



HAL
open science

Contributions to unbiased diagrammatic methods for interacting fermions

Riccardo Rossi

► **To cite this version:**

Riccardo Rossi. Contributions to unbiased diagrammatic methods for interacting fermions. Condensed Matter [cond-mat]. Université Paris sciences et lettres, 2017. English. NNT : 2017PSLEE091 . tel-01704724v2

HAL Id: tel-01704724

<https://theses.hal.science/tel-01704724v2>

Submitted on 14 Oct 2021

HAL is a multi-disciplinary open access archive for the deposit and dissemination of scientific research documents, whether they are published or not. The documents may come from teaching and research institutions in France or abroad, or from public or private research centers.

L'archive ouverte pluridisciplinaire **HAL**, est destinée au dépôt et à la diffusion de documents scientifiques de niveau recherche, publiés ou non, émanant des établissements d'enseignement et de recherche français ou étrangers, des laboratoires publics ou privés.

Laboratoire de Physique Statistique
Département de Physique de l'École Normale Supérieure



THÈSE de DOCTORAT

specialité: Physique Statistique

présentée par

Riccardo ROSSI

pour obtenir le titre de Docteur
de l'Université de recherche Paris Sciences et Lettres.

**Contributions to unbiased diagrammatic methods
for interacting fermions**

Soutenue le 18 septembre 2017 devant le jury composé de:

Pavel BUIVIDOVICH	Rapporteur
Evgeny KOZIK	Examineur
Olivier PARCOLLET	Examineur
Guido PUPILLO	Examineur
Jean-Bernard ZUBER	Président
Wilhelm ZWARGER	Rapporteur
Kris VAN HOUCKE	Directeur de thèse
Félix WERNER	Directeur de thèse

Contents

Introduction	9
Overview	13
I Large-order behavior and resummation for the unitary Fermi gas	15
1 Introduction	17
1.1 The unitary Fermi gas	17
1.2 The unitary Fermi gas as the continuum limit of lattice models	20
1.3 Diagrammatic dressing: bare, ladder, and bold expansions	21
2 Summary of main results	24
3 Large-order behavior for the pressure in the ladder scheme	29
3.1 Shifted action for the ladder scheme	29
3.2 Obtaining the large-order behavior for the pressure from the partition function	30
3.3 Integration over fermions	32
3.4 Saddle point for the large-order behavior of the determinant	34
3.5 Functional integration in the large- n limit	35
4 Analytic reconstruction by conformal-Borel transform	39
4.1 Unicity of Taylor coefficients	39
4.2 Borel summability and conformal mapping	40
5 Generalizations	43
5.1 Borel summability of the self-energies in the ladder expansion	43
5.2 Alternative view: discontinuities near the origin	48
5.3 Discussion of the bold scheme	51
6 Numerical results	53
7 Conclusions and outlook	55

Appendices of Part I	60
A Shifted action for the ladder scheme	60
B Interchanging thermodynamic and large-order limit	61
C Renormalized Fredholm determinants	62
D Large-field behavior of the determinant	67
E No imaginary-time dependence of the instanton	71
F Sobolev bound	72
G Variational principle	73
H High and low temperature limits of the action functional	74
I Symmetric decreasing rearrangement	75
J Gaussian zero modes	76
K Gaussian integration	78
L Bound on derivatives	81
M Unicity of analytic continuation	82
N Ramis's theorem	84
O Consistency condition for the maximal analytic extension	89
P Construction of the conformal map	90
Q Some properties of Gevrey asymptotic series	93
R Dispersion relation	95
S Pair propagator in terms of the η fields	96
T Generalized Pauli formulas	96
U Numerical computation of the minimum of the action	97
V Legendre-Bateman expansion	98
W Discontinuities of the bold self-energies	99

**II Connected determinant diagrammatic Monte Carlo:
polynomial complexity despite fermionic sign 103**

**Article 1: Determinant Diagrammatic Monte Carlo in the thermo-
dynamic limit 105**

Article 2: Polynomial complexity despite the fermionic sign 111

Complements 117

1 The recursive formula for many-variable formal power series . . .	117
2 Example: two-body interactions with a linear quadratic shift . . .	120
2.1 Calculation of $a_E(V)$	121
2.2 Monte Carlo integration and computational cost of the non-deterministic part	122
2.3 Generalizations	122

2.4	Computation of physical correlation functions	123
3	Polynomial-time scaling	124
Conclusion and outlook		127
Appendices of Part II		129
A	Computational cost of the recursive formula	129
B	Computational cost of the determinants	130
C	Hybrid sampling	130
D	Binary representation	131
III Multivaluedness of the Luttinger-Ward functional and applicability of dressed diagrammatic schemes		135
1	Introduction and overview	138
2	The dangers of dressing	139
2.1	The formal definition of the bold series	140
2.2	The Kozik-Ferrero-Georges branch of the Luttinger-Ward functional	142
2.3	Misleading convergence of the bold scheme	143
3	An insightful model	144
3.1	Feynman diagrams definition	145
3.2	Grassmann integral representation	145
3.3	The KFG branch of the toy model	146
3.4	Misleading convergence of the bold scheme within the toy model	149
4	Semi-bold scheme: partial dressing with no misleading convergence	151
4.1	Shifted-action expansion	151
4.2	Semi-bold scheme	153
5	Applicability of the bold scheme	154
6	Conclusions and outlook	156
Article 3: Skeleton series and multivaluedness of the self-energy functional in zero space-time dimensions		157
Article 4: Shifted-action expansion and applicability of dressed diagrammatic schemes		165
Bibliography		171

Abstract

This thesis contributes to the development of unbiased diagrammatic approaches to the quantum many-body problem, which consist in computing expansions in Feynman diagrams to arbitrary order with no small parameter. The standard fermionic sign problem - exponential increase of statistical error with volume - does not affect these methods as they work directly in the thermodynamic limit. Therefore they are a powerful tool for the simulation of quantum matter.

Part I of the thesis is devoted to the unitary Fermi gas, a model of strongly-correlated fermions accurately realized in cold-atom experiments. We show that physical quantities can be retrieved from the divergent diagrammatic series by a specifically-designed conformal-Borel transformation. Our results, which are in good agreement with experiments, demonstrate that a diagrammatic series can be summed reliably for a fermionic theory with no small parameter.

In Part II we present a new efficient algorithm to compute diagrammatic expansions to high order. All connected Feynman diagrams are summed at given order in a computational time much smaller than the number of diagrams. Using this technique one can simulate fermions on an infinite lattice in polynomial time. As a proof-of-concept, we apply it to the weak-coupling Hubbard model, obtaining results with record accuracy.

Finally, in Part III we address the problem of the misleading convergence of dressed diagrammatic schemes, which is related to a branching of the Luttinger-Ward functional. After studying a toy model, we show that misleading convergence can be ruled out for a large class of diagrammatic schemes, and even for the fully-dressed scheme under certain conditions.

Résumé

Cette thèse contribue au développement d'approches diagrammatiques systématiques pour le problème quantique à N corps, qui consistent à calculer une expansion en diagrammes de Feynman à un ordre arbitraire sans contrainte de paramètre petit. La forme standard du problème de signe fermionique - augmentation exponentielle de l'erreur statistique avec le volume - n'affecte pas ces méthodes car elles fonctionnent directement dans la limite thermodynamique. Par conséquent, elles sont un outil puissant pour la simulation de la matière quantique.

La partie I de la thèse est consacrée au gaz de Fermi unitaire, un modèle de fermions fortement corrélés réalisé avec précision dans des expériences d'atomes froids. Nous montrons que les quantités physiques peuvent être extraites de la série diagrammatique divergente par une transformation de Borel conforme spécifiquement conçue. Nos résultats, qui sont en accord avec les expériences, démontrent qu'une série diagrammatique peut être resommée de manière fiable pour une théorie fermionique sans contrainte de paramètre petit.

Dans la partie II, nous présentons un nouvel algorithme pour calculer les expansions diagrammatiques à ordre élevé. Tous les diagrammes Feynman connectés sont sommés à un ordre donné avec un temps de calcul beaucoup plus petit que le nombre de diagrammes. En utilisant cette technique, on peut simuler des fermions sur un réseau infini en temps polynomial. Pour preuve, nous l'appliquons au modèle d'Hubbard à couplage faible, en obtenant des résultats avec une précision record.

Enfin, dans la partie III, nous abordons le problème de la convergence erronée des schémas diagrammatiques habillés, qui est lié à une ramification de la fonctionnelle de Luttinger-Ward. Après avoir étudié un modèle-jouet, nous montrons que le caractère erroné de la convergence peut être exclu pour une grande classe de schémas diagrammatiques, et aussi pour le schéma complètement habillé, sous certaines conditions.

Introduction

For interacting bosonic systems in thermal equilibrium, numerically exact Quantum Monte Carlo methods have proven to be extremely effective in accurately predicting the thermodynamic behavior [1, 2, 3, 4]. In most cases of physical interest, fermionic degrees of freedom are present. Unfortunately, the same Monte Carlo methods that were proven to be successful for bosons face severe difficulties when dealing with fermions: the Monte Carlo variance of the observables is much greater than their value, this is the infamous sign problem [5, 6, 7, 8]. More precisely, we can define the fermionic sign problem as the exponential increase of computational time with system size and inverse temperature. For most cases of physical interest (e.g. repulsive Hubbard model away from half-filling), traditional Monte Carlo techniques are affected by the sign problem. This means that at low temperature it is very difficult to simulate large lattice sizes, and the extrapolation to the physical thermodynamic limit is in many cases beyond our current (and at least near future) computational capabilities.

A possible solution that has been proposed is quantum simulation. For example, one can use ultra-cold atoms experiments to simulate models of strongly interacting fermions using nature instead of the computer. This route has been very successful for the unitary Fermi gas [9, 10, 11, 12, 13, 14], that can now be simulated in the lab with very high accuracy and controllability. The simulation of the Hubbard model has recently achieved very promising successes [15, 16, 17, 18, 19]. In particular, the low-temperature regime has been reached and long-range anti-ferromagnetic order has been observed [20], and experimental efforts are underway to reach even lower temperatures.

In this text we will focus on a class of theoretical methods that address the problem of the simulation of strongly-correlated Fermi systems from a different perspective than traditional Quantum Monte Carlo methods. The main idea is very simple: Feynman diagrams can be formulated directly in the thermodynamic limit (even at zero temperature if we want to), so that the traditional form of sign problem (that is, the exponential increase of computational time with system size and inverse temperature) is not present by construction. When a diagrammatic scheme is convergent we are able to get arbitrarily close to the exact result with

controlled error bars given enough computer time, provided that we have a way to compute arbitrarily high expansion orders. For this reason, we can refer to these diagrammatic methods as “unbiased”. This distinguishes them from low-order diagrammatic computations, where the error bar is difficult to estimate and does not vanish in the limit of infinite computer time.

In order to compute the high-order expansion, it is useful to use Monte Carlo. For this reason, this class of approaches is called Diagrammatic Monte Carlo [21]. Diagrammatic Monte Carlo was first applied to the polaron problem [22, 23, 24, 25, 26, 27]. It was later shown to be applicable to fermionic many-body problems [28, 29, 30, 31, 32, 12], and to frustrated spin systems [33, 34, 35]. While the original technique explicitly sampled Feynman diagram topologies, alternative computational approaches are also being developed [36, 37, 38, 39]. Recently, it was shown that Diagrammatic Monte Carlo can be applied to the large- N limit of matrix field theories [40, 41].

Remarkably, one can argue that dealing with fermions instead of bosons is even advantageous for Diagrammatic Monte Carlo methods. This fact was referred to as “sign blessing” [33, 42], to contrast it with the fermionic sign problem encountered in traditional Quantum Monte Carlo methods. The main advantage of using diagrammatic expansions is the enhanced convergence properties of the series in the fermionic case. Another advantage is the possibility of grouping fermionic Feynman diagrams into determinants, which is used in some Diagrammatic Monte Carlo algorithms [37, 38].

Let us first discuss the convergence properties. For bosons, the diagrammatic series always has a zero radius of convergence. Indeed, all diagrams contribute with the same sign, and therefore one expects that the order n is proportional to the number of Feynman diagrams at order n , which is always of order $n!$. This can be shown using standard Lipatov techniques [43, 44, 45]. Fermionic Feynman diagrams have different signs, and there are generally strong cancellations within the same order of expansion. For fermions on a lattice at non-zero temperature, the cancellation is nearly perfect, and one has a finite radius of convergence. This has been seen numerically [28, 29, 32, 38], and it has also been proven mathematically [46]¹. For fermions in continuous space, one has in general zero radius of convergence in high-enough dimensions (higher than 2 in most cases), but the divergence is much milder than for bosons. For example, as we will see in Part I of this text, for the unitary Fermi gas the order n is proportional to $(n!)^{1/5}$. Having a zero radius of convergence is not an insurmountable problem: if certain conditions are verified, one can obtain controlled results by using a Borel resummation technique. However, from a computational point of view,

¹In the special case of the half-filled two-dimensional Hubbard model on the honeycomb lattice, the radius of convergence is finite even at zero temperature [47].

this is always expected to be worse. For wildly diverging diagrammatic series one needs to compute the order- n with a very high relative precision, there is loosely speaking a big sign problem between different orders that come with different signs.² This is the case of φ^4 theory, in which the required relative precision increases rapidly with order. In essence, Diagrammatic Monte Carlo is expected to work well when one has either a non-zero radius of convergence (fermions on a lattice at non-zero temperature), or a mildly divergent series (e.g. the unitary Fermi gas).

The second advantage of having a fermionic sign in Feynman diagrams is the possibility of grouping the sum of all diagrams (connected and disconnected) using determinants, which can be computed in polynomial time, while for bosons we can group the sum of all diagrams using permanents, which can be computed in exponential time.

A very useful tool available in diagrammatic techniques is the possibility of working with dressed objects. This turns out to be helpful in many situations, and it is even mandatory in order to define the model in some case (e.g. the unitary Fermi gas can be defined in the continuum limit only after we have summed up ladder diagrams up to infinite order).

When considering unbiased diagrammatic schemes, one is generally confronted with these fundamental problems:

- **Choice of diagrammatic expansion:** First of all, one has to choose an unperturbed action in order to perform a diagrammatic expansion, and it is important to understand which choices lead to a well-defined perturbation theory. For example, for the unitary Fermi gas the expansion in the bare coupling constant is not well-defined in the continuum limit, and one has to dress the interaction in order to have a meaningful continuous-space zero-range theory³.

An even more subtle problem is to understand when the use of diagrammatic dressing is justified from a mathematical point of view, as it was found that fully-dressed diagrammatic expansion for Hubbard-like lattice models have fundamental problems [48] that can even lead to convergence towards an unphysical result. This problem is studied for lattice models in Part III of this text.

- **Computation of high-order terms:** Once the diagrammatic expansion has been chosen, one has to compute the coefficients of the expansion. For low-order computations, performing a brute-force enumeration of Feynman diagram topologies and computing the integrals over the internal variables

²This fact was pointed out to us by N. Prokofiev and B. Svistunov.

³See Section 1.3 of Part I for more details

one-by-one is feasible. In order to go to high orders in a systematic way, it is convenient to treat the topologies of the diagrams and internal variables at the same level and to build a Markov chain in this space (this is the most common version of Diagrammatic Monte Carlo), or even to perform first the sum over (symmetrized) Feynman diagram topologies and then perform stochastically the integral over internal variables (this is the basis of determinant techniques). We have contributed to the determinant approach by introducing a new algorithm, which has a polynomial-time computational complexity for a convergent series. This is presented in Part II.

- **Convergence properties and resummation:** After computing the coefficients of the diagrammatic expansions, one has to reconstruct the physical answer from them, if at all possible. If we are inside the radius of convergence, direct summation of the diagrammatic series yields an exponentially convergent result. If we are outside the radius of convergence, one has to use resummation techniques to compute the physical answer. We have solved this problem for the unitary Fermi gas in Part I, where we have computed the large-order behavior of various diagrammatic expansions and we have shown that a specifically designed conformal-Borel transform is able to resum the diagrammatic series.

Overview

This thesis is devoted to the study of mathematical and computational aspects of diagrammatic expansions. It is divided in three independent parts, which can be read in any order. Let us give a brief overview of the different parts:

- **Part I: Large-order behavior and resummation for the unitary Fermi gas:** In this part we deal with the problem of convergence of diagrammatic series in the case of the unitary Fermi gas. We show here that various diagrammatic series for this system have a zero radius of convergence by computing the large-order asymptotic behavior. We show that it is possible to recover the physical result from series coefficients by using a specifically built conformal-Borel resummation technique, which uses the information on the large-order behavior in an “optimal” way. We then present the results of the application of this resummation technique to the normal phase of the unitary Fermi gas, using Diagrammatic Monte Carlo for computing the series of Feynman diagrams. As the work presented in this part is still unpublished, we decided to present arguments and derivations in a fairly detailed way.
- **Part II: Connected determinant diagrammatic Monte Carlo: polynomial-time complexity despite fermionic sign:** In this part we present a new algorithm to compute diagrammatic expansions at high order, and we show that this algorithm has a polynomial-time computational complexity.

Article 1 [38] presents the new algorithm for computing diagrammatic expansions. It allows to consider directly the sum of all connected Feynman diagrams at once at fixed space-time positions of interactions vertices. In this way, the thermodynamic limit can be taken for free. Moreover, considering the sum of all (symmetrized) topologies at once (this is done using a recursive formula and a determinant representation) allows for massive cancellations between diagrams, greatly reducing the variance of the Monte Carlo simulation. This allows to compute diagrammatic expansions

with a cost which increases only exponentially with order, which is to be contrasted with the factorial cost of the standard diagrammatic technique.

Article 2 [49] underlines the power of diagrammatic techniques for fermionic systems, showing in particular that the algorithm of Article 1 has a polynomial-time computational scaling: the total error bar on thermodynamic-limit quantities goes down polynomially with CPU time.

We then provide a minimalist technical supplement for Article 1. We discuss some proofs concerning the recursive formula, computational cost and Monte Carlo implementation of the new connected determinant diagrammatic Monte Carlo algorithm. We also provide a discussion of computational complexity, extending Article 2.

- **Part III: Multivaluedness of Luttinger-Ward functional and applicability of dressed diagrammatic schemes:** This part is dedicated to the problem of misleading convergence of Bold Diagrammatic Monte Carlo. This problem has been raised by the work of Kozik et al., showing that the self-energy expressed in terms of the fully-dressed one-particle propagator has at least two branches. As a consequence, the Bold Diagrammatic Monte Carlo scheme can converge in some parts of the parameter space towards a wrong unphysical solution. The main result of this chapter is to show that at least when certain conditions are satisfied, this “apocalyptic” scenario is impossible, so that one can safely use Bold Diagrammatic Monte Carlo. Moreover, we propose a new partially-dressed scheme for which the misleading convergence is impossible.

Part I

Large-order behavior and resummation for the unitary Fermi gas

In this part of the text we discuss the computation of the large-order behavior of various systematic diagrammatic expansions for the unitary Fermi gas. We find that for all considered diagrammatic schemes, the order- n diagrammatic expansion diverges like $(n!)^{1/5}$. In particular, the radius of convergence of the series is zero. By using the shifted-action formalism, we are able to prove that the series can be resummed by a carefully designed conformal-Borel transform, which uses the information on the large-order behavior and on the analytic structure in an “optimal” way. We then show how it is possible to include the resummation algorithm in the Diagrammatic Monte Carlo procedure, obtaining controlled numerical results for the normal phase of the unitary Fermi gas.

After a short introduction, we summarize the main results of this part of the dissertation. We then proceed with the derivations, relying on appendices for the most technical parts. Finally, we present numerical results. ⁴

1 Introduction

1.1 The unitary Fermi gas

We consider a gas of spin-1/2 fermions in three dimensions, interacting with a short-range attractive interaction [9]. At low energy, the two-body scattering is dominated by the scattering between different spin particles in the spin-zero channel. The form of the s-wave scattering amplitude for particles of relative momentum \mathbf{k} is constrained by the optical theorem, which is a consequence of unitarity

$$f_k = -\frac{1}{ik + u(k)}, \quad u(k) \in \mathbb{R} \quad (1)$$

so that we have the bound

$$|f_k| \leq \frac{1}{k} \quad (2)$$

The unitary gas ideally saturates this bound, $f_k^{(\text{unitary})} = -1/ik$. In practice, for a unitary gas to be realized we require that f_k is of this form for typical values of momentum in the gas. We expand $u(k)$ for small k

$$u(k) = \frac{1}{a} - \frac{1}{2}r_e k^2 + O(k^4) \quad (3)$$

where a is the scattering length and r_e is the effective range of the interaction. Let k_F be the Fermi momentum and $k_T := \sqrt{3T}$ the thermal de Broglie momentum⁵,

⁴Work done in collaboration with Takahiro Ohgoe, Kris Van Houcke and Félix Werner. I was responsible for the resummation part of the code.

⁵We choose the mass of the particles equal to 1, and $\hbar = 1$.

where T is the temperature. The typical value of the relative momentum between two particles will be of the order of the maximum between k_F and k_T . Thus, we must have

$$k_F r_e \ll 1, \quad k_T r_e \ll 1 \quad (4)$$

to be in the universal regime where the details of the interaction apart from the scattering length are not important. Moreover, every dimensionless intensive quantity is a function of only $k_F a$ and T/E_F , where $E_F := k_F^2/2$. The unitary gas is obtained for $1/(k_F a) = 0$, exactly at the point where a two-body bound state of zero energy is present.⁶

It is interesting to study the evolution of the properties of the gas as a function of $k_F a$. When $k_F a \rightarrow 0^-$, one has a weakly attractive Fermi gas, which experiences a superfluid phase transition at an exponentially small critical temperature, well described by BCS theory. $k_F a \rightarrow 0^+$ corresponds to the strong coupling regime. The attractive interaction between particles is very strong and for temperatures lower than $1/a^2$ the gas is composed of tightly bound molecules of one spin up and one spin down particle, of size $\sim k_F a$ smaller than the distance between different molecules. We can describe this regime as a weakly interacting gas of molecules of spin zero. These spin-less bosons experience Bose-Einstein condensation at low enough temperature. Let us remark that the mechanism for superfluidity is very different for $k_F a \rightarrow 0^\pm$, in the BCS regime the Cooper pairs are highly delocalized in space, while in the BEC regime we have a condensate of bosonic molecules of small size [50, 51]. In the middle of the BCS-BEC crossover (see [52] and Refs. therein) stands the strongly interacting unitary Fermi gas, which cannot be described using any of these two weakly interacting pictures (see Figure 1).

In the following we consider the unpolarized case where the number of spin-up particles is equal to the number of spin-down particles, but there is no fundamental limitation to extend our approach to the polarized gas.

The unitary Fermi gas is the subject of an intense experimental activity in cold-atoms laboratories. The first conclusive condensation of a Fermi gas was achieved in [54] by showing the presence of a vortex lattice in the rotating superfluid gas. For other pioneering experiments, see [55, 9] and references therein. Recent achievements include the study of the Josephson effect [56], the investigation of transport properties through a quantum point contact [57], and of counterflow in a mixture of superfluid Fermi and Bose gases [58, 59, 60].

The experiments which are most directly relevant to the calculations presented in this manuscript are the measurements of the thermodynamic properties

⁶Therefore, the unitary gas has only one parameter, which can be chosen to be the temperature over the Fermi-energy T/E_F , or the chemical potential over the temperature μ/T (which is more natural in the grand-canonical formalism we use).

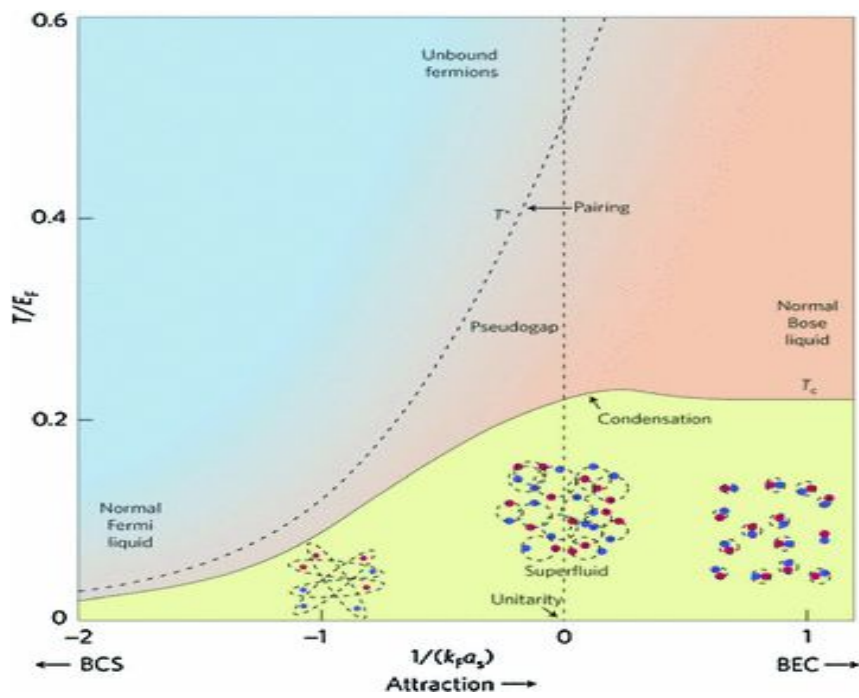


Figure 1: Expected phase diagram for the BCS-BEC crossover (image taken from [53]). In the x -axis we have the inverse dimensionless scattering length, and on the y axis we have the dimensionless temperature. The unitary Fermi gas is obtained for $1/k_F a = 0$.

of the homogeneous gas at thermal equilibrium. The equation of state of the homogeneous gas was obtained in [61, 11, 62, 63, 12, 64, 65]. The measurement of the so-called contact parameter (which determines the large-momentum behavior of the momentum distribution, as well as the short-distance behavior of the pair distribution function) has been done so far for the inhomogeneous trapped gas in [66, 67, 68, 69, 62, 14, 70, 71]. The homogeneous-gas contact was extracted using zero-temperature local-density approximation [62, 14] or by probing the central region of the cloud [70, 71].

Photoemission spectroscopy experiments [72, 73] (first proposed in [74]) should greatly benefit from the recently introduced flat traps [75]. Another interesting quantity is the shear viscosity, measured in [76, 77], and theoretically investigated in [78].

1.2 The unitary Fermi gas as the continuum limit of lattice models

In this section we will discuss how to construct the unitary Fermi gas as the continuum limit of lattice models with zero-range interactions. This is only an intermediate step needed for the derivations, we will always take the continuum limit analytically before the numerical calculations, which are performed directly in the continuum (and thermodynamic) limit. This is an important advantage with respect to lattice Quantum Monte Carlo computations, for which even in the non-polarised regime where there is no sign problem, the double extrapolation to the continuum and thermodynamic limits is hard to achieve in a controlled way [79, 80, 81, 82].

The unitary limit is universal in the sense that if the range of the interaction is short enough the physical properties of the gas will depend only on the scattering length. The first example we consider is the attractive Hubbard model for a cubic lattice:

$$\hat{H} = -t \sum_{\mathbf{r} \sim \mathbf{r}', \sigma} \hat{c}_\sigma^\dagger(\mathbf{r}) \hat{c}_\sigma(\mathbf{r}') + U \sum_{\mathbf{r}} (\hat{c}_\uparrow^\dagger \hat{c}_\uparrow \hat{c}_\downarrow^\dagger \hat{c}_\downarrow)(\mathbf{r}) \quad (5)$$

where the first sum run over neighboring sites \mathbf{r} and \mathbf{r}' . One can find a bound state of two particles with different spins with zero energy for

$$\left(\frac{t}{U}\right)_{\text{dimer}} = -\frac{1}{4(2\pi)^3} \int_{[-\pi, \pi]^3} \frac{d^3\mathbf{k}}{3 - \sum_{j=1}^3 \cos(k_j)} = -0.1263655\dots \quad (6)$$

Let b be the lattice spacing. Then, one can show (see, e.g., [83]) that in order to obtain a gas with an s-wave scattering length a one has to take the limit $b \rightarrow 0$ at fixed density $n := \nu/b^3$, where b is the lattice spacing and ν is the filling

factor, with interaction given by

$$\frac{t}{\bar{U}} = \left(\frac{t}{\bar{U}} \right)_{\text{dimer}} + \frac{b}{8\pi a} \quad (7)$$

For convenience, we will consider in the following a lattice model with a quadratic dispersion relation, which is equivalent to the Hubbard model in the continuum limit:

$$\hat{H} = \sum_{\sigma} \int_{\text{BZ}} \frac{d^3\mathbf{k}}{(2\pi)^3} \frac{k^2}{2} \hat{\psi}_{\mathbf{k},\sigma}^{\dagger} \hat{\psi}_{\mathbf{k},\sigma} + g_0 b^3 \sum_{\mathbf{r} \in b\mathbb{Z}^3} (\hat{\psi}_{\uparrow}^{\dagger} \hat{\psi}_{\uparrow} \hat{\psi}_{\downarrow}^{\dagger} \hat{\psi}_{\downarrow})(\mathbf{r}) \quad (8)$$

where

$$\{\hat{\psi}_{\sigma}(\mathbf{r}), \hat{\psi}_{\sigma'}(\mathbf{r}')\} = 0, \quad \{\hat{\psi}_{\sigma}(\mathbf{r}), \hat{\psi}_{\sigma'}^{\dagger}(\mathbf{r}')\} = b^{-3} \delta_{\sigma,\sigma'} \delta_{\mathbf{r},\mathbf{r}'} \quad (9)$$

and g_0 is chosen according to [83]

$$\frac{1}{g_0} = \frac{1}{4\pi a} - \int_{\text{BZ}} \frac{d^3k}{(2\pi)^3} \frac{1}{k^2} \quad (10)$$

1.3 Diagrammatic dressing: bare, ladder, and bold expansions

From the previous expression we see that $g_0 \underset{b \rightarrow 0^+}{=} 0^-$. Moreover, if we write a bare expansion in powers of g_0 for the pressure for instance

$$p_{\text{bare}}(g_0) \underset{\text{Taylor}}{=} \sum_{n=0}^{\infty} g_0^n p_{\text{bare},n} \quad (11)$$

we see that in order to have a non-trivial system, we must have at least for some n

$$|p_{\text{bare},n}| \underset{b \rightarrow 0^+}{=} \infty \quad (12)$$

The reason for this is that the ladder diagrams are divergent in the continuum limit. Therefore, one has to solve the two-body scattering problem before taking the continuum limit. We introduce (see, e.g., [84]):

$$\Gamma^{(0)} \quad \square = \bullet + \begin{array}{c} \circlearrowleft \\ \bullet \quad \bullet \\ \circlearrowright \end{array} + \begin{array}{c} \circlearrowleft \quad \circlearrowleft \\ \bullet \quad \bullet \quad \bullet \\ \circlearrowright \quad \circlearrowright \end{array} + \dots$$

Γ_0 has a non-trivial continuum limit. For completeness, we give the expression of Γ_0 :

$$\Gamma_0^{-1}(\mathbf{p}, \Omega_n) = \frac{1}{g_0} - \Pi_{\text{bubble}}(\mathbf{p}, \Omega_n) \quad (13)$$

where \mathbf{p} is the momentum, $\Omega_n \in 2\pi\mathbb{Z}/\beta$ is the Matsubara bosonic frequency, and Π_{bubble} is the $G_0 G_0$ bubble

$$\Pi_{\text{bubble}}(\mathbf{p}, \Omega_n) := \int \frac{d^3 k}{(2\pi)^3} \frac{1 - n_{\uparrow}^{(0)}(\mathbf{p}/2 + \mathbf{k}) - n_{\downarrow}^{(0)}(\mathbf{p}/2 - \mathbf{k})}{i\Omega_n + 2\mu - \epsilon_{\mathbf{p}/2+\mathbf{k}} - \epsilon_{\mathbf{p}/2-\mathbf{k}}} \quad (14)$$

where $\mu := (\mu_{\uparrow} + \mu_{\downarrow})/2$ is the mean chemical potential, $\epsilon_{\mathbf{p}}$ is the (quadratic) dispersion relation, and $n_{\sigma}^{(0)}$ is the non-interacting Fermi-Dirac momentum distribution. The Γ_0 diagrams are obtained from the g_0 diagrams by replacing g_0 by Γ_0 ; moreover the diagrams containing $(G_0 G_0)$ bubbles must be removed (to avoid double counting). For the pressure, for instance, we obtain

$$p_{\text{ladd}}[\Gamma_0] \underset{\text{Taylor}}{=} \sum_{n=0}^{\infty} p_{\text{ladd},n}[\Gamma_0] \quad (15)$$

where for $n \geq 2$, $p_{\text{ladd},n}$ is built from Feynman diagrams containing n Γ_0 lines⁷. One has that every term of this expansion is well-defined in the continuum limit:

$$\lim_{b \rightarrow 0^+} p_{\text{ladd},n}[\Gamma_0] \in \mathbb{R} \quad (16)$$

The ladder approximation consists in summing up all ladder diagrams to infinity, in our formalism the ladder approximation for the pressure corresponds to order zero of the ladder expansion, $p \approx p_{\text{ladd},0}$ (for applications of the ladder approximation to the unitary Fermi gas, see [85, 86]).

In order to enhance convergence properties and (more importantly) to extend the applicability region to lower temperatures, we need to use more general diagrammatic dressing. Indeed, $p_{\text{ladd},n}$ is well-defined only if Γ_0 has no poles. This is true for temperatures higher than the pairing temperature T^* , see Figure 1. In order to study the system in the lower temperature interval $T_c < T \leq T^*$, one has to sum up more general classes of diagrams. A particularly elegant dressing is the “bold” dressing (or fully-dressed scheme). It consists in using the fully-dressed fermion propagators G and pair propagator Γ to build perturbative expansions. For a formal definition of the bold scheme, see Section 5.3. Let G be the Green’s function

$$G(\mathbf{r}, \tau) := -\langle \varphi_{\uparrow}(\mathbf{r}, \tau) \bar{\varphi}_{\uparrow}(\mathbf{0}, 0) \rangle \quad (17)$$

⁷We want to stress that the ladder expansion we consider here is formally exact: every Feynman diagram is included in the expansion.

where φ and $\bar{\varphi}$ are Grassmann fields. Let Γ be the pair propagator:

$$\Gamma(\mathbf{r}, \tau) := g_0 \delta(\mathbf{r}, \tau) - g_0^2 \langle (\bar{\varphi}_\downarrow \bar{\varphi}_\uparrow)(\mathbf{x}, \tau) (\varphi_\uparrow \varphi_\downarrow)(\mathbf{0}, 0) \rangle \quad (18)$$

Then, we simply re-express every physical quantity (e.g. the pressure) in a formal series in G and Γ :

$$p_{\text{bold}}[G, \Gamma] = \sum_{n=0}^{\infty} p_{\text{bold},n}[G, \Gamma] \quad (19)$$

where $p_{\text{bold},n}$ is built on Feynman diagrams having n Γ lines (to avoid double counting, one has to forbid diagrams that fall apart upon cutting two G -lines or two Γ -lines).

The self-energy Σ and the pair self-energy Π are defined by the Dyson equations:

$$\Sigma := G_0^{-1} - G^{-1}, \quad \Pi := \Gamma_0^{-1} - \Gamma^{-1} \quad (20)$$

We can then define the “boldified” self-energies diagrammatic series $\Sigma_{\text{bold}}[G, \Gamma]$ and $\Pi_{\text{bold}}[G, \Gamma, G_0] = \Pi_{\text{bubble}}[G] - \Pi_{\text{bubble}}[G_0] + \tilde{\Pi}_{\text{bold}}[G, \Gamma]$ ⁸. The propagators G and Γ are computed from truncated self-consistent Dyson’s equations

$$\sum_{n=1}^{\mathcal{N}} \Sigma_{\text{bold},n}[G_{\mathcal{N}}, \Gamma_{\mathcal{N}}] := G_0^{-1} - G_{\mathcal{N}}^{-1} \quad (21)$$

$$\Pi_{\text{bubble}}[G_{\mathcal{N}}] - \Pi_{\text{bubble}}[G_0] + \sum_{n=2}^{\mathcal{N}} \tilde{\Pi}_{\text{bold},n}[G_{\mathcal{N}}, \Gamma_{\mathcal{N}}] := \Gamma_0^{-1} - \Gamma_{\mathcal{N}}^{-1} \quad (22)$$

and one computes G and Γ from

$$G = \lim_{\mathcal{N} \rightarrow \infty} G_{\mathcal{N}}, \quad \Gamma = \lim_{\mathcal{N} \rightarrow \infty} \Gamma_{\mathcal{N}} \quad (23)$$

Without entering into details, let us just mention another interesting diagrammatic scheme to consider, the \mathcal{M} -semi-bold scheme introduced in Article 4 [87], where $\mathcal{M} \in \mathbb{N}$. One has that $\mathcal{M} = 0$ corresponds to the ladder scheme, while $\mathcal{M} \rightarrow \infty$ corresponds to the bold scheme.⁹ It would be interesting to implement the $\mathcal{M} = 1$ semi-bold scheme as the order $\mathcal{N} = 1$ approximation corresponds to the scheme introduced in [88, 89], which was found to be remarkably accurate for the unitary Fermi gas.¹⁰

⁸The first order is special (it is the difference of the bubbles GG and G_0G_0 , it is not a functional of G and Γ), and needs to be treated separately. This is due to the fact that the natural definition of pair self-energy would be $\tilde{\pi} := g_0^{-1} - \Gamma^{-1}$, which can be written as a functional $\tilde{\pi}_{\text{bold}}[G, \Gamma]$ of G and Γ . Unfortunately, $\tilde{\pi}_{\text{bold},1}[G, \Gamma] \equiv \Pi_{\text{bubble}}[G]$ is infinite in the continuum limit. Therefore, it is better to work with the “unnatural” definition.

⁹The advantage of the semi-bold scheme over the bold one is that by construction it does not suffer from the problems to be described in Part III.

¹⁰In particular, the scheme of [88, 89] predicts a phase transition at a temperature $T = T_1^*$

2 Summary of main results

Before presenting the original work with the detailed derivations, we summarize the main results of this part of the dissertation.

For a given physical quantity f_{physical} (like the pressure, a correlation function, or a self-energy) and for a given diagrammatic scheme denoted by “diag”¹¹, we introduce a function $f_{\text{diag}}(z)$ of a complex parameter z such that its Taylor series is equal order-by-order to the diagrammatic expansion:

$$f_{\text{diag}}(z) \underset{\text{Taylor}}{=} \sum_{n=0}^{\infty} z^n f_{\text{diag},n} \quad (24)$$

where $f_{\text{diag},n} = \lim_{w \rightarrow 0^+} \frac{1}{n!} \frac{d^n f_{\text{diag}}(w)}{dw^n}$ is the order- n diagrammatic expansion of f_{physical} for the considered diagrammatic scheme “diag”. We construct this $f_{\text{diag}}(z)$ by introducing an action $S_{\text{diag}}^{(z)}$ depending on the complex parameter z . We impose by construction that $S_{\text{diag}}^{(z=1)} = S_{\text{physical}}$, so that

$$f_{\text{diag}}(z=1) = f_{\text{physical}} \quad (25)$$

One of the most important problems that we consider in this part of the dissertation is the determination of the large-order behavior of the Taylor coefficients $f_{\text{diag},n}$. We first present a detailed derivation for the pressure computed with the “ladder scheme” (the diagrammatic series without ladder diagrams). We start from a finite-size model on a lattice (but the continuum limit will be taken soon after) in order to have a well-defined partition function, from which we deduce the large-order behavior for the pressure. After discussing the pressure within the ladder expansion, we generalize our results to include more general correlation functions, and more general diagrammatic schemes, even if the rigour of the computation decreases with the “distance” from the pressure of the ladder scheme. We expect that in general, for every quantity f and for every diagrammatic scheme, one has¹²

$$f_{\text{diag},n} \underset{n \rightarrow \infty}{=} (n/5)! A_{\text{diag}}^{-n} \text{Re exp} \left\{ \frac{4\pi i n}{5} - U_{\text{diag},1} e^{4\pi i/5} n^{4/5} + O(n^{3/5}) \right\} \quad (26)$$

which is very close to the critical temperature T_c . This means that the 1-semi-bold scheme (which is a just a perturbation theory on top of the approximation of [88, 89]) is meaningful down to temperature $T = T_1^*$, therefore it can be applied essentially in the whole normal phase.

¹¹“diag” can be in practice “ladd” (for the ladder expansion), “bold” (for the fully-dressed expansion) or “semi – bold” (for the semi-bold scheme introduced in [87]). See section 1.3

¹²It would be extremely difficult to find or to fit numerically this type of behavior for several reasons:

- The term $\cos \left[4\pi/5 - \sum_{k=1}^4 n^{(5-k)/5} U_{\text{diag},k} \sin((5-k)\pi/5) + \phi_0 + O(n^{-1/5}) \right]$ is an highly oscillatory function of n . A small correction in the phase has potentially a big

where $A_{\text{diag}} > 0$ ¹³ and $U_{\text{diag},1} \in \mathbb{R}$ depend only on the diagrammatic scheme considered, they are the same for every correlation function. For example, for the ladder scheme, one has

$$A_{\text{ladd}} = A_{\sharp} \inf_{\eta} \frac{-\langle \eta | \Gamma_0^{-1} | \eta \rangle}{\left(\int d^3 \mathbf{r} d\tau |\eta(\mathbf{r}, \tau)|^{5/2} \right)^{4/5}}, \quad U_{\text{ladd},1} = 5^{1/5} A_{\text{ladd}} \quad (27)$$

where $A_{\sharp} := \frac{1}{\pi^2} \left(\frac{4}{5\Gamma(3/4)^8} \right)^{1/5}$. The bosonic η field that minimizes the functional defining A_{diag} is called an instanton in the literature¹⁴.

Let us remark that the Taylor series in equation (24) has a zero radius of convergence as $f_{\text{diag},n} \sim (n!)^{1/5}$. However, the divergence is much milder than the divergence one would have for a bosonic theory, where the order- n typically contributes as $n!$. This behavior is very easy to justify: each diagram contributes with the same sign for bosonic systems, and there are $n!$ of them at order n . However, we cannot apply this argument to fermionic systems, as the diagrams come with different signs.¹⁵

We can interpret this result in terms of Dyson collapse:¹⁶ We turn the phase of our artificial coupling constant z and we look for instabilities for $|z| \rightarrow 0^+$.

effect on the value of $f_{\text{diag},n}$. The mere knowledge of A_{diag} and $U_{\text{diag},1}$ is not enough, one has to compute $U_{\text{diag},k}$ for $k \in \{1, 2, 3, 4\}$ and ϕ_0 , which is very hard to do.

- The correction to this behavior is quite large even for large n (it decays as $O(n^{-1/5})$).
- $\cos(4\pi/5 - \sum_{k=1}^4 U_{\text{diag},k} \sin((5-k)\pi/5) + \phi_0 + O(n^{-1/5}))$ can be zero or very close to zero for some n . For these values of n , other instanton configurations with action $A'_{\text{diag}} > A_{\text{diag}}$ can in principle have a dominant contribution to the value of $f_{\text{diag},n}$.

These problems are not present in ϕ^4 theory, where the large-order behavior calculation was tested numerically.

Given the difficulty to perform numerical checks, we believe that it is important to provide an accurate derivation for this scaling, and this is one of the main objectives of this part of the dissertation.

¹³This is true obviously only when the particular diagrammatic scheme considered is meaningful. See Section 1.3 for a discussion of the meaningfulness of various diagrammatic scheme in the normal phase.

¹⁴Instanton means a field which lasts for an “instant” of imaginary time. In our case the name is probably misleading as we will show that there is no imaginary-time dependence. Even if we think that probably soliton would be a better name in our case, we will use instanton for compatibility with literature on instantons.

¹⁵At high orders, the number of diagrams contributing with positive sign is the same as the number of diagrams contributing with negative sign.

¹⁶Even if the physical interpretation is appealing, we choose not to follow this route for the derivations if alternatives are available. The reason is that one has to analytically continue the functional integral in any direction of the complex plane, while the naive definition works only for phases which are smaller than some angle (in our case $|\arg z| < 2\pi/5$). This analytic continuation can be done in several ways. The simplest one is to add a phase to the modulus

A collapse means an infinite density, so it is natural to apply the Thomas-Fermi approximation, which becomes exact in this limit. This semi-classical approximation for the large-order behavior of fermionic theories was discussed in pioneering works for Yukawa theory [90] and for Quantum Electro-Dynamics [91, 92, 93]. The Thomas-Fermi approximation allows to explicitly perform the integration over fermionic degrees of freedom, leaving us with an effective bosonic theory (in our case for the pairing field). It was first shown for φ^4 theories in [43, 44] that one can make an asymptotically exact computation of the large-order behavior of perturbation theory by performing a saddle point approximation of the bosonic functional integral. The solution of the saddle point equations is called the instanton, which must be localized in space in order to give a finite contribution in the thermodynamic limit. As the collapse happens at the level of the functional integral, it must be shared by every correlation function.

As the Taylor series diverges, we cannot obtain a result to arbitrary precision by simply summing the Taylor series¹⁷. Moreover, the knowledge of the asymptotic behavior of $f_{\text{diag},n}$ (or even the exact knowledge of all the $f_{\text{diag},n}$) is not sufficient to completely determine $f_{\text{diag}}(z)$. For example, one could add functions with zero Taylor series for $z \rightarrow 0^+$

$$e^{-z^{-\rho}} \underset{\text{Taylor}}{=} \sum_{n=0}^{\infty} z^n \cdot 0 \quad (28)$$

with $\rho > 0$. Then, one has $f_{\text{diag}}(z) + e^{-z^{-\rho}} \underset{\text{Taylor}}{=} \sum_{n=0}^{\infty} z^n f_{\text{diag},n}$. The shifted-action construction is essential in order to provide the additional non-perturbative information on the analytic properties of $f_{\text{diag}}(z)$ needed to uniquely recover

of the field (which naively should be always zero), but then one has to assume that the contour can be deformed to pass through saddle points. A more natural analytic continuation uses the so-called Lefschetz thimbles, which are contours of steepest descent where the action is real, so that the integral over a thimble is always well-defined. The singularities of the functional are caused by changes in the choosing of these thimbles. In particular, the discontinuities (i.e. differences in contour choosing) are naturally expressed in terms of integrals over saddle points, where thimbles merge. While being a very effective theory for integral of one or several real or complex variables, its application to functional integrals is, to our knowledge, uncontrolled in most cases, as it is difficult to see how thimbles are chosen. However, for the fully-dressed (i.e. bold) scheme, we are obliged to use these empirical arguments, as we have found the more solid techniques too cumbersome to apply.

¹⁷One should also remark that if the value of A is very large nothing prevents in principle to obtain very good numerical estimates by stopping the Taylor series at order \mathcal{N} (this is the case of Quantum Electro-Dynamics). However, for the unitary Fermi gas the value of A in the strongly correlated regime is not large (for example, for the bold scheme, it goes to zero when approaching the critical temperature). Moreover, in this thesis we discuss only numerically exact diagrammatic methods, which are able to compute quantities with arbitrary numerical precision given enough computer time.

$f_{\text{diag}}(1) = f_{\text{physical}}$ from the diagrammatic coefficients $(f_{\text{diag},n})_{n \in \mathbb{N}}$. The information needed to compute $f_{\text{diag}}(z)$ from the Taylor series is the region in which the function is analytic, and an uniform bound of derivatives in this region. This result follows from a version of the Phragmén-Lindelöf principle: Suppose that $f_{\text{diag}}(z)$ is analytic in the region $W_R^\epsilon := \{z \in \mathbb{C} \mid 0 < |z| < R, |\arg z| < \pi/10 + \epsilon\}$, for some $\epsilon > 0$ and $R > 0$. Suppose that the derivatives of $f_{\text{diag}}(z)$ satisfy the bound for $z \in W$:

$$\left| \frac{1}{n!} \frac{d^n f_{\text{diag}}(z)}{dz^n} \right| \leq C \tilde{A}^{-n} (n/5)! \quad (29)$$

for some $C, \tilde{A} > 0$, and that $f_{\text{diag},n} := \lim_{z \rightarrow 0, z \in W} \frac{1}{n!} \frac{d^n f_{\text{diag}}(z)}{dz^n}$ is well-defined.

Then, these properties uniquely define $f_{\text{diag}}(z)$, in the sense that if a function has the same Taylor expansion and satisfies these properties, then it must coincide with f_{diag} for $z \in W$.¹⁸ We can prove these properties with the shifted-action formalism.

At this point, we know that $f_{\text{diag}}(z)$ is uniquely determined by the sequence $(f_{\text{diag},n})_{n \in \mathbb{N}}$, but how can we reconstruct it from the finite sequence $(f_{\text{diag},n})_{0 \leq n \leq \mathcal{N}}$? A powerful technique is the conformal-Borel method, which uses the information we have gathered so far on $f_{\text{diag}}(z)$ in an “optimal” way. We introduce

$$E(t) := \frac{1}{t} t^{5\delta} \exp\{-t^5 - b_1 t^4 - b_2 t^3\} \quad (30)$$

where $\delta > 0$, $b_1, b_2 \in \mathbb{R}$ are for the moment arbitrary¹⁹. We introduce the (generalized) Borel transform $B_{\text{diag}}(z)$ of $f_{\text{diag}}(z)$ for $|z| < A_{\text{diag}}$ by

$$B_{\text{diag}}(z) := \sum_{n=0}^{\infty} z^n \frac{f_{\text{diag},n}}{\mu_n} \quad (31)$$

where $\mu_n := \int_0^\infty dt E(t) t^n$. One has $\mu_n \underset{n \rightarrow \infty}{=} (n/5)! e^{-b_1(n/5)^{4/5} + O(n^{3/5})}$. At this point, a version of Ramis’s theorem (which we re-derived independently, see Appendix N), allows us to recover $f_{\text{diag}}(z)$ by the inverse Borel transformation:

¹⁸It is interesting to see how these assumptions fail for the function $e^{-z^{-\rho}}$. For $\rho \geq 5$, the function is unbounded in $z \in W$ and the derivative bounds cannot be satisfied already at order 0. For $0 < \rho < 5$, the function and the derivatives are bounded, but they do not satisfy the $(n/5)!$ bound. Indeed for $z = x > 0$, one has $\frac{d^n f(x)}{dx^n} \underset{x \rightarrow 0^+}{=} e^{-x^{-\rho}} (\rho^n / x^{(\rho+1)n} (1 + O(x^\rho)))$. If we evaluate this expression for $x = ((1 + 1/\rho)n)^{-1/\rho}$, one has $\frac{d^n f(x)}{dx^n} \sim (n!)^{1+1/\rho}$, an expression that cannot be bound by $(n!)^{1+1/5}$.

¹⁹In practical computations, we fix $\delta = 1$ for definiteness, b_1 is constrained by a consistency condition (see footnote 20), and b_2 is a free parameter that we use to improve numerical convergence.

1. $B_{\text{diag}}(z)$ can be analytically continued in a neighborhood of the positive real axis.
2. The expression

$$f_{\text{diag}}^{(B)}(z) := \int_0^\infty dt E(t) B_{\text{diag}}(zt) \quad (32)$$

is well-defined for $0 \leq z < R'$, $R' > 0$, and in this region one has

$$f_{\text{diag}}^{(B)}(z) = f_{\text{diag}}(z) \quad (33)$$

The last point we need to discuss is how to achieve in practice point 1: the analytic continuation of $B_{\text{diag}}(z)$. A very powerful way to do this is by using a conformal mapping, assuming that we know the position of the singularities of $B_{\text{diag}}(z)$ in the complex plane. From the large-order behavior (26) we see that $B_{\text{diag}}(z)$ is analytic for $|z| < A_{\text{diag}}$, and it has singularities at $z = A_{\text{diag}} e^{\pm 4\pi i/5}$. We know that $B_{\text{diag}}(z)$ is analytic in a neighborhood of the positive real axis. At this point we *assume* that $B_{\text{diag}}(z)$ can be analytically continued everywhere in the complex plane, except in $\mathcal{C} := \{z \in \mathbb{C} \mid |z| \geq A_{\text{diag}}, |\arg z| = 4\pi/5\}$. This assumption is internally consistent only if a condition on b_1 is satisfied.²⁰

Let \mathcal{D} be the open unit disc, and let $h : \mathcal{D} \rightarrow \mathbb{C} \setminus \mathcal{C}$ be an holomorphic function (in other words, a conformal mapping) such that

- h is one-to-one.
- $h(0) = 0$
- $h(w)^* = h(w^*)$

Then, h is completely determined.²¹ We introduce for all $w \in \mathcal{D}$ such that $|h(w)| < A_{\text{diag}}$, the Borel transform in the w variable:

$$\tilde{B}_{\text{diag}}(w) := B_{\text{diag}}(h(w)) \quad (34)$$

But $\tilde{B}_{\text{diag}}(w)$ can be analytically extended in $w \in \mathcal{D}$ as it has no singularities in the open unit disc. Moreover, the explicit analytic continuation is given by its Taylor series

$$\tilde{B}_{\text{diag}}(w) = \sum_{n=0}^{\infty} w^n \tilde{B}_{\text{diag},n}, \quad |w| < 1 \quad (35)$$

²⁰The condition is $|\theta_B(b_1)| < \pi/5$, where $\theta_B(b_1) := \arg[\exp(i\pi/5)U_1 - b_1/5^{4/5}]$, see Appendix O for the derivation.

²¹The explicit expression is $h(w) = \frac{4\nu^\nu(1-\nu)^{1-\nu}A_{\text{diag}}w}{(1+w)^{2(1-\nu)}(1-w)^{2\nu}}$ evaluated for $\nu = 4/5$.

From this, we can obtain an explicit analytic continuation of $B_{\text{diag}}(z)$ for $z \in \mathbb{C} \setminus \mathcal{C}$ by

$$B_{\text{diag}}(z) := \sum_{n=0}^{\infty} (h^{-1}(z))^n \tilde{B}_{\text{diag},n} \quad (36)$$

The first \mathcal{N} coefficients of the Taylor expansion of \tilde{B}_{diag} , $(\tilde{B}_{\text{diag},n})_{n=0}^{\mathcal{N}}$, are linearly related to $(f_{\text{diag},n})_{n=0}^{\mathcal{N}}$. If we then further assume that $f(z)$ can be analytically continued for $0 < z < R''$, $R'' > 1$, we can compute f_{physical} from

$$\begin{aligned} f_{\text{physical}} &= f_{\text{diag}}(1) = f_{\text{diag}}^{(B)}(1) = \int_0^1 dw h'(w) E(h(w)) \lim_{\mathcal{N} \rightarrow \infty} \sum_{n=0}^{\mathcal{N}} w^n \tilde{B}_{\text{diag},n} = \\ &= \lim_{\mathcal{N} \rightarrow \infty} \sum_{n=0}^{\mathcal{N}} f_{\text{diag},n} \mathcal{B}_n^{(\mathcal{N})} \end{aligned} \quad (37)$$

The error which results from the truncation of the procedure at order \mathcal{N} is (nearly) exponentially small $O(\exp[-(1.56\dots)A_{\text{diag}}^{1/9} \mathcal{N}^{8/9}])$.

This concludes the summary of our mathematical construction. Numerical results are discussed in Section 6.

3 Large-order behavior for the pressure in the ladder scheme

3.1 Shifted action for the ladder scheme

We consider the diagrammatic expansion for the pressure for definiteness, whose physical value is p_{physical} . We introduce a function $p_{\text{ladd}}[\Gamma_0, z]$ such that

1. The Taylor expansion in the complex parameter z gives us the diagrammatic expansion

$$p_{\text{ladd}}[\Gamma_0, z] \stackrel{\text{Taylor}}{=} \sum_{n=0}^{\infty} z^n p_{\text{ladd},n}[\Gamma_0] \quad (38)$$

where $p_{\text{ladd},n}[\Gamma_0]$ is the order- n diagrammatic contribution of the ladder expansion.

2. The function evaluated at $z = 1$ gives us back the physical answer

$$p_{\text{ladd}}[\Gamma_0, z = 1] = p_{\text{physical}} \quad (39)$$

It is clear that the function $p_{\text{ladd}}[\Gamma_0, z]$ must be defined in a non-perturbative way, we cannot rely on the Taylor series as it could have (and it has as we will see) a zero radius of convergence. This non-perturbative definition is provided by a shifted action $S_{\text{ladd}}^{(z)}$ [87]. For the pressure, we write

$$p_{\text{ladd}}[\Gamma_0, z] := \lim_{\nu \rightarrow \infty} \frac{1}{\beta \mathcal{V}} \log \int \mathcal{D}[\varphi, \bar{\varphi}, \eta, \bar{\eta}] e^{-S_{\text{ladd}}^{(z)}} \quad (40)$$

where one imposes by construction

$$S_{\text{ladd}}^{(z=1)} = S_{\text{physical}} \quad (41)$$

For the ladder scheme, it can be shown that in our case one has (see Appendix A):

(Shifted action for the ladder scheme):

$$S_{\text{ladd}}^{(z)} = -\langle \varphi | G_0^{-1} | \varphi \rangle - \langle \eta | \Gamma_0^{-1} | \eta \rangle - z \langle \eta | \Pi_{\text{bubble}} | \eta \rangle + \sqrt{z} (\langle \eta | \varphi_{\downarrow} \varphi_{\uparrow} \rangle + \langle \varphi_{\downarrow} \varphi_{\uparrow} | \eta \rangle). \quad (42)$$

where $\varphi, \bar{\varphi}$ are spin-1/2 fields, $\eta, \bar{\eta}$ is a complex field, and $z \in \mathbb{C}$.

We had defined Γ_0 and Π_{bubble} in Equations (13) and (14).

We can use this action to define z -dependent correlation functions. For example, for the Green's function G , one has

$$G_{\text{ladd}}[\Gamma_0, z](\mathbf{r}, \tau) = - \frac{\int \mathcal{D}[\varphi, \bar{\varphi}, \eta, \bar{\eta}] e^{-S_{\text{ladd}}^{(z)}} \varphi_{\uparrow}(\mathbf{r}, \tau) \bar{\varphi}_{\uparrow}(\mathbf{0}, 0)}{\int \mathcal{D}[\varphi, \bar{\varphi}, \eta, \bar{\eta}] e^{-S_{\text{ladd}}^{(z)}}} \quad (43)$$

A Taylor expansion of G_{ladd} in z is equivalent to the ladder diagrammatic expansion:

$$G_{\text{ladd}}[\Gamma_0, z] \underset{\text{Taylor}}{=} \sum_{n=0}^{\infty} z^n G_{\text{ladd},n}[\Gamma_0] \quad (44)$$

where $G_{\text{ladd},n}[\Gamma_0]$ is the order- n contribution of the ladder expansion built with Γ_0 . From Equation (41), one has moreover that $G_{\text{ladd}}[\Gamma_0, z=1] = G_{\text{physical}}$. Let us finally remark that we can apply the same construction to every correlation function.

3.2 Obtaining the large-order behavior for the pressure from the partition function

We know that $S_{\text{ladd}}^{(z)}$ is not well-defined in the continuum limit ($\langle \eta | \Pi_{\text{bubble}} | \eta \rangle$ diverges in this limit). Thus we cannot take the continuum limit where the

lattice spacing b goes to zero at this stage. We also work for the moment at large (but finite) volume \mathcal{V} . We consider the normalized partition function

$$\tilde{Z}_{\text{ladd}}(\mathcal{V}, z) := \frac{\int \mathcal{D}[\eta, \bar{\eta}, \varphi, \bar{\varphi}] e^{-S_{\text{ladd}}^{(z)}[\varphi, \bar{\varphi}, \eta, \bar{\eta}]}}{\int \mathcal{D}[\eta, \bar{\eta}, \varphi, \bar{\varphi}] e^{-S_{\text{ladd}}^{(0)}[\varphi, \bar{\varphi}, \eta, \bar{\eta}]}} \quad (45)$$

(the denominator is just a z -independent number). One has

$$p_{\text{ladd}}(z) = p_{\text{ladd}}(0) + \lim_{\mathcal{V} \rightarrow \infty} \frac{1}{\beta \mathcal{V}} \ln \tilde{Z}_{\text{ladd}}(\mathcal{V}, z) \quad (46)$$

We expand the partition function in a formal power series in z , which is built from Feynman diagrams built from bare propagators G_0 and Γ_0 with no ($G_0 G_0$) bubble diagrams

$$\tilde{Z}_{\text{ladd}}(\mathcal{V}, z) \underset{\text{Taylor}}{=} 1 + \sum_{n=1}^{\infty} \tilde{Z}_{\text{ladd},n}(\mathcal{V}) z^n \quad (47)$$

We would like to deduce the large- n behavior of $p_{\text{ladd},n}$ from the large-order behavior of $\tilde{Z}_{\text{ladd},n}(\mathcal{V})$. $\tilde{Z}_{\text{ladd},n}(\mathcal{V})$ can be decomposed in contributions coming from disconnected parts:

$$\tilde{Z}_{\text{ladd},n}(\mathcal{V}) = \sum_{\mathcal{C}=1}^n \tilde{Z}_{\text{ladd},n,\mathcal{C}}(\mathcal{V}) \quad (48)$$

where $Z_{\text{ladd},n,\mathcal{C}}(\mathcal{V})$ is the contribution of all Feynman diagrams contributing to the order n ladd partition function which can be divided in \mathcal{C} connected parts. One has

$$\frac{\tilde{Z}_{\text{ladd},n,\mathcal{C}}(\mathcal{V})}{\mathcal{V}^{\mathcal{C}}} \underset{\mathcal{V} \rightarrow \infty}{=} \tilde{z}_{\text{ladd},n,\mathcal{C}} + O(e^{-\lambda \mathcal{V}^\alpha}) \quad (49)$$

for some positive λ , α and $\tilde{z}_{\text{ladd},n,\mathcal{C}}$.²²

The linked-cluster theorem implies that

$$p_{\text{ladd},n} = \tilde{z}_{\text{ladd},n,1} \quad (50)$$

therefore, we only need to compute $\tilde{z}_{\text{ladd},n,1}$. The strategy then it is very simple: we compute the term of $\tilde{Z}_{\text{ladd},n}(\mathcal{V})$ linear in \mathcal{V} , this will be proportional to the contribution for the pressure. More precisely:

²²We sketch here the proof of this simple fact. The factor $\mathcal{V}^{\mathcal{C}}$ is simply due to the integration over the positions of the connected parts. The fermionic propagator G_0 goes to zero always exponentially at large distance, the same is true for the bosonic propagator Γ_0 if the ladder series is meaningful (that is, for temperatures higher than T^* , see Figure 1 and the discussion of Section 1.3). Therefore, the contribution of a connected part at finite volume differs from the contribution at infinite volume by an exponentially small contribution of the order of $e^{-\lambda \mathcal{V}^{1/3}}$.

Suppose that there exists a \tilde{p}_n (which is not a function of volume \mathcal{V} and lattice spacing b) such that

$$\lim_{\mathcal{V} \rightarrow \infty} \lim_{n \rightarrow \infty} \lim_{b \rightarrow 0^+} \frac{\tilde{Z}_{\text{ladd},n}(\mathcal{V})}{\beta \mathcal{V} \tilde{p}_n} = 1 \quad (51)$$

Then, one has $\lim_{n \rightarrow \infty} \frac{\tilde{p}_n}{p_{\text{ladd},n}} = 1$.

This is shown in Appendix B.

Now, Equation (51) tells us that we have to first take the continuum limit where the lattice spacing b goes to zero. Then, we will compute the large-order behavior of the perturbative expansion at finite (but very large) volume \mathcal{V} . Only at the end we will take the thermodynamic limit $\mathcal{V} \rightarrow \infty$. The limit can exist only if $|\tilde{z}_{\text{ladd},n,1}|$ goes to infinity with n faster than any exponential of n (we will see that this is the case), otherwise the terms $\tilde{z}_{\text{ladd},n,\mathcal{C}}$ where \mathcal{C} is of order n will dominate because they increase exponentially fast with volume and \mathcal{C} .

3.3 Integration over fermions

One of the main advantages of the functional integral method is the possibility to perform generalized semi-classical (or saddle-point) calculations. Unfortunately, this is not possible for Grassmann integrals. For this reason, we would like to integrate them out to obtain a purely bosonic effective action. Accordingly, we perform the functional integration over the fermions in \tilde{Z} in (45) to obtain:

$$\tilde{Z}_{\text{ladd}}(\mathcal{V}, z) = \frac{\int \mathcal{D}[\eta, \bar{\eta}] e^{\langle \eta | \Gamma_0^{-1} | \eta \rangle + z \langle \eta | \Pi_{\text{bubble}}[G_0] | \eta \rangle} \det(\mathbb{1} + \sqrt{z} \hat{\Upsilon})}{\int \mathcal{D}[\eta, \bar{\eta}] e^{\langle \eta | \Gamma_0^{-1} | \eta \rangle}} \quad (52)$$

where we have defined:

$$\hat{\Upsilon} := \begin{pmatrix} 0 & \hat{G}_0 \hat{\eta} \\ -\hat{G}_0^\dagger \hat{\eta}^\dagger & 0 \end{pmatrix} \quad (53)$$

The determinant, at non-zero lattice spacing, is an entire function of order 1 (the terms in \sqrt{z}^{2n+1} gives zero contribution, see Appendix C). However, the determinant is divergent in the continuum limit, as shown in Equation (C.17). Luckily, the Π_{bubble} term is here exactly to compensate this divergence and to leave us with a finite answer:

(Renormalized determinant): The expression

$$\det_4(\mathbb{1} + \sqrt{z}\hat{\Upsilon}) := e^{z\langle\eta|\Pi_{\text{bubble}}[G_0]|\eta\rangle} \det(\mathbb{1} + \sqrt{z}\hat{\Upsilon}) \quad (54)$$

is well defined in the continuum limit $b \rightarrow 0^+$.

The proof of this result is presented in Appendix C. Moreover, one can show that the renormalized determinant \det_4 is an entire function (see Appendix C):

(\det_4 is entire): If $\int_{\mathbb{R}^3} d^3\mathbf{r} \int_0^\beta d\tau |\eta(\mathbf{r}, \tau)|^4 < \infty$, then $\det_4(\mathbb{1} + \sqrt{z}\hat{\Upsilon})$ is an entire function of z .

We study the large z behavior of \det_4 , which can be computed with a Thomas-Fermi (or quasi-local) approximation (see Appendix D):

(Thomas-Fermi asymptotics): For $|\arg z| < \pi$, one has

$$\det_4(\mathbb{1} + \sqrt{z}\hat{\Upsilon}) \underset{|z| \rightarrow \infty}{=} \exp\left(-g_{TF} z^{5/4} \int dX |\eta(X)|^{5/2} + O(z)\right) \quad (55)$$

where $g_{TF} > 0$.

We see therefore that \det_4 is an entire function of order $5/4$. From this we can deduce a first important consequence. If we write

$$\tilde{Z}_{\text{ladd}}(\mathcal{V}, z) = \frac{\int \mathcal{D}[\eta, \bar{\eta}] e^{\langle\eta|\Gamma_0^{-1}|\eta\rangle} \det_4(\mathbb{1} + \sqrt{z}\hat{\Upsilon})}{\int \mathcal{D}[\eta, \bar{\eta}] e^{\langle\eta|\Gamma_0^{-1}|\eta\rangle}} \quad (56)$$

we see that \tilde{Z} is the integral of an entire functional of η . For a finite range of integration, this function cannot have singularities. However, the range of the integration over the η field is unbounded, so convergence problems can be present. From the large η behavior of \det_4 (55), we see that the integral is absolutely convergent for

$$|\arg z| < \frac{2\pi}{5} \quad (57)$$

This means that \tilde{Z} is an analytic function of z in this region. When we take the logarithm to compute the pressure $p_{\text{ladd}}(z)$, we see that (apart from possible phase transitions given by zeros of \tilde{Z}), $p_{\text{ladd}}(z)$ will be an analytic function in the same domain. We are therefore led to the following *conjecture*

(Analyticity domain): There exists $R > 0$ such that $p_{\text{ladd}}(z)$ is analytic for $0 < |z| < R$, $|\arg z| < 2\pi/5$,

3.4 Saddle point for the large-order behavior of the determinant

We have seen that the continuum limit $b \rightarrow 0^+$ can be taken safely. Let us now turn to the next limit, that is, the large- n behavior of $\tilde{Z}_{\text{ladd},n}(\mathcal{V})$, for a very large but finite volume \mathcal{V} .

For every $z \in \mathbb{C}$, we can write

$$\det_4(1 + \sqrt{z}\hat{\Upsilon}) = \sum_{n=0}^{\infty} q_n[\eta, \bar{\eta}] z^n \quad (58)$$

so that

$$\tilde{Z}_{\text{ladd},n}(\mathcal{V}) = \langle q_n[\eta, \bar{\eta}] \rangle_{\Gamma_0} \quad (59)$$

where we have introduced a shorthand notation for the Gaussian functional integral mean over the field η :

$$\langle \cdot \rangle_{\Gamma_0} := \frac{\int \mathcal{D}[\eta, \bar{\eta}] e^{\langle \eta | \Gamma_0^{-1} | \eta \rangle}}{\int \mathcal{D}[\eta, \bar{\eta}] e^{\langle \eta | \Gamma_0^{-1} | \eta \rangle}} \quad (60)$$

The next step is the computation of $q_n[\eta, \bar{\eta}]$. We can write the Cauchy integral formula for \det_4 :

$$q_n[\eta, \bar{\eta}] = \oint_{\mathcal{C}_0} \frac{dz}{2\pi i} \frac{\det_4(\mathbb{1} + \sqrt{z}\hat{\Upsilon})}{z^{n+1}} =: \oint_{\mathcal{C}_0} \frac{dz}{2\pi i} e^{-S_{4,n}(z)} \quad (61)$$

We know that, in general, the large- n behavior is determined by the singularities of the function nearest to the origin. But \det_4 is an entire function, and the only singularities of an entire function are at $|z| = \infty$. Therefore, we expect that only the behavior for $|z| \rightarrow \infty$ can be relevant in the large- n limit.

Following this intuition, we deform the contour to values of z of order $n^{4/5}$ (there are no constraints on the integration contour as the integrand is entire).

Indeed, we find that our intuition is correct as there are two saddle points at:²³

$$z = z_c^\pm := \frac{e^{\pm 4\pi i/5}}{\left(\frac{5}{4}g_{TF} \int |\eta|^{5/2}\right)^{4/5}} n^{4/5} + O(n^{3/5}) \quad (62)$$

One has

$$\operatorname{Re} S_{4,n}(z_c^\pm) = \frac{4n}{5} \log \frac{n}{e} - \frac{4n}{5} \log \left(\frac{5}{4} g_{TF} \int |\eta|^{5/2} \right) + O(n^{4/5}) \quad (63)$$

$$\operatorname{Im} S_{4,n}(z_c^\pm) = \pm \frac{4\pi n}{5} + O(n^{4/5}) \quad (64)$$

so that

$$q_n[\eta, \bar{\eta}] \underset{n \rightarrow \infty}{\sim} (n!)^{-4/5} \left(\frac{5}{4} g_{TF} \int |\eta|^{5/2} \right)^{\frac{4n}{5}} \operatorname{Re} \exp \left(\frac{4\pi i n}{5} + O(n^{4/5}) \right) \quad (65)$$

3.5 Functional integration in the large- n limit

We now compute $\tilde{Z}_{\text{ladd},n}$ by performing the functional integration over the bosonic η field. At leading order²⁴, we have to compute

$$I_n := \left\langle \left(\int dX |\eta(X)|^{5/2} \right)^{4n/5} \right\rangle_{\Gamma_0} \quad (66)$$

This integral is somewhat similar to the integral $\int_0^\infty dx e^{-x^2} x^{2n} \sim n!$, which can be computed by Laplace's method for large n by expanding around $x = \sqrt{n}$.²⁵

²³ In this text, we only discuss the computation at leading order for simplicity. The computation of the first correction is straightforward, while the sub-leading terms are increasingly hard to obtain. However, we will see that all the information we need is contained in the leading term (the A^{-n} term in the asymptotic behavior). The first correction (the $\exp\{U_1 e^{4\pi i/5} n^{4/5}\}$ term) gives a (non-trivial) constraint on the parameter b_1 of the Borel transform (see Appendix O). All the sub-leading corrections (which would be $\exp\{U_k e^{(5-k)i\pi/5} n^{(5-k)/5}\}$ for $k \geq 2$) are irrelevant, their knowledge cannot be used in the numerical algorithm, and accordingly we did not compute them.

²⁴ See footnote 23.

²⁵ This is one of the main advantages of using this direct technique compared to the alternative methods, which use an analytic continuation of the functional integral and saddle points in the fields η and $\bar{\eta}$ (and z in some case). In our case, we only need to apply Laplace's method, which clearly works even for functional integrals.

Inspired by this, we write an effective action for the functional integration defining I_n :

$$S_{\text{eff},n}[\eta, \bar{\eta}] := -\langle \eta | \Gamma_0^{-1} | \eta \rangle - \frac{4n}{5} \log \int dX |\eta(X)|^{5/2} \quad (67)$$

We re-scale the η field $\eta(X) = \sqrt{n} \lambda(X)$ to obtain

(Effective action for large- n):

$$S_{\text{eff},n}[\eta, \bar{\eta}] = n s_{\text{eff}}[\lambda, \bar{\lambda}] - n \log n \quad (68)$$

where

$$s_{\text{eff}}[\lambda, \bar{\lambda}] := -\langle \lambda | \Gamma_0^{-1} | \lambda \rangle - \frac{4}{5} \log \int dX |\lambda(X)|^{5/2} \quad (69)$$

We see therefore that we have the canonical form needed for the application of the Laplace method. We do not need to turn the contour of integration for λ and $\bar{\lambda}$ in the complex plane (we look for Laplace points, if they exist we can apply Laplace's method). Therefore, we have $(\bar{\lambda}_c)^* = \lambda_c$. We need to minimize the action s_{eff} :

$$\frac{\delta s_{\text{eff}}[\lambda_c, \lambda_c^*]}{\delta \lambda_R(\mathbf{r}, \tau)} = 0, \quad \frac{\delta s_{\text{eff}}[\lambda_c, \lambda_c^*]}{\delta \lambda_I(\mathbf{r}, \tau)} = 0 \quad (70)$$

where $\lambda = \lambda_R + i\lambda_I$. In Appendix E, we show that

(No imaginary-time dependence): For $\mathbf{r} \in \mathbb{R}^3$ and $\tau \in [0, \beta]$, one has

$$\lambda_c(\mathbf{r}, \tau) = \lambda_c(\mathbf{r}) \quad (71)$$

if for every $\mathbf{p} \in \mathbb{R}^3$ and $p_4 \in 2\pi\mathbb{Z}/\beta$, $p_4 \neq 0$, one has

$$\text{Im } \Gamma_0^{-1}(\mathbf{p}, p_4) \neq 0 \quad (72)$$

We assume from now on that the previous condition is verified. Therefore, $\lambda_c(\mathbf{r})$ is a time-independent ‘‘instanton’’ (instanton means a classical solution of the classical equations that lasts for ‘‘an instant’’ of time). It is important to underline that the previous condition is only a sufficient condition to affirm that λ_c is a static-instanton and not a proper instanton.

It is useful at this point to introduce the operator R_0^{-1} , that is the operator $-\Gamma_{0,R}^{-1}$ restricted to act on time-independent fields. In momentum space

$$R_0^{-1}(\mathbf{p}) := -\Gamma_{0,R}^{-1}(\mathbf{p}, p_4 = 0) \quad (73)$$

We define for a spatial field $\lambda(\mathbf{r}) \in \mathbb{C}$, $\mathbf{r} \in \mathbb{R}^3$, an “action” functional $A_S[\lambda] \in \mathbb{R}$

$$A_S[\lambda] := \frac{\langle \lambda | R_0^{-1} | \lambda \rangle}{\left(\int d^3\mathbf{r} |\lambda(\mathbf{r})|^{5/2} \right)^{4/5}} \quad (74)$$

It is possible to prove that the action functional is strictly positive (see Appendix (F)) and has an absolute minimum:

$$A_S := \min_{\lambda} A_S[\lambda] > 0 \quad (75)$$

The action functional goes to infinity in the low-density limit, and it is zero at the pair-forming temperature T^* :

$$\lim_{\beta\mu \rightarrow -\infty} A_S = \infty. \quad \lim_{T \downarrow T^*} A_S = 0 \quad (76)$$

as it is proved in Appendix H. This means that perturbation theory becomes essentially “convergent” at high temperature, and that it is very difficult to sum the ladder expansion (which is an expansion in powers of Γ_0) when we approach the (pseudo) critical point T^* where Γ_0 has a pole. We now present a variational principle (proved in Appendix G) which is very useful for numerical computations (see Appendix V for a discussion of the numerical calculation):

(Variational principle): The Laplace point solution $\lambda_c = \lambda_c(\mathbf{r})$ is a minimum of the action functional (74)

$$\lambda_c \in \operatorname{argmin} A_S[\lambda] \quad (77)$$

(the minima of the functional are related by $\lambda_c(\mathbf{r}) \mapsto w \lambda_c(R\mathbf{r} + \mathbf{r}_0)$, $w \in \mathbb{C} \setminus \{0\}$, $\mathbf{r}_0 \in \mathbb{R}^3$, and R is a rotation matrix)

The following result is fundamental for the numerical computation of the instanton (see Appendix I for the proof)

(Properties of the solution): The action functional A_S is minimized by a real radially symmetric field ($\lambda_c(\mathbf{r}) \in \mathbb{R}$, $\lambda_c(\mathbf{r}) = \lambda_c(\mathbf{r}')$ if $|\mathbf{r}| = |\mathbf{r}'|$) if $u(|\mathbf{r}|) := R_0^{1/2}(\mathbf{r}) > 0$ and $u'(r) < 0$.

We have seen therefore that we can find a Laplace point instanton $\eta_c = \sqrt{n} \lambda_c$ to compute the functional integral over η and $\bar{\eta}$ in the large- n limit. We can expand the effective action $S_{\text{eff},n}$ around one of the instanton solutions $\eta = \sqrt{n} \lambda_c + v$, and we divide the fluctuations in real and imaginary part $v = v_R + i v_I$:

$$S_{\text{eff},n}[\eta, \bar{\eta}] = -n \log n + n s_c + (v_R \ v_I) S_{\text{eff},2}[\eta_c, \bar{\eta}_c] \begin{pmatrix} v_R \\ v_I \end{pmatrix} + O(v^3) \quad (78)$$

where

$$s_c := s[\lambda_c, \bar{\lambda}_c] = 1 + \log \left(\beta^{\frac{1}{5}} A_S \right) \quad (79)$$

At this point, we would like to perform the Gaussian integral over v to get the contribution at leading order. However, the matrix $S_{\text{eff},2}$ has zero modes,

$$S_{\text{eff},2} \begin{pmatrix} v_R^{(0)} \\ v_I^{(0)} \end{pmatrix} = 0, \text{ hence the Gaussian approximation for these modes does}$$

not work [45, 94]. This is related to the fact that the instanton λ_c breaks symmetries of the action, namely translation invariance and multiplication of the field λ by a complex number of unit modulus. Explicitly, one has that for every θ and \mathbf{r}_0 , $e^{i\theta} \lambda_c(\mathbf{r} + \mathbf{r}_0)$ minimizes the action functional, the action does not vary along these directions. We need to integrate over θ and \mathbf{r}_0 exactly, and then perform the Gaussian integral for the non-zero modes that we call collectively v . One can show (see Appendix J) that

$$\mathcal{D}[\eta, \bar{\eta}] \propto d\theta d^3 \mathbf{r}_0 \mathcal{D}[v', \bar{v}'] \quad (80)$$

where v' are fluctuations orthogonal to the change of θ and \mathbf{r}_0 . We are disregarding here n^γ multiplicative corrections, at this order of approximation they are sub-leading as we are already disregarding terms of order $O(e^{\# n^{k/5}})$ with $k \in \{1, 2, 3, 4\}$. The integration over θ gives a constant, while the integration over \mathbf{r}_0 gives a volume factor \mathcal{V} . It remains therefore the Gaussian integration

$$\frac{\int \mathcal{D}[v, \bar{v}] \exp \left\{ -(v_R \ v_I) S_{\text{eff},2}[\eta_c, \bar{\eta}_c] \begin{pmatrix} v_R \\ v_I \end{pmatrix} \right\}}{\int \mathcal{D}[\eta, \bar{\eta}] e^{\langle \eta | \Gamma_0^{-1} | \eta \rangle}} = \frac{\det' S_{\text{eff},2}^{-1/2}}{\det(-\Gamma_0)} \quad (81)$$

where $v_R(\mathbf{r}, r_4) := \text{Re } v(\mathbf{r}, r_4)$, $v_I(\mathbf{r}, r_4) := \text{Im } v(\mathbf{r}, r_4)$. \det' is defined as the determinant computed in the space orthogonal to the zero modes (otherwise, it is trivially zero). One might think that the ratio of the determinants increases exponentially with the volume, as it is the ratio of two partition functions. However, loosely speaking, the operators $S_{\text{eff},2}$ and Γ_0^{-1} differ only in a finite region of space because λ_c decays exponentially fast. In Appendix K we prove that this

ratio has a finite thermodynamic limit, and it is independent of n . In the end, at leading order, we can write for $n \rightarrow \infty$

$$I_n = \left\langle \left(\int_{\Gamma_0} d\mathbf{r}, \tau |\eta(\mathbf{r}, \tau)|^{5/2} \right)^{4n/5} \right\rangle \propto \mathcal{V} n! (\beta^{1/5} A_S)^{-n} \quad (82)$$

Using equations (59),(65), one has for $n \rightarrow \infty$

$$\tilde{Z}_{\text{ladd},n}(\mathcal{V}) \underset{n \rightarrow \infty}{=} \mathcal{V} (n!)^{1/5} \left(\frac{4^{4/5} \beta^{1/5} A_S}{(5g_{TF})^{4/5}} \right)^{-n} \left(\text{Re} e^{\frac{4\pi i n}{5} + O(n^{4/5})} + O((A_S/A')^N) \right) \quad (83)$$

where $A' > A_S$ is a (possible) contribution from a local minima of the effective action. Using Equation (51), we arrive at

(Large-order asymptotic behavior):

$$p_{\text{ladd},n} \underset{n \rightarrow \infty}{=} (n/5)! A_{\text{ladd}}^{-n} \text{Re} e^{\frac{4\pi i n}{5} + O(n^{4/5})} \quad (84)$$

$$\text{and } A_{\text{ladd}} := \frac{4^{4/5} \beta^{1/5} A_S}{5g_{TF}^{4/5}}.$$

4 Analytic reconstruction by conformal-Borel transform

4.1 Unicity of Taylor coefficients

We can write a bound on the derivatives for $|\arg w| < 3\pi/10$ (see Appendix L)

$$\left| \frac{1}{n!} \frac{d^n}{dz^n} p_{\text{ladd}}(z) \right| \leq C_B \tilde{A}^{-n} (n/5)! \quad (85)$$

for every $\tilde{A} > A_{\text{ladd}}$. The fundamental result that will allow to reconstruct $p_{\text{ladd}}(z)$ from its diagrammatic series is the following unicity theorem:

(Unicity of Taylor coefficients): Let $f(z)$ be an analytic function in $W_R^\epsilon := \{z \in \mathbb{C} \mid 0 < |z| < R, |\arg z| < \pi/10 + \epsilon\}$, for some $R > 0$ and $\epsilon > 0$. Suppose that f is infinitely derivable in the origin

$$f_n := \lim_{z \rightarrow 0, z \in W_R^\epsilon} \frac{1}{n!} \frac{d^n}{dz^n} f(z) \quad (86)$$

and for $z \in W_R^\epsilon$

$$\left| \frac{1}{n!} \frac{d^n}{dz^n} f(z) \right| \leq C_B A^{-n} (n/5)! \quad (87)$$

Suppose that $g(z)$ satisfies the same conditions as $f(z)$. Then, $g(z) = f(z)$ for $z \in W_R^\epsilon$.

This theorem is proved in Appendix M.

4.2 Borel summability and conformal mapping

As we have seen $p_{\text{ladd}}(z)$ is analytic in W_R^ϵ , and it satisfies the bound (85), so it is completely determined by the asymptotic series according to the theorem of the previous section. It turns out that the Borel transform is a way to reconstruct this analytic function from the Taylor coefficients:²⁶

(Borel summability): Under the conditions (86) and (87) on $f(z)$, we introduce the Borel transform of f for $|z| < A$ as

$$B(z) := \sum_{n=0}^{\infty} \frac{f_n}{\Gamma(n/5 + 1)} \quad (88)$$

Then, $B(z)$ can be continued to a neighborhood of the positive real axis, and we have for $0 \leq x < R$

$$f(x) = 5 \int_0^\infty \frac{dt}{t} t^5 e^{-t^5} B(xt) \quad (89)$$

This result is a generalization of Watson's theorem [95], due to Ramis [96]. We have derived it in a slightly different form, see Appendix N for a proof. We see therefore that if $R > 1$, we can compute $f(1)$ (which is the physical result)

²⁶In the enunciation of the theorem, for simplicity, the parameters b_1 and b_2 of the Borel transform are set to zero and the parameter δ is set to one.

with the Borel technique by only knowing the coefficients of the diagrammatic expansion.

We introduce the (slightly more general) Borel transform of p_{ladd} , for $|z| < A_{\text{ladd}}$ we write

$$B_{\text{ladd}}(z) := \sum_{n=0}^{\infty} \frac{p_{\text{ladd},n}}{\mu_n} z^n \quad (90)$$

where

$$\mu_n(b_1, b_2, \delta) := \int_0^{\infty} dt E(t) t^n \quad (91)$$

and $^{27}E(t) := t^{5\delta-1} \exp\{-t^5 - b_1 t^4 - b_2 t^3\}$. From the large-order behavior of $p_{\text{ladd},n}$, we see that $B(z)$ has essential singularities at $z = e^{\pm \frac{4\pi i}{5}} A_{\text{ladd}}$. Sub-leading Laplace points (configurations with action A') will give singularities for $z = e^{\pm \frac{4\pi i}{5}} A'$, with $A' > A_{\text{ladd}}$. We are therefore led to the following *conjecture*

(Maximal analytic extension): There exists an analytic continuation of $B_{\text{ladd}}(z)$ in $\mathbb{C} \setminus \mathcal{C}_{A_{\text{ladd}}}$, where $\mathcal{C}_A := \{z \in \mathbb{C} \mid |\arg z| = 4\pi/5, |z| \geq A\}$ if $|\theta_B(b_1)| < \pi/5$, where $\theta_B(b_1) := \arg[\exp(i\pi/5)U_{\text{ladd},1} - b_1/5^{4/5}]$.

The necessity of the condition on b_1 is proved in Appendix O, but we want to stress that it is not clear that this condition is also sufficient.

Let us remark that if $U_1 \neq 0$, one has to use a non-zero b_1 .

We now explicitly construct this analytic continuation. The strategy is very simple. We will provide an invertible conformal map $h = h(w)$ that maps the the unitary disk $\mathcal{D} := \{w \in \mathbb{C} \mid |w| < 1\}$ onto the set $\mathbb{C} \setminus \mathcal{C}_A$. We require also that the origin is mapped into the origin ($z(0) = 0$). This has to be required to ensure that the expansion for $z \rightarrow 0$ is equivalent to the expansion for $w \rightarrow 0$. The last requirement is that this map must be real $h(w^*)^* = h(w)$. It turns out that there exists a unique conformal map with these properties (see Appendix P):

²⁷From the large- n behavior of $\mu_n \underset{n \rightarrow \infty}{=} (n/5)! e^{-b_1(n/5)^{4/5} + O(n^{3/5})}$ we see that b_1 is essentially a counterterm to the term in U_1 , b_2 is a counterterm to the term in U_2 and so on. δ eliminates power law scaling like n^α , it should not be relevant at large-enough n because is sub-dominant with respect to the corrections to scaling of order $\exp(O(n^{(5-k)/5}))$ with $k \in \{1, 2, 3, 4\}$. Numerically, we have found a weak dependence of the result on this parameter, and accordingly we have set $\delta = 1$. b_1 is constrained by a consistency condition (see Appendix O). We have fixed b_1 such that $|\theta(b_1)| = \pi/10$. For this choice, the Borel transform has an oscillatory discontinuity, which seems heuristically the best choice. The mathematical convergence of the technique does not depend on the value of the parameter b_2 , but the rate of the convergence numerically does. We have chosen b_2 in order to have a somewhat ‘‘smooth’’ convergence, even if we have not tried to optimize b_2 in a systematic way.

(Conformal map): Let $h : \mathcal{D} \rightarrow \mathbb{C} \setminus \mathcal{C}_A$ be an analytic function such that:

- h is one-to-one.
- $h(0) = 0$.
- $h(w^*)^* = h(w)$.

Then, one has

$$h(w) := \frac{4^{9/5} A w}{5(1+w)^{2/5}(1-w)^{8/5}} \quad (92)$$

We now use the conformal map $h(w)$ for $A \equiv A_{\text{ladd}}$. For all $|h(w)| < A_{\text{ladd}}$, we introduce the Borel transform \tilde{B}_{ladd} in the w variable:

$$\tilde{B}_{\text{ladd}}(w) := B_{\text{ladd}}(h(w)) = \sum_{n=0}^{\infty} (h(w))^n B_{\text{ladd},n} = \sum_{n=0}^{\infty} (h(w))^n \frac{p_{\text{ladd},n}}{\mu_n} \quad (93)$$

Then, it is easy to show that the function $\tilde{B}_{\text{ladd}}(w)$ is analytic at least for $|h(w)| < A_{\text{ladd}}$. We expand $\tilde{B}_{\text{ladd}}(w)$ in a Taylor series

$$\tilde{B}_{\text{ladd}}(w) = \sum_{n=0}^{\infty} w^n \tilde{B}_{\text{ladd},n} \quad (94)$$

This Taylor series converges for $|w| < 1$ because the function \tilde{B}_{ladd} has no singularity in the unitary disk, which is equivalent to saying that $B_{\text{ladd}}(z)$ has no singularity for $z \in \mathbb{C} \setminus \mathcal{C}_{A_{\text{ladd}}}$. As $h(w)$ is invertible, we can analytically continue $B_{\text{ladd}}(z)$ for $z \in \mathbb{C} \setminus \mathcal{C}_{A_{\text{ladd}}}$ in an explicit way using \tilde{B}_{ladd}

$$B_{\text{ladd}}(z) := \tilde{B}_{\text{ladd}}(h^{-1}(z)) = \sum_{n=0}^{\infty} (h^{-1}(z))^n \tilde{B}_{\text{ladd},n} \quad (95)$$

One can easily prove that the function $B_{\text{ladd}}(z)$ defined in this way is analytic. The vector $(\tilde{B}_{\text{ladd},n})_{n=0}^{\mathcal{N}}$ is linearly related to the vector $(p_{\text{ladd},n})_{n=0}^{\mathcal{N}}$ ²⁸.

$$\tilde{B}_{\text{ladd},0} = \frac{p_{\text{ladd},0}}{\mu_0}, \quad \tilde{B}_{\text{ladd},n} = \sum_{k=1}^n m_{nk} \frac{A_{\text{ladd}}^k}{\mu_k(b_1, b_2, \delta)} p_{\text{ladd},k} \quad (97)$$

²⁸The explicit relation is for $n \geq 1$ and $1 \leq k \leq n$:

$$m_{nk} = \left(\frac{4^{9/5}}{5}\right)^k \sum_{j=0}^{n-k} (-1)^j \binom{2k/5 + j - 1}{2k/5 - 1} \binom{3k/5 + n - j - 1}{8k/5 - 1} \quad (96)$$

At this point, we write

$$\begin{aligned}
p_{\text{physical}} &= p_{\text{ladd}}(1) = \int_0^\infty dt E(t) B_{\text{ladd}}(t) = \int_0^1 dw h'(w) E(h(w)) \tilde{B}_{\text{ladd}}(w) = \\
&= \sum_{n=0}^{\infty} \tilde{B}_{\text{ladd},n} h_n = \lim_{\mathcal{N} \rightarrow \infty} \sum_{n=0}^{\mathcal{N}} \tilde{B}_{\text{ladd},n} h_n
\end{aligned} \tag{98}$$

where $h_n(A_{\text{ladd}}, b_1, b_2, \delta) := \int_0^\infty dt E(t) (h^{-1}(t))^n$. We finally arrive at

(Conformal-Borel resummation):

$$p_{\text{physical}} = \lim_{\mathcal{N} \rightarrow \infty} \sum_{n=0}^{\mathcal{N}} \mathcal{B}_n^{(\mathcal{N})} p_{\text{ladd},n} \tag{99}$$

where $\mathcal{B}_0^{(\mathcal{N})} := 1$ and for $n \geq 1$:

$$\mathcal{B}_n^{(\mathcal{N})}(A_{\text{ladd}}, b_1, b_2, \delta) := \frac{A_{\text{ladd}}^n}{\mu_n(b_1, b_2, \delta)} \sum_{k=n}^{\mathcal{N}} h_k(A_{\text{ladd}}, b_1, b_2, \delta) m_{kn} \tag{100}$$

One also has that $\lim_{\mathcal{N} \rightarrow \infty} \mathcal{B}_n^{(\mathcal{N})} = 1$.

We see therefore that the problem of reconstructing $p_{\text{ladd}}(z)$ from the coefficients $(p_{\text{ladd},n})_{n=0}^{\mathcal{N}}$ is explicitly solved.

5 Generalization to correlation functions and to the fully-dressed diagrammatic scheme

In this section, we show how it is possible to generalize the large-order behavior computation to the correlation functions, and how to consider more general diagrammatic schemes.

5.1 Borel summability of the self-energies in the ladder expansion

The computation for the pressure is not generalizable as it is to correlation functions, as they are expressed as ratio of partition-like functions. The strategy

is then very simple: we compute the large-order behavior for each partition-like function, and we deduce the large-order behavior of the correlation function. In this section we are interested in bounding the large-order behavior, in the next section we will make explicit predictions for it. In order to manipulate such ratios of partition functions, which are given by asymptotic series which respect certain bounds, it is very useful to introduce the concept of Gevrey asymptotic series:

(Gevrey asymptotic series): Let $A > 0$. A formal power series $\sum_{n=0}^{\infty} z^n f_n$ is Gevrey asymptotic of type $(5, A)$ to the function $f(z)$ if there exists $R > 0$ and $\epsilon > 0$ such that $f(z)$ is analytic for $z \in W_R^\epsilon := \{z \in \mathbb{C} \mid 0 < |z| < R, |\arg z| < \pi/10 + \epsilon\}$ and such that for every $0 < \epsilon_A < 1$, there exists $C < \infty$ such that for every $N \in \mathbb{N}$ and $z \in W_R^\epsilon$ one has

$$\left| f(z) - \sum_{n=0}^{N-1} f_n z^n \right| \leq C \left(\frac{|z|}{A(1 - \epsilon_A)} \right)^N (N/5)! \quad (101)$$

In this case, we will write

$$f(z) \hat{=}^A_5 \sum_{n=0}^{\infty} f_n z^n \quad (102)$$

One can show that the bounds of section 4.1 are sufficient to have a Gevrey asymptotic series (see Appendix M)

(Derivative bounds imply Gevrey asymptotics): Let $f(z)$ be an analytic function in $W_R^\epsilon := \{z \in \mathbb{C} \mid 0 < |z| < R, |\arg z| < \pi/10 + \epsilon\}$, for some $R > 0$ and $\epsilon > 0$. Suppose that f is infinitely derivable in the origin and

$$f_n := \lim_{z \rightarrow 0, z \in W_R^\epsilon} \frac{1}{n!} \frac{d^n}{dz^n} f(z) \quad (103)$$

and for every $0 < \epsilon_A < 1$, there exists $C < \infty$ such that for every $z \in W_R^\epsilon$ and $n \in \mathbb{N}$

$$\left| \frac{1}{n!} \frac{d^n}{dz^n} f(z) \right| \leq C_B (A(1 - \epsilon_A))^{-n} (n/5)! \quad (104)$$

Then

$$f(z) \hat{=}^A_5 \sum_{n=0}^{\infty} f_n z^n \quad (105)$$

We can then use this result to write:

$$p_{\text{ladd}}(z) \hat{=}^A_{\hat{=}^A_{\text{ladd}}} \sum_{n=0}^{\infty} z^n p_{\text{ladd},n} \quad (106)$$

We can restate Ramis's theorem using Gevrey asymptotic series

(Borel summability): Suppose

$$f(z) \hat{=}^A_{\hat{=}^A} \sum_{n=0}^{\infty} z^n f_n \quad (107)$$

Then, for all x such that $0 \leq x < R$, $R > 0$, $f(x)$ is given by the inverse Borel transform introduced before.

Note that the unicity result of Section 4.1 is then concisely stated as follows: if $f(z) \hat{=}^A_{\hat{=}^A} \sum_{n=0}^{\infty} f_n z^n$ and $g(z) \hat{=}^A_{\hat{=}^A} \sum_{n=0}^{\infty} g_n z^n$, then there exists $R > 0$ and $\epsilon > 0$ such that $f(z) = g(z)$ for $z \in W_R^\epsilon$ (it is a slightly generalized version, see Appendix M for the proof).

This notion is useful for the following properties: suppose that

$$f(z) \hat{=}^A_{\hat{=}^A} \sum_{n=0}^{\infty} f_n z^n, \quad g(z) \hat{=}^A_{\hat{=}^A} \sum_{n=0}^{\infty} g_n z^n \quad (108)$$

Then, one has

$$(f + g)(z) \hat{=}^A_{\hat{=}^A} \sum_{n=0}^{\infty} z^n f_n + \sum_{n=0}^{\infty} z^n g_n \quad (109)$$

$$(fg)(z) \hat{=}^A_{\hat{=}^A} \left(\sum_{n=0}^{\infty} z^n f_n \right) \cdot \left(\sum_{n=0}^{\infty} z^n g_n \right) \quad (110)$$

$$\frac{1}{f(z)} \hat{=}^A_{\hat{=}^A} \left(\sum_{n=0}^{\infty} z^n f_n \right)^{-1} \quad (111)$$

where on r.h.s we have operations between formal power series. We refer to Appendix Q for the proof²⁹.

We would like to discuss now how to bound the large-order behavior for the self-energies using this formalism. It is shown in Appendix S that we can write an

²⁹These properties are also proven in [97], even if the proof for the last property is more elementary in the Appendix of this text.

expression for the pair propagator Γ (see Section 1.3 for the definition) directly in the continuum limit

$$\Gamma_{\text{physical}}(\mathbf{x}, \tau) = -\langle \bar{\eta}(\mathbf{x}, \tau) \eta(\mathbf{0}, 0) \rangle \quad (112)$$

For general z , we define Γ_{ladd} by

$$\Gamma_{\text{ladd}}(\mathbf{x}, \tau; z) := -\langle \bar{\eta}(\mathbf{x}, \tau) \eta(\mathbf{0}, 0) \rangle_{S_{\text{ladd}}^{(z)}} \stackrel{\text{Taylor}}{=} \sum_{n=0}^{\infty} \Gamma_{\text{ladd},n}(\mathbf{x}, \tau) z^n \quad (113)$$

where $\Gamma_{\text{ladd},n}$ is the order- n of ladder expansion built from Γ_0 . Let us remark that $\Gamma_{\text{ladd}}(z=0) = \Gamma_0$ and $\Gamma_{\text{ladd}}(z=1) = \Gamma_{\text{physical}}$. The formal power series in z is built from ladder-less diagrams.

Let us define

$$\gamma_{\text{ladd}}(\mathbf{x}, \tau; z) := -\frac{\int \mathcal{D}[\eta, \bar{\eta}, \varphi, \bar{\varphi}] \bar{\eta}(\mathbf{x}, \tau) \eta(\mathbf{0}, 0) e^{-S_{\text{ladd}}^{(z)}}}{\int \mathcal{D}[\eta, \bar{\eta}, \varphi, \bar{\varphi}] e^{-S_{\text{ladd}}^{(0)}}} \quad (114)$$

One has

$$\Gamma_{\text{ladd}}(\mathbf{x}, \tau; z) = \gamma_{\text{ladd}}(\mathbf{x}, \tau; z) \frac{1}{\tilde{Z}_{\text{ladd}}(z)} \quad (115)$$

We can study the series for $\gamma_{\text{ladd}}(\mathbf{x}, \tau; z)$ in the same way as we have done for $\tilde{Z}_{\text{ladd}}(z)$, finding the same result at leading order (with an additional prefactor given by the convolution of two instantons):

$$\gamma_{\text{ladd},n}(\mathbf{x}, \tau) \stackrel{n \rightarrow \infty}{=} \left(\int d^3 \mathbf{r}_0 \lambda_c(\mathbf{x} + \mathbf{r}_0) \lambda_c(\mathbf{r}_0) \right) A_{\text{ladd}}^{-n} \cos \left(\frac{4\pi n}{5} + O(n^{\frac{4}{5}}) \right) \left(\frac{n}{5} \right)! \quad (116)$$

Following the same arguments, one can show that

$$\gamma_{\text{ladd}}(\mathbf{x}, \tau; z) \hat{=} \hat{A}_{\text{ladd}} \sum_{n=0}^{\infty} \gamma_{\text{ladd},n}(\mathbf{x}, \tau) z^n \quad (117)$$

and have already seen that (at finite volume \mathcal{V})

$$\tilde{Z}_{\text{ladd}}(z) \hat{=} \hat{A}_{\text{ladd}} \sum_{n=0}^{\infty} z^n \tilde{Z}_{\text{ladd},n} \quad (118)$$

We see that Γ_{ladd} is the product of a function with Gevrey- $(5, A_{\text{ladd}})$ asymptotics with the inverse of a function with Gevrey- $(5, A_{\text{ladd}})$ asymptotics, therefore according to properties (110) and (111), Γ_{ladd} must have Gevrey- $(5, A_{\text{ladd}})$ asymptotics:

$$\Gamma_{\text{ladd}}(\mathbf{x}, \tau; z) \hat{=} \hat{A}_{\text{ladd}} \sum_{n=0}^{\infty} \Gamma_{\text{ladd},n}(\mathbf{x}, \tau) z^n \quad (119)$$

Hence, the series for Γ can be resummed by a Borel transform according to Ramis's theorem.

Now, the pair self-energy Π_{ladd} is defined by $\Pi_{\text{ladd}}(z) = \Gamma_0^{-1} - \Gamma_{\text{ladd}}^{-1}(z)$, so that

(Borel summability of the pair self-energy):

$$\Pi_{\text{ladd}}(z) \stackrel{\hat{=} A_{\text{ladd}}}{=} \sum_{n=1}^{\infty} z^n \Pi_{\text{ladd},n} \quad (120)$$

so we find that also the series for Π_{ladd} is resumable by a Borel transform.

We would like to discuss the large-order behavior of the self-energy. Unfortunately, the analysis is not as straightforward as for the pair propagator because the fermion propagator G is not an entire function when expressed in terms of the η fields. In Appendix T, we prove generalizations of Pauli's formula, and in particular (T.10)

$$(z \Pi_{\text{bubble}} + \Pi_{\text{ladd}}(z)) : \Gamma_{\text{ladd}}(z) = \Sigma_{\text{ladd}}(z) : G_{\text{ladd}}(z) \quad (121)$$

where $f : g$ means $\beta^{-1} \sum_{p_4} \int d^3 \mathbf{p} f_{\mathbf{p}, p_4} g_{\mathbf{p}, p_4}$, where \mathbf{p} is the momentum and p_4 is the Matsubara frequency, that can be bosonic or fermionic depending on the function. We thus have

$$\Sigma_{\text{ladd}}(z) : G_{\text{ladd}}(z) = \frac{1}{\beta} \sum_{p_4 \in 2\mathbb{Z}\pi/\beta} \int d^3 \mathbf{p} \frac{z \Pi_{\text{bubble}}(\mathbf{p}, p_4) + \Pi_{\text{ladd}}(\mathbf{p}, p_4; z)}{\Gamma_0(\mathbf{p}, p_4)^{-1} - \Pi_{\text{ladd}}(\mathbf{p}, p_4; z)} \quad (122)$$

so we see that $\Sigma_{\text{ladd}}(z) : G_{\text{ladd}}(z)$ is the integral of rational functions that admits Gevrey asymptotics, so that one is lead to conjecture

$$\begin{aligned} \Sigma_{\text{ladd}}(z) : G_{\text{ladd}}(z) &= \frac{1}{\beta} \sum_{p_4 \in (2\mathbb{Z}+1)\pi/\beta} \int d^3 \mathbf{p} \frac{\Sigma_{\text{ladd}}(\mathbf{p}, p_4; z)}{G_0(\mathbf{p}, p_4)^{-1} - \Sigma_{\text{ladd}}(\mathbf{p}, p_4; z)} = \\ &\stackrel{\hat{=} A_{\text{ladd}}}{=} \sum_{n=1}^{\infty} f_n z^n \end{aligned} \quad (123)$$

for some f_n . From that expression, one is lead to induce that

(Borel summability of the self-energy):

$$\Sigma_{\text{ladd}}(z) \stackrel{\wedge}{=} \frac{A_{\text{ladd}}}{5} \sum_{n=1}^{\infty} \Sigma_{\text{ladd},n} z^n \quad (124)$$

These properties allow us to prove that the ladder expansion is Borel summable, but in principle we cannot say anything about the large-order behavior apart that is bounded by $(n/5)!(A_{\text{ladd}}(1 - \epsilon_A))^{-n}$ for every $0 < \epsilon_A < 1$. In order to make more precise predictions, and to extend the analysis to more involved diagrammatic schemes, we need the more intuitive analysis of the following section.

5.2 Alternative view: discontinuities near the origin

It is a well-known fact that for analytic functions with non-zero radius of convergence of the Taylor expansion at the origin, the large-order behavior of the coefficients is determined by the properties of the singularity nearest to the point of expansion. Having a zero radius of convergence means that there are singularities exactly at zero distance from the point of expansion, otherwise it is straightforward to show that the radius of convergence would be finite. We have extended the Borel transform $B(z)$ of $p_{\text{ladd}}(z)$ to $z \in \mathbb{C} \setminus \{z \in \mathbb{C} \mid |z| \geq A_{\text{ladd}}, |\arg z| = 4\pi/5\}$. As before, we write (in this section we drop the b_1 and b_2 parameters of the Borel transform for simplicity)

$$p_{\text{ladd}}(z) = 5 \int_0^{\infty} \frac{dt}{t} t^{5\delta} e^{-t^5} B_{\text{ladd}}(zt) \quad (125)$$

This gives in principle the possibility to analytically extend p_{ladd} to $\{z \in \mathbb{C} \mid |z| < R\} \setminus \mathcal{C}_0$, where $\mathcal{C}_0 := \{z \in \mathbb{C} \mid z \neq 0, |\arg z| = 4\pi/5\}$, for some $R > 0$. We will see that f has singularities for $|\arg z| = 4\pi/5$. A very important object in the following is the discontinuity

$$\text{Disc}(g, z_0) := \lim_{\epsilon \downarrow 0} g(z_0 e^{i0^+}) - g(z_0 e^{-i0^+}) \quad (126)$$

If g is real, then $\text{Disc}(g, x e^{i\theta})^* = -\text{Disc}(g, x e^{-i\theta})$. p_{ladd} has discontinuities for $|\arg z| = 4\pi/5$ (for definiteness, we consider only $\arg z = 4\pi/5$)

$$\begin{aligned} \text{Disc}(p_{\text{ladd}}, x e^{4\pi i/5}) &= \frac{5}{x^{5\delta}} \int_{A_{\text{ladd}}}^{\infty} \frac{dt}{t} t^{5\delta} e^{-t^5/x^5} \text{Disc}(B_{\text{ladd}}, t e^{4\pi i/5}) = \\ &= \frac{5 e^{-\left(\frac{A_{\text{ladd}}}{x}\right)^5}}{x^{5\delta}} \int_0^{\infty} \frac{dt}{t + A_{\text{ladd}}} (t + A_{\text{ladd}})^{5\delta} e^{-\frac{1}{x^5} \sum_{k=1}^5 C_{5,k} t^k A_{\text{ladd}}^{5-k}} \times \\ &\times \text{Disc}(B_{\text{ladd}}, (t + A_{\text{ladd}}) e^{4\pi i/5}) \end{aligned} \quad (127)$$

where $C_{5,k} := \binom{5}{k}$. By changing variable $u = 5tA_{\text{ladd}}^4/x^5$, we find that at leading order for small x one has

$$\begin{aligned} \text{Disc}(p_{\text{ladd}}, x e^{4\pi i/5}) &= \\ &\simeq \frac{e^{-\left(\frac{A_{\text{ladd}}}{x}\right)^5}}{(x/A_{\text{ladd}})^{5(\delta-1)}} \int_0^\infty du e^{-u} \text{Disc}(B_{\text{ladd}}, (A_{\text{ladd}} + x^5 u/(5A_{\text{ladd}}^4)) e^{4\pi i/5}) \end{aligned} \quad (128)$$

so that we expect that $\text{Disc}(f, x e^{\pm 4\pi i/5}) \sim e^{-(A_{\text{ladd}}/x)^5}$ for small x , it is smaller than any power of x as expected. In Appendix R we prove the following useful formula, which is a generalization of the formula presented in [98]

(Dispersion relation): Suppose $f(z)$ is analytic in $\{z \in \mathbb{C} \mid |z| < R, |\arg z| \neq 4\pi/5\}$ and that the following limit exists

$$\lim_{x \downarrow 0} \frac{1}{n!} \frac{d^n}{dx^n} f(x) =: f_n \quad (129)$$

Then for $r < R$ one has

$$f_n = \oint_{|z|=r} \frac{dz}{2\pi i} \frac{f(z)}{z^{n+1}} - \sum_{s \in \{-1,1\}} s e^{-\frac{4\pi i s n}{5}} \int_0^r \frac{dt}{2\pi i} \frac{\text{Disc}(f, t e^{4\pi i s/5})}{t^{n+1}} \quad (130)$$

One has

$$\left| \oint_{|z|=r} \frac{dz}{2\pi i} \frac{f(z)}{z^{n+1}} \right| \leq \frac{1}{r^n} \sup_{|z|=r} |f(z)| \quad (131)$$

from which we see that only the integral over the discontinuity can give a factorial contribution. If we try

$$\text{Disc}(p_{\text{ladd}}, x e^{4\pi i/5}) \underset{x \downarrow 0}{=} \exp\left(-\left(\frac{A_{\text{ladd}}}{x}\right)^5 + O(x^{-4})\right) \quad (132)$$

we get the right large-order behavior for $p_{\text{ladd},n}$.

We are then led to study the algebra of exponentially small discontinuities. Suppose that $f(z)$ and $g(z)$ are analytic functions for $|\arg z| \neq 4\pi/5$ and $|z| < R$,

with $f(0) \neq 0$. Suppose further that

$$\text{Disc}(f, xe^{\pm 4\pi i/5}) \underset{x \downarrow 0}{=} \exp \left(- \left(\frac{A_{\text{ladd}}}{x} \right)^5 + O(x^{-4}) \right) \quad (133)$$

$$\text{Disc}(g, xe^{\pm 4\pi i/5}) \underset{x \downarrow 0}{=} \exp \left(- \left(\frac{A_{\text{ladd}}}{x} \right)^5 + O(x^{-4}) \right) \quad (134)$$

Then

$$\text{Disc}(fg, xe^{\pm 4\pi i/5}) \underset{x \downarrow 0}{=} f(0) \text{Disc}(g, xe^{\pm 4\pi i/5}) + g(0) \text{Disc}(f, xe^{\pm 4\pi i/5}) \quad (135)$$

$$\text{Disc}(1/f, xe^{\pm 4\pi i/5}) \underset{x \downarrow 0}{=} - \frac{\text{Disc}(f, xe^{\pm 4\pi i/5})}{f(0)^2} \quad (136)$$

Let us apply these properties to compute the discontinuity of Γ_{ladd} :

$$\text{Disc}(\Gamma_{\text{ladd}}, xe^{\pm 4\pi i/5}) \underset{x \downarrow 0}{=} \text{Disc}(\gamma_{\text{ladd}}, xe^{\pm 4\pi i/5}) \quad (137)$$

as $|\text{Disc}(\tilde{Z}_{\text{ladd}}, xe^{\pm 4\pi i/5})| = O(x^5 |\text{Disc}(\gamma_{\text{ladd}}, xe^{\pm 4\pi i/5})|) \ll |\text{Disc}(\gamma_{\text{ladd}}, xe^{\pm 4\pi i/5})|$ for $x \downarrow 0$ ³⁰. From this result we can derive directly

$$\Gamma_{\text{ladd},n} \underset{n \rightarrow \infty}{=} \gamma_{\text{ladd},n} \quad (138)$$

and a similar behavior can be derived for $\Pi_{\text{ladd},n}$

(Large-order behavior for the pair self-energy):

$$\Pi_{\text{ladd},n}(\mathbf{r}, \tau) \underset{n \rightarrow \infty}{\sim} \int_{1,2} \Gamma_0(\mathbf{r} - \mathbf{r}_1, \tau - \tau_1) \gamma_{\text{ladd},n}(\mathbf{r}_1 - \mathbf{r}_2, \tau_1 - \tau_2) \Gamma_0(\mathbf{r}_1, \tau_1) \quad (139)$$

One can derive in this way a similar expression for $\Sigma_{\text{ladd},n}$.

³⁰This is due to the fact that γ_{ladd} contains the fields $\eta(\mathbf{r}, \tau) \bar{\eta}(\mathbf{0}, 0)$, which are of order $1/|z|^5$.

5.3 Discussion of the bold scheme

There is no difficulty in repeating the analysis of the previous section for general partially dressed schemes, like the semi-bold scheme introduced in [87]. However, for the bold scheme introduced in Section 1.3, the analysis cannot be applied without changes, as there are singularities coming from the fact that the shifted action itself is singular at the origin, as it is built self-consistently with the self-energy Σ and pair self Π which are singular at the origin³¹. It is then clear that in the fully-bold case we cannot expect the same level of rigour as for other schemes, but we will try nevertheless to give rather convincing arguments.

First of all, we need to define the bold scheme in a more formal way than in Section 1.3. We can define these series in a completely formal way starting from the bare expansion³². We remind that

$$\Sigma_{\text{ladd}}[G_0, z\Gamma_0] \underset{\text{Taylor}}{=} \sum_{n=1}^{\infty} z^n \Sigma_{\text{ladd},n}[G_0, \Gamma_0] \quad (140)$$

$$\Pi_{\text{ladd}}[G_0, z\Gamma_0] \underset{\text{Taylor}}{=} \sum_{n=1}^{\infty} z^{n-1} \Pi_{\text{ladd},n}[G_0, \Gamma_0] \quad (141)$$

which can be generated from the action $S_{\text{ladd}}^{(z)}[G_0, \Gamma_0]$ of Section 4.1:

$$S_{\text{ladd}}^{(z)}[G_0, g_0] = -\langle \varphi | G_0^{-1} | \varphi \rangle - \langle \eta | \Gamma_0^{-1} | \eta \rangle - z \langle \eta | \Pi_{\text{bubble}}[G_0] | \eta \rangle + \sqrt{z} (\langle \eta | \varphi_{\downarrow} \varphi_{\uparrow} \rangle + \langle \varphi_{\downarrow} \varphi_{\uparrow} | \eta \rangle) \quad (142)$$

We now formally define the bold series by

$$\Sigma_{\text{ladd}}[G_0(z), \Gamma_0(z)] \underset{\text{Taylor}}{=} \sum_{n=1}^{\infty} z^n \Sigma_{\text{bold},n}[G, \Gamma] \quad (143)$$

$$\Pi_{\text{ladd}}[G_0(z), \Gamma_0(z)] + \Pi_{\text{bubble}}[G_0(z)] \underset{\text{Taylor}}{=} \Pi_{\text{bubble}}[G] + \sum_{n=2}^{\infty} z^{n-1} \tilde{\Pi}_{\text{bold},n}[G, \Gamma] \quad (144)$$

³¹In principle, as we will discuss in Part III, there is another potential fundamental difficulty with the bold scheme: it turns out that for certain lattice models, like the Hubbard model near half-filling, there are branch-cut singularities in the shifted action. In the following, we *assume* that we do not face this type of problems. An argument for this assumption is that we are considering the continuum limit which corresponds to vanishing filling factor, while this problem was encountered only near half filling.

³²We remark that the bare expansion in g_0 is defined only at finite lattice spacing b . The continuum limit must be taken afterwards.

where

$$G_0(z)^{-1} := G^{-1} + \sum_{n=1}^{\infty} z^n \Sigma_{\text{bold},n}[G, \Gamma] \quad (145)$$

$$\Gamma_0(z)^{-1} := (z\Gamma)^{-1} + \Pi_{\text{bubble}}[G] - \Pi_{\text{bubble}}[G_0(z)] + \sum_{n=2}^{\infty} z^{n-1} \tilde{\Pi}_{\text{bold},n}[G, \Gamma] \quad (146)$$

where $\Pi_{\text{bubble}}[G]$ is the particle-particle bubble GG . These equations can be solved in the field of formal power series for every G and Γ , and one can obtain the formal expression of $\Sigma_{\text{bold},n}[G, \Gamma]$ and $\tilde{\Pi}_{\text{bold},n}[G, \Gamma]$ in terms of $\Sigma_{\text{ladd},m}[G, \Gamma]$ and $\Pi_{\text{ladd},m}[G, \Gamma]$ for $m \leq n$.

At this point we would like to use as before a shifted action, that reproduces the bold series order-by-order, and such that its evaluation at $z = 1$ gives the physical action. This shifted action can be constructed self-consistently if we assume to know the analytic continuation of the bold self-energy Σ_{bold} and the bold pair self-energy Π_{bold} ³³, such that

$$\Sigma_{\text{bold}}[G, \Gamma, z] \underset{\text{Taylor}}{=} \sum_{n=1}^{\infty} z^n \Sigma_{\text{bold},n}[G, \Gamma] \quad (147)$$

$$\tilde{\Pi}_{\text{bold}}[G, \Gamma, z] \underset{\text{Taylor}}{=} \sum_{n=2}^{\infty} z^n \tilde{\Pi}_{\text{bold},n}[G, \Gamma] \quad (148)$$

Note that we can impose that $\Sigma[G, \Gamma, z] = \Sigma[G, z\Gamma, 1]$, $\tilde{\Pi}_{\text{bold}}[G, \Gamma, z] = z \tilde{\Pi}_{\text{bold}}[G, z\Gamma, 1]$. Then, reasoning in the same way as in Appendix A, the bold shifted action is

$$S_{\text{bold}}^{(z)}[G, \Gamma] := -\langle \varphi | G^{-1} + \Sigma_{\text{bold}}[G, \Gamma, z] | \varphi \rangle + \langle \eta | \Gamma^{-1} + z \Pi_{\text{bubble}}[G] + \tilde{\Pi}_{\text{bold}}[G, \Gamma, z] | \eta \rangle + \sqrt{z} (\langle \eta | \varphi_{\downarrow} \varphi_{\uparrow} \rangle + \langle \varphi_{\downarrow} \varphi_{\uparrow} | \eta \rangle) \quad (149)$$

We expect Σ_{bold} and $\tilde{\Pi}_{\text{bold}}$ to have singularities for infinitesimally small z at some angle in the complex plane. In practice, Σ_{bold} and $\tilde{\Pi}_{\text{bold}}$ are just the resummed bold series. But resummed in which way? We can answer this question by considering the following consistency condition: The propagators G and Γ can be computed with the shifted-action formalism, and are in principle functions of z . But they must be trivial functions of z , the propagators expressed in terms of themselves are given by a series with only one term

$$G_{\text{bold}}(z) = G, \quad \Gamma_{\text{bold}}(z) = \Gamma \quad (150)$$

³³We start from order 2 in the equation for $\tilde{\Pi}$ because $\Pi_{\text{bold},1}[G, G_0] = \Pi_{\text{bubble}}[G] - \Pi_{\text{bubble}}[G_0]$ is not a functional of only G and Γ .

In particular, the discontinuity of the propagators must be zero:

$$\text{Disc}(G_{\text{bold}}, xe^{\pm 4\pi i/5}) = 0, \quad \text{Disc}(\Gamma_{\text{bold}}, xe^{\pm 4\pi i/5}) = 0 \quad (151)$$

Let us summarize what we have discussed: we can formally express G and Γ in terms of functional integrals of the shifted action $S_{\text{bold}}^{(z)}$. We have seen in the previous sections that the functional integration is responsible for discontinuities for infinitesimally small value of z . Here, we have an additional source of discontinuities, as the action itself is discontinuous. We must therefore require that in the case of the computation of G and Γ these two sources of discontinuities compensate exactly. This is enough to induce the large-order behavior and the analytic structure of Σ_{bold} and Π_{bold} . We show in Appendix W that Π_{bold} and Σ_{bold} have the same analytical structure, and the same large-order behavior after the replacement of the expression defining A_{ladd} of Γ_0 with Γ , and with an additional term in the expression for the first correction $U_{\text{bold},1}$

$$A_{\text{bold}} = A_{\#} \inf_{\eta} \frac{-\langle \eta | \Gamma^{-1} | \eta \rangle}{\|\eta\|_{5/2}^2}, \quad U_{\text{bold},1} = 5^{\frac{1}{5}} A_{\text{bold}} - 5^{\frac{1}{5}} A_{\#} \frac{\langle \eta_c | \tilde{\Pi}_{\text{bold}} | \eta_c \rangle}{\|\eta_c\|_{5/2}^2} \quad (152)$$

6 Numerical results

In this section we show some results obtained by integrating the resummation technique described in the previous sections into the Diagrammatic Monte Carlo algorithm [84]. We will present results in the high-temperature and the degenerate regimes of the normal phase of the unitary Fermi gas. We have full momentum - Matsubara frequency resolution for the Green's function and the pair propagator, but here we only present results for thermodynamic quantities, like the density

$$n := 2G(\mathbf{r} = 0, \tau = 0^-) \quad (153)$$

the order-parameter susceptibility (which diverges at the s-wave superfluid phase transition):

$$\chi := -\Gamma(\mathbf{p} = 0, \Omega_n = 0) \quad (154)$$

and the contact parameter (see, e.g., [83]):

$$\mathcal{C} := -\Gamma(\mathbf{r} = 0, \tau = 0^-) \quad (155)$$

The contact parameter is defined from the k^{-4} tail of the momentum distribution

$$\lim_{|\mathbf{k}| \rightarrow \infty} |\mathbf{k}|^4 n(\mathbf{k}) = \mathcal{C} \quad (156)$$

and is proportional to the density of small-distance pairs:

$$\langle \hat{n}_\uparrow(\mathbf{r}) \hat{n}_\downarrow(\mathbf{0}) \rangle \underset{r \rightarrow 0}{=} \frac{\mathcal{C}}{(4\pi)^2 r^2} \quad (157)$$

The error bars in our plots contain all sources of error (which are the statistical uncertainty of the Monte Carlo procedure and an estimate of the systematic error coming from our grid and cutoffs).

We see in Figure 2 that Diagrammatic Monte Carlo is able to achieve a 4-digit accuracy in the high-temperature regime for the density and the susceptibility with the ladder scheme. This is due to the (almost) convergent property of the series (we have seen in Appendix H that A_{diag} goes to infinity for $\beta\mu \rightarrow -\infty$). In general, we remark that bold and ladder schemes agree on every quantity, with a slower convergence for the bold scheme.³⁴

In the degenerate regime of Figure 3, we have the possibility to compare with cold-atom experiments [12]. In the plot we also add the old (uncontrolled) Lindelöf resummation technique used in [12, 99], which is justified only for series with a non-zero radius of convergence³⁵. Note the consistency between the theoretical estimates. The experimental result for the density is compatible within the error bar.

In Figure 4 we illustrate that it is crucial to resum the diagrammatic series in the degenerate regime, by comparing the results with and without resummation. Indeed, when the value of A_{diag} is $\lesssim 1$ there is no small expansion parameter. For $\beta\mu = 0$ (the case of Figure 4), one has $A_{\text{ladd}} \approx 0.949$ and $A_{\text{bold}} \approx 0.961$.

In Figure 7 we show various estimations for the fourth virial coefficient of the unitary Fermi gas, and we compare it with our equation of state at high temperature. The Figure sheds light on a controversy. The experiments of ENS [11] and of MIT [12] are in disagreement by a factor of 2 with a conjecture of Endo and Castin [100]. The dedicated Path Integral Quantum Monte Carlo simulation of Yan and Blume [101] is not able to discriminate between these two values. Our results for the equation of state suggest a very natural explanation for this disagreement: the experimental estimations are extrapolations obtained from data points with $\zeta \gtrsim 1$, where the apparent value of b_4 is nearly the double

³⁴We have not tried to properly optimize the parameter b_2 of the Borel transform for the bold scheme, because for each b_2 we need a different run of the code and the convergence was already good enough.

³⁵Lindelöf resummation cannot converge if we go to high-enough orders. Nevertheless, for the finite order we consider, it appears to give a quite accurate estimate. This can be understood with the following (naïve) argument. Suppose we would like to resum the series $\sum_n a_n$. The Lindelöf technique consists in dividing each term of the series by $e^{\epsilon n \log n} \sim (n!)^\epsilon$, and then try to extrapolate the sum $\sum_n a_n e^{-\epsilon n \log n}$ to $\epsilon \rightarrow 0^+$ in order to obtain the resummed value. As in our case $a_n \sim (n!)^{1/5}$, we see that we cannot take an ϵ smaller than $1/5$, which is nevertheless a “small” number. Hence, one expects the systematic error to be small.

of the conjectured value. This unexpected structure of the virial expansion means that contributions from many-body physics are relevant already at fairly high-temperature, hence the unitary Fermi gas is a “true” many-body system in a wide region of the normal phase.

7 Conclusions and outlook

In this part of the dissertation we have seen how one can compute the large-order behavior of various diagrammatic expansions for a strongly correlated Fermi system in the continuous space. Using this information, combined with essential non-perturbative analytic properties, we have shown that we can obtain controlled diagrammatic results for the normal phase of the unitary Fermi gas. This is a non-trivial problem because the diagrammatic series has a zero radius of convergence. We have found that a specifically designed conformal-Borel transform allows us to resum the series and compute the physical result.

After extending our bold computations to lower temperatures down to T_c , we will compute the single-particle spectral function using numerical analytic continuation (see [102] for recent progress on this delicate numerical procedure) and compare with experimental spectra and existing lowest-order diagrammatic studies [103, 104, 86].

The method can be applied as well to a non-infinite s -wave scattering length, allowing us to study the BCS-BEC crossover. It is also possible to generalize the formalism to the superfluid phase by introducing anomalous propagators.

It will be particularly interesting to study the polarized gas, where the fate of the superfluid state is much debated [105]. The limit case of complete polarization (only one spin down particle, the polaron) has already been studied extensively theoretically [22, 23, 106, 24, 27], and experimentally [107, 108].

A model amenable with similar techniques would be the 2D Fermi gas with zero-range interactions (see [109, 110, 111] for the large-order behavior of the 2D Yukawa field theory), which is already the subject of theoretical [112, 113, 25, 26] and experimental studies [114, 115, 116, 117, 118].

Another interesting and fundamental problem is the homogeneous electron gas, also known as jellium model. For jellium one can apply a modified version of the Dyson argument [119] to show that the radius of convergence is zero (the role of positrons is played by the positive ions of the jellium). The analysis presented in this text suggests the possibility of computing the large-order behavior for jellium and to construct a corresponding conformal-Borel resummation technique.

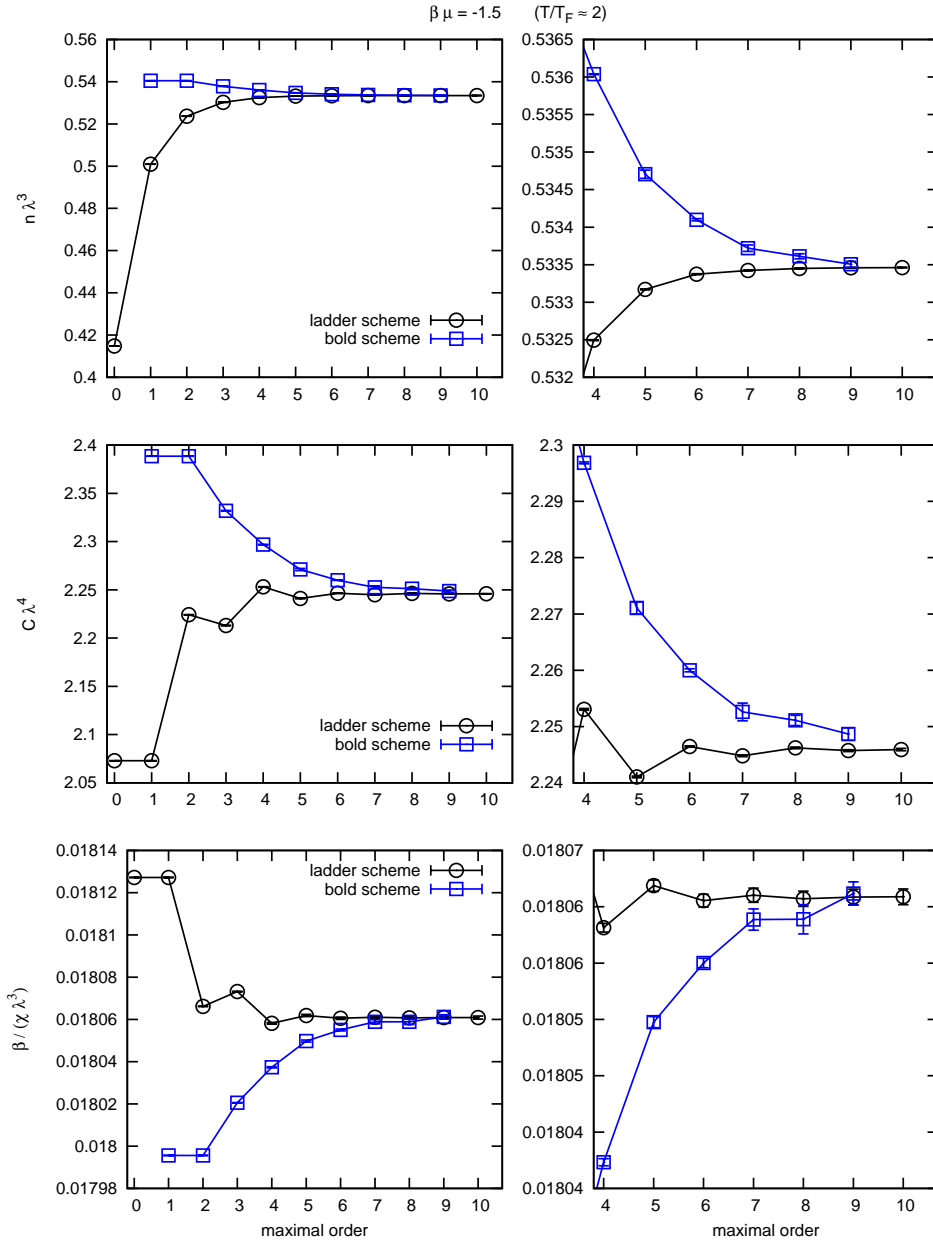


Figure 2: Dimensionless density $n\lambda^3$, contact parameter $\mathcal{C}\lambda^4$, and inverse order-parameter susceptibility $\beta/(\chi\lambda^3)$ as a function of maximal order of expansion \mathcal{N} , for $\beta\mu = -1.5$, where $\lambda = \sqrt{2\pi\beta}$ is the thermal de Broglie wavelength.

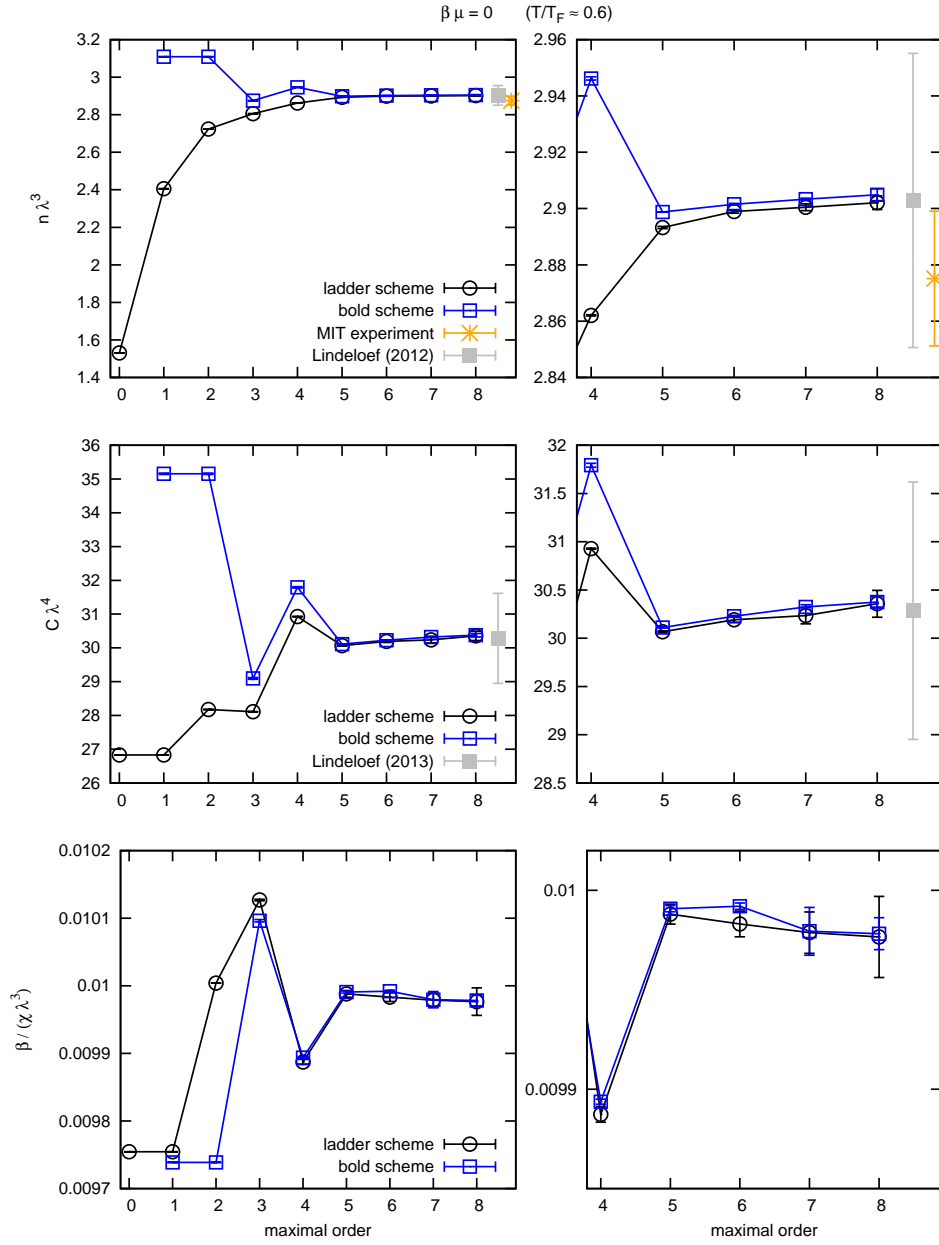


Figure 3: Dimensionless density $n\lambda^3$, contact parameter $C\lambda^4$, and inverse order-parameter susceptibility $\beta/(\chi\lambda^3)$ as a function of maximal order of expansion \mathcal{N} , for $\beta\mu = 0$.

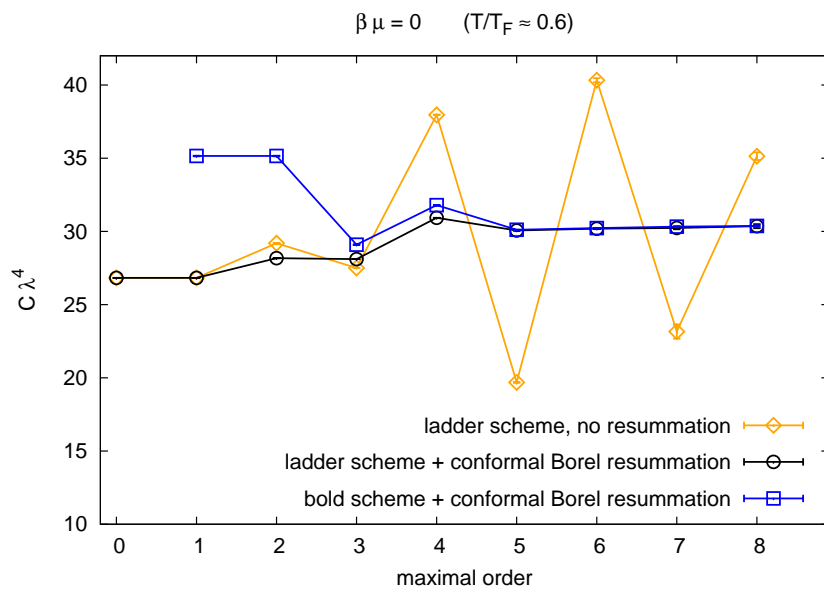


Figure 4: Dimensionless contact parameter $\mathcal{C}\lambda^4$ as a function of maximal order of expansion \mathcal{N} .

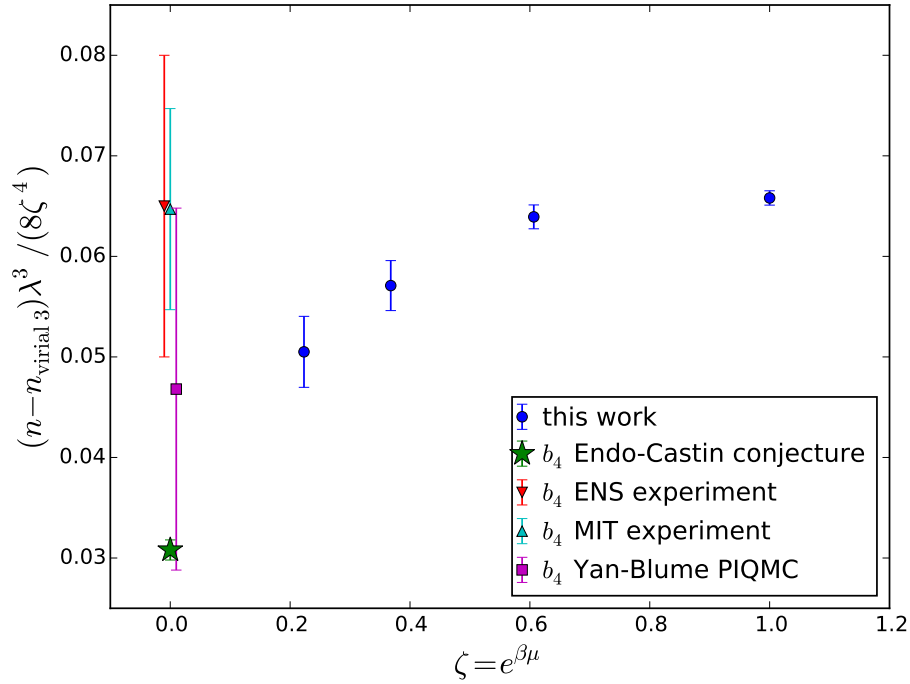


Figure 5: Density n relative to the density computed from the third order virial expansion $n_{\text{virial3}} := 2\lambda^{-3} \sum_{k=1}^3 k b_k \zeta^k$ ($\lambda = \sqrt{2\pi\beta}$, and b_k is k -th virial coefficient), divided by $8\zeta^4$. One has that $\frac{n - n_{\text{virial3}}}{8\zeta^4} \lambda^3 = b_4 + O(\zeta)$ as $\zeta \rightarrow 0$. The blue circles are obtained with the ladder-scheme conformal-Borel DiagMC. The green star is the conjecture of Endo and Castin [100]. The cyan and red triangles are experimental estimations of ENS [11] and MIT [12] labs. The violet square was obtained with a Path-Integral Quantum Monte Carlo simulation by Yan and Blume [101].

Appendices of Part I

A Shifted action for the ladder scheme

From the hamiltonian (8), we can build the action

$$S_{\text{physical}}^{(\text{Grassmann})} = -\langle \varphi | G_0^{-1} | \varphi \rangle + g_0 b^3 \sum_{\mathbf{r} \in b\mathbb{Z}^3} \int_0^\beta d\tau (\bar{\varphi}_\uparrow \bar{\varphi}_\downarrow \varphi_\downarrow \varphi_\uparrow)(\mathbf{r}, \tau) \quad (\text{A.1})$$

where φ and $\bar{\varphi}$ are Grassmann fields and τ is the imaginary time. We perform an Hubbard-Stratonovich transformation in the particle-particle channel identical to the one used in [120], to get

$$S_{\text{physical}} = -\langle \varphi | G_0^{-1} | \varphi \rangle - \frac{1}{g_0} \langle \eta | \eta \rangle + \langle \eta | \varphi_\downarrow \varphi_\uparrow \rangle + \langle \varphi_\downarrow \varphi_\uparrow | \eta \rangle \quad (\text{A.2})$$

where η is a bosonic field. We will consider a slightly more general action

$$S_{\text{bare}}[g_0] = -\langle \varphi | G_0^{-1} | \varphi \rangle - \langle \eta | g_0^{-1} | \eta \rangle + \langle \eta | \varphi_\downarrow \varphi_\uparrow \rangle + \langle \varphi_\downarrow \varphi_\uparrow | \eta \rangle \quad (\text{A.3})$$

where g_0 is an arbitrary operator. We introduce the (finite-volume) bare pressure

$$p_{\text{bare}}[g_0] := \frac{1}{\beta \mathcal{V}} \log \int \mathcal{D}[\varphi, \bar{\varphi}, \eta, \bar{\eta}] e^{-S_{\text{bare}}[g_0]} \quad (\text{A.4})$$

We can formally write for $z \in \mathbb{C}$

$$p_{\text{bare}}[z g_0] \stackrel{\text{Taylor}}{=} \sum_{n=0}^{\infty} z^n p_{\text{bare},n}[g_0] \quad (\text{A.5})$$

We would like to eliminate the ladder diagrams, which are built from the particle-particle bubble $\Pi_{\text{bubble}}[G_0]$:

$$\Pi_{\text{bubble}}[G_0](\mathbf{r}, \tau) := -G_0(\mathbf{r}, \tau)^2 \quad (\text{A.6})$$

and we call Γ_0 the sum of ladder diagrams. It is easy to see that for a given g_0 , Γ_0 satisfies the following operator equation

$$\Gamma_0^{-1} = g_0^{-1} - \Pi_{\text{bubble}}[G_0] \quad (\text{A.7})$$

Suppose that for a given Γ_0 we choose $g_0 = g_0(z)$ such that

$$g_0(z) := ((z\Gamma_0)^{-1} + \Pi_{\text{bubble}}[G_0])^{-1} \quad (\text{A.8})$$

We then define for a given Γ_0

$$p_{\text{ladd}}(z) := p_{\text{bare}}[g_0(z)] \quad (\text{A.9})$$

Then, one has

$$p_{\text{ladd}}(z) \underset{\text{Taylor}}{=} \sum_{n=0}^{\infty} z^n p_{\text{ladd},n}[\Gamma_0] \quad (\text{A.10})$$

The previous equation follows simply from the fact that an order- n Feynman diagram for the ladder scheme has n Γ_0 lines, so it will have a contribution proportional to z^n . We are then in the position to introduce the shifted action for the ladder scheme as

$$S_{\text{ladd}}^{(z)} := S_{\text{bare}}[g_0(z)] \quad (\text{A.11})$$

where Γ_0 is chosen to be the physical Γ_0 . The final result (Eq. (42)) is obtained by re-scaling η and $\bar{\eta}$ by \sqrt{z} ³⁶

B Interchanging thermodynamic and large-order limit

We have by hypothesis that $\lim_{\mathcal{V} \rightarrow \infty} \lim_{n \rightarrow \infty} \log \frac{\tilde{Z}_{\text{ladd},n}(\mathcal{V})}{\mathcal{V}} - \log \tilde{p}_n = 0$. One has

$$\log \frac{\tilde{Z}_{\text{ladd},n}(\mathcal{V})}{\mathcal{V}} = \log \tilde{z}_{\text{ladd},n,1} + \log \left(1 + \frac{\mathcal{V} \sum_{\mathcal{C}=2}^n \tilde{z}_{\text{ladd},n,\mathcal{C}} \mathcal{V}^{\mathcal{C}-2}}{\tilde{z}_{\text{ladd},n,1}} + O(e^{-\lambda \mathcal{V}^\alpha}) \right) \quad (\text{B.1})$$

Let $s_n := \log \tilde{p}_n - \log \tilde{z}_{\text{ladd},n,1}$. Suppose that for $\mathcal{C} > k$, $1 < k \leq n$, one has

$$\lim_{n \rightarrow \infty} \frac{\tilde{z}_{\text{ladd},n,\mathcal{C}}}{\tilde{z}_{\text{ladd},n,1}} = 0 \quad (\text{B.2})$$

and

$$\lim_{n \rightarrow \infty} \frac{\tilde{z}_{\text{ladd},n,k}}{\tilde{z}_{\text{ladd},n,1}} \neq 0 \quad (\text{B.3})$$

then one has $\lim_{\mathcal{V} \rightarrow \infty} \lim_{n \rightarrow \infty} \log \left(1 + \frac{\mathcal{V} \sum_{\mathcal{C}=2}^n \tilde{z}_{\text{ladd},n,\mathcal{C}} \mathcal{V}^{\mathcal{C}-2}}{\tilde{z}_{\text{ladd},n,1}} + O(e^{-\lambda \mathcal{V}^\alpha}) \right) - s_n = \lim_{\mathcal{V} \rightarrow \infty} (k-1) \log \mathcal{V} = \infty$ for every choice of s_n . Therefore, one has

$$\lim_{n \rightarrow \infty} \frac{\tilde{z}_{\text{ladd},n,\mathcal{C}}}{\tilde{z}_{\text{ladd},n,1}} = 0 \quad (\text{B.4})$$

for $\mathcal{C} > 1$, which implies $s_n = 0$.

³⁶This re-scaling does not produce any measurable effect as we will always compute quantities which are ratios of functional integrals.

C Renormalized Fredholm determinants

We consider the discretized Hilbert space $\mathcal{H}_b = L^2(\mathcal{L}_b \times [0, \beta])$, which consists in functions anti-periodic in imaginary time, where $\mathcal{L}_b := b\mathbb{Z}^3$ is the lattice of spacing b , with scalar product

$$\langle f|g \rangle := \sum_{\mathbf{x} \in b\mathbb{Z}^3} \int_0^\beta d\tau f^*(\mathbf{x}, \tau) g(\mathbf{x}, \tau) \quad (\text{C.1})$$

\mathcal{H}_b is separable, in the sense that there exists a countable orthonormal basis given by localized deltas of Kronecker in space and Matsubara plane waves. We define \mathcal{H}_0 as $L^2(\mathbb{R}^3 \times [0, \beta])$. For a (one-body) operator $\hat{O} : \mathcal{H}_b \rightarrow \mathcal{H}_b$ we define $|\hat{O}| := (\hat{O}^\dagger \hat{O})^{1/2}$. The trace of an operator \hat{O} is defined

$$\text{Tr } \hat{O} := \sum_{n=1}^{\infty} \langle \phi_n | \hat{O} \phi_n \rangle \quad (\text{C.2})$$

where $(\phi_n)_{n \in \mathbb{N}}$ is an orthonormal basis of \mathcal{H}_b .

(Trace-class operators): Let $b \geq 0$. We say that the operator $\hat{O} : \mathcal{H}_b \rightarrow \mathcal{H}_b$ is p -trace class for $p \in \mathbb{N}_+$ if

$$\|\hat{O}\|_p := (\text{Tr } |\hat{O}|^p)^{1/p} < \infty \quad (\text{C.3})$$

In his case, we write $\hat{O} \in \mathcal{C}_p$.

We will not try to introduce the determinant of operators formally, we will just suppose that we can extend the properties of the finite-dimensional version without difficulty. It can be shown that this can be done for Fredholm determinants:

(Fredholm determinant): Suppose $\hat{O} \in \mathcal{C}_1$. For $z \in \mathbb{C}$ we define

$$f(z) := \det(\mathbb{1} + z \hat{O}) \quad (\text{C.4})$$

Then, f is entire. More generally, $\det(\mathbb{1} + \hat{O}(z))$ is entire if $\hat{O}(z)$ is an entire function with values in \mathcal{C}_1 .

We will prove it for \hat{O} diagonalizable. The general proof can be found in [121]. We compute the determinant in the basis where \hat{O} is diagonal

$$f(z) = \prod_{n=1}^{\infty} (1 + z \lambda_n) =: \sum_{n=0}^{\infty} f_n z^n \quad (\text{C.5})$$

where λ_n is a left eigenvalue of \hat{O} such that $|\lambda_n| \geq |\lambda_{n+1}|$. One has

$$f_n = \sum_{i_1 < i_2 < \dots < i_n; i_1, i_2, \dots, i_n \in \mathbb{N}_+} \lambda_{i_1} \lambda_{i_2} \dots \lambda_{i_n} = \frac{1}{n!} \sum_{i_1, i_2, \dots, i_n \in \mathbb{N}_+, i_j \neq i_k} \lambda_{i_1} \lambda_{i_2} \dots \lambda_{i_n} \quad (\text{C.6})$$

One has

$$|f_n| \leq \frac{1}{n!} \sum_{i_1, i_2, \dots, i_n \in \mathbb{N}_+} |\lambda_{i_1} \lambda_{i_2} \dots \lambda_{i_n}| = \frac{\|\hat{O}\|_1^n}{n!} \quad (\text{C.7})$$

We have also proved that

Suppose $\hat{O} \in \mathcal{C}_1$. We have

$$|\det(\mathbb{1} + \hat{O})| \leq e^{\|\hat{O}\|_1} \quad (\text{C.8})$$

We now introduce the renormalized determinant

(Renormalized determinant): For $\hat{O} \in \mathcal{C}_n$, we define

$$\det_n(\mathbb{1} + \hat{O}) := \det \left[(\mathbb{1} + \hat{O}) \exp \left(\sum_{k=1}^{n-1} \frac{(-1)^k}{k} \hat{O}^k \right) \right] \quad (\text{C.9})$$

We justify now the definition of the renormalized determinant. Suppose $\hat{O} \notin \mathcal{C}_1$. Then the “bare” determinant

$$\det(\mathbb{1} + \hat{O}) = \prod_{j=1}^{\infty} (1 + \lambda_j) = \exp \left(\sum_{j=1}^{\infty} \log(1 + \lambda_j) \right) \quad (\text{C.10})$$

is not guaranteed to be well-defined, as the sum can be divergent in this case. The idea is to consider

$$\det_n(\mathbb{1} + \hat{O}) = \prod_{j=1}^{\infty} (1 + \lambda_j) e^{\sum_{k=1}^{n-1} (-\lambda_j)^k / k} = \exp \left[\sum_{j=1}^{\infty} \left(\log(1 + \lambda_j) + \sum_{k=1}^{n-1} (-\lambda_j)^k / k \right) \right] \quad (\text{C.11})$$

Using the fact that for some C

$$\left| \log(1 + x) + \sum_{k=1}^{n-1} (-x)^k / k \right| \leq C |x|^n \quad (\text{C.12})$$

one can write

$$\sum_{j=1}^{\infty} \left| \log(1 + \lambda_j) + \sum_{k=1}^{n-1} (-\lambda_j)^k / k \right| \leq C \|\hat{O}\|_n^n \quad (\text{C.13})$$

from which we see that the renormalized determinant is well-defined for $\hat{O} \in \mathcal{C}_n$.

Let $\hat{O} \in \mathcal{C}_n$. We introduce

$$f(z) := \det_n(\mathbb{1} + z \hat{O}) \quad (\text{C.14})$$

Then f is entire. More generally, $\det_n(\mathbb{1} + \hat{O}(z))$ is entire if $\hat{O}(z)$ is an entire function with values in \mathcal{C}_n .

We consider the function

$$f(z) := \det(\mathbb{1} + \sqrt{z} \hat{\Upsilon}) \quad (\text{C.15})$$

where we defined:

$$\hat{\Upsilon} := \begin{pmatrix} 0 & \hat{G}_0 \hat{\eta} \\ -\hat{G}_0^\dagger \hat{\eta}^\dagger & 0 \end{pmatrix} \quad (\text{C.16})$$

The operator $\hat{\Upsilon}$ is not trace-class 2 in the continuum limit.

$$\|\hat{\Upsilon}\|_2^2 := \text{Tr} \hat{\Upsilon}^\dagger \hat{\Upsilon} \underset{b \downarrow 0}{=} \infty \quad (\text{C.17})$$

Indeed

$$\begin{aligned} \text{Tr} \hat{\Upsilon}^\dagger \hat{\Upsilon} &= 2 \int dX |\eta(X)|^2 \int dY G_0(Y) G_0(Y) = \\ &= -2 \Pi_{\text{bubble}}[G_0](P=0) \int dX |\eta(X)|^2 \end{aligned} \quad (\text{C.18})$$

As $\Pi_{\text{bubble}}(P=0) \sim 1/b$ for small b , we would have to require that $\|\eta\|_2 = 0$, but this means that the field η must be zero almost everywhere. Let us compute

$$\begin{aligned} \|\hat{\Upsilon}\|_4^4 &= \text{Tr} [(\hat{\Upsilon}^\dagger \hat{\Upsilon})^2] = 2 \int dX dY DQ |\eta(X)|^2 |\eta(Y)|^2 e^{iQ(X-Y)} \times \\ &\times \int DP |G_0(P)|^2 |G_0(P+Q)|^2 \end{aligned} \quad (\text{C.19})$$

Let us introduce

$$\lambda(X) := |\eta(X)|^2 \quad (\text{C.20})$$

We can then write

$$\|\hat{\Upsilon}\|_4^4 = 2 \int DQ |\lambda_Q|^2 K_4(Q) \quad (\text{C.21})$$

where

$$K_4(Q) := \int DP |G_0(P)|^2 |G_0(P+Q)|^2 \quad (\text{C.22})$$

$K_4(Q)$ is well defined in the continuum limit. We can derive a simple bound on $\|\hat{\Upsilon}\|_4$

$$\|\hat{\Upsilon}\|_4^4 \leq C_4 \|\eta\|_4^4 \quad (\text{C.23})$$

where

$$C_4 := 2 \sup_Q |K_4(Q)| \quad (\text{C.24})$$

and

$$\|\eta\|_4^4 = \int dX |\eta(X)|^4 \quad (\text{C.25})$$

Let us show that $C_4 < \infty$. By using the Cauchy-Schwartz inequality, one has

$$C_4 = K_4(Q=0) = \int DP |G_0(P)|^4 = \frac{1}{\beta} \sum_{n \in \mathbb{Z}} \int \frac{d^3 p}{(\omega_n^2 + \xi_p^2)^2} \quad (\text{C.26})$$

We introduce $p_F := \sqrt{2m\mu}$ for $\mu > 0$ and $p_F = 0$ for $\mu < 0$. We divide the integral in two parts:

$$\begin{aligned} & \frac{1}{\beta} \sum_{n \in \mathbb{Z}} \int \frac{d^3 p}{(\omega_n^2 + \xi_p^2)^2} = \\ & = \frac{1}{\beta} \sum_{n \in \mathbb{Z}} \int_{p < p_F+1} \frac{d^3 p}{(\omega_n^2 + \xi_p^2)^2} + \frac{1}{\beta} \sum_{n \in \mathbb{Z}} \int_{p > p_F+1} \frac{d^3 p}{(\omega_n^2 + \xi_p^2)^2} =: I_1 + I_2 \end{aligned} \quad (\text{C.27})$$

We write

$$|I_1| \leq \frac{1}{\beta} \sum_{n \in \mathbb{Z}} \int_{p < p_F+1} \frac{d^3 p}{\omega_n^4} = \frac{(p_F+1)^3 \beta^3}{3\pi^6} \sum_{n=0}^{\infty} \frac{1}{(2n+1)^4} < \infty \quad (\text{C.28})$$

For I_2 , we use the identity

$$\frac{1}{(a_1 + a_2)^2} \leq \frac{1}{2a_1 a_2} \quad (\text{C.29})$$

We have

$$|I_2| \leq \frac{\beta}{\pi^2} \sum_{n=0}^{\infty} \frac{1}{(2n+1)^2} \int_{p > p_F+1} \frac{d^3 p}{\xi_p^2} \quad (\text{C.30})$$

There exists a constant C such that $\xi_p^2 \geq C_F^{-1} p^4$ for $p > p_F + 1$. We can then write

$$|I_2| \leq \frac{C_F \beta}{\pi^2} \sum_{n=0}^{\infty} \frac{1}{(2n+1)^2} \int_{p > p_F+1} \frac{d^3 p}{p^4} < \infty \quad (\text{C.31})$$

Therefore, we arrive at

Suppose that $\eta \in L^4(\mathbb{R}^3 \times [0, \beta])$. Then $\hat{\Upsilon} \in \mathcal{C}_4$.

We introduce

$$f_4(z) := \det_4(\mathbb{1} + \sqrt{z} \hat{\Upsilon}) \quad (\text{C.32})$$

From theorem (C.14), f_4 is an entire function of $w := \sqrt{z}$, that can be expanded in an always convergent power series (for $z \notin \mathbb{R}^-$)

$$f_4(z) = \sum_{n=0}^{\infty} f_{4,n} z^{n/2} \quad (\text{C.33})$$

Let $R > 0$ such that for $|z| < R$, $f_4(z) \neq 0$. One has $R > 0$ because an entire function is continuous and $f_4(0) = 1$. For $|z| < R$, we introduce

$$l_4(z) := \log f_4(z) = - \sum_{n=4}^{\infty} \frac{(-\sqrt{z})^n}{n} \text{Tr} \hat{\Upsilon}^n \quad (\text{C.34})$$

It is easy to show that for $n \in \mathbb{N}$

$$\text{Tr} \hat{\Upsilon}^{2n+1} = 0 \quad (\text{C.35})$$

so that for $|z| < R$

$$l_4(z) = - \sum_{n=2}^{\infty} \frac{z^n}{2n} \text{Tr} \hat{\Upsilon}^{2n} \quad (\text{C.36})$$

Exponentiating the previous equation one has for $|z| < R$

$$f_4(z) = \exp \left(- \sum_{n=2}^{\infty} \frac{z^n}{2n} \text{Tr} \hat{\Upsilon}^{2n} \right) = \sum_{n=0}^{\infty} f_{4,2n} z^n \quad (\text{C.37})$$

which proves that $f_{4,2n+1} = 0$. As this series converges for all $z \in \mathbb{C}$, we have that $f_4(z)$ is an entire function of z . We have then shown the following:

Suppose that $\eta \in L^4(\mathbb{R}^3 \times [0, \beta])$. We define

$$f_4(z) := \det_4(\mathbb{1} + \sqrt{z} \hat{\Upsilon}[\eta, \bar{\eta}]) \quad (\text{C.38})$$

with

$$\hat{\Upsilon}[\eta, \bar{\eta}] := \begin{pmatrix} 0 & \hat{G}_0 \hat{\eta} \\ -\hat{G}_0^\dagger \hat{\eta}^\dagger & 0 \end{pmatrix} \quad (\text{C.39})$$

$$\hat{\eta} := \int dX \eta(X) |X\rangle\langle X|, \quad \hat{G}_0 := \int DP G_0(P) |P\rangle\langle P| \quad (\text{C.40})$$

Then, f_4 is an entire function of z .

Let us discuss the bold case. In the bold case, one would have that $\hat{\Upsilon}$ is dependent on z

$$\hat{\Upsilon}(z) := \begin{pmatrix} 0 & \hat{G}_0(z) \hat{\eta} \\ -\hat{G}_0(z)^\dagger \hat{\eta}^\dagger & 0 \end{pmatrix} \quad (\text{C.41})$$

$\hat{\Upsilon}(z)$ is not an entire function of z , because

$$G_0^{-1}(z) = G^{-1} + \Sigma_{\text{bold}}[G, \Gamma, z] \quad (\text{C.42})$$

and Σ_{bold} is a function which have singularities at zero distance from the origin. Therefore, we cannot say that $f_4(z)$ in this case it is an entire function of z , and a different path has to be followed.

D Large-field behavior of the determinant

It is well known that the large external potential limit in quantum mechanics is given by a quasi-local approximation. Indeed, as the wavelength of the particle is proportional the inverse of the square root of the potential depth, the particle experience an essentially flat potential over one wavelength.

The integration over fermions gives the partition function of a (one-particle) imaginary-time quantum-mechanical system with a (pairing) external potential, with anti-periodic boundary conditions in the imaginary-time direction. It seems clear physically that we can apply therefore the quasi-local (or Thomas-Fermi) approximation. We just need now to justify this physical picture.

It is easier to compute the large- z behavior of the logarithmic derivative of

\det_4 :

$$\begin{aligned}
& \frac{d}{dz} \log \det_4(1 + \sqrt{z} \hat{Y}) = \\
& = \langle \eta | \Pi_{\text{bubble}}[G_0] | \eta \rangle + \frac{d}{dz} \log \frac{\int \mathcal{D}[\varphi, \bar{\varphi}] e^{\langle \varphi | G_0^{-1} | \varphi \rangle - \sqrt{z} (\langle \eta | \varphi_{\downarrow} \varphi_{\uparrow} \rangle + \langle \varphi_{\downarrow} \varphi_{\uparrow} | \eta \rangle)}}{\int \mathcal{D}[\varphi, \bar{\varphi}] e^{\langle \varphi | G_0^{-1} | \varphi \rangle}} = \\
& = \langle \eta | \Pi_{\text{bubble}}[G_0] | \eta \rangle - \frac{1}{2\sqrt{z}} (\langle \eta | \langle \varphi_{\downarrow} \varphi_{\uparrow} \rangle_{M(z)} \rangle + \langle \langle \varphi_{\downarrow} \varphi_{\uparrow} \rangle_{M(z)} | \eta \rangle)
\end{aligned} \tag{D.1}$$

where

$$\langle \cdot \rangle_{M(z)} := \frac{\int \mathcal{D}[\phi, \bar{\phi}] e^{\langle \phi | M^{-1}(z) | \phi \rangle}}{\int \mathcal{D}[\phi, \bar{\phi}] e^{\langle \phi | M^{-1}(z) | \phi \rangle}}. \tag{D.2}$$

$$(M(z))^{-1} = \begin{pmatrix} G_{0;\uparrow}^{-1} & \sqrt{z} \eta \\ \sqrt{z} \bar{\eta} & -G_{0;\downarrow}^{-1} \end{pmatrix} \tag{D.3}$$

and ϕ is a Nambu field

$$\phi := \begin{pmatrix} \varphi_{\uparrow} \\ \bar{\varphi}_{\downarrow} \end{pmatrix}, \quad \bar{\phi} := (\bar{\varphi}_{\uparrow} \quad \varphi_{\downarrow}) \tag{D.4}$$

We then have

$$\begin{aligned}
& \frac{d}{dz} \log \det_4(1 + \sqrt{z} \hat{Y}) = \langle \eta | \Pi_{\text{bubble}}[G_0] | \eta \rangle + \\
& + \frac{1}{2\sqrt{z}} \int_X (\bar{\eta}(X) M_{12}^{(z)}(X, X) + M_{21}^{(z)}(X, X) \eta(X))
\end{aligned} \tag{D.5}$$

We write

$$M^{(z)} = -D^{(z)} \begin{pmatrix} -G_{0;\downarrow}^{-1} & -\sqrt{z} \eta \\ -\sqrt{z} \bar{\eta} & G_{0;\uparrow}^{-1} \end{pmatrix} \tag{D.6}$$

where

$$[(G_{0;\uparrow}^{-1} G_{0;\downarrow}^{-1} + z \bar{\eta} \eta) D^{(z)}] (X, Y) = \delta(X - Y) \tag{D.7}$$

Let us study this equation for $D^{(z)}$ in the limit $z \rightarrow \infty$. Suppose we set up a perturbation theory starting from the local term $z|\eta|^2$, which could dominate in the $z \rightarrow \infty$. The solution at order zero would be

$$D_{\text{first try}}^{(z)}(X, Y) = \frac{\delta(X - Y)}{z|\eta(X)|^2} \tag{D.8}$$

but then the first perturbative correction $G_{0;\uparrow}^{-1} G_{0;\downarrow}^{-1} D_{\text{first try}}^{(z)}$ would be of order $\frac{1}{b^4}$, and we could not take the continuum limit $b \downarrow 0$ before the $z \rightarrow \infty$ limit. We

need to look for a smeared delta solution which is smooth at the space scale b (and similarly for imaginary time). $D^{(z)}$ will have a width of order $|z|^{-1/4}$ in space and $|z|^{-1/2}$ in imaginary time. The local solution $\sim \delta(X - Y)$ is reproduced only in the limit $z \rightarrow \infty$. We define the Thomas-Fermi length l_{TF} and the Thomas-Fermi time τ_{TF} as

$$l_{TF}(Y) := \frac{1}{\sqrt{m} |z^{1/2} \eta(Y)|}, \quad \tau_{TF}(Y) := \frac{1}{|z^{1/2} \eta(Y)|} \quad (\text{D.9})$$

Let b the lattice spacing and ϵ_τ the discretization length of imaginary time (the one that was introduced to construct the functional integral). One has to impose

$$l_{TF}(Y) \gg b, \quad \tau_{TF}(Y) \gg \epsilon_\tau \quad (\text{D.10})$$

in order for the width to be well defined. Let l_η and τ_η the typical length and time scale of the η field. In the Thomas-Fermi region $|\mathbf{x} - \mathbf{y}| \lesssim l_{TF}(Y)$, $|x_4 - y_4| \lesssim \tau_{TF}(Y)$, one has

$$\frac{|\eta(X)|^2 - |\eta(Y)|^2}{|\eta(Y)|^2} = O\left(\frac{l_{TF}(Y)}{l_\eta}, \frac{\tau_{TF}(Y)}{\tau_\eta}\right) \quad (\text{D.11})$$

which is of order $|z|^{-1/4}$. In this region, we can write the approximated equation:

$$(G_{0,\uparrow}^{-1} G_{0,\downarrow}^{-\dagger} D_{TF}^{(z)})(X, Y) + z |\eta(Y)|^2 D_{TF}^{(z)}(X, Y) = \delta(X - Y) \quad (\text{D.12})$$

whose solution defines $D_{TF}^{(z)}$:

(Thomas-Fermi ansatz):

$$D_{TF}^{(z)}(X, Y) = \int DP \frac{e^{iP(X-Y)}}{G_{0,\uparrow}^{-1}(P) G_{0,\downarrow}^{-1}(-P) + z |\eta(Y)|^2} \quad (\text{D.13})$$

which is just the propagator for a quasi-local configuration. We write

$$D^{(z)} = D_{TF}^{(z)} + \sum_{n=1}^{\infty} D_{TF,n}^{(z)} \quad (\text{D.14})$$

where

$$[(D_{TF}^{(z)})^{-1} D_{TF,n+1}^{(z)}](X, Y) := z(|\eta(Y)|^2 - |\eta(X)|^2) D_{TF,n}^{(z)}(X, Y) \quad (\text{D.15})$$

We introduce for each $f(X, Y)$

$$f(P|Y) := \int dX e^{-iPX} f(X + Y, Y) \quad (\text{D.16})$$

One has

$$\begin{aligned} D_{TF, n+1}^{(z)}(P|Y) = & \\ - \sum_{(n_x, n_y, n_z, l) \neq (0, 0, 0, 0)} & \frac{z [(i\partial_x)^{n_x} (i\partial_y)^{n_y} (i\partial_z)^{n_z} (i\partial_\tau)^l |\eta(Y)|^2]}{n_x! n_y! n_z! l!} \times \\ \times D_{TF}^{(z)}(P|Y) \partial_{p_x}^{n_x} \partial_{p_y}^{n_y} \partial_{p_z}^{n_z} \partial_\omega^l & D_{TF, n}^{(z)}(P|Y) \end{aligned} \quad (\text{D.17})$$

We introduce

$$d_{n_x, n_y, n_z, l, k}^{(z)}(P|Y) := p_x^{n_x} p_y^{n_y} p_z^{n_z} \omega^l \left(D_{TF}^{(z)}(P|Y) \right)^k \quad (\text{D.18})$$

One has for $z \rightarrow \infty$

$$d_{n_x, n_y, n_z, l, k}^{(z)}(Y, Y) = O(z^{(n_x + n_y + n_z + 2l + 5 - 4k)/4}) \quad (\text{D.19})$$

We see therefore that we have to bound the maximal P power of $D_{TF, n}^{(z)}$. Suppose that $D_{TF, n}^{(z)}$ has a certain P power. Then, $D_{TF, n+1}^{(z)}$ has at least two $D_{TF, n}^{(z)}$ more and three p more, that gives a factor $O(z^{(3-8)/4}) = O(z^{-5/4})$. Putting the pieces together, one has

$$\begin{aligned} O(D_{TF, n+1}^{(z)}(Y, Y)) &= O(z) O(z^{-5/4}) O(D_{TF, n}^{(z)}(Y, Y)) = \\ &= O(z^{-1/4}) O(D_{TF, n}^{(z)}(Y, Y)) \end{aligned} \quad (\text{D.20})$$

We see that the correction is of the order we expected: neglecting the space variation of $|\eta|^2$ gives a factor $z^{-1/4}$ more at most (an imaginary time variation would have given a factor $z^{-1/2}$). We have then shown that $D_{TF}^{(z)}$ is the dominant term for $z \rightarrow \infty$. Using the definition of $M^{(z)}$ (equation D.6), we have

$$(M_{TF}^{(z)})_{12}(X, Y) = \sqrt{z} \int DP \frac{e^{iP(X-Y)} \eta(Y)}{G_{0,\uparrow}^{-1}(P) G_{0,\downarrow}^{-1}(-P) + z |\eta(Y)|^2} \quad (\text{D.21})$$

We can write

$$\begin{aligned} \frac{d}{dz} \log \det_4(1 + \sqrt{z} \hat{Y}) &= \langle \eta | \tilde{\Pi}_0 | \eta \rangle + \\ + z \int dX DP & \frac{|\eta(X)|^4}{G_{0,\uparrow}^{-1}(P) G_{0,\downarrow}^{-1}(-P) [G_{0,\uparrow}^{-1}(P) G_{0,\downarrow}^{-1}(-P) + z |\eta(X)|^2]} + O(1) \end{aligned} \quad (\text{D.22})$$

where

$$\tilde{\Pi}_0(P) := \Pi_{\text{bubble}}(P) - \Pi_{\text{bubble}}(P=0) \quad (\text{D.23})$$

$\tilde{\Pi}_0$ admits a continuous limit, unlike Π_{bubble} . In the integral over P for large $z|\eta(X)|^2$, only the large P momentum behavior is important. In this limit, we obtain

$$\frac{d}{dz} \log \det_4(\mathbb{1} + \sqrt{z}\hat{Y}) = -\frac{5}{4}z^{1/4}g_{TF} \int dX |\eta(X)|^{5/2} + O(1) \quad (\text{D.24})$$

where

$$g_{TF} := \frac{4}{5} \int \frac{d^3k}{(2\pi)^3} \left(\frac{1}{k^2} - \frac{1}{\sqrt{k^4+4}} \right) = \frac{4}{5} \frac{\Gamma(3/4)^2}{\sqrt{2\pi}\pi^2} = 0.0485588\dots \quad (\text{D.25})$$

so that \det_4 is an entire function of order $5/4$:

$$\det_4(\mathbb{1} + \sqrt{z}\hat{Y}) \underset{z \rightarrow \infty}{=} \exp \left(-g_{TF} z^{5/4} \int dX |\eta(X)|^{5/2} + O(z) \right) \quad (\text{D.26})$$

Let us briefly discuss the bold case. In this case, one has to take the limit where $z \rightarrow 0$ and $z|\eta|^2$ goes to infinity, as discussed in the dissertation. For small z , we write $G_0(z) = G + O(z)$. As G and G_0 share the same asymptotic behavior when $P \rightarrow \infty$, the Thomas-Fermi computation is the same.

E No imaginary-time dependence of the instanton

The stationary point equation that minimize the action can be written

$$-\Gamma_0^{-1}|\lambda_c\rangle = \frac{(\bar{\lambda}_c^{1/4}\lambda_c^{5/4})(\mathbf{r}, \tau)}{\sum_{\mathbf{r}} \int d\tau |\lambda_c(\mathbf{r}, \tau)|^{5/2}} \quad (\text{E.1})$$

$$-\langle \lambda_c | \Gamma_0^{-1} = \frac{(\bar{\lambda}_c^{5/4}\lambda_c^{1/4})(\mathbf{r}, \tau)}{\sum_{\mathbf{r}} \int d\tau |\lambda_c(\mathbf{r}, \tau)|^{5/2}} \quad (\text{E.2})$$

Dividing Γ_0^{-1} in its real and imaginary parts

$$\Gamma_{0,R}^{-1} := \frac{\Gamma_0^{-1} + \Gamma_0^{-\dagger}}{2}, \quad \Gamma_{0,I}^{-1} := \frac{\Gamma_0^{-1} - \Gamma_0^{-\dagger}}{2i} \quad (\text{E.3})$$

one has

$$\Gamma_{0,I}^{-1}|\lambda_c\rangle = 0 \quad (\text{E.4})$$

$$-\Gamma_{0,R}^{-1}|\lambda_c\rangle = \frac{(\bar{\lambda}_c^{1/4}\lambda_c^{5/4})(\mathbf{r}, \tau)}{\int d\mathbf{r}, \tau |\lambda_c(\mathbf{r}, \tau)|^{5/2}} \quad (\text{E.5})$$

A simple consequence is

$$-\langle \lambda_c | \Gamma_{0,R}^{-1} | \lambda_c \rangle = 1 \quad (\text{E.6})$$

Translation invariance, rotation invariance, and hermicity imply

$$\Gamma_{0,R}^{-1}(\mathbf{p}, \pm|p_4|) = \Gamma_{0,R}^{-1}(|\mathbf{p}|, |p_4|), \quad \Gamma_{0,I}^{-1}(\mathbf{p}, \pm|p_4|) = \pm\Gamma_{0,I}^{-1}(|\mathbf{p}|, |p_4|) \quad (\text{E.7})$$

where \mathbf{p} is the momentum and $p_4 \in 2\pi\mathbb{Z}/\beta$ is the Matsubara frequency. From (E.4), we have for every momentum P

$$\Gamma_{0,I}^{-1}(\mathbf{p}, p_4) = 0 \quad \vee \quad \lambda_c(\mathbf{p}, p_4) = 0 \quad (\text{E.8})$$

Let us note first that $\Gamma_{0,I}^{-1}(\mathbf{p}, 0) = 0$. Using the explicit formula from [12], one has

$$\Gamma_{0,I}^{-1}(\mathbf{p}, p_4) = p_4 \int_{\mathbb{R}^3} \frac{d^3k}{(2\pi)^3} \frac{1 - n^{(0)}(\mathbf{p}/2 + \mathbf{k}) - n^{(0)}(\mathbf{p}/2 - \mathbf{k})}{p_4^2 + (2\mu - |\mathbf{p}|^2/4 - k^2)^2} \quad (\text{E.9})$$

so one has the condition

$$\int_{\mathbb{R}^3} \frac{d^3k}{(2\pi)^3} \frac{1 - n^{(0)}(\mathbf{p}/2 + \mathbf{k}) - n^{(0)}(\mathbf{p}/2 - \mathbf{k})}{p_4^2 + (2\mu - |\mathbf{p}|^2/4 - k^2)^2} \neq 0 \quad (\text{E.10})$$

F Sobolev bound

In this section, we will use the spatial norm $\|\lambda\|_\alpha := (\int d^3x |\lambda(\mathbf{x})|^\alpha)^{1/\alpha}$. We call $R_0^{1/2}$ the square root of the positive operator R_0 . We write

$$A_S[\lambda] = \frac{\|R_0^{-1/2}\lambda\|_2^2}{\|\lambda\|_{5/2}^2} = \frac{\|\tilde{\lambda}\|_2^2}{\|R_0^{1/2}\tilde{\lambda}\|_{5/2}^2} \quad (\text{F.1})$$

where $\tilde{\lambda} = R_0^{-1/2}\lambda$. As $R_0^{1/2}$ is translation-invariant, its action on $\tilde{\lambda}$ can be written as a convolution in the space-time representation (let $\tilde{r}_0(\mathbf{x} - \mathbf{y}) := \langle \mathbf{x} | R_0^{1/2} | \mathbf{y} \rangle$)

$$\|R_0^{1/2}\tilde{\lambda}\|_{5/2} = \|\tilde{r}_0 * \tilde{\lambda}\|_{5/2} \leq \|\tilde{r}_0\|_{\frac{10}{9}} \|\tilde{\lambda}\|_2 \quad (\text{F.2})$$

where we used Young's inequality $\|f * g\|_r \leq \|f\|_p \|g\|_q$, which is valid for $1/p + 1/q = 1/r + 1$. We therefore have proved that

$$A_S[\lambda] \geq \|\tilde{r}_0\|_{\frac{10}{9}}^{-2} \quad (\text{F.3})$$

We now prove that $\|\tilde{r}\|_{10/9}$ is finite. For small \mathbf{p} , rotation invariance and positivity implies

$$R_0^{-1}(\mathbf{p}) = -\mu_B + \frac{p^2}{2m_B} + O(p^4) \quad (\text{F.4})$$

with $\mu_B < 0$ and $m_B > 0$. We see therefore that $\tilde{r}(\mathbf{x})$ goes to zero exponentially for large $|\mathbf{x}|$. For large \mathbf{p} , one has [122]

$$R_0^{-1}(\mathbf{p}) \underset{|\mathbf{p}| \rightarrow \infty}{=} \frac{1}{4\pi} \sqrt{\frac{|\mathbf{p}|^2}{4} - 2\mu} \propto |\mathbf{p}| \quad (\text{F.5})$$

This implies that for small $|\mathbf{r}|$, the function \tilde{r} will have a power-law singularity

$$\tilde{r}(\mathbf{r}) \underset{|\mathbf{r}| \rightarrow 0}{\propto} |\mathbf{r}|^{-3/2} \quad (\text{F.6})$$

which nevertheless gives a finite 10/9 norm.

G Variational principle

Suppose $\lambda \in \text{argmin } A_S[\lambda']$. Then by functional derivation we obtain

$$R_0^{-1}|\lambda\rangle = -\langle \lambda | R_0^{-1} | \lambda \rangle \frac{\bar{\lambda}^{1/4} \lambda^{5/4}}{\int d^3x |\lambda(\mathbf{x})|^{5/2}} \quad (\text{G.1})$$

We consider the equation for $\rho > 0$

$$R_0^{-1}|\lambda_\rho\rangle = \rho \bar{\lambda}_\rho^{1/4} \lambda_\rho^{5/4} \quad (\text{G.2})$$

Then one has

$$\lambda_\rho = \frac{\lambda_1}{\rho^2} \quad (\text{G.3})$$

Moreover, λ_ρ is a solution of equation (G.1) for every ρ . Then, as (E.5) is the equation G.2 for some $\rho = \rho_c$, this means that λ_c satisfies the same equation as λ_{ρ_c} . We note that the functional $A_S[\lambda]$ is invariant under dilation $w \in \mathbb{C} \setminus \{0\}$, translation of $\mathbf{r}_0 \in \mathbb{R}^3$ and rotation by R :

$$A_S[\lambda] = A_S[\lambda'] \quad (\text{G.4})$$

where $\lambda'(\mathbf{r}) = w \lambda(R\mathbf{r} + \mathbf{r}_0)$.

H High and low temperature limits of the action functional

For $s \in \mathbb{R}$, we define

$$\lambda_s(\mathbf{r}) := \lambda(e^s \mathbf{r}) \quad (\text{H.1})$$

and we define (in momentum space)

$$R_s^{-1}(\mathbf{p}) := R_0^{-1}(e^s \mathbf{p}) \quad (\text{H.2})$$

By explicating the dependence of A_S on R_0 , one has

$$A_S[R_0, \lambda_s] = e^{-\frac{3s}{5}} A_S[R_s, \lambda] \quad (\text{H.3})$$

For $\beta\mu \rightarrow -\infty$ or $|\mathbf{p}| \rightarrow \infty$, one has [12]

$$R_0^{-1}(\mathbf{p}) = \frac{1}{4\pi} \sqrt{\frac{|\mathbf{p}|^2}{4} - 2\mu} + O(e^{\beta\mu}) \quad (\text{H.4})$$

Let $\mu(x) = \mu_0 e^x$, with $\mu_0 < 0$. By choosing $s = x/2$, one has for $\mu_0 \rightarrow -\infty$

$$A_S[R_0(\mu(x)), \lambda_s] = e^{\frac{x}{5}} A_S[R_0(\mu_0), \lambda] \quad (\text{H.5})$$

Let $f^{(x)}$ the field that minimizes $A_S(\mu(x))$ for chemical potential equal to $\mu(x)$, and let $A_S(\mu(x)) = A_S[R_0(\mu(x)), f^{(x)}]$ be this minimal value. Then, using equation (H.3), we write

$$A_S(\mu(x)) = A_S[R_0(\mu(x)), f^{(x)}] = e^{x/5} A_S[R_0(\mu_0), f_{-x/2}^{(x)}] \geq e^{x/5} A_S(\mu_0) \quad (\text{H.6})$$

that implies that $A_S(\mu)$ goes to infinity as least as fast as $(-\mu)^{1/5}$ when $\mu \rightarrow -\infty$. Let us consider the low-temperature limit, where T approach $T_c^{(0)}$ from above. In this limit, one has

$$R_0^{-1}(\mathbf{p}) = -\mu_B + \frac{p^2}{2m_B} + O(p^4) \quad (\text{H.7})$$

where $\mu_B = 0$ at $T = T_c^{(0)}$. For simplicity, we will consider the case where $\mu_B \uparrow 0$ with m_B fixed. We write $\mu_B(x) = e^x \mu_B$, we choose $s = x/2$. One has

$$R_0^{-1}(e^{x/2} p) = e^x \left(-\mu_B + \frac{p^2}{2m_B} + O(e^x) \right) \quad (\text{H.8})$$

so that for $\mu_B \rightarrow -\infty$ one has

$$A_S(\mu_B(x)) \leq A_S[R_0(\mu_B(x)), \lambda_s] = e^{\frac{7x}{10}} A_S[R_0(\mu_B), \lambda] \quad (\text{H.9})$$

so that in this limit one has that $A_S(\mu_B)$ goes to zero at least like $|\mu_B|^{-\frac{7}{10}}$.

I Symmetric decreasing rearrangement

We use the theory of symmetric (or radial) decreasing rearrangements in order to prove that the instanton solution can be chosen real and radial. For a non-negative continuous function $f(\mathbf{r}) \geq 0$, we define the symmetric decreasing rearrangement $f^\sharp : \mathbb{R}^3 \rightarrow \mathbb{R}^+$ by

$$f^\sharp(\mathbf{r}) = t \tag{I.1}$$

where t is chosen to satisfy $\text{Vol}\{\mathbf{x} \in \mathbb{R}^3 \mid f(\mathbf{x}) \geq t\} = 4\pi|\mathbf{r}|^3/3$. f^\sharp has these properties

- f^\sharp is a radial function ($f^\sharp(\mathbf{x}) = f^\sharp(\mathbf{y})$ if $|\mathbf{x}| = |\mathbf{y}|$)
- $f^\sharp(\mathbf{r}) \geq 0$
- $\frac{d}{dx} f^\sharp(x \mathbf{r}) < 0$

Inversely, these properties characterize a symmetric decreasing arranged function, $f = |f|^\sharp$ if and only if the above properties are satisfied for f . The norm is not changed by the rearrangement

$$\|f\|_\alpha = \||f|^\sharp\|_\alpha \tag{I.2}$$

We now prove a rearrangement inequality (the proof was provided on *mathoverflow.net* by Christian Remling, but we reproduce it here)

$$\|f * g\|_p \leq \||f|^\sharp * |g|^\sharp\|_p \tag{I.3}$$

We will use this version of the Hölder inequality

$$\|u\|_p = \sup_{\|h\|_q=1} \|h u\|_1 \tag{I.4}$$

with $1/p + 1/q = 1$. We write

$$\|f * g\|_p \leq \||f| * |g|\|_p = \sup_{\|h\|_q=1} \|h(|f| * |g|)\|_1 \tag{I.5}$$

We now use Riesz rearrangement inequality

$$\begin{aligned} \sup_{\|h\|_q=1} \|h(|f| * |g|)\|_1 &= \sup_{\|h\|_q=1} \||h|(|f| * |g|)\|_1 \leq \\ &\leq \sup_{\|h\|_q=1} \||h|^\sharp(|f|^\sharp * |g|^\sharp)\|_1 = \sup_{\|h\|_q=1} \||h|^\sharp(|f|^\sharp * |g|^\sharp)\|_1 = \\ &= \||f|^\sharp * |g|^\sharp\|_p \end{aligned} \tag{I.6}$$

□

With the same notations as in section F, using (I.3) one has

$$A_S[\lambda] = \tilde{A}_S[\tilde{\lambda}] := \frac{\|\tilde{\lambda}\|_2^2}{\|\tilde{r} * \tilde{\lambda}\|_{5/2}^2} \geq \frac{\|\tilde{\lambda}^\sharp\|_2^2}{\|\tilde{r}^\sharp * \tilde{\lambda}^\sharp\|_{5/2}^2} \quad (\text{I.7})$$

If we assume that

$$\tilde{r}(\mathbf{r}) = |\tilde{r}^\sharp(\mathbf{r})| \quad (\text{I.8})$$

we have proved

$$\tilde{A}_S[\tilde{\lambda}] \geq \tilde{A}_S[|\tilde{\lambda}^\sharp|] \quad (\text{I.9})$$

that implies that we can choose $\tilde{\lambda}_c = |\tilde{\lambda}_c^\sharp| > 0$. In particular, we find that

$$\lambda_c = R_0^{1/2} \tilde{\lambda}_c \quad (\text{I.10})$$

is a radial real function.

J Gaussian zero modes

Suppose that the action is invariant by $S_{\text{eff}}[\eta, \bar{\eta}] = S_{\text{eff}}[T_\alpha \eta, \bar{T}_\alpha \bar{\eta}]$, where α is a real number and T_α is some operator acting on η . Suppose that $T_\alpha \eta_c \neq \eta_c$. We write

$$T_\alpha \eta_c = \eta_c + \alpha \partial_\alpha \eta_c + \alpha^2 \partial_{\alpha\alpha} \eta_c / 2 + O(\alpha^3) \quad (\text{J.1})$$

Let $\partial_\alpha \eta_c = v_R^{(0)} + i v_I^{(0)}$. Then

$$\begin{aligned} S_{\text{eff}}[T_\alpha \eta_c, \bar{T}_\alpha \bar{\eta}_c] - S_{\text{eff}}[\eta_c, \bar{\eta}_c] &= \\ &= \frac{\alpha^2}{2} (v_R^{(0)} \quad v_I^{(0)}) S_{\text{eff},2}[\eta_c, \bar{\eta}_c] \begin{pmatrix} v_R^{(0)} \\ v_I^{(0)} \end{pmatrix} + O(\alpha^3) = 0 \end{aligned} \quad (\text{J.2})$$

We see therefore that $S_{\text{eff},2}[\eta_c, \bar{\eta}_c] \begin{pmatrix} v_R^{(0)} \\ v_I^{(0)} \end{pmatrix} = 0$. In our case the role of α is played by an angle $\alpha_0 := \theta \in (\pi, \pi]$ and a translation vector $\vec{\alpha} := \mathbf{r}_0 \in \mathbb{R}^3$, as $S_{\text{eff}}[\eta_c, \bar{\eta}_c] = S_{\text{eff}}[\eta'_c, \bar{\eta}'_c]$, where $\eta'_c(\mathbf{r}) = (T_\alpha \eta_c)(\mathbf{r}) = e^{i\theta} \eta_c(\mathbf{r} + \mathbf{r}_0)$. The rotation invariance and the time translation invariance are unbroken. We can then write the zero modes $\{v_l^{(0)}\}_{0 \leq l \leq 3}$ (we have chosen $\eta_c(\mathbf{r})$ real):

$$v_0^{(0)}(\mathbf{r}, r_4) = i e^{i\theta} \eta_c(\mathbf{r} + \mathbf{r}_0) = \begin{pmatrix} -\sin \theta \eta_c(\mathbf{r} + \mathbf{r}_0) \\ \cos \theta \eta_c(\mathbf{r} + \mathbf{r}_0) \end{pmatrix} \quad (\text{J.3})$$

$$v_j^{(0)}(\mathbf{r}, r_4) = e^{i\theta} \partial_j \eta_c(\mathbf{r} + \mathbf{r}_0) = \begin{pmatrix} \cos \theta \partial_j \eta_c(\mathbf{r} + \mathbf{r}_0) \\ \sin \theta \partial_j \eta_c(\mathbf{r} + \mathbf{r}_0) \end{pmatrix} \quad (\text{J.4})$$

for $j \in \{1, 2, 3\}$. We introduce the scalar product that is natural for the Gaussian integration:

$$v \cdot u := \int dX (v_R u_R + v_I u_I)(X) \quad (\text{J.5})$$

The zero modes are orthogonal:

$$v_0^{(0)} \cdot v_j^{(0)} = 0 \quad (\text{J.6})$$

$$\begin{aligned} v_i^{(0)} \cdot v_j^{(0)} &= \int_0^\beta dr_4 \int d^3\mathbf{r} \partial_i \eta_c(\mathbf{r}) \partial_j \eta_c(\mathbf{r}) = \\ &= \delta_{ij} \frac{\beta}{3} \int d^3\mathbf{r} (f'_c(|\mathbf{r}|))^2 =: \delta_{ij} \|v_i^{(0)}\|_2^2 \end{aligned} \quad (\text{J.7})$$

$$v_0^{(0)} \cdot v_0^{(0)} = \int_0^\beta dr_4 \int d^3\mathbf{r} \bar{\eta}_c(\mathbf{r}) \eta_c(\mathbf{r}) = \beta \int d^3\mathbf{r} |\eta_c(\mathbf{r})|^2 =: \|v_0^{(0)}\|_2^2 \quad (\text{J.8})$$

where $i, j \in \{1, 2, 3\}$ and $\eta_c(\mathbf{r}) = f_c(|\mathbf{r}|)$. To simplify the computation, we will assume that θ and \mathbf{r}_0 are very small. In this limit, we can parametrize a general η field in this way

$$\eta(\mathbf{r}, r_4) = \eta_c(\mathbf{r}) + \sum_{n=0}^{\infty} a_n v_n(\mathbf{r}, r_4) \quad (\text{J.9})$$

where the first four terms in the sum are given by the zero-modes at zero θ and \mathbf{r}_0

$$a_0 := \theta \|v_0^{(0)}\|_2, \quad a_j := (\mathbf{r}_0)_j \|v_j^{(0)}\|_2 \quad (\text{J.10})$$

for $j \in \{1, 2, 3\}$, and

$$v_l(\mathbf{r}, r_4) := \frac{v_l^{(0)}}{\|v_l^{(0)}\|_2} \quad (\text{J.11})$$

for $l \in \{0, 1, 2, 3\}$, and $\{v_n\}_{n \geq 4}$ is a basis (that we assume numerable for simplicity) of the space orthogonal to $\{v_l^{(0)}\}_{0 \leq l \leq 3}$. As $\{v_n\}_{n \geq 0}$ is an orthonormal basis, the change of variables from $\eta(\mathbf{r}, r_4)$ to a_n has unitary Jacobian

$$\mathcal{D}[\eta, \bar{\eta}] = \prod_{n=0}^{\infty} da_n = \left(\prod_{l=0}^3 \|v_l^{(0)}\|_2 \right) d\theta d^3\mathbf{r}_0 \prod_{n=4}^{\infty} da_n \quad (\text{J.12})$$

By translation (and θ) invariance, this result must be true for every \mathbf{r}_0 and θ . Note that each of the norms is proportional to \sqrt{n} .

K Gaussian integration

We introduce

$$U[\eta, \bar{\eta}] := -\frac{4n}{5} \log \int dX |\eta(X)|^{5/2} \quad (\text{K.1})$$

In this section we use the norm

$$\|f\|_{5/2} = \left(\int dX |f(X)|^{5/2} \right)^{2/5} \quad (\text{K.2})$$

One has (we remind that $\eta_c = \sqrt{n} \eta_c$)

$$\frac{\delta^2 U[\eta_c, \bar{\eta}_c]}{\delta \bar{\eta}(X) \delta \bar{\eta}(Y)} = \frac{1}{(2\|\lambda_c\|_{5/2})^2} \left[-(u_c(\mathbf{x}))^{1/2} \delta(X - Y) + 5(u_c(\mathbf{x})u_c(\mathbf{y}))^{3/2} \right] \quad (\text{K.3})$$

$$\frac{\delta^2 U[\eta_c, \bar{\eta}_c]}{\delta \bar{\eta}(X) \delta \eta(Y)} = \frac{5}{(2\|\lambda_c\|_{5/2})^2} \left[-(u_c(\mathbf{x}))^{1/2} \delta(X - Y) + (u_c(\mathbf{x})u_c(\mathbf{y}))^{3/2} \right] \quad (\text{K.4})$$

where we have chosen $\eta_c(\mathbf{x})$ real and $u_c(\mathbf{x}) := \eta_c(\mathbf{x})/\|\eta_c\|_{5/2}$. One has

$$\begin{aligned} U_{RR}(X, Y) &:= \frac{1}{2} \frac{\delta^2 U[\eta_c, \bar{\eta}_c]}{\delta \eta_R(X) \delta \eta_R(Y)} = \\ &= \frac{1}{2\|\lambda_c\|_{5/2}^2} \left[-3(u_c(\mathbf{x}))^{1/2} \delta(X - Y) + 5(u_c(\mathbf{x})u_c(\mathbf{y}))^{3/2} \right] \end{aligned} \quad (\text{K.5})$$

$$U_{RI}(X, Y) := \frac{\delta^2 U[\eta_c, \bar{\eta}_c]}{\delta \eta_R(X) \delta \eta_I(Y)} = 0$$

$$U_{II}(X, Y) := \frac{1}{2} \frac{\delta^2 U[\eta_c, \bar{\eta}_c]}{\delta \eta_I(X) \delta \eta_I(Y)} = \frac{1}{\|\lambda_c\|_{5/2}^2} \left[-(u_c(\mathbf{x}))^{1/2} \delta(X - Y) \right]$$

We have then

$$S_{\text{eff},2} = \begin{pmatrix} -\Gamma_{0,R}^{-1} + U_{RR} & -i\Gamma_{0,I}^{-1} \\ i\Gamma_{0,I}^{-1} & -\Gamma_{0,R}^{-1} + U_{II} \end{pmatrix} \quad (\text{K.6})$$

Let us verify that $S_{\text{eff},2}$ has $i\lambda_c(\mathbf{r})$ and $\partial_j \lambda_c(\mathbf{r})$ as zero modes. For the θ mode, we have

$$S_{\text{eff},2} \begin{pmatrix} 0 \\ \lambda_c \end{pmatrix} = \begin{pmatrix} i\Gamma_{0,I}^{-1} \lambda_c \\ (-\Gamma_{0,R}^{-1} + U_{II}) \lambda_c \end{pmatrix} \quad (\text{K.7})$$

The saddle point equations imply

$$\Gamma_{0,I}^{-1} \lambda_c = 0 \quad (\text{K.8})$$

$$\left[(-\Gamma_{0,R}^{-1} + U_{II}) \lambda_c \right](X) = \frac{\lambda_c(\mathbf{x})^{3/2}}{\int dZ |\lambda_c(\mathbf{z})|^{5/2}} - \frac{\lambda_c(\mathbf{x})^{3/2}}{\int dZ |\lambda_c(\mathbf{z})|^{5/2}} = 0 \quad (\text{K.9})$$

For the translation modes, one has for $j \in \{1, 2, 3\}$

$$S_{\text{eff},2} \begin{pmatrix} \partial_j \lambda_c \\ 0 \end{pmatrix} = \begin{pmatrix} (-\Gamma_{0,R}^{-1} + U_{RR}) \partial_j \lambda_c \\ i\Gamma_{0,I}^{-1} \partial_j \lambda_c \end{pmatrix} \quad (\text{K.10})$$

$$[\Gamma_{0,I}^{-1} \partial_j \lambda_c](X) = \partial_j \int dY \Gamma_{0,I}^{-1}(X - Y) \lambda_c(\mathbf{y}) = 0 \quad (\text{K.11})$$

$$\begin{aligned} [(-\Gamma_{0,R}^{-1} + U_{RR}) \partial_j \lambda_c](X) &= - \int dY \Gamma_{0,R}^{-1}(X - Y) \partial_j \lambda_c(\mathbf{y}) + \\ &- \frac{3(\lambda_c(\mathbf{x}))^{1/2} \partial_j \lambda_c(\mathbf{x})}{2\|\lambda_c\|_{5/2}^{5/2}} + \frac{2(\lambda_c(\mathbf{x}))^{3/2}}{\|\lambda_c\|_{5/2}^3} \int dY \partial_j (\lambda_c(\mathbf{y}))^{5/2} = \\ &= -\partial_j \int dY \Gamma_{0,R}^{-1}(X - Y) \lambda_c(\mathbf{y}) - \frac{\partial_j (\lambda_c(\mathbf{x}))^{3/2}}{\|\lambda_c\|_{5/2}^{5/2}} = 0 \end{aligned} \quad (\text{K.12})$$

We now note that $S_{\text{eff},2}$ is a non-negative operator when acting to the space orthogonal to the zero modes. Otherwise, by moving the instanton η_c in the direction of one of its negative eigenvalues v_{neg} by a small amount ϵ we could find a field $\eta_c^{(\text{lower})} = \eta_c + \epsilon v_{\text{neg}}$ with lower action. We now add the zero-modes $v_i^{(0)}$ (for $\theta = 0$ and $\mathbf{r}_0 = 0$) to $S_{\text{eff},2}$ giving them eigenvalues equal to one:

$$\begin{aligned} S_{\text{eff},2}^{(\text{zero})} &:= S_{\text{eff},2} + \sum_{l=0}^4 \frac{v_l^{(0)} \otimes v_l^{(0)}}{\|v_l^{(0)}\|^2} = \\ &= \begin{pmatrix} -\Gamma_{0,R}^{-1} + U_{RR} + \sum_{j=1}^3 \frac{v_j^{(0)} \otimes v_j^{(0)}}{\|v_j^{(0)}\|_2^2} & -i\Gamma_{0,I}^{-1} \\ i\Gamma_{0,I}^{-1} & -\Gamma_{0,R}^{-1} + U_{II} + \frac{v_0^{(0)} \otimes v_0^{(0)}}{\|v_0^{(0)}\|_2^2} \end{pmatrix} \end{aligned} \quad (\text{K.13})$$

We can then write

$$\det S_{\text{eff},2}^{(\text{zero})} = \det' S_{\text{eff},2} \quad (\text{K.14})$$

where \det' is the determinant computed in the space orthogonal to the zero modes, and \det is computed in the usual unrestricted space. We now write

$$S_{\text{eff},2}^{(\text{zero})} = -\mathbb{F}_0^{-1} + \hat{B} \quad (\text{K.15})$$

where

$$-\mathbb{F}_0^{-1} := \begin{pmatrix} -\Gamma_{0,R}^{-1} & -i\Gamma_{0,I}^{-1} \\ i\Gamma_{0,I}^{-1} & -\Gamma_{0,R}^{-1} \end{pmatrix} \quad (\text{K.16})$$

$$\hat{B} := \begin{pmatrix} U_{RR} + \frac{\sum_j \partial_j \lambda_c \otimes \partial_j \lambda_c}{\|\partial_1 \lambda_c\|_2^2} & 0 \\ 0 & U_{II} + \frac{\lambda_c \otimes \lambda_c}{\|\lambda_c\|_2^2} \end{pmatrix} \quad (\text{K.17})$$

We can then write:

$$\begin{aligned} & \frac{\int \mathcal{D}[v, \bar{v}] \exp \left\{ -(v_R \ v_I) S_{\text{eff},2}[\eta_c, \bar{\eta}_c] \begin{pmatrix} v_R \\ v_I \end{pmatrix} \right\}}{\int \mathcal{D}[\eta, \bar{\eta}] e^{\langle \eta | \Gamma_0^{-1} | \eta \rangle}} = \frac{\det' S_{\text{eff},2}^{-1/2}}{\det(-\Gamma_0^{1/2})} = \\ & = \frac{\det [S_{\text{eff},2}^{(\text{zero})}]^{-1/2}}{\det((-\Gamma_0)^{1/2})} = \frac{\det(-\Gamma_0^{-1})^{1/2}}{\det[-\Gamma_0^{-1} + \hat{B}]^{1/2}} = \det \left(\mathbb{1} - (-\Gamma_0^{-1} + \hat{B})^{-1} \hat{B} \right)^{1/2} \end{aligned} \quad (\text{K.18})$$

In order for the Fredholm determinant to be well defined, $(-\Gamma_0^{-1} + \hat{B})^{-1} \hat{B}$ must be trace-class one. We write

$$\|(-\Gamma_0^{-1} + \hat{B})^{-1} \hat{B}\|_1 \leq \|(-\Gamma_0^{-1} + \hat{B})^{-1}\|_\infty \|\hat{B}\|_1 \quad (\text{K.19})$$

We have seen that $S_{\text{eff},2}^{(\text{zero})}$ is non-negative. We now *assume* that $S_{\text{eff},2}^{(\text{zero})} = -\Gamma_0^{-1} + \hat{B}$ is positive and gapped, this implies

$$\|(-\Gamma_0^{-1} + \hat{B})^{-1}\|_\infty < \infty \quad (\text{K.20})$$

We now bound the norm of \hat{B} :

$$\left\| U_{II} + \frac{\lambda_c \otimes \lambda_c}{\|\lambda_c\|_2^2} \right\|_1 \leq \|U_{II}\|_1 + \left\| \frac{\lambda_c \otimes \lambda_c}{\|\lambda_c\|_2^2} \right\|_1 = 1 + \frac{\beta}{\|\lambda_c\|_{5/2}^2} \int d^3x |u_c(\mathbf{x})|^{1/2} \quad (\text{K.21})$$

$$\begin{aligned} & \left\| U_{RR} + \frac{\sum_j \partial_j \lambda_c \otimes \partial_j \lambda_c}{\|\partial_1 \lambda_c\|_2^2} \right\|_1 \leq \\ & \leq 3 + \frac{3\beta}{2\|\lambda_c\|_{5/2}^2} \int d^3x |u_c(\mathbf{x})|^{1/2} + \frac{5\beta}{2\|\lambda_c\|_{5/2}^2} \int d^3x |u_c(\mathbf{x})|^3 \end{aligned} \quad (\text{K.22})$$

so we find that if λ_c is square root and cubic integrable (and it is, as it decays exponentially), we have:

$$\|\hat{B}\|_1 = \left\| U_{II} + \frac{\lambda_c \otimes \lambda_c}{\|\lambda_c\|_2^2} \right\|_1 + \left\| U_{RR} + \frac{\sum_j \partial_j \lambda_c \otimes \partial_j \lambda_c}{\|\nabla \lambda_c\|_2^2} \right\|_1 < \infty \quad (\text{K.23})$$

Using $|\det(\mathbb{1} + \hat{Y})| \leq e^{\|\hat{Y}\|_1}$ if $\|\hat{Y}\|_1 < \infty$ (see [121]), we can explicitly give an upper bound for the ratio of the two partition functions

$$\det \left(\mathbb{1} - (-\Gamma_0^{-1} + \hat{B})^{-1} \hat{B} \right)^{1/2} \leq \exp \left(\|(-\Gamma_0^{-1} + \hat{B})^{-1}\|_\infty \|\hat{B}\|_1 / 2 \right) \quad (\text{K.24})$$

To obtain a lower bound, we write

$$\det \left(\mathbb{1} - (-\Gamma_0^{-1} + \hat{B})^{-1} \hat{B} \right)^{1/2} = \frac{1}{\det(\mathbb{1} - \Gamma_0 \hat{B})^{1/2}} \quad (\text{K.25})$$

$$\det(\mathbb{1} - \Gamma_0 \hat{B})^{1/2} \leq \exp\left(\|\Gamma_0\|_\infty \|\hat{B}\|_1/2\right) \quad (\text{K.26})$$

So we can write

$$0 < C_L^{(\det)} \leq \det\left(\mathbb{1} - (-\Gamma_0^{-1} + \hat{B})^{-1} \hat{B}\right)^{1/2} \leq C_R^{(\det)} < \infty \quad (\text{K.27})$$

where $C_L^{(\det)} := e^{-\|\Gamma_0\|_\infty \|\hat{B}\|_1/2}$ and $C_R^{(\det)} := e^{\|(-\Gamma_0^{-1} + \hat{B})^{-1}\|_\infty \|\hat{B}\|_1/2}$. We see therefore that the ratio of the determinants is finite in the thermodynamic limit $\mathcal{V} \rightarrow \infty$.

L Bound on derivatives

One has that the functional integral is (formally) absolutely convergent for $|\arg z| < 2\pi/5$, so we can interchange differentiation and integration to obtain

$$\frac{d^n}{dw^n} \tilde{Z}_{\text{ladd}}(w) = n! \langle q_n^{(w)}[\eta, \bar{\eta}] \rangle_{\Gamma_0} \quad (\text{L.1})$$

where

$$q_n^{(w)}[\eta, \bar{\eta}] := \oint_{\mathcal{C}_w} \frac{dz}{2\pi i} \frac{\det_4(\mathbb{1} + \sqrt{z} \hat{Y})}{(z-w)^{n+1}} = \oint_{\mathcal{C}_w} \frac{dz}{2\pi i} \frac{\det_4(\mathbb{1} + \sqrt{z} \hat{Y})}{z^{n+1}} (1-w/z)^{-n-1} \quad (\text{L.2})$$

where \mathcal{C}_w is a contour that contains w . As before, for large n , we find two saddle points for large values of z , $|z_c| = O(n^{4/5})$, $|\arg z_c| = 4\pi/5$. One has

$$|1 - w/z_c|^{-n-1} < 1 \quad (\text{L.3})$$

for $|\arg w| < 3\pi/10$. One has then

$$|q_n^{(w)}[\eta, \bar{\eta}]| \lesssim e^{-\text{Re } S_{4,n}(z_c)} \sim (n!)^{-4/5} \left(\frac{5}{4} g_{TF} \int |\eta|^{5/2}\right)^{\frac{4n}{5}} \quad (\text{L.4})$$

so that

$$\left| \frac{1}{n!} \frac{d^n}{dw^n} \tilde{Z}_{\text{ladd}}(w) \right| \lesssim (n!)^{-4/5} \left(\frac{5}{4} g_{TF}\right)^{\frac{4n}{5}} I_n \quad (\text{L.5})$$

By using equation (82) for the large-order behavior of I_n , we get the sought result:

$$\left| \frac{1}{n!} \frac{d^n}{dw^n} \tilde{Z}_{\text{ladd}}(w) \right| \lesssim \mathcal{V} (n!)^{1/5} (A')^{-n} \quad (\text{L.6})$$

from which we deduce the bound for the derivatives of p_{ladd} .

M Unicity of analytic continuation

We introduce some useful definitions and properties of formal Taylor series. The notation is inspired from [97].

(Gevrey asymptotics): Let $A > 0$ and $\rho \geq 1$. A formal power series $\sum_{n=0}^{\infty} z^n f_n$ is Gevrey asymptotic of type (ρ, A) to a function $f(z)$ if there exists $R > 0$ and $\epsilon > 0$ such that $f(z)$ is analytic for $z \in W_R^\epsilon := \{z \in \mathbb{C} \mid 0 < |z| < R, |\arg z| < \pi/(2\rho) + \epsilon\}$ and such that for every $0 < \epsilon_A < 1$, there exists $C < \infty$ such that for every n and $z \in W_R^\epsilon$ one has

$$\left| f(z) - \sum_{n=0}^{N-1} f_n z^n \right| \leq C \left(\frac{|z|}{A(1 - \epsilon_A)} \right)^N (N/\rho)! \quad (\text{M.1})$$

In this case, we will write

$$f(z) \hat{=}^A_\rho \sum_{n=0}^{\infty} f_n z^n \quad (\text{M.2})$$

We now show that every analytic function that satisfies some bounds on derivatives admits a “strong” asymptotic series (see [123] for a similar discussion) of Gevrey type:

(Equivalence between Taylor expansions and Gevrey asymptotics): Let $A > 0$ and $\rho \geq 1$. Suppose there exists $R > 0$ and $\epsilon > 0$ such that the function $f(z)$ is analytic for $z \in W_R^\epsilon := \{z \in \mathbb{C} \mid 0 < |z| < R, |\arg z| < \pi/(2\rho) + \epsilon\}$, such that

$$f_n := \lim_{z \rightarrow 0, z \in W_R^\epsilon} \frac{1}{n!} \frac{d^n f(z)}{dz^n} \quad (\text{M.3})$$

and such that for every $\epsilon_A > 0$ there exists $C < \infty$ such that for every $N \in \mathbb{N}$ and $z \in W_R^\epsilon$ one has

$$\left| \frac{1}{N!} \frac{d^N f(z)}{dz^N} \right| \leq C (A + \epsilon_A)^{-N} (N/\rho)! \quad (\text{M.4})$$

Then

$$f(z) \hat{=}^A_\rho \sum_{n=0}^{\infty} z^n f_n \quad (\text{M.5})$$

The proof is straightforward. The Taylor formula with Lagrange's remainder for the analytic function f for $z, w \in W_R^\epsilon := \{z \in \mathbb{C} \mid |\arg z| < \pi/(2\rho) + \epsilon, 0 < |z| < R\}$ is ($0 < x < 1$):

$$\begin{aligned} \left| f(z) - \sum_{n=0}^{N-1} \frac{(z-w)^n}{n!} \frac{d^n}{dw^n} f(w) \right| &\leq \frac{|z-w|^N}{N!} \left| \frac{d^N}{d\zeta^N} f(\zeta) \right|_{\zeta=w+x(z-w)} \leq \\ &\leq \frac{|z-w|^N}{N!} \sup_{\zeta \in W_R^\epsilon} \left| \frac{d^N}{d\zeta^N} f(\zeta) \right| \leq C \left(\frac{|z-w|}{A+\epsilon_A} \right)^N (N/\rho)! \end{aligned} \quad (\text{M.6})$$

By taking the limit $w \rightarrow 0$, we can then obtain that the Taylor expansion for $z \rightarrow 0$ is not only an asymptotic series, but it is a strong asymptotic series. The unicity result is just a simple application of Phragmen-Lindelof principle. We start by stating an intermediate result. For every $\rho > 0$, there exists $C > 0$ and $B > 0$ such that for $|z| < R$

$$\min_{N \in \mathbb{N}^+} |z|^N (N/\rho)! \leq C e^{-B|z|^{-\rho}} \quad (\text{M.7})$$

This is proved by using Stirling bound on factorial. We now use the well-known Phragmén-Lindelöf principle:

(Phragmén-Lindelöf principle): Let $f(z)$ be an analytic function in $D_\rho^\epsilon := \{z \in \mathbb{C} \mid \operatorname{Re} z^{-\rho+\epsilon} > R^{-\rho+\epsilon}\}$ for some $\rho > \epsilon > 0$, and $R > 0$. Suppose further that for $z \in D_\rho^\epsilon$ f satisfies the bound:

$$|f(z)| \leq C e^{-B|z|^{-\rho}} \quad (\text{M.8})$$

Then, f is identically zero on D_ρ^ϵ .

We can then prove the fundamental unicity result for functions with Gevrey asymptotics:

(Unicity of functions with Gevrey asymptotics): Let $\rho \geq 1$, and $A > 0$. Suppose that

$$f(z) \stackrel{A}{\underset{\rho}{\asymp}} \sum_{n=0}^{\infty} z^n f_n \quad (\text{M.9})$$

Suppose that

$$g(z) \stackrel{A}{\underset{\rho}{\asymp}} \sum_{n=0}^{\infty} z^n f_n \quad (\text{M.10})$$

Then, for $z \in W_R^\epsilon$, one has

$$g(z) = f(z) \quad (\text{M.11})$$

In order to prove this result, we write for $z \in W_R^\epsilon$

$$|f(z) - g(z)| \leq \left| f(z) - \sum_{n=0}^{N^*-1} z^n f_n \right| + \left| g(z) - \sum_{n=0}^{N^*-1} z^n f_n \right| \quad (\text{M.12})$$

where $N^* = \operatorname{argmin} \left| \frac{z}{A} \right|^N (N/\rho)!$. Using Equation (M.7), we can then write for some $C' > 0$ and $B > 0$:

$$|f(z) - g(z)| \leq C' e^{-B|z|^{-\rho}} \quad (\text{M.13})$$

Now we use Phragmén-Lindelöf principle to show that $f(z) - g(z)$ is identically zero on W_R^ϵ .

N Ramis's theorem

In this section we consider $\rho \geq 1$. We present a generalization of Watson's theorem for $\rho \neq 1$ [95]. This generalization was presented by Ramis in [96]. We present an alternative derivation of a slightly different version of the theorem.

(Ramis's Theorem): Let $A > 0$, and $\rho \geq 1$. Let $f(z)$ such that (we use the notation introduced in Equation (M.2))

$$f(z) \stackrel{A}{\underset{\rho}{\asymp}} \sum_{n=0}^{\infty} z^n f_n \quad (\text{N.1})$$

We define the Borel transform of f as

$$B(z) := \sum_{n=0}^{\infty} \frac{f_n}{\Gamma(n/\rho + 1)} z^n \quad (|z| < A) \quad (\text{N.2})$$

Then, the function $B(z)$ can be continued analytically for $|\arg z| < \epsilon$. We define for $|\arg z| < \epsilon$ and $|z| < R'$, $R' > 0$

$$f_B(z) := \rho \int_0^{\infty} \frac{dt}{t} t^\rho e^{-t^\rho} B(zt) \quad (\text{N.3})$$

$f_B(z)$ can be continued analytically in the region W_R^ϵ , and in this region we have

$$f_B(z) = f(z), \quad z \in W_R^\epsilon \quad (\text{N.4})$$

Proof: We introduce the Mittag-Leffler function for $\rho \geq 1$

$$E_{\frac{1}{\rho}}(z) := \sum_{n=0}^{\infty} \frac{z^n}{\Gamma(n/\rho + 1)} \quad (\text{N.5})$$

One has the asymptotic expansion for $|z| \rightarrow \infty$ [124]:

$$E_{\frac{1}{\rho}}(z) \underset{|z| \rightarrow \infty}{=} \rho e^{z^\rho} + O\left(\frac{1}{z}\right) \quad (\text{N.6})$$

for $|\arg z| < \frac{\pi}{2\rho}$. We have

$$E_{\frac{1}{\rho}}(z) \underset{|z| \rightarrow \infty}{=} O\left(\frac{1}{z}\right) \quad (\text{N.7})$$

for $\frac{\pi}{2\rho} \leq |\arg z| \leq \pi$. In particular, we have the bound

$$|E_{\frac{1}{\rho}}(z)| \leq C_{\text{Mittag}} e^{|z|^\rho} \quad (\text{N.8})$$

for $|z| > R/\rho^{1/\rho} > 0$, for some R . We define the (non-perturbative) Borel transform B_{NP} of f by

$$B_{NP}(z) := \oint_{\partial W_R^\epsilon} \frac{dw}{2\pi i} \frac{f(w)}{w} E_{\frac{1}{\rho}}\left(\frac{z}{w}\right) \quad (\text{N.9})$$

We see that the integral is absolutely convergent for $|\arg z| < \epsilon$, where it defines an analytic function. It is bounded by

$$\begin{aligned} & |B_{NP}(z) - f(0)| \leq \\ & \leq \frac{R}{\pi} \left(1 + \frac{\pi}{2\rho} + \epsilon\right) \sup_{w \in \partial W_R^\epsilon} \left| \frac{f(w) - f(0)}{w} \right| \sup_{w \in \partial W_R^\epsilon} \left| E_{\frac{1}{\rho}} \left(\frac{z}{w} \right) \right| \leq \quad (\text{N.10}) \\ & \leq C_{\text{Bor}} e^{|z|/R^\rho} \end{aligned}$$

where $C_{\text{Bor}} < \infty$ as

$$\sup_{w \in \partial W_R^\epsilon} \left| \frac{f(w) - f(0)}{w} \right| < \infty \quad (\text{N.11})$$

A simple application of Lebesgue dominated convergence theorem, gives for $n \geq 0$

$$\oint_{\partial W_R^\epsilon} \frac{dw}{2\pi i} \frac{w^n}{w} E_{\frac{1}{\rho}} \left(\frac{z}{w} \right) = \frac{z^n}{\Gamma(n/\rho + 1)} \quad (\text{N.12})$$

(we need to modify the contour ∂W_R^ϵ to a contour that contains the origin, this can be done by adding an infinitesimally small contour to the left of the origin whose contribution is zero). We introduce

$$R_N(z) := f(z) - \sum_{n=0}^{N-1} f_n z^n, \quad R_N^B(z) := B_{NP}(z) - \sum_{n=0}^{N-1} \frac{f_n}{\Gamma(n/\rho + 1)} z^n \quad (\text{N.13})$$

Let us write

$$\begin{aligned} |R_N^B(z)| &= \left| \oint_{\partial W_r^\epsilon} \frac{dw}{2\pi i} \frac{R_N(w)}{w} E_{\frac{1}{\rho}} \left(\frac{z}{w} \right) \right| \leq \\ &\leq \frac{C_1}{r} \left(\frac{r}{A} \right)^N e^{|z|^\rho/r^\rho} \Gamma(N/\rho + 1) \end{aligned} \quad (\text{N.14})$$

where $0 < r \leq R$. We choose $r = \rho^{1/\rho} |z| N^{-1/\rho}$ to optimize the bound (we can do that for $|z| < (R/\rho^{1/\rho})N^{1/\rho}$), getting

$$|R_N^B(z)| \leq C_2 N^\alpha \left(\frac{|z|}{A} \right)^N, \quad |z| < (R/\rho^{1/\rho})N^{1/\rho} \wedge |\arg z| < \epsilon \quad (\text{N.15})$$

for some $C_2 \geq 0$ and $\alpha \geq 0$ and $|z| < (R/\rho^{1/\rho})N^{1/\rho}$. We see that $R_N^B(z)$ goes to zero for $|z| < A$ as $N \rightarrow \infty$, so we have

$$B_{NP}(z) = \sum_{n=0}^{\infty} \frac{f_n}{\Gamma(n/\rho + 1)} z^n \equiv B(z), \quad |z| < A \wedge |\arg z| < \epsilon \quad (\text{N.16})$$

We see therefore that $B_{NP}(z)$ is the analytic continuation of $B(z)$ for $|\arg z| < \epsilon$, and we will call this analytic extension $B(z)$. For $|z| \geq (R/\rho^{1/\rho})N^{1/\rho}$, we use the bound for $r = R$ (with the correction of (N.8))

$$|R_N^B(z)| \leq C_3 \left(\frac{R}{A}\right)^N e^{|z|^\rho/R^\rho} \Gamma(N/\rho + 1) \quad (\text{N.17})$$

which is valid for $|z| \geq (R/\rho^{1/\rho})N^{1/\rho}$ and $|\arg z| < \epsilon$. The inverse Borel transform of B is defined by (we consider $\text{Im } z > 0$)

$$f_B(z) := \frac{\rho}{(ze^{-i\epsilon})^\rho} \int_0^\infty \frac{dt}{t} t^\rho e^{-t^\rho/(ze^{-i\epsilon})^\rho} B(te^{i\epsilon}) \quad (\text{N.18})$$

Let us compute where this integral is absolutely convergent:

$$\left| t^\rho e^{-t^\rho/(ze^{-i\epsilon})^\rho} B(te^{i\epsilon}) \right| \leq C_{\text{Bor}} e^{-t^\rho \left(\frac{\cos(\rho\theta - \epsilon)}{r^\rho} - \frac{1}{R^\rho} \right)} \quad (\text{N.19})$$

for $z = re^{i\theta}$. R' is defined by

$$\frac{\cos(\frac{\pi}{2} - \epsilon/2)}{R'^\rho} > \frac{1}{R^\rho} \quad (\text{N.20})$$

for small ϵ we have

$$R' < R \left(\frac{2}{\epsilon}\right)^{\frac{1}{\rho}} \quad (\text{N.21})$$

Therefore $f_B(z)$ is analytic for $\{z \in \mathbb{C} \mid \text{Im } z > 0\} \cap W_{R'}^{\frac{\epsilon}{2\rho}}$. For small $\arg z$, we can turn the contour over t and write

$$f_B(z) := \frac{\rho}{z^\rho} \int_0^\infty \frac{dt}{t} t^\rho e^{-t^\rho/z^\rho} B(t) \quad (\text{N.22})$$

that shows that f_B can be extended to an analytic function for $z \in W_{R'}^{\frac{\epsilon}{2\rho}}$. We introduce

$$R_N^I(z) := f_B(z) - \sum_{n=0}^{N-1} f_n z^n \quad (\text{N.23})$$

Now we show that there exists $C_I > 0$ and $A_I > 0$ such that

$$|R_N^I(z)| \leq C_I \left(\frac{|z|}{A_I}\right)^N \Gamma(N/\rho + 1) \quad (\text{N.24})$$

We write

$$\begin{aligned} R_N^I(z) &= \frac{\rho}{(ze^{-i\epsilon})^\rho} \int_0^\infty \frac{dt}{t} t^\rho e^{-t^\rho/(ze^{-i\epsilon})^\rho} R_N^B(te^{i\epsilon}) = \\ &= I_N^m(z) + I_N^M(z) \end{aligned} \quad (\text{N.25})$$

where

$$I_N^m(z) := \frac{\rho e^{i\epsilon\rho}}{(ze^{-i\epsilon})^\rho} \int_0^{(R/\rho^{1/\rho})N^{1/\rho}} \frac{dt}{t} t^\rho e^{-t^\rho/(ze^{-i\epsilon})^\rho} R_N^B(te^{i\epsilon}) \quad (\text{N.26})$$

$$I_N^M(z) := \frac{\rho e^{i\epsilon\rho}}{(ze^{-i\epsilon})^\rho} \int_{(R/\rho^{1/\rho})N^{1/\rho}}^\infty \frac{dt}{t} t^\rho e^{-t^\rho/(ze^{-i\epsilon})^\rho} R_N^B(te^{i\epsilon}) \quad (\text{N.27})$$

One has for $z = r e^{i\theta}$

$$\begin{aligned} |I_N^m(z)| &\leq \frac{C_2 \rho}{r^\rho A^N} \int_0^{(R/\rho^{1/\rho})N^{1/\rho}} \frac{dt}{t} t^\rho e^{-t^\rho \frac{\cos(\rho\theta - \epsilon)}{r^\rho}} t^N < \\ &< \frac{C_2 \rho N^\alpha}{r^\rho A^N} \int_0^\infty \frac{dt}{t} t^\rho e^{-t^\rho \frac{\cos(\rho\theta - \epsilon)}{r^\rho}} t^N = \\ &= \frac{C_2 \rho N^\alpha r^N}{A^N} (\cos(\rho\theta - \epsilon))^{-\frac{N}{\rho} - 1} \Gamma(N/\rho + 1) \leq \\ &\leq \frac{C_2 \rho N^\alpha r^N}{A^N} (\cos(\pi/2 - \epsilon/2))^{-\frac{N}{\rho} - 1} \Gamma(N/\rho + 1) < \\ &< C_2 \rho N^\alpha \left(\frac{R|z|}{R'A} \right)^N \Gamma(N/\rho + 1) \end{aligned} \quad (\text{N.28})$$

One has for $z = r e^{i\theta}$ (we introduce $\lambda := \frac{\cos(\rho\theta - \epsilon)}{r^\rho} - \frac{1}{R^\rho}$)

$$\begin{aligned} |I_N^M(z)| &\leq \frac{C_3 \rho}{r^\rho} \left(\frac{R}{A} \right)^N \Gamma(N/\rho + 1) \int_{(R/\rho^{1/\rho})N^{1/\rho}}^\infty dt t^{\rho-1} e^{-\lambda t^\rho} \leq \\ &\leq \frac{C_3 \lambda^{-1}}{r^\rho} \left(\frac{R e^{\frac{1}{\rho}}}{A} \right)^N \Gamma(N/\rho + 1) \exp\left(-\frac{R^\rho \cos(\pi/2 - \epsilon/2) N}{\rho r^\rho} \right) \end{aligned} \quad (\text{N.29})$$

where Γ_{inc} is the incomplete Gamma function. We write for $z \in W_{R'}^{\epsilon/2}$

$$e^{-\frac{R^\rho \cos(\pi/2 - \epsilon/2)}{\rho} \frac{1}{|z|^\rho}} \leq \frac{e^{-\frac{R^\rho \cos(\pi/2 - \epsilon/2)}{\rho R'^\rho}}}{R'^{-1} |z|} =: C_5 |z| \quad (\text{N.30})$$

and

$$\lambda^{-1} \leq \frac{|z|^\rho}{\cos(\pi/2 - \epsilon/2)} \quad (\text{N.31})$$

so that

$$|I_N^M(z)| \leq C_6 \left(\frac{R e^{\frac{1}{\rho}} C_5 |z|}{A} \right)^N \Gamma(N/\rho + 1) \quad (\text{N.32})$$

We can then write

$$|R_N^I(z)| \leq C_I(A_I) \left(\frac{|z|}{A_I} \right)^N \Gamma(N/\rho + \delta) \quad (\text{N.33})$$

for A_g such that

$$A_I < A \min \left(\frac{R}{R'}, \frac{1}{C_5 R e^{\frac{1}{\rho}}} \right) \quad (\text{N.34})$$

We see that f and f_B have identical strong asymptotic series in the region $W_{R'}^{\frac{\epsilon}{2\rho}}$, where they are analytical. By the Phragmén-Lindelöf principle of the previous section, we have

$$f_B(z) = f(z), \quad z \in W_{R'}^{\frac{\epsilon}{2\rho}} \quad (\text{N.35})$$

It is then possible to extend f_B by analytic continuation to the whole W_R^{ϵ} , the analytic extension being given by f . \square

O Consistency condition for the maximal analytic extension

We have seen that the Borel transform $B(z)$ has the Taylor expansion $\sum_{n=0}^{\infty} z^n B_n$ for $|z| < A$. One has

$$B_n \underset{n \rightarrow \infty}{=} A^{-n} \operatorname{Re} \exp \left(\frac{4\pi i n}{5} + (b_1/5^{4/5} - U_1 e^{\frac{4\pi i}{5}}) n^{4/5} + O(n^{3/5}) \right) \quad (\text{O.1})$$

If we assume that B is analytic for $z \in \mathbb{C} \setminus \mathcal{C}$ and decreases sufficiently fast at infinity, we can write

$$B_n = \oint \frac{dz}{2\pi i} \frac{B(z)}{z^{n+1}} = -2 \operatorname{Re} e^{-\frac{4\pi i n}{5}} \int_A^{\infty} \frac{dt}{2\pi i} \frac{\operatorname{Disc}(B, t e^{4\pi i/5})}{t^{n+1}} \quad (\text{O.2})$$

where for $z_0 \in \mathbb{C}$ we have defined

$$\operatorname{Disc}(f, z_0) := f(z_0 e^{-i0^+}) - f(z_0 e^{i0^+}) \quad (\text{O.3})$$

We introduce for $u \geq 0$

$$S_{\operatorname{disc}}(u) := -\log \operatorname{Disc}(B, A(1+u)e^{4\pi i/5}) \quad (\text{O.4})$$

so that we can write

$$B_n = -2 A^{-n} \operatorname{Re} e^{-\frac{4\pi i n}{5}} \int_0^{\infty} \frac{du}{2\pi i} \frac{e^{-S_{\operatorname{disc}}(u)}}{(1+u)^{n+1}} \quad (\text{O.5})$$

It is clear that for large n only $u \ll 1$ will be important in the integral, so we can hope to compute the integral by the saddle-point method. For small u , we assume that

$$S_{\text{disc}}(u) \underset{u \rightarrow 0^+}{=} \frac{s_{\text{disc}} e^{i\phi}}{u^\alpha} \quad (\text{O.6})$$

with $s_{\text{disc}} > 0$ and $-\pi < \phi < \pi$. We now look for a saddle point. In order to get a contribution of order $n^{4/5}$, one has to choose $\alpha = 4$. The saddle point nearest to the integration contour is at

$$u_c = \left(\frac{4 s_{\text{disc}} e^{i\phi}}{n} \right)^{\frac{1}{5}} \quad (\text{O.7})$$

which gives a contribution to B_n of

$$B_n \underset{n \rightarrow \infty}{\sim} -2 A^{-n} \text{Re} \exp \left(-\frac{4\pi i n}{5} - \frac{5}{4^{4/5}} (s_{\text{disc}})^{\frac{1}{5}} e^{i\phi/5} n^{4/5} + O(n^{3/5}) \right) \quad (\text{O.8})$$

Comparing with (O.1), we have

$$U_1 e^{\frac{4\pi i}{5}} - b_1 / 5^{4/5} = \frac{5}{4^{4/5}} (s_{\text{disc}})^{\frac{1}{5}} e^{i\phi/5} \quad (\text{O.9})$$

where $-\pi < \phi < \pi$ and $s_{\text{disc}} > 0$.

P Construction of the conformal map

We first recall the Schwartz integral formula: for an analytic function f in the *closed* unit disk, one has

$$f(z) = i \text{Im} f(0) + \frac{1}{2\pi i} \oint_{|\zeta|=1} \frac{d\zeta}{\zeta} \frac{\zeta + z}{\zeta - z} \text{Re} f(\zeta) \quad (\text{P.1})$$

We define the open unit disk as

$$\mathcal{D} := \{z \in \mathbb{C} \mid |z| < 1\} \quad (\text{P.2})$$

We start by proving a simple extension of the Schwartz formula that works in an *open* unit disk.

(Generalized Schwartz integral formula): We define

$$f(z) = iC_0 + \frac{1}{2\pi i} \oint_{|\zeta|=1} \frac{d\zeta}{\zeta} \frac{\zeta + z}{\zeta - z} h(-i \log \zeta) \quad (\text{P.3})$$

where $C_0 \in \mathbb{R}$ and $h : (-\pi, \pi] \rightarrow [-M, M]$, $M > 0$, is a bounded integrable function. Then, f is an analytic function in \mathcal{D} . Let h_n be the n -th Fourier coefficient of h :

$$h_n := \int_{-\pi}^{\pi} \frac{d\theta}{2\pi} e^{-in\theta} h(\theta), \quad n \in \mathbb{Z} \quad (\text{P.4})$$

Then, when the series of $\{h_n e^{in\theta}\}_{n \in \mathbb{Z}}$ converges, one has

$$\lim_{z \rightarrow e^{i\theta}} \operatorname{Re} f(z) = \sum_{n \in \mathbb{Z}} h_n e^{in\theta} \quad (\text{P.5})$$

Proof: Without loss of generality, we consider the case where $C_0 = 0$. Let $z \in \mathcal{D}$. Then, we can write

$$\begin{aligned} f(z) &= \sum_{n=0}^{N-1} \frac{z^n}{2\pi i} \int_{-\pi}^{\pi} d\phi e^{-i\phi(n+1)} (e^{i\phi} + z) h(\phi) + \\ &+ \frac{z^N}{2\pi i} \int_{-\pi}^{\pi} d\phi e^{-i\phi(n+1)} \frac{e^{i\phi} + z}{e^{i\phi} - z} h(\phi) \end{aligned} \quad (\text{P.6})$$

One has

$$\left| \frac{z^N}{2\pi i} \int_{-\pi}^{\pi} d\phi e^{-i\phi(n+1)} \frac{e^{i\phi} + z}{e^{i\phi} - z} h(\phi) \right| \leq |z|^N \frac{1 + |z|}{1 - |z|} M \xrightarrow{N \rightarrow \infty} 0 \quad (\text{P.7})$$

so that we have for $z \in \mathcal{D}$

$$f(z) = h_0 + 2 \sum_{n=1}^{\infty} h_n z^n \quad (\text{P.8})$$

where $|h_n| \leq M$, so the series converges. Suppose now that the series $\sum_{n=1}^{\infty} h_n e^{in\theta}$ converges, using Abel's theorem we have

$$\lim_{z \rightarrow e^{i\theta}} \operatorname{Re} f(z) = h_0 + 2 \operatorname{Re} \sum_{n=1}^{\infty} h_n e^{in\theta} = \sum_{n \in \mathbb{Z}} h_n e^{in\theta} \quad (\text{P.9})$$

□

(Constuction of the conformal map): Let g be an invertible analytic function, $g : \mathcal{D} \rightarrow \mathbb{C} \setminus \{z \in \mathbb{C} \mid |z| > A, |\arg z| = \nu\pi\}$, with $A > 0$ and $0 < \nu < 1$, such that $g(0) = 0$ and $g(w)^* = g(w^*)$. Then

$$g(w) = \frac{a_{cf} A w}{(1+w)^{2(1-\nu)}(1-w)^{2\nu}} \quad (\text{P.10})$$

where $a_{cf} := 4\nu^\nu(1-\nu)^{1-\nu}$

Proof: One has that $\partial\mathcal{D}$ has to be mapped on $\{z \in \mathbb{C} \mid |z| > A, |\arg z| = \nu\pi\}$ if one wants the map to be invertible. In particular, we know that

$$|\arg g(w)| = \nu\pi \quad (\text{P.11})$$

for $|w| = 1$. Continuity arguments, with the reality condition $g(w)^* = g(w^*)$ imply that

$$\arg g(e^{i\theta}) = \nu\pi \operatorname{sign} \theta \quad (\text{P.12})$$

for $\theta \in (-\pi, \pi)$. We remark that

$$\Phi(w) := -i \log \frac{g(w)}{w} \quad (\text{P.13})$$

is an analytic function in \mathcal{D} . We introduce for $\theta \in (-\pi, 0) \cup (0, \pi)$

$$h(\theta) := \lim_{w \rightarrow e^{i\theta}} \operatorname{Re} \Phi(w) = \nu\pi \operatorname{sign} \theta - \theta \quad (\text{P.14})$$

and

$$h(0) = h(\pm\pi) = 0 \quad (\text{P.15})$$

Then, by applying our improved Schwartz formula, we can write

$$\Phi(w) = i \operatorname{Im} \Phi(0) + \frac{1}{2\pi i} \oint_{|\zeta|=1} \frac{d\zeta}{\zeta} \frac{\zeta+z}{\zeta-z} h(-i \log \zeta) \quad (\text{P.16})$$

We have for $w \in \mathcal{D}$:

$$\Phi(w) = i \operatorname{Im} \Phi(0) + 2i(1-\nu) \log(1+w) + 2i\nu \log(1-w) \quad (\text{P.17})$$

so that

$$g(w) = e^{-\operatorname{Im} \Phi(0)} \frac{w}{(1+w)^{2(1-\nu)}(1-w)^{2\nu}} \quad (\text{P.18})$$

By considering the preimage of $te^{i\nu\pi}$, $t > 0$, it is easy to see that

$$g(w) = \frac{a_{cf} A w}{(1+w)^{2(1-\nu)}(1-w)^{2\nu}} \quad (\text{P.19})$$

with $a_{cf} = 4\nu^\nu(1-\nu)^{1-\nu}$. One also has

$$g(e^{i\theta_{\text{cut}}}) := Ae^{i\nu\pi}, \quad \tan \frac{\theta_{\text{cut}}}{2} = \sqrt{\frac{\nu}{1-\nu}} \quad (\text{P.20})$$

□

Q Some properties of Gevrey asymptotic series

For two formal Taylor series $\sum_n f_n z^n$ and $\sum_n g_n z^n$, we define addition and multiplication in the usual way

$$\sum_{n=0}^{\infty} f_n z^n + \sum_{n=0}^{\infty} g_n z^n = \sum_{n=0}^{\infty} (f_n + g_n) z^n \quad (\text{Q.1})$$

$$\left(\sum_{n=0}^{\infty} f_n z^n \right) \left(\sum_{n=0}^{\infty} g_n z^n \right) = \sum_{n=0}^{\infty} \left(\sum_{m=0}^n f_{n-m} g_m \right) z^n \quad (\text{Q.2})$$

and for $f_0 \neq 0$ we can define the inverse multiplication as:

$$\left(\sum_{n=0}^{\infty} f_n z^n \right)^{-1} = \sum_{n=0}^{\infty} c_n z^n \quad (\text{Q.3})$$

where $c_0 = 1/f_0$ and c_n satisfies a recursive formula for $n \geq 1$:

$$c_n = -\frac{1}{f_0} \sum_{m=0}^{n-1} f_{n-m} c_m \quad (\text{Q.4})$$

(Algebraic properties of Gevrey asymptotic series): Suppose that $f(z) \hat{=}^A_{\rho} \sum_n f_n z^n$ and $g(z) \hat{=}^A_{\rho} \sum_n g_n z^n$, then

$$(f+g)(z) \hat{=}^A_{\rho} \sum_{n=0}^{\infty} f_n z^n + \sum_{n=0}^{\infty} g_n z^n \quad (\text{Q.5})$$

$$(fg)(z) \hat{=}^A_{\rho} \left(\sum_{n=0}^{\infty} f_n z^n \right) \left(\sum_{n=0}^{\infty} g_n z^n \right) \quad (\text{Q.6})$$

Suppose that $f_0 \neq 0$. Then

$$\frac{1}{f(z)} \hat{=}^A_{\rho} \left(\sum_{n=0}^{\infty} f_n z^n \right)^{-1} \quad (\text{Q.7})$$

Proof: Let us show (Q.6). Let us define

$$R_N^h(z) := h(z) - \sum_{n=0}^{N-1} h_n z^n \quad (\text{Q.8})$$

for $h \in \{f, g\}$. We write

$$\begin{aligned} & \left| f(z)g(z) - \sum_{n=0}^{N-1} (fg)_n z^n \right| \leq \\ & \leq |f(z)R_N^g(z)| + \left| \sum_{n=0}^{N-1} g_n z^n R_{N-n}^f(z) \right| \leq \\ & \leq C^2 \left(\frac{|z|}{A-\eta} \right)^N (N!)^{1/\rho} + C^2 \left(\frac{|z|}{A-\eta} \right)^N \sum_{n=0}^{N-1} (n!)^{\frac{1}{\rho}} ((N-n)!)^{\frac{1}{\rho}} \leq \\ & \leq C^2 (N+1) \left(\frac{|z|}{A-\eta} \right)^N (N!)^{\frac{1}{\rho}} \end{aligned} \quad (\text{Q.9})$$

where $C = C(\eta)$. Let $c(\delta)$ such that $1+x \leq c(\delta)e^{\delta x}$ for $x > 0$ and $\delta > 0$, where $c(\delta) = e^{\delta-1}/\delta$. We can then write for $\eta' := A(1-e^{-\delta}) + \eta e^{-\delta}$

$$\left| f(z)g(z) - \sum_{n=0}^{N-1} (fg)_n z^n \right| \leq c(\delta) C^2(\eta) \left(\frac{|z|}{A-\eta'} \right)^N (N!)^{\frac{1}{\rho}} \quad (\text{Q.10})$$

η' can be made arbitrarily small by choosing δ and η small.

We now consider the reciprocal function $(1/f)(z)$. If $f_0 \neq 0$, $(1/f)(z)$ is analytic for some $|z| < R'$, $|\arg z| < \pi/(2\rho) + \epsilon$. Without loss of generality, we assume that $f_0 = 1$, and we write $f(z) = 1 - zg(z)$, and let $G < 1/R'$ such that $|g(z)| < G$. One has

$$\begin{aligned} & \left| \frac{1}{1-zg(z)} - \sum_{n=0}^{N-1} (f^{-1})_n z^n \right| \leq \left| \frac{1 - (zg(z))^N}{1 - zg(z)} - \sum_{n=0}^{N-1} (f^{-1})_n z^n \right| + \left| \frac{(zg(z))^N}{1 - zg(z)} \right| \leq \\ & \leq \left| \frac{1 - (zg(z))^N}{1 - zg(z)} - \sum_{n=0}^{N-1} (f^{-1})_n z^n \right| + \frac{G^N}{1 - R'G} |z|^N \end{aligned} \quad (\text{Q.11})$$

$$\begin{aligned} & \left| \frac{1 - (zg(z))^N}{1 - zg(z)} - \sum_{n=0}^{N-1} (f^{-1})_n z^n \right| = \left| \sum_{n=1}^{N-1} (zg(z))^n - \sum_{n=1}^{N-1} (f^{-1})_n z^n \right| = \\ & = \left| \sum_{n=1}^{N-1} z^n R_{N-n}^{g^n}(z) \right| \leq \sum_{n=1}^{N-1} |z|^n |R_{N-n}^{g^n}(z)| \end{aligned} \quad (\text{Q.12})$$

By applying Eq.(Q.10) recursively, one can easily show that there exists $C = C(\eta) < \infty$ and $c = c(\eta) < \infty$ such that

$$|R_{N-n}^{g^n}(z)| \leq C c^n \frac{|z|^{N-n}}{(A+\eta)^N} [(N-n)!]^{\frac{1}{\rho}} = C \frac{|z|^{N-n}}{(A+\eta)^N} (N!)^{\frac{1}{\rho}} \prod_{k=N-n+1}^N \frac{c}{k^{\frac{1}{\rho}}} \quad (\text{Q.13})$$

Let us consider N greater than $N^* \geq c^\rho$. Then, we can write

$$|R_{N-n}^{g^n}(z)| \leq \frac{|z|^{N-n}}{(A+\eta)^N} (N!)^{\frac{1}{\rho}} \lambda^n \quad (\text{Q.14})$$

with $\lambda < 1$. We then write for $N > N^*$

$$\begin{aligned} \left| \frac{1}{1-zg(z)} - \sum_{n=0}^{N-1} (f^{-1})_n z^n \right| &\leq \frac{C}{1-\lambda} \frac{|z|^N}{(A+\eta)^N} (N!)^{\frac{1}{\rho}} + \frac{G^N}{1-R'G} |z|^N \leq \\ &\leq \frac{C'}{1-\lambda} \frac{|z|^N}{(A+\eta)^N} (N!)^{\frac{1}{\rho}} \end{aligned} \quad (\text{Q.15})$$

□

R Dispersion relation

We will show that for every $0 < x < R$ one has

$$\frac{1}{n!} \frac{d^n}{dx^n} f(x) = \oint_{|z|=r} \frac{dz}{2\pi i} \frac{f(z)}{(z-x)^{n+1}} - \sum_{s \in \{-1,1\}} s e^{\frac{4\pi i s}{5}} \int_0^r \frac{dt}{2\pi i} \frac{\text{Disc}(f, t e^{4\pi i s/5})}{(t e^{4\pi i s/5} - x)^{n+1}} \quad (\text{R.1})$$

The sought result is obtained by taking the limit $x \downarrow 0$ in this formula. We start by writing the integral representation for the derivative

$$\frac{1}{n!} \frac{d^n}{dx^n} f(x) = \oint_{\partial W_{\epsilon,r}} \frac{dz}{2\pi i} \frac{f(z)}{(z-x)^{n+1}} = \oint_{\partial W_{\epsilon,r} \cup \partial W'_{\epsilon,r}} \frac{dz}{2\pi i} \frac{f(z)}{(z-x)^{n+1}} \quad (\text{R.2})$$

where $0 < \epsilon < x$, $x < r < R$, $W_{\epsilon,r} := \{z \in \mathbb{C} \mid |z-\epsilon| < r, |\arg(z-\epsilon)| \leq 4\pi/5\}$, $W'_{\epsilon,r} := \{z \in \mathbb{C} \mid |z+\epsilon| < r, 4\pi/5 \leq |\arg(z+\epsilon)| \leq \pi\}$. We take the limit $\epsilon \downarrow 0$, and we obtain (R.1).

□

S Pair propagator in terms of the η fields

If we denote the partition function for $z = 1$ by $Z_{\text{ladd}}(1) = \int \mathcal{D}[\eta, \bar{\eta}, \varphi, \bar{\varphi}] e^{-S_{\text{ladd}}^{(1)}}$. We write

$$\begin{aligned} 0 &= \frac{1}{Z_{\text{ladd}}(1)} \int \mathcal{D}[\eta, \bar{\eta}, \varphi, \bar{\varphi}] \frac{\delta}{\delta \bar{\eta}(X)} \frac{\delta}{\delta \eta(0)} e^{-S_{\text{ladd}}^{(1)}} = \\ &= \frac{\delta(X)}{g_0} + \langle (\varphi_{\downarrow} \varphi_{\downarrow})(X) (\bar{\varphi}_{\uparrow} \bar{\varphi}_{\downarrow})(0) \rangle + \frac{1}{g_0^2} \langle \eta(X) \bar{\eta}(0) \rangle + \\ &\quad - \frac{1}{g_0} \langle \eta(X) (\bar{\varphi}_{\uparrow} \bar{\varphi}_{\downarrow})(0) \rangle - \frac{1}{g_0} \langle (\varphi_{\downarrow} \varphi_{\uparrow})(X) \eta(0) \rangle \end{aligned} \quad (\text{S.1})$$

The three point vertex is related to the two-point bosonic function:

$$\begin{aligned} 0 &= \frac{1}{Z_{\text{ladd}}(1)} \int \mathcal{D}[\eta, \bar{\eta}, \varphi, \bar{\varphi}] \frac{\delta}{\delta \eta(0)} \eta(X) e^{-S_{\text{ladd}}^{(1)}} = \\ &= \delta(X) + \frac{1}{g_0} \langle \eta(X) \bar{\eta}(0) \rangle - \langle \eta(X) (\bar{\varphi}_{\uparrow} \bar{\varphi}_{\downarrow})(0) \rangle \end{aligned} \quad (\text{S.2})$$

$$\begin{aligned} 0 &= \frac{1}{Z_{\text{ladd}}(1)} \int \mathcal{D}[\eta, \bar{\eta}, \varphi, \bar{\varphi}] \frac{\delta}{\delta \bar{\eta}(X)} \bar{\eta}(0) e^{-S_{\text{ladd}}^{(1)}} = \\ &= \delta(X) + \frac{1}{g_0} \langle \eta(X) \bar{\eta}(0) \rangle - \langle (\varphi_{\downarrow} \varphi_{\uparrow})(X) \bar{\eta}(0) \rangle \end{aligned} \quad (\text{S.3})$$

We can then write

$$- \langle \eta(X) \bar{\eta}(0) \rangle = g_0 \delta(X) - g_0^2 \langle (\varphi_{\downarrow} \varphi_{\downarrow})(X) (\bar{\varphi}_{\uparrow} \bar{\varphi}_{\downarrow})(0) \rangle = \Gamma(X) \quad (\text{S.4})$$

T Generalized Pauli formulas

We define $\tilde{p}_{\text{ladd}}(z) := p_{\text{ladd}}(z) - p_{\text{ladd}}(0)$, which can also be expressed in terms of a functional integral with the shifted action:

$$\tilde{p}_{\text{ladd}}(z) = \lim_{\nu \rightarrow \infty} \frac{1}{\beta \mathcal{V}} \log \frac{\int \mathcal{D}[\eta, \bar{\eta}, \varphi, \bar{\varphi}] e^{-S_{\text{ladd}}^{(z)}}}{\int \mathcal{D}[\eta, \bar{\eta}, \varphi, \bar{\varphi}] e^{-S_{\text{ladd}}^{(0)}}} \quad (\text{T.1})$$

$\tilde{p}_{\text{ladd}}(z)$ is a functional of G_0 and Γ_0 , and we write explicitly $\tilde{p}_{\text{ladd}}[G_0, \Gamma_0, z]$. We evaluate this functional for $G_0(\lambda) = \lambda G_0$, $\lambda > 0$. Π_{bubble} is the product of two G_0 , so one has $\Pi_{\text{bubble}}(\lambda) = \lambda^2 \Pi_{\text{bubble}}$. By performing a change of variable $\varphi = \sqrt{\lambda} \varphi'$, $\bar{\varphi} = \sqrt{\lambda} \bar{\varphi}'$, we see that

$$\tilde{p}_{\text{ladd}}[\lambda G_0, \Gamma_0, z] = \tilde{p}_{\text{ladd}}[G_0, \Gamma_0, \lambda^2 z] \quad (\text{T.2})$$

By differentiating with respect to λ and setting $\lambda = 1$, one obtains

$$\int DP G_{0;P} \frac{\delta \tilde{p}_{\text{ladd}}[G_0, \Gamma_0, z]}{\delta G_{0;P}} = 2z \frac{d}{dz} \tilde{p}_{\text{ladd}}[G_0, \Gamma_0, z] \quad (\text{T.3})$$

We compute

$$\begin{aligned} \frac{\delta}{\delta G_{0;P}} \frac{1}{\beta \mathcal{V}} \log \int \mathcal{D}[\eta, \bar{\eta}, \varphi, \bar{\varphi}] e^{-S_{\text{ladd}}^{(z)}} &= \\ = 2z \mathcal{F}[G_0(X) \Gamma_{\text{ladd}}(-X; z)](P) + 2G_{0;P}^{-2} G_{\text{ladd};P}(z) \end{aligned} \quad (\text{T.4})$$

We introduce

$$f : g := \int DP f_P g_P = \int dX f(-X)g(X) \quad (\text{T.5})$$

so that we have

$$z \frac{d}{dz} p_{\text{ladd}}[G_0, \Gamma_0, z] = -z \Pi_{\text{bubble}} : \Gamma_{\text{ladd}}(z) + \Sigma_{\text{ladd}}(z) : G_{\text{ladd}}(z) \quad (\text{T.6})$$

where $\Sigma_{\text{ladd}}(z) := G_0^{-1} - G_{\text{ladd}}^{-1}(z)$. We evaluate the functional $\tilde{p}_{\text{ladd}}[G_0, \Gamma_0, z]$ at $\Gamma_0(\lambda) = \lambda \Gamma_0$, $\lambda > 0$. By performing a change of variable $\eta = \sqrt{\lambda} \eta'$, $\bar{\eta} = \sqrt{\lambda} \bar{\eta}'$, one has

$$\tilde{p}_{\text{ladd}}[G_0, \lambda \Gamma_0, z] = \tilde{p}_{\text{ladd}}[G_0, \Gamma_0, \lambda z] \quad (\text{T.7})$$

By differentiating with respect to λ and setting $\lambda = 1$, one obtains

$$\int DP \Gamma_{0;P} \frac{\delta \tilde{p}_{\text{ladd}}[G_0, \Gamma_0, z]}{\delta \Gamma_{0;P}} = z \frac{d}{dz} \tilde{p}_{\text{ladd}}[G_0, \Gamma_0, z] \quad (\text{T.8})$$

so that

$$z \frac{d}{dz} p_{\text{ladd}}[G_0, \Gamma_0, z] = \Pi_{\text{ladd}}(z) : \Gamma_{\text{ladd}}(z) \quad (\text{T.9})$$

that implies

$$(z \Pi_{\text{bubble}} + \Pi_{\text{ladd}}(z)) : \Gamma_{\text{ladd}}(z) = \Sigma_{\text{ladd}}(z) : G_{\text{ladd}}(z) \quad (\text{T.10})$$

$$(\Pi_{\text{bubble}}(X) \equiv -[G_0(X)]^2).$$

U Numerical computation of the minimum of the action

The strategy is very simple, we expand $\lambda_c(r)$ using the convenient Legendre-Bateman basis $\{\mathcal{R}_n\}_{n \in \mathbb{N}}$ (introduced in Appendix V):

$$\lambda_c(r) = \mathcal{R}_0(l, r) + \sum_{n=1}^{\mathcal{N}_c} \lambda_n \mathcal{R}_n(l, r) \quad (\text{U.1})$$

where $\lambda_n \in \mathbb{R}$. Remark that the coefficient of \mathcal{R}_0 (which is formally λ_0) has been set equal to one. We can do that because the solution is invariant by multiplication of a scalar and it is positive, so that the scalar product between \mathcal{R}_0 and λ_c is non-zero. We write the 3d Fourier transform of λ_c as

$$\lambda_c(p) = \mathcal{B}_0(l, p) + \sum_{n=1}^{\mathcal{N}_c} \lambda_n \mathcal{B}_n(l, p) \quad (\text{U.2})$$

At this point it is easy to write an explicit expression for the action functional evaluated with this expansion:

$$A_S[\lambda_c] = \frac{\sum_{n,m=0}^{\mathcal{N}_c} \lambda_n \lambda_m \int d^3p R_0^{-1}(p) \mathcal{B}_n(l, p) \mathcal{B}_m(l, p)}{(\int d^3r (\sum_{n=0}^{\mathcal{N}_c} \lambda_n \mathcal{R}_n(l, r))^{5/2})^{4/5}} =: F(l, \{\lambda_n\}_{n=1}^{\mathcal{N}_c}) \quad (\text{U.3})$$

and the parameter l and $\{\lambda_n\}_{n=1}^{\mathcal{N}_c}$ are variationally chosen³⁷. Already the zeroth-order ($\mathcal{N}_c = 0$) gives a variational action which is correct to a few percent³⁸, and we use in practice high values of $\mathcal{N}_c \sim 10 - 15$ in order to control the error.

V Legendre-Bateman expansion

We would like to introduce a very useful basis of radial functions. We have not found references in the literature for this basis, but it should be very well-known given the very convenient analytical and numerical properties. Let $l > 0$. We define for $n \geq 0$ and for $r \geq 0$:

$$\mathcal{R}_n(l, r) := \frac{(-1)^n \tilde{P}_{2n+1}(\tanh(r/l))}{\sqrt{2\pi l} r \cosh(r/l)} \quad (\text{V.1})$$

where \tilde{P}_n is the normalized Legendre polynomial of order n . This set of functions has the following properties

- $\{\mathcal{R}_n\}$ is an orthonormal set in \mathbb{R}^3 .
- $\{\mathcal{R}_n\}$ is a complete basis of square-integrable smooth radial even functions in \mathbb{R}^3 .

³⁷We choose to variationally set l in order to have a better solution, even if it can be computed from the large- r behavior of $\lambda_c(\mathbf{r})$ (by linearizing the non-linear integral equations for λ_c).

³⁸The qualitative shape of $\lambda_c(r)$ was determined analytically (it is a (node-less) decreasing smooth function for every r , exponentially decaying for large r), and the numerical computation adds no qualitative features. We remind however that the error on λ_c is always higher than the error on A_S , as we are using a variational method.

- For large r , they decay exponentially

$$\mathcal{R}_n(l, r) \underset{r \rightarrow \infty}{=} (-1)^n \sqrt{\frac{4n+3}{\pi l}} \frac{e^{-r/l}}{r} \quad (\text{V.2})$$

- Their Fourier transform is related to the Bateman polynomials

$$\mathcal{B}_n(l, p) := \int d^3r e^{-i\mathbf{p}\cdot\mathbf{r}} \mathcal{R}_n(l, r) = 2\pi\sqrt{l} \frac{B_{2n+1}(pl)}{p \cosh(\pi pl/2)} \quad (\text{V.3})$$

- $\{\mathcal{R}_n\}$ and $\{\mathcal{B}_n\}$ admit a recursion relation.

W Discontinuities of the bold self-energies

First of all, let us show that the discontinuities of Σ_{bold} and $\tilde{\Pi}_{\text{bold}}$ must be related. Using Equation (T.10) for $G_0(z) := (G^{-1} + \Sigma_{\text{bold}}(z))^{-1}$ and $\Gamma_0(z) := ((z\Gamma)^{-1} + \tilde{\Pi}_{\text{bold}}[G, \Gamma, z]/z + \Pi_{\text{bubble}}[G] - \Pi_{\text{bubble}}[G_0(z)])^{-1}$, one has

$$(z\Pi_{\text{bubble}}[G] + \tilde{\Pi}_{\text{bold}}[G, \Gamma, z]) : \Gamma = \Sigma_{\text{bold}}[G, \Gamma, z] : G \quad (\text{W.1})$$

so that

$$\text{Disc}(\tilde{\Pi}_{\text{bold}}, z) : \Gamma = \text{Disc}(\Sigma_{\text{bold}}, z) : G \quad (\text{W.2})$$

hence the discontinuities of Σ_{bold} and $\tilde{\Pi}_{\text{bold}}$ must be of the same order.

In order to gain insight into the problem, let us consider a zero-dimensional toy model. Let us define $f(z)$ by an integral over some integration path \mathcal{P}_z in the complex plane:

$$f(z) := \int_{\mathcal{P}_z} dw e^{-S_z(w)} \quad (\text{W.3})$$

where the contour \mathcal{P}_z for $z \geq 0$ is just the positive real axis. We suppose that the action $S_z(w)$ is positive for real w and real z , but it is complex for general z and w . \mathcal{P}_z always starts from the origin and goes towards $|w| = \infty$ in such a way that the action $S_z(w)$ is always positive along this path. The integration path can be chosen to be a continuous function of z , apart from exceptional points where the integration path encounters saddle points for the action $S_z(w)$, that is when $\partial_w S_z(w) = 0$. If the action is continuous as a function of z , these are the only points where the function $f(z)$ can have discontinuities. It is possible to show that the discontinuities are given exactly by the integral over saddle points

$$\text{Disc}(f, z_0) = \int_{\mathcal{S}_{z_0}} dw e^{-S_z(w)} \quad (\text{W.4})$$

where $\mathcal{S}_{z_0} := \mathcal{P}_{z_0 e^{i0^+}} - \mathcal{P}_{z_0 e^{-i0^+}}$ is the steepest descent integration path over the saddle point. When $|z_0|$ is small enough, in many cases one can compute the integral by the saddle point approximation:

$$\text{Disc}(f, z_0) \Big|_{|z_0| \rightarrow 0^+} = e^{-S_{z_0}(w_c)} \sqrt{\frac{2\pi}{\partial_w^2 S_{z_0}(w_c)}} \quad (\text{W.5})$$

where w_c is such that $\partial_w S_{z_0}(w_c)$. This is the case that we have encountered so far, with $|\arg z_0| = 4\pi/5$ and

$$e^{-S_{z_0}(w_c)} \sim e^{-\left(\frac{A}{|z_0|}\right)^5} \quad (\text{W.6})$$

from which we see that the discontinuity is exponentially small.

We need now to generalize this formula to allow for discontinuous actions. We write

$$\text{Disc}(f, z_0) = \int_{\mathcal{S}_z} dw \text{Cont}(e^{-S_z(w)}, z_0) + \int_{Y_z} dw \text{Disc}(e^{-S_z(w)}, z_0) \quad (\text{W.7})$$

where we have introduced

$$\text{Cont}(g, u) := g(ue^{i0^+}) + g(ue^{-i0^+}) \quad (\text{W.8})$$

and $Y_z := \mathcal{P}_{z_0 e^{i0^+}} + \mathcal{P}_{z_0 e^{-i0^+}}$ is a Y -shaped integration path.

We *assume* that these formulas can be applied with no modifications to functional integrals. Let us consider the computation of the pair propagator within the fully-dressed (aka bold) scheme

$$\Gamma_{\text{bold}}[G, \Gamma, z] := -\frac{\int \mathcal{D}[\varphi, \bar{\varphi}, \eta, \bar{\eta}] e^{-S_{\text{bold}}^{(z)} \eta \bar{\eta}}}{\int \mathcal{D}[\varphi, \bar{\varphi}, \eta, \bar{\eta}] e^{-S_{\text{bold}}^{(z)}}} \quad (\text{W.9})$$

(we dropped the space-time dependence on the fields for simplicity). The bold action is given by

$$\begin{aligned} S_{\text{bold}}^{(z)}[G, \Gamma] = & -\langle \varphi | G^{-1} + \Sigma_{\text{bold}}[G, \Gamma, z] | \varphi \rangle - \langle \eta | \Gamma^{-1} + \tilde{\Pi}_{\text{bold}}[G, \Gamma, z] | \eta \rangle + \\ & + \sqrt{z} (\langle \eta | \varphi_{\downarrow} \varphi_{\uparrow} \rangle + \langle \varphi_{\downarrow} \varphi_{\uparrow} | \eta \rangle) \end{aligned} \quad (\text{W.10})$$

We are interested in the behavior for small z . We suppose that the discontinuities of Σ_{bold} and $\tilde{\Pi}_{\text{bold}}$ are exponentially small in this limit, so that we can write

$$\text{Disc}(e^{-S_{\text{bold}}^{(z)}}, z) \Big|_{|z| \rightarrow 0} = e^{-S_{\text{bold}}^{(0)}} \left(\langle \varphi | \text{Disc}(\Sigma_{\text{bold}}, z) | \varphi \rangle + \langle \eta | \text{Disc}(\tilde{\Pi}_{\text{bold}}, z) | \eta \rangle \right) \quad (\text{W.11})$$

We introduce

$$\tilde{Z}_{\text{bold}}(z) := \frac{\int \mathcal{D}[\varphi, \bar{\varphi}, \eta, \bar{\eta}] e^{-S_{\text{bold}}^{(z)}}}{\int \mathcal{D}[\varphi, \bar{\varphi}, \eta, \bar{\eta}] e^{-S_{\text{bold}}^{(0)}}} \quad (\text{W.12})$$

Using Equation (W.8), we have

$$\text{Disc}(\tilde{Z}_{\text{bold}}, z) \Big|_{|z| \rightarrow 0^+} = \frac{\int_{\mathcal{S}_z} \mathcal{D}[\varphi, \bar{\varphi}, \eta, \bar{\eta}] e^{-S_{\text{bold}}^{(z)}}}{\int \mathcal{D}[\varphi, \bar{\varphi}, \eta, \bar{\eta}] e^{-S_{\text{bold}}^{(0)}}} - 2 \text{Disc}(\Sigma_{\text{bold}}, z) : G \quad (\text{W.13})$$

We introduce

$$\gamma_{\text{bold}}[G, \Gamma, z] := - \frac{\int \mathcal{D}[\varphi, \bar{\varphi}, \eta, \bar{\eta}] e^{-S_{\text{bold}}^{(z)}} \eta \bar{\eta}}{\int \mathcal{D}[\varphi, \bar{\varphi}, \eta, \bar{\eta}] e^{-S_{\text{bold}}^{(0)}}} \quad (\text{W.14})$$

One has

$$\begin{aligned} \text{Disc}(\gamma_{\text{bold}}, z)(X) \Big|_{|z| \rightarrow 0^+} &= - \frac{\int_{\mathcal{S}_z} \mathcal{D}[\varphi, \bar{\varphi}, \eta, \bar{\eta}] e^{-S_{\text{bold}}^{(z)}} \eta(X) \bar{\eta}(0)}{\int \mathcal{D}[\varphi, \bar{\varphi}, \eta, \bar{\eta}] e^{-S_{\text{bold}}^{(0)}}} + \\ &- 2 (\text{Disc}(\Sigma_{\text{bold}}, z) : G) \Gamma(X) + \int_{Y_1, Y_2} \text{Disc}(\tilde{\Pi}_{\text{bold}}(Y_1 - Y_2), z) \Gamma(Y_2) \Gamma(X - Y_1) \end{aligned} \quad (\text{W.15})$$

Finally, we have

$$\begin{aligned} 0 = \text{Disc}(\Gamma_{\text{bold}}, z)(X) \Big|_{|z| \rightarrow 0^+} &= - \frac{\int_{\mathcal{S}_z} \mathcal{D}[\varphi, \bar{\varphi}, \eta, \bar{\eta}] e^{-S_{\text{bold}}^{(z)}} \eta(X) \bar{\eta}(0)}{\int \mathcal{D}[\varphi, \bar{\varphi}, \eta, \bar{\eta}] e^{-S_{\text{bold}}^{(0)}}} + \\ &+ \int_{Y_1, Y_2} \text{Disc}(\tilde{\Pi}_{\text{bold}}(Y_1 - Y_2), z) \Gamma(Y_2) \Gamma(X - Y_1) \end{aligned} \quad (\text{W.16})$$

This implies that the discontinuity of $\tilde{\Pi}_{\text{bold}}$ must be of equal to the discontinuity computed from the saddle point with the Thomas-Fermi approximation. For $|z| \rightarrow 0^+$, we have $\tilde{\Pi}_{\text{bold}} = O(|z| \Sigma_{\text{bold}}) = O(|z|^2)$, and we obtain at leading order

$$A := A_{\sharp} \inf_{\eta} \frac{-\langle \eta | \Gamma^{-1} | \eta \rangle}{\|\eta\|_{5/2}^2} \quad (\text{W.17})$$

similarly to the bare case.

Part II

**Connected determinant
diagrammatic Monte Carlo:
polynomial complexity despite
fermionic sign**

Article 1: Determinant Diagrammatic Monte Carlo in the thermodynamic limit



Determinant Diagrammatic Monte Carlo Algorithm in the Thermodynamic Limit

Riccardo Rossi*

Laboratoire de Physique Statistique de l'École Normale Supérieure, 75005 Paris, France

(Received 15 December 2016; published 25 July 2017)

We present a simple trick that allows us to consider the sum of all connected Feynman diagrams at fixed position of interaction vertices for general fermionic models, such that the thermodynamic limit can be taken analytically. With our approach one can achieve superior performance compared to conventional diagrammatic Monte Carlo algorithm, while rendering the algorithmic part dramatically simpler. By considering the sum of all connected diagrams at once, we allow for massive cancellations between different diagrams, greatly reducing the sign problem. In the end, the computational effort increases only exponentially with the order of the expansion, which should be contrasted with the factorial growth of the standard diagrammatic technique. We illustrate the efficiency of the technique for the two-dimensional Fermi-Hubbard model.

DOI: 10.1103/PhysRevLett.119.045701

Finding an efficient method to solve the quantum many-body problem is of fundamental physical importance. A promising strategy to gain insight is represented by quantum simulators. For example, experimentalists working with cold atoms in optical lattices are able to realize one of the most prominent models of strongly correlated electrons, the Hubbard model. A study of its equation of state at low temperature has been reported in Ref. [1]. Moreover, short-range antiferromagnetic correlations have been observed [2–6], and, very recently, even a long-range antiferromagnetic state was realized [7].

From the theoretical side, making predictions for strongly correlated fermionic systems is a very challenging problem. Quantum Monte Carlo methods are affected by the infamous sign problem when dealing with fermionic models, which in general precludes reaching low-temperature and large system sizes (see Refs. [8,9] and references therein). The simulation time to obtain a given precision scales exponentially with the system size and the inverse of the temperature. In the strongly correlated regime, it is then very difficult to extrapolate to the thermodynamic limit (TL). However, the fermionic sign gives an unexpected advantage when considering fermionic perturbation theory. For bosonic theories, typically, the perturbative expansion has a zero radius of convergence. This is due to the factorial number of Feynman diagrams all contributing with the same sign. For fermions, strong cancellations between different diagrams at fixed order lead in general to a finite convergence radius on a lattice at finite temperature. This happens because for sufficiently small interactions of whatever sign (or phase) the system is stable on a lattice at nonzero temperature. This was seen numerically [10,11], and even proved mathematically for the Hubbard model at high enough temperature [12]. Perturbation theory is therefore a powerful tool to study fermionic

theories. By analytic continuation, any point of the phase diagram which is in the same phase as the perturbative starting point can be reached in principle, provided that one has a method to compute the diagrammatic series to high order. At the moment, there are two numerical methods to evaluate diagrammatic expansions at high order, determinant diagrammatic Monte Carlo (DDMC), and diagrammatic Monte Carlo (DiagMC) simulations. Major recent achievements of DiagMC simulations are the study of the normal phase of the unitary Fermi gas [13], the determination of the ground state phase diagram of the Hubbard model up to filling factor 0.7 and interactions $U/t \leq 4$ [14], and the settlement of the Bose-metal issue [15]. Given the power and the versatility of the technique, systematic diagrammatic extensions of dynamical mean field theory are now being studied [16,17].

In DiagMC simulations [10,11,18,19] one expresses the perturbative expansion in terms of connected Feynman diagrams, which can be written directly in the TL. One then performs a random walk in the space of topologies and of integration variables of Feynman diagrams. In DDMC simulations [20–22] one computes finite-volume perturbative contributions, considering at once the sum of all Feynman diagrams (connected and disconnected) at fixed position of interaction vertices. One lets the interaction vertices perform a random walk in the space-time simulation volume. In principle, in order to compute the sum of all Feynman diagrams, one should consider all possible connections between these vertices, of which there are a factorial number. However, it has been pointed out that all these fermionic permutations can be grouped in determinants, which can be computed in polynomial time. In addition, summing all diagrams together already accounts for massive cancellations. For example, the Hubbard model at half filling has no sign problem within DDMC simulations, because the sum of all diagrams at a

given order is positive definite for every vertex configuration; in contrast the individual diagrams considered by DiagMC simulations have positive and negative signs. The major downside of DDMC simulations is that one has to consider a finite-size system, and this is a serious problem in the generic case where one has a sign problem. Intensive quantities, like the density or the energy per site, are computed in DDMC simulations as the ratio of two quantities which increase exponentially with the volume.

In this Letter we present a way to compute directly these intensive quantities, such that the thermodynamic limit can be taken analytically. It is then clear that the traditional form of sign problem is not present. As we consider the sum of all connected Feynman diagrams at once, we already account for cancellations between different diagrams at the same order, greatly reducing the variance in the sampling. In the end, the total computational cost increases only exponentially with the order, which is to be compared with the factorial increase of the standard diagrammatic technique. We provide numerical proof of the efficiency of the technique by applying it to the two-dimensional Hubbard model at low temperature and weak coupling, where the series is fast converging. We compute the radius of convergence of the series, which is determined by a phase transition happening for negative values of the interaction.

Let us present an intuitive diagrammatic derivation of the analytical result of this work. As pointed out in Refs. [20–22], we can express the sum of all diagrams with fixed space-time position of interaction vertices in terms of determinants. This is due to the fact that a determinant accounts for all the possible connections between vertices, with the right sign for fermions. In this way it is clear that one generates all diagrams, connected and disconnected. We would like to remove disconnected diagrams, as we know that only connected diagrams will contribute to intensive quantities [23]. Let us consider a disconnected diagram. It can be divided in a part which is connected to the external points of the function we are looking at, and another part which is not connected to it (see Fig. 1). This correspondence is one to one. It is then clear that we can write a recursive formula for the connected part: we subtract from the set of all diagrams (connected or not) those which can be divided in a connected part and a disconnected part. Let $c_E(V)$ be the sum of connected diagrams contributing to a correlation function with a set of external points represented by E , and with interaction vertices $V = \{v_1, \dots, v_n\}$ at fixed space-time position. Similarly, let $a_E(V)$ be the sum of all diagrams, connected and disconnected. In particular, $a_\emptyset(V)$ denotes all diagrams with interaction vertices V and no external points (they are the diagrams contributing to the grand-partition function). $a_{E'}(V')$ is easy to compute for every E' and V' as it can be expressed in terms of determinants, but we are interested in obtaining $c_E(V)$. If we know $c_E(S)$ for all S proper subset of V , we can compute $c_E(V)$ from

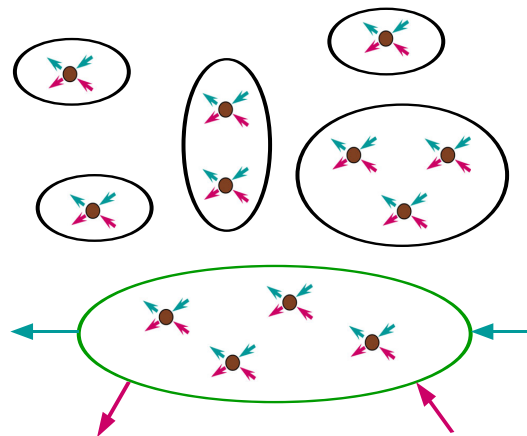


FIG. 1. A twelve-order disconnected contribution for the four-point correlation function. The big arrows represent the external lines, while the points with small arrows represent two-particle interaction vertices. The ellipses represent connected parts. The green ellipse represents all the diagrams contributing to the connected part with four interaction vertices at fixed space-time position. The black ellipses can be considered collectively as arising from connected + disconnected diagrams with no external lines.

$$c_E(V) = a_E(V) - \sum_{S \subset V} c_E(S) a_\emptyset(V \setminus S). \quad (1)$$

If one wants to compute the grand-canonical free energy (the pressure for an homogeneous system), which has no external points, one has to render one of the vertices “special” and consider connectedness with respect to it. If the vertices are indistinguishable, in order to obtain the n th order diagrammatic contribution for the correlation function one has to divide by $n!$ after summation of $c_E(V)$ over space-time position of v_1, \dots, v_n . The integral of $c_E(V)$ over the space-time positions of the v_1, \dots, v_n is convergent, in other words, one can consider directly the TL where the positions of the interaction vertices are unconstrained. The integration over the space-time position of the vertices is performed with a standard Markov chain Monte Carlo algorithm. We sample a linear combination of the order n and the order $n - 1$ for normalization purposes, but alternatively one could use order-changing updates as in the usual DDMC and DiagMC implementations.

Let us discuss how the computational cost varies with the order $n = |V|$. The time to compute $a_E(S)$ and $a_\emptyset(S)$ for all $S \subset V$ scales like $n^3 2^n$ (n^3 is the cost to compute the determinant of a $n \times n$ matrix, and we have to compute 2^n determinants roughly of this size). It can be shown that the number of arithmetic operations needed to get $c_E(V)$ from the recursive formula (1) is proportional to 3^n , which is the main contribution for n large enough. The observables we sample are not sign definite, this is reminiscent of the

fermionic sign problem. The crucial advantage of this technique over DiagMC simulations is that we eliminate topologies from configuration space. In the case where all diagrams have the same sign, this is not a big advantage. However, in fermionic models this is not at all the case, there is an almost perfect cancellation between different diagram topologies occurring with opposite signs. The cancellations are so strong that the sum over the diagrams at a certain order divided by the same sum taken with absolute values goes to zero factorially like the number of diagrams; this can be seen as a consequence of having a finite radius of convergence. This means that if one samples topologies one by one, like in DiagMC simulations, a factorial “sign problem” is encountered (see Ref. [24] for a more detailed discussion). We see, therefore, that the trick of summing over all connected topologies allows us to greatly alleviate this reminiscence of the sign problem, leaving us with a sign problem from the integration over the space-time positions of interaction vertices that increases at most exponentially with the number of vertices. One might wonder if paying an exponential cost to remove disconnected topologies is really worth it, as we could compute the sum of *all* topologies in polynomial time, as it is done in DDMC simulations. The advantage of considering only connected diagrams is that we do not suffer from the traditional form of sign problem, that is, the prohibitive scaling of computational time with system size. An analogous situation was found in the context of out-of-equilibrium impurity models [25], where in order to consider the long time evolution it was found advantageous to pay an exponential cost for each Monte Carlo step to explicitly eliminate disconnected diagrams [26]. For these reasons, we are able to reach higher orders than DiagMC simulations, even without resumming classes of diagrams more complicated than tadpoles (for the Hubbard model DiagMC simulations arrive at order ~ 6 for both the bare and bold series). Unlike DDMC simulations, the sign problem does not limit us to work at half filling or with attractive interactions.

We now discuss the results obtained by implementing this method for the two-dimensional Hubbard model. Without loss of generality we can set the hopping parameter t to one. We consider inverse temperature $\beta = 8$, repulsive on-site interaction parameter $U = 2$, at density $n = 0.875\ 00(2)$ near to half filling. All our error bars correspond to 1 standard deviation. We resum all bare tadpole diagrams, whose effect is to shift the chemical potential $\mu(U) = \mu_0 + Un_0/2$, where μ_0 is the chemical potential needed to get the density n_0 in the absence of interactions (this corresponds to the first-order semibold scheme introduced in Ref. [27]). This is useful because one has a smaller density shift as a function of U . We compare thermodynamical quantities with DiagMC benchmarks from Ref. [9]. We find compatible results, with error bars 1 order of magnitude smaller (see Fig. 2). We estimate the chemical potential at fixed density $n = 0.875$

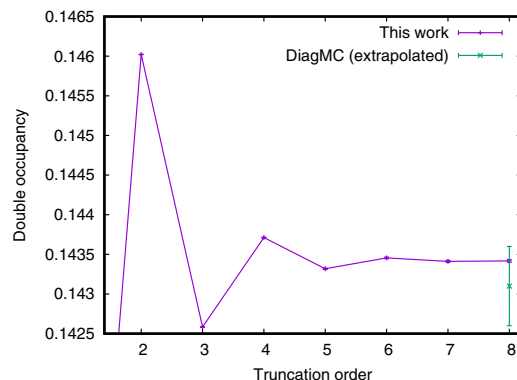


FIG. 2. Double occupancy as a function of truncation order, for $\beta = 8$, $U = 2$ and $n = 0.875\ 00(2)$. The DiagMC number is taken from Ref. [9] and it refers to infinite-order extrapolation of the bold series for $n = 0.875$.

to be $\mu = 0.55978(7)$, while DiagMC simulation gives $\mu_{\text{Diag}} = 0.558(3)$. For the energy per site, we have $E = -1.25992(6)$, while $E_{\text{Diag}} = -1.2600(6)$. As the entropy is relevant for experiments in optical lattices, we also give the value of the entropy per site $S = 0.1958(4)$. We have pushed the computations up to eleven orders for the pressure (let us note that for the pressure we have 1 order more for free) as the error bars continued to stay bounded (see Fig. 3), spending seven thousand CPU hours. Let us only remark here that the exponential cost to go to higher orders is compensated by an exponential convergence as a function of the order for a convergent series, resulting in an error bar that decays as a power law as a function of computer time [24]. We have estimated the radius of convergence of the series in U by looking at coefficients; see Fig. 4. This is compatible with a phase transition happening at $U = -5.1(1)$, when the system

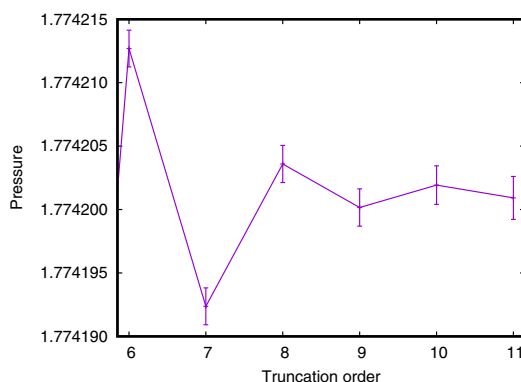


FIG. 3. Pressure as a function of truncation order, for $\beta = 8$, $U = 2$, and $n = 0.875\ 00(2)$.

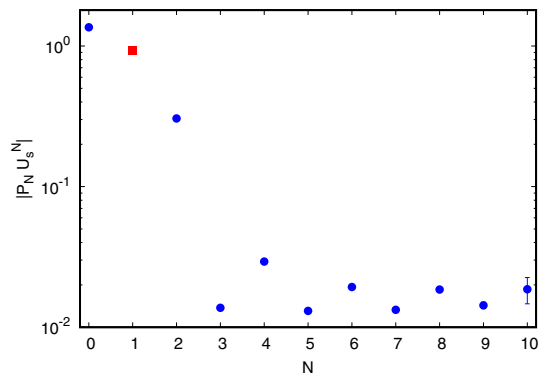


FIG. 4. $|P_N U_s^N|$ as a function of the expansion order N , where $U_s = -5.1$ and P_N is the coefficient of the series for the pressure, $P(U) = \sum_{N=0}^{\infty} P_N U^N$. The blue circle points correspond to positive values of $P_N U_s^N$, while the red square point corresponds to a negative value. We see that starting from order ~ 5 we are in the high-order asymptotic regime. This implies that the radius of convergence of the series is $R = 5.1(1)$.

is electron doped $n > 1$. This is in qualitative agreement with the established phase diagram for the attractive Hubbard model [28]. The subleading alternating structure shown in Fig. 4 is compatible with an additional singularity around $U = 6$, but further work is needed to rule out other possibilities. In principle, the series converges exponentially for $|U| < 5.1$. In practice, in order to get accurate results for moderate values of interactions it is necessary to perform analytical continuation or resummation of the series in order to accelerate (or extend) the convergence.

We stress that there is no fundamental difference in the sampling between different physical quantities, as we expect the external points to play a minor role at high-enough orders. In the high-order limit, external points can be thought as “boundary terms,” the bulk being the large number of internal interaction vertices. This intuition is supported by the universality of large-order behavior of perturbation theory, which is independent of the configuration of the external points [29]. Nevertheless, there exist simple modifications of the procedure that can improve numerical sampling in a decisive way. The simplest modification is to consider the unlegged Green’s function, which can be further divided in a fully dressed tadpole diagram, and another part. In this way one can obtain statistics for all values of the Green’s function at once, as the diagrams depend on the external points only through these legs in the space-time representation, gaining as well two more orders. To go further, one has to sample the self-energy. We want to get rid of one-particle reducible diagrams. A general one-particle reducible diagram can be divided in a part which is one-particle irreducible with respect to one of the external points, and another part consisting of a diagram for the Green’s function. We can

then derive a recursive formula for the self-energy of the same form as Eq. (1).

Finally, we note that it is possible to generalize the method to more general diagrammatic schemes by the use of a shifted action [27], where one has to consider additional interaction vertices that act as counterterms.

In conclusion, we have presented an elementary yet efficient method for the computation of high-order perturbative expansions of general fermionic models directly in thermodynamic limit. Formally, this method has superior algorithmic properties than DiagMC simulations. We have verified the formal arguments by providing numerical proof for the low-temperature Hubbard model at small interaction, obtaining results that are the state of the art in this regime. We have computed the radius of convergence of the series, which shows that the bare series is convergent up to moderate value of interaction strength. Moreover, we have shown that achieving such high orders can be used to detect singularities of thermodynamical functions, which are known to indicate phase transitions.

A natural continuation of this work would be the study of the pseudogap regime of the two-dimensional Hubbard model, where the new algorithm has the potential to extend to lower temperature the DiagMC results of Ref. [30].

I am grateful to Kris Van Houcke and Félix Werner for useful suggestions, constant support of the project, and help with writing the manuscript. I thank Boris Svistunov for fruitful discussions and for proposing improvements of the manuscript. I acknowledge useful discussions with Tommaso Comparin. This work has been partially supported by the Simons Foundation within the Many Electron Collaboration framework. Simulations ran on the cluster *MesoPSL* (Region Ile-de-France/Grant No. ANR-10-EQPX-29-01).

* Also at CNRS, Université de recherche Paris Sciences et Lettres, UPMC, Université Paris Diderot, Sorbonne Universités, and Sorbonne Paris-Cité.
riccardo.rossi@ens.fr

- [1] E. Cocchi, L. A. Miller, J. H. Drewes, M. Koschorreck, D. Pertot, F. Brennecke, and M. Köhl, *Phys. Rev. Lett.* **116**, 175301 (2016).
- [2] R. A. Hart, P. M. Duarte, T.-L. Yang, X. Liu, T. Paiva, E. Khatami, R. T. Scalettar, N. Trivedi, D. A. Huse, and R. G. Hulet, *Nature (London)* **519**, 211 (2015).
- [3] D. Greif, G. Jotzu, M. Messer, R. Desbuquois, and T. Esslinger, *Phys. Rev. Lett.* **115**, 260401 (2015).
- [4] M. F. Parsons, A. Mazurenko, C. S. Chiu, G. Ji, D. Greif, and M. Greiner, *Science* **353**, 1253 (2016).
- [5] L. W. Cheuk, M. A. Nichols, K. R. Lawrence, M. Okan, H. Zhang, E. Khatami, N. Trivedi, T. Paiva, M. Rigol, and M. W. Zwierlein, *Science* **353**, 1260 (2016).
- [6] J. H. Drewes, L. A. Miller, E. Cocchi, C. F. Chan, N. Wurz, M. Gall, D. Pertot, F. Brennecke, and M. Köhl, *Phys. Rev. Lett.* **118**, 170401 (2017).

- [7] A. Mazurenko, C. S. Chiu, G. Ji, M. F. Parsons, M. Kanász-Nagy, R. Schmidt, F. Grusdt, E. Demler, D. Greif, and M. Greiner, *Nature (London)* **545**, 462 (2017).
- [8] M. Troyer and U.-J. Wiese, *Phys. Rev. Lett.* **94**, 170201 (2005).
- [9] J. P. F. LeBlanc, A. E. Antipov, F. Becca, I. W. Bulik, G. K.-L. Chan, C.-M. Chung, Y. Deng, M. Ferrero, T. M. Henderson, C. A. Jiménez-Hoyos *et al.* (Simons Collaboration on the Many-Electron Problem), *Phys. Rev. X* **5**, 041041 (2015).
- [10] K. Van Houcke, E. Kozik, N. Prokof'ev, and B. Svistunov, *Phys. Procedia* **6**, 95 (2010).
- [11] E. Kozik, K. Van Houcke, E. Gull, L. Pollet, N. Prokof'ev, B. Svistunov, and M. Troyer, *Europhys. Lett.* **90**, 10004 (2010).
- [12] G. Benfatto, A. Giuliani, and V. Mastropietro, *Ann. Inst. Henri Poincaré* **7**, 809 (2006).
- [13] K. Van Houcke, F. Werner, E. Kozik, N. Prokof'ev, B. Svistunov, M. Ku, A. Sommer, L. Cheuk, A. Schirotzek, and M. Zwierlein, *Nat. Phys.* **8**, 366 (2012).
- [14] Y. Deng, E. Kozik, N. V. Prokof'ev, and B. V. Svistunov, *Europhys. Lett.* **110**, 57001 (2015).
- [15] J. Gukelberger, E. Kozik, L. Pollet, N. Prokof'ev, M. Sigrist, B. Svistunov, and M. Troyer, *Phys. Rev. Lett.* **113**, 195301 (2014).
- [16] S. Isakov, A. E. Antipov, and E. Gull, *Phys. Rev. B* **94**, 035102 (2016).
- [17] J. Gukelberger, E. Kozik, and H. Hafermann, arXiv: 1611.07523 [*Phys. Rev. B* (to be published)].
- [18] S. A. Kulagin, N. Prokof'ev, O. A. Starykh, B. Svistunov, and C. N. Varney, *Phys. Rev. Lett.* **110**, 070601 (2013).
- [19] A. S. Mishchenko, N. Nagaosa, and N. Prokof'ev, *Phys. Rev. Lett.* **113**, 166402 (2014).
- [20] E. Bourovski, N. Prokof'ev, and B. Svistunov, *Phys. Rev. B* **70**, 193101 (2004).
- [21] A. N. Rubtsov, V. V. Savkin, and A. I. Lichtenstein, *Phys. Rev. B* **72**, 035122 (2005).
- [22] E. Burovski, N. Prokof'ev, B. Svistunov, and M. Troyer, *Phys. Rev. Lett.* **96**, 160402 (2006).
- [23] A.-A. Abrikosov, L.-P. Gorkov, I.-E. Dzyaloshinski, and R. A. Silverman, *Methods of Quantum Field Theory in Statistical Physics* (Dover, New York, 1976).
- [24] R. Rossi, N. Prokof'ev, B. Svistunov, K. Van Houcke, and F. Werner, *Europhys. Lett.* **118**, 10004 (2017).
- [25] R. E. V. Profumo, C. Groth, L. Messio, O. Parcollet, and X. Waintal, *Phys. Rev. B* **91**, 245154 (2015).
- [26] In this context one starts from a noninteracting state and let the system evolve in real time. Observables are computed in power series of the interaction potential, whose coefficients can be expressed in terms of determinants. The use of the recursive formula for eliminating disconnected diagrams is not necessary here, because the sum over the Keldish indices directly eliminates disconnected diagrams.
- [27] R. Rossi, F. Werner, N. Prokof'ev, and B. Svistunov, *Phys. Rev. B* **93**, 161102 (2016).
- [28] T. Paiva, R. R. dos Santos, R. T. Scalettar, and P. J. H. Denteneer, *Phys. Rev. B* **69**, 184501 (2004).
- [29] J. Zinn-Justin, *Quantum Field Theory and Critical Phenomena*, 4th ed. (Clarendon Press, New York, 2002).
- [30] W. Wu, M. Ferrero, A. Georges, and E. Kozik, *Phys. Rev. B* **96**, 041105 (2017).

Article 2: Polynomial complexity despite the fermionic sign

Polynomial complexity despite the fermionic sign

R. ROSSI¹, N. PROKOF'EV^{2,3}, B. SVISTUNOV^{2,3,4,5,1}, K. VAN HOUCKE¹ and F. WERNER⁵

¹*Laboratoire de Physique Statistique, Ecole Normale Supérieure, UPMC, Université Paris Diderot, CNRS
24 rue Lhomond, 75005 Paris, France*

²*Department of Physics, University of Massachusetts - Amherst, MA 01003, USA*

³*National Research Center "Kurchatov Institute" - 123182 Moscow, Russia*

⁴*Wilczek Quantum Center, Zhejiang University of Technology - Hangzhou 310014, China*

⁵*Laboratoire Kastler Brossel, Ecole Normale Supérieure, UPMC, CNRS, Collège de France
24 rue Lhomond, 75005 Paris, France*

received 29 March 2017; accepted in final form 10 May 2017

published online 30 May 2017

PACS 02.70.Ss – Quantum Monte Carlo methods

PACS 71.10.Fd – Lattice fermion models (Hubbard model, etc.)

Abstract – It is commonly believed that in unbiased quantum Monte Carlo approaches to fermionic many-body problems, the infamous sign problem generically implies prohibitively large computational times for obtaining thermodynamic-limit quantities. We point out that for convergent Feynman diagrammatic series evaluated with a recently introduced Monte Carlo algorithm (see Rossi R., arXiv:1612.05184), the computational time increases only polynomially with the inverse error on thermodynamic-limit quantities.

Copyright © EPLA, 2017

The notion of fermion sign problem (FSP) was originally formulated in the context of auxiliary-field, path-integral and diffusion quantum Monte Carlo (QMC) methods [1–4]. There, it was observed that the computational time required for calculating properties of the fermionic system to a given accuracy scales exponentially with the system volume. Later, the notion of FSP was implicitly extended to an arbitrary QMC approach dealing with interacting fermions, referring to the stochastic sampling of a non-sign-definite quantity with a near cancellation between positive and negative contributions. Sign-free Monte Carlo (MC) algorithms were emerging only as exceptions confirming the rule: In each such case, the absence of FSP was due to some special property of the simulated model (see, e.g., [5–11] and references therein). Nowadays the FSP is generally perceived as one of the most important unsolved problems in the field of numerical studies of interacting fermionic systems in dimensions $d > 1$ (see footnote ¹).

The main message of this letter follows from a simple observation. Suppose some quantity Q is computed from a limit $Q = \lim_{n \rightarrow \infty} Q_n$, with an exponentially fast convergence, $|Q - Q_n| \sim e^{-\#n}$ (where $\#$ denotes some positive

constant). Then in order to compute Q up to an error $|Q - Q_n| = \epsilon$ it is sufficient to take $n \sim \ln \epsilon^{-1}$. Hence, even if the computational time increases exponentially as a function of n , $t \sim e^{\#n}$, the increase of t as a function of ϵ^{-1} is only polynomial, $\ln t \sim \ln \epsilon^{-1}$.

This observation applies to the simulation of interacting fermions by the algorithm introduced in ref. [12], denoted hereafter by the acronym CDet, for connected determinant diagrammatic MC. This algorithm works directly in the thermodynamic limit since it evaluates the series of *connected* Feynman diagrams. It exploits two advantages of the fermionic sign: First, for fermions on a lattice at finite temperature, the series has a finite radius of convergence, so that the convergence as a function of diagram order n is exponential; second, a factorial number of connected Feynman diagrams can be evaluated in exponential time using determinants (and a recursive formula).

In general, sign-alternation of observables simulated by MC methods is neither sufficient nor necessary to state that the problem is intractable. One should rather focus on what we will call the “computational complexity problem” (CCP) instead of the FSP. The key question is the one that is most relevant practically²: How easily

¹Frustrated spin and frustrated bosonic (with restricted on-site Hilbert space) lattice models can be mapped to a system of interacting fermions and thus are part of the present discussion.

²We closely follow ideas expressed by D. Ceperley at the Meeting of the *Simons Collaboration on the Many-Electron Problem*, New York, November 19–20, 2015.

can one indefinitely increase the accuracy of the computed thermodynamic-limit answer? This leads to the following definition of the CCP that can be applied to any numerical scheme. Let Q be the intensive quantity of interest in the thermodynamic limit. *A numerical scheme is said to have CCP if the computational time t required to obtain Q with an error ϵ diverges faster than any polynomial function of $\epsilon^{-1} \rightarrow \infty$. The CCP is considered to be solved if*

$$t(\epsilon) = O(\epsilon^{-\alpha}). \quad (1)$$

Note that we consider unbiased methods, *i.e.*, $\epsilon \rightarrow 0$ is the difference between computed value and *exact* value.

In what follows, we show in some detail that CDet solves the CCP, at least at finite temperature and small enough interaction. In parallel, we also discuss the conventional diagrammatic Monte Carlo approach (hereafter denoted by DiagMC) in which the sum over diagram topologies is done stochastically [13]. We then show that the conventional FSP leads to a CCP for path-integral and auxiliary-field QMC.

In quantum Monte Carlo, one typically generates configurations \mathcal{C} according to a conveniently chosen unnormalised probability distribution $P(\mathcal{C})$ that is positive. Any sign alternation is taken into account when collecting statistics, and is absorbed into the quantity $A(\mathcal{C})$ that is being measured. The average with respect to P ,

$$\langle A \rangle_P = \frac{\sum_{\mathcal{C}} P(\mathcal{C}) A(\mathcal{C})}{\sum_{\mathcal{C}} P(\mathcal{C})}, \quad (2)$$

is estimated through

$$\frac{1}{N_{MC}} \sum_{i=1}^{N_{MC}} A(\mathcal{C}_i), \quad (3)$$

with N_{MC} the number of MC measurements and \mathcal{C}_i the configuration at the i -th measurement. By the central limit theorem, the 1σ statistical error on (3) is given by

$$\epsilon_{\text{stat}} = \sigma_A \sqrt{\frac{2 \tau_{\text{auto}} + 1}{N_{MC}}}, \quad (4)$$

with τ_{auto} the integrated autocorrelation time and $\sigma_A^2 = \langle A^2 \rangle_P - \langle A \rangle_P^2$ the variance on individual measurements.

We now specialize to CDet and DiagMC. We consider the computation of an observable (*e.g.*, density or double occupancy). For convenience, we make two simplifications regarding the Monte Carlo algorithm. We expect that this does not change the final CCP scaling. The first simplification is that a separate simulation is performed for each order, while the normalisation factors z_n (see below) are known. The second simplification is that in DiagMC, rather than sampling the self-energy diagrams and then obtaining observables from the Dyson equation, we consider here sampling the diagrams for the observable (including one-particle reducible diagrams), so that external variables are simply fixed (to zero in space and

imaginary-time representation). A DiagMC configuration is then defined by a Feynman diagram topology together with values of the internal variables X . In CDet a configuration is defined only by the internal variables X (the space and imaginary-time coordinates of the interaction vertices), while the weight of a configuration is given by the sum over all possible connected diagram topologies connecting the internal and external vertices.

Let us denote the contribution of a diagram of topology \mathcal{T} for fixed internal variables X by $\mathcal{D}(\mathcal{T}, X)$. Let a_n be the sum of all Feynman diagrams of order n :

$$a_n = \int dX \sum_{\mathcal{T} \in \mathcal{S}_n} \mathcal{D}(\mathcal{T}, X), \quad (5)$$

with \mathcal{S}_n the set of all diagram topologies at order n . This can be rewritten in the form of eq. (2):

$$a_n = \langle A_n \rangle_{P_n}, \quad (6)$$

with the unnormalised distribution to be sampled chosen to be

$$\begin{cases} P_n(\mathcal{T}, X) = |\mathcal{D}(\mathcal{T}, X)| & \text{(DiagMC),} \\ P_n(X) = \left| \sum_{\mathcal{T} \in \mathcal{S}_n} \mathcal{D}(\mathcal{T}, X) \right| & \text{(CDet)} \end{cases} \quad (7)$$

and

$$A_n = \begin{cases} z_n \text{ sign}[\mathcal{D}(\mathcal{T}, X)] & \text{(DiagMC),} \\ z_n \text{ sign} \left[\sum_{\mathcal{T} \in \mathcal{S}_n} \mathcal{D}(\mathcal{T}, X) \right] & \text{(CDet)} \end{cases} \quad (8)$$

with the normalization factors

$$z_n = \begin{cases} \int dX \sum_{\mathcal{T} \in \mathcal{S}_n} |\mathcal{D}(\mathcal{T}, X)| & \text{(DiagMC),} \\ \int dX \left| \sum_{\mathcal{T} \in \mathcal{S}_n} \mathcal{D}(\mathcal{T}, X) \right| & \text{(CDet).} \end{cases} \quad (9)$$

So, in DiagMC the diagrams are sampled according to the distribution $|\mathcal{D}(\mathcal{T}, X)|$, while in CDet diagrams are grouped together via determinants and in the MC part of the algorithm one samples X according to the distribution $|\sum_{\mathcal{T} \in \mathcal{S}_n} \mathcal{D}(\mathcal{T}, X)|$. In what follows we neglect the statistical error on the normalisation factors z_n since they are obtained by sampling a sign-positive quantity.

Here we consider fermions on a lattice at finite temperature, so that the radius of convergence of the diagrammatic series is finite [12–14]. Assuming that we are inside the radius of convergence, the convergence is exponential,

$$|a_n| \underset{n \rightarrow \infty}{=} O(R^{-n}) \quad (10)$$

with $R > 1$ a constant. Here and in what follows we omit multiplicative constants and power laws which do not affect the dominant scaling behavior.

The number of diagrams scales factorially with the order n . For CDet, however, one takes into account cancellations between different diagram topologies. More specifically, we expect that for fermions on a lattice at finite temperature,

$$z_n \underset{n \rightarrow \infty}{\sim} R_D^{-n} n! \quad (\text{DiagMC}), \quad (11)$$

$$z_n \underset{n \rightarrow \infty}{\sim} R_C^{-n} \quad (\text{CDet}) \quad (12)$$

with R_D and R_C positive constants³.

Let us discuss the behavior of the average sign, $\langle \text{sign} \rangle := \langle \text{sign} A_n \rangle_{P_n} = a_n/z_n$, as a function of the order n . For DiagMC, we see that $\langle \text{sign} \rangle$ tends to zero factorially, a manifestation of the near-compensation between different diagrams. For CDet, $\langle \text{sign} \rangle$ tends to zero exponentially in the generic case where $R_C < R$.

As a result, the variance on individual measurements behaves as

$$\sigma_{A_n} = z_n \sqrt{1 - \langle \text{sign} \rangle_{P_n}^2} \underset{n \rightarrow \infty}{\sim} z_n, \quad (13)$$

which, together with eq. (4), gives for the statistical error bar on the n -th order contribution a_n

$$\epsilon_{\text{stat}}(n) \underset{n \rightarrow \infty}{\sim} z_n \sqrt{\frac{2 \tau_{\text{auto}}(n) + 1}{N_{MC}(n)}}. \quad (14)$$

Here $\tau_{\text{auto}}(n)$ is expected to increase at most polynomially with n , which we have checked numerically for CDet; we will neglect this n -dependence of τ_{auto} since it will not affect the final scalings. An appropriate dependence $N_{MC}(n)$ of the number of MC steps on order will be specified below.

Note that the relative statistical error given by the absolute value of $\epsilon_{\text{stat}}(n)/a_n \propto z_n/a_n = 1/\langle \text{sign} \rangle_{P_n}$ diverges factorially for DiagMC and exponentially for CDet. This can be viewed as a sign problem for diagrammatic Monte Carlo methods, limiting the order that can be reached. On the other hand, the exponential convergence (10), which is only possible thanks to the fermionic sign, implies that reaching very high orders is not necessary, as we now quantify.

The assumption of exponential convergence implies that the systematic error due to the finite diagram-order cut-off N ,

$$\epsilon_{\text{sys}}(N) = \sum_{n=N+1}^{\infty} a_n, \quad (15)$$

decreases exponentially,

$$\epsilon_{\text{sys}}(N) \underset{N \rightarrow \infty}{\sim} O(R^{-N}). \quad (16)$$

To achieve a final error $\sim \epsilon$, it is then natural to work in a regime where systematic and statistical errors are on the

³Equation (12) is a natural conjecture given eq. (10); its rigorous proof may be obtained using techniques similar to those of ref. [15] (see ref. [16]). Equation (11) is plausible since this is the generic large-order behavior for bosonic theories [17].

same order. We thus choose N such that $R^{-N} \sim \epsilon$, and we take a computational time t such that the total statistical error is $\epsilon_{\text{stat}} \sim \epsilon$. Neglecting correlations between different orders, we have $\epsilon_{\text{stat}}^2 \simeq \sum_{n=0}^N \epsilon_{\text{stat}}(n)^2$, which leads us to choose $N_{MC}(n)$ such that $\epsilon_{\text{stat}}(n)$ is n -independent. Equation (14) together with eqs. (11), (12) then yield

$$t_n \underset{n \rightarrow \infty}{\sim} \begin{cases} \frac{1}{\epsilon^2} \frac{(n!)^2}{R_D^{2n}} & (\text{DiagMC}), \\ \frac{1}{\epsilon^2} \left(\frac{3}{R_C}\right)^n & (\text{CDet}), \end{cases} \quad (17)$$

where the factor 3 for CDet comes from the fact that the computational time per MC step is $\sim 3^n$, because of the recursive formula that needs to be evaluated in order to eliminate disconnected diagrams [12]. As a result, for DiagMC most time is spent sampling the highest order, while for CDet this is the case only for $R_C < \sqrt{3}$. Finally, we get

$$t(\epsilon) \sim \epsilon^{-\# \ln(\ln \epsilon^{-1})} \quad (\text{DiagMC}), \quad (18)$$

$$t(\epsilon) \sim \epsilon^{-\alpha} \quad (\text{CDet}). \quad (19)$$

Hence polynomial scaling is nearly reached with DiagMC, and is achieved with CDet. The exponent for CDet is given by

$$\alpha = 2 + \frac{\ln(3/R_C^2)}{\ln R} \quad (20)$$

if $R_C < \sqrt{3}$.

The case $R_C > \sqrt{3}$ is particularly instructive. Here, most time is spent sampling low diagram orders, and one has $\alpha = 2$, which is the best scaling one can achieve in any Monte Carlo computation. We thus conclude that fermionic sign —all by itself— does not necessarily leads to *any* qualitative effect on the scaling of computational time with ϵ .

The above scalings are not purely academic considerations, as we illustrate with an example for CDet. We analyse the computation, reported in ref. [12], of the pressure of Fermi-Hubbard model in two dimensions. The diagrammatic scheme is a bare series with bare tadpoles taken into account through a shift of the chemical potential. The Hubbard parameters are: interaction $U = 2$, chemical potential $\mu = 0.55978$ and inverse temperature $\beta = 8$ (with hopping = 1); this corresponds to a density $n = 0.87500(2)$. Figure 1(a) shows that $|a_n|$ approaches an exponential behavior R^{-n} with $R = 2.5(1)$, while fig. 1(b) shows that z_n approaches R_C^{-n} with $R_C = 0.75(3)$ (see footnote ⁴). We can make three important observations. First, the exponent $\alpha = 3.8(2)$ is not too large. Second, we clearly reach the asymptotic regime where eqs. (12), (16), and therefore also eq. (19), are valid. Third, $|a_n|$ at low n is ~ 100 times larger than the extrapolation to low orders of the large-order behavior shown by the straight line in

⁴For the density and the kinetic energy, we find the same value of R_C within our error bars.

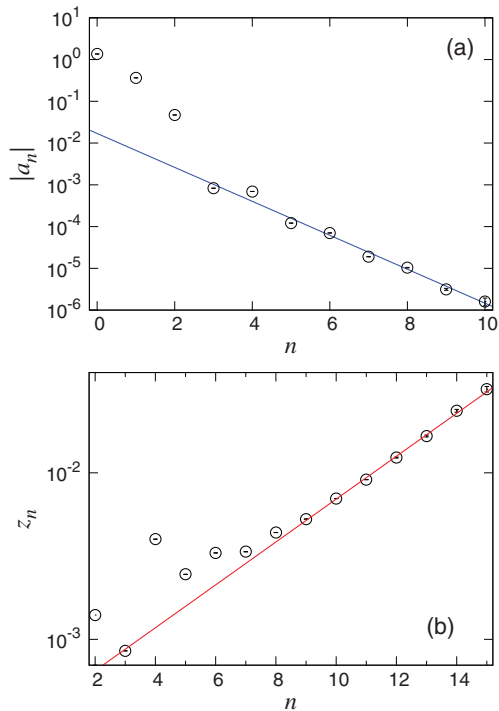


Fig. 1: (Colour online) (a) Absolute value of the sum of all order- n diagrams $|a_n|$, and (b) weight z_n of the order- n configuration space of connected determinant diagrammatic Monte Carlo, for the pressure of the Fermi-Hubbard model (at $U = 2$, $\beta = 8$, $n \simeq 0.875$). The lines are linear fits to the data at large n .

fig. 1(a). These three observations explain why it was possible to obtain a $\sim 10^{-6}$ relative accuracy for the pressure in ref. [12]. Interestingly, the second and third observations hold independently of U (with $\mu(U) = \mu_0 + Un_0/2$ as in [12]). In contrast, α diverges when U tends to the critical value $U_c = 2R(U = 2) \simeq 5.1$ such that $R(U_c) = 1$. Divergent-series summation methods may allow to approach this point and even to go beyond it; we leave this for future study.

To avoid possible confusion, let us remark that we do not claim any connection between our results and the computational complexity theory of computer science. In this theory, a “problem instance” is defined by \mathcal{N} parameters, and the P complexity class is defined by polynomial scaling of computational time *with respect to* \mathcal{N} for $\mathcal{N} \rightarrow \infty$ (in the worst case with respect to all possible instances). In the spin-glass problem discussed in [18], an instance is a disorder realisation, and \mathcal{N} is the number of random couplings (which happens to coincide with the system volume). In contrast, here we consider problems defined by a *fixed* (usually small) number of model-parameters (*e.g.*, T , U and μ for the Hubbard model in the thermodynamic limit).

We turn to “traditional” QMC, by which we mean here path-integral or auxiliary-field QMC. We consider the computation of an intensive quantity at finite temperature. Generically the FSP leads to an exponential scaling with spatial volume and inverse temperature of the average sign, and hence, due to eq. (4), of the statistical error (see, *e.g.*, [1,2,4,10]):

$$\epsilon_{\text{stat}}(L) \underset{L \rightarrow \infty}{\sim} \frac{e^{\#\beta L^d}}{\sqrt{t}}, \quad (21)$$

where L is the linear system size.

Beside the statistical error, we also need to take into account the systematic error $\epsilon_{\text{sys}}(L)$ coming from the finite size L . The total error ϵ entering the CCP is $\epsilon \sim \epsilon_{\text{stat}}(L) + \epsilon_{\text{sys}}(L)$. We assume that finite-size corrections decrease exponentially,

$$\epsilon_{\text{sys}}(L) \underset{L \rightarrow \infty}{\sim} e^{-\#L}, \quad (22)$$

which is expected generically (away from second-order phase transitions and at finite temperature). For a given computational time t , the optimal strategy is to choose L so that $\epsilon_{\text{sys}} \sim \epsilon_{\text{stat}}$, which yields

$$t(\epsilon) \sim e^{\#\beta(\ln \epsilon^{-1})^d}. \quad (23)$$

So for $d > 1$ the scaling of t with ϵ^{-1} is quasi-polynomial and there is a CCP. In one dimension there is no CCP, which is another illustration of the simple observation presented in the introduction.

Apart from these asymptotic scalings, there are also practical advantages of diagrammatic methods over traditional QMC. For traditional QMC, the condition for getting close to the thermodynamic limit is typically L much larger than the correlation length. Equation (21) then yields a computational time $t \propto e^{\#2\beta L^d}$ which is often prohibitive, meaning that one cannot get close to the thermodynamic limit, and that one cannot even reach the asymptotic scaling regimes (22), (23). The situation is very different in diagrammatic expansions, where as shown by the above example, the asymptotic regime is accessible, and, moreover, the lowest orders typically set the scale while higher-order contributions are merely corrections.

In conclusion, unbiased numerical methods for solving quantum many-fermion problems should be evaluated on the basis of their scaling of computational time with respect to the final error bar on thermodynamic-limit quantities. The presence of a fluctuating sign does not suffice to say that a problem is intractable by Monte Carlo. Nothing prevents in principle a polynomial scaling of the CPU time *vs.* the inverse error bar. We demonstrated that such polynomial complexity is indeed achieved by the recently proposed CDet method when inside the radius of convergence of the Feynman diagrammatic series. Since this method offers the possibility to calculate properties of many-fermion systems in polynomial time, it is fair to

say that the sign problem has become irrelevant here and a numerical solution to the many-fermion problem is available, at least in some region of parameter space.

We acknowledge support from ERC Grant Thermodynamix (NP and FW), the Simons Foundation's Many Electron Collaboration, the National Science Foundation under the grant PHY-1314735, and the MURI Program New Quantum Phases of Matter from AFOSR (NP and BS). Some of us are members of Paris Sciences et Lettres, Sorbonne Universités (RR, KVH and FW) and Sorbonne Paris-Cité (RR and KVH).

REFERENCES

- [1] LOH E. Y., GUBERNATIS J. E., SCALETTAR R. T., WHITE S. R., SCALAPINO D. J. and SUGAR R. L., *Phys. Rev. B*, **41** (1990) 9301.
- [2] CEPERLEY D. M., *Path integral Monte Carlo methods for fermions*, in *Monte Carlo and Molecular Dynamics of Condensed Matter Systems*, edited by BINDER K. and CICCOTTI G., Vol. **49** (Editrice Compositori, Bologna, Italy) 1996.
- [3] CEPERLEY D. M., *Quantum Monte Carlo Methods for Fermions*, in *Proceedings of the Les Houches Summer School, Session 56, Strongly Interacting Fermions and High T_c Superconductivity*, edited by DOUCOT B. and ZINN-JUSTIN J. (Elsevier) 1995.
- [4] ASSAAD F. F. and EVERTZ H. G., *World-line and Determinantal Quantum Monte Carlo Methods for Spins, Phonons and Electrons*, in *Computational Many-Particle Physics*, edited by FEHSKE H., SCHNEIDER R. and WEIßE A., *Lect. Notes Phys.*, Vol. **739** (Springer) 2008, pp. 277–356.
- [5] CHANDRASEKHARAN S. and WIESE U.-J., *Phys. Rev. Lett.*, **83** (1999) 3116.
- [6] BERG E., METLITSKI M. A. and SACHDEV S., *Science*, **338** (2012) 1606.
- [7] WEI Z. C., WU C., YI LI, ZHANG S. and XIANG T., *Phys. Rev. Lett.*, **116** (2016) 250601.
- [8] ALET F., DAMLE K., and PUJARI S., *Phys. Rev. Lett.*, **117** (2016) 197203.
- [9] HONECKER A., WESSEL S., KERKDYK R., PRUSCHKE T., MILA F. and NORMAND B., *Phys. Rev. B*, **93** (2016) 054408.
- [10] IAZZI M., SOLUYANOV A. A. and TROYER M., *Phys. Rev. B*, **93** (2016) 115102.
- [11] CAPPONI S., *J. Phys.: Condens. Matter*, **29** (2017) 043002.
- [12] ROSSI R., arXiv:1612.05184.
- [13] VAN HOUCKE K., KOZIK E., PROKOF'EV N. and SVISTUNOV B., *Phys. Procedia*, **6** (2010) 95.
- [14] BENFATTO G., GIULIANI A. and MASTROPIETRO V., *Ann. Henri Poincaré*, **7** (2006) 809.
- [15] ABDESSELAM A. and RIVASSEAU V., *Lett. Math. Phys.*, **44** (1998) 77.
- [16] MAGNEN J., private communication.
- [17] ZINN-JUSTIN J., *Phys. Rep.*, **70** (1981) 109.
- [18] TROYER M. and WIESE U.-J., *Phys. Rev. Lett.*, **94** (2005) 170201.

Complements

We present now a short complement on the technical parts of Article 1. We also provide an extended discussion of computational complexity, which is the subject of Article 2.

1 The recursive formula for many-variable formal power series

We introduce an elegant and powerful framework to formalize diagrammatic expansions.

In order to motivate this formalism, let us start with an example. We consider the Green's function G of the Hubbard model. It can be computed for small enough interaction strength U by a (bare) diagrammatic expansion:

$$G(U) = \sum_{n=0}^{\infty} U^n G_n \quad (1)$$

where G_n can be expressed as a space-time integral over the position of the interaction vertices X_0, \dots, X_{n-1} :

$$G_n = \frac{1}{n!} \int_{X_0, \dots, X_{n-1}} G(\{X_0, \dots, X_{n-1}\}) \quad (2)$$

We wish to consider directly the integrand $G_n(\{X_0, \dots, X_{n-1}\})$ of this expansion. For this reason, we introduce a space-time dependent coupling constant $U(X)$, and we consider the expansion of G as before:³⁹

$$\begin{aligned} G[U] &= \sum_{n=0}^{\infty} \frac{1}{n!} \int_{X_0, \dots, X_{n-1}} G(\{X_0, \dots, X_{n-1}\}) \prod_{j=0}^{n-1} U(X_j) \\ &= \sum_{n=0}^{\infty} \int_{X_0 \leq X_1 \leq \dots \leq X_{n-1}} G(\{X_0, \dots, X_{n-1}\}) \prod_{j=0}^{n-1} U(X_j) \end{aligned} \quad (3)$$

³⁹We define an order relation on space-time coordinate: $X = (\mathbf{x}, x_4) \leq Y = (\mathbf{y}, y_4)$ if $x_4 \leq y_4$.

But this is just the Taylor expansion of the many-variable function $G[U]$, $G(\{X_0, \dots, X_{n-1}\})$ is just a coefficient of this Taylor expansion. We would therefore like to promote each $U(X)$ to an independent variable.

Inspired by this idea, we are lead to study properties of general many-variable formal power series. Let \mathcal{I} be a discrete set with an order relation: $\forall v_1, v_2 \in \mathcal{I}, v_1 \neq v_2$, then either $v_1 < v_2$ or $v_2 < v_1$. The discreteness of the set is not important, we only use it for notational simplicity. We introduce this notation for many-variable formal power series:

(Many-variable formal power series):

$$F[\xi] = \sum_{n=0}^{\infty} \sum_{v_0 \leq \dots \leq v_{n-1}} F(\{v_0, \dots, v_{n-1}\}) \prod_{j=0}^{n-1} \xi_{v_j} = \sum_V F(V) \xi^V \quad (4)$$

where $F(\{v_0, \dots, v_{n-1}\}) \in \mathbb{C}$ and $V = \{v_0, \dots, v_{n-1}\}$ is a multiset built on \mathcal{I} .

V must be a multiset in the previous formula ⁴⁰, but if the set \mathcal{I} represent continuous variables like imaginary time (and this is the typical case) we can just consider V to be a set without repeated elements. Here ξ_{v_j} plays the role of a bookkeeping parameter. Note the useful property

$$\xi^V \xi^W = \xi^{V \cup W} \quad (5)$$

where the union \cup is the union between multiset (for example, $\{v\} \cup \{v\} = \{v, v\}$). $F[\xi]$ can be thought as the generating functional of the functions $F(V)$. We say that two functionals $F[\xi]$ and $H[\xi]$ are identical if

$$F[\xi] = H[\xi] \quad \Leftrightarrow \quad F(V) = H(V) \quad \forall V \quad (6)$$

for every V . We define algebraic operations of formal power series in the standard way:

$$F[\xi] + H[\xi] = \sum_V (F(V) + H(V)) \xi^V \quad (7)$$

$$F[\xi] H[\xi] = \sum_V \left(\sum_{S \subseteq V} F(S) H(V \setminus S) \right) \xi^V \quad (8)$$

⁴⁰We would like to stress that V is a multiset, it can have repeated elements. The limiting case is obtained when \mathcal{I} consists only of one element, which is obtained for simple Taylor expansion in the interaction strength. In this case, if we call the v the only element of \mathcal{I} , one has that $V \in \{\emptyset, \{v\}, \{v, v\}, \{v, v, v\}, \dots\}$, that corresponds to $1, U, U^2, U^3$ and so on.

We would like to compute a “correlation function” $c[\xi]$, which is given by the ratio of formal power series

$$c[\xi] = \frac{a[\xi]}{z[\xi]}, \quad z(\emptyset) \neq 0 \quad (9)$$

We will be interested in computing the coefficients of $c[\xi]$ in terms of the coefficients of $a[\xi]$ and $z[\xi]$ in an efficient way. We write

$$a[\xi] = \sum_V a(V) \xi^V = c[\xi] z[\xi] = \sum_V \left(\sum_{S \subseteq V} c(S) z(V \setminus S) \right) \xi^V \quad (10)$$

where we used (8). We use (6) for comparing term by term:

$$a(V) = \sum_{S \subseteq V} c(S) z(V \setminus S) \quad (11)$$

We therefore arrive at the fundamental recursive formula:

(Recursive formula): Suppose that we have to compute the ratio of two many-variable formal power series:

$$c[\xi] = \frac{a[\xi]}{z[\xi]} \quad (12)$$

and $z(\emptyset) \neq 0$. Then we can use the following recursive formula:

$$c(V) = \frac{a(V)}{z(\emptyset)} - \sum_{S \subsetneq V} c(S) \frac{z(V \setminus S)}{z(\emptyset)} \quad (13)$$

Let us consider the “free-energy”

$$p[\xi] = \log z[\xi] \quad (14)$$

We first compute

$$\left(\sum_{v \in \mathcal{I}} \xi^v \frac{\partial}{\partial \xi^v} \right) \xi^V = |V| \xi^V \quad (15)$$

We write

$$\sum_v \xi^v \partial_{\xi^v} p[\xi] = \sum_V |V| p(V) \xi^V = \frac{\sum_v \xi^v \partial_{\xi^v} z[\xi]}{z[\xi]} = \frac{\sum_V |V| z(V) \xi^V}{\sum_V z(V) \xi^V} \quad (16)$$

We can apply then the recursive formula (12) to show

(Recursive formula for the free-energy): Suppose that

$$p[\xi] = \log z[\xi] \quad (17)$$

and $z(\emptyset) \neq 0$. Then $p(\emptyset) = \log z(\emptyset)$ and for $V \neq \emptyset$ one has

$$p(V) = z(V) - \sum_{S \subsetneq V} \frac{|S|}{|V|} p(S) z(V \setminus S) \quad (18)$$

In Appendix A we calculate the cost of applying the recursive formula when V is a set (i.e. when all the elements of V are different, this is the most expensive case and the one which is usually encountered), which is found to be of order $O(3^n)$ for $|V| = n$:

(Cost of the recursive formula): There exists an algorithm that computes $c(V)$ in $3^n - 2^n$ arithmetic operations ($n := |V|$) knowing $a(S)$ and $z(S)$ for all $S \subseteq V$.

2 Example: two-body interactions with a linear quadratic shift

We will limit ourselves for definiteness to discuss a lattice model with two-body interactions. Schematically, the action is

$$S_{\text{physical}} := - \int_{\chi, \zeta} \bar{\psi}(\chi) (G_0^{-1} \psi)(\chi) + \int_{\chi, \zeta} U(\chi, \zeta) \bar{\psi} \psi(\chi) \bar{\psi} \psi(\zeta) \quad (19)$$

where χ and ζ are collective spin-space-imaginary time variables, $\chi = (\chi_0, \vec{\chi}, \chi_4)$, $\chi_0 \in \{\uparrow, \downarrow\}$, $\vec{\chi} \in \mathbb{Z}^d$, $\chi_4 \in [0, \beta]$ (β is the inverse temperature). We introduce a shifted-action with a linear quadratic shift:

$$\begin{aligned} S[\xi] := & - \int_{\chi, \zeta} \bar{\psi}(\chi) (\tilde{G}_1^{-1} \psi)(\chi) + \int_{\chi, \zeta} \xi(\chi, \zeta) (\bar{\psi} \psi - \alpha)(\chi) (\bar{\psi} \psi - \alpha)(\zeta) + \\ & - \int_{\chi, \zeta} U(\chi, \zeta) \alpha(\chi) \alpha(\zeta) \end{aligned} \quad (20)$$

Here the ξ are just formal bookkeeping parameters. In this case the set \mathcal{I} is continuous $\mathcal{I} = (\{\uparrow, \downarrow\} \times \mathbb{Z}^d \times [0, \beta])^2$. Note that we have also added a mean-field-like shift $\alpha(\chi)$ to the interaction.

We impose that the shifted-action is equal to the physical action when evaluated for $\xi = U$:

$$S[U] = S_{\text{physical}} \quad (21)$$

2.1 Calculation of $a_E(V)$

We define

$$a_E[\xi] := (-1)^m \frac{\int \mathcal{D}[\psi, \bar{\psi}] e^{-S[\xi]} \left(\prod_{j=0}^{m-1} \psi(\rho^{(j)}) \bar{\psi}(\delta^{(j)}) \right)}{\int \mathcal{D}[\psi, \bar{\psi}] e^{-S[0]}} \quad (22)$$

where $E := \{(\rho^{(j)}, \delta^{(j)})\}_{j \in \{0, \dots, m-1\}}$. We would like to compute $a_E(V)$, defined by

$$a_E[\xi] = \sum_{n=0}^{\infty} \int_{\chi^{(0)}, \zeta^{(0)}, \dots, \chi^{(n-1)}, \zeta^{(n-1)}} \frac{a_E(V)}{n!} \prod_{j=0}^{n-1} \xi(\chi_j, \zeta_j) = \int_V a_E(V) \xi^V \quad (23)$$

where $V := \{(\chi^{(j)}, \zeta^{(j)})\}_{j \in \{0, \dots, n-1\}}$. Wick's theorem allows us to compute $a_E(V)$ exactly in terms of determinants:

(Wick's theorem): Let $E := \{(\rho^{(j)}, \delta^{(j)})\}_{j \in \{0, \dots, m-1\}}$ and $V := \{(\chi^{(j)}, \zeta^{(j)})\}_{j \in \{0, \dots, n-1\}}$. One has

$$a_E(V) = \det \tilde{\mathcal{G}} \quad (24)$$

where for $a, b \in \{0, \dots, m+2n-1\}$ one has

$$\tilde{G}_{ab} := \tilde{G}_1(\eta_a, \gamma_b) - \lambda_a \delta_{ab} \quad (25)$$

$$\begin{aligned} \eta_a &:= \begin{cases} \rho^{(a)} & 0 \leq a \leq m-1 \\ \chi^{(a-m)} & m \leq a \leq m+n-1 \\ \zeta^{(a-n-m)} & m+n \leq a \leq m+2n-1 \end{cases} \\ \gamma_a &:= \begin{cases} \delta^{(a)} & 0 \leq a \leq m-1 \\ \chi^{(a-m)} & m \leq a \leq m+n-1 \\ \zeta^{(a-n-m)} & m+n \leq a \leq m+2n-1 \end{cases} \\ \lambda_a &:= \begin{cases} 0 & 0 \leq a \leq m-1 \\ \alpha(\chi^{(a-m)}) & m \leq a \leq m+n-1 \\ \alpha(\zeta^{(a-n-m)}) & m+n \leq a \leq m+2n-1 \end{cases} \end{aligned} \quad (26)$$

We estimate in Appendix B the cost of computing a_E

If $|V| = n$, for large n one needs $O(n^3 2^n)$ arithmetic operations to compute $a_E(S)$ and $a_\emptyset(S)$ for all $S \subseteq V$.

2.2 Monte Carlo integration and computational cost of the non-deterministic part

We consider now a general correlation function:

$$c_E[\xi] := (-1)^m \frac{\int \mathcal{D}[\psi, \bar{\psi}] e^{-S[\xi]} \left(\prod_{j=0}^{m-1} \psi(\rho^{(j)}) \bar{\psi}(\delta^{(j)}) \right)}{\int \mathcal{D}[\psi, \bar{\psi}] e^{-S[\xi]}} = \frac{a_E[\xi]}{a_\emptyset[\xi]} \quad (27)$$

where $E := \{(\rho^{(j)}, \delta^{(j)})\}_{j=0}^{m-1}$. We write

$$c_E[\xi] = \sum_{n=0}^{\infty} \int_{\chi^{(0)}, \zeta^{(0)}, \dots, \chi^{(n-1)}, \zeta^{(n-1)}} \frac{c_E(V)}{n!} \prod_{j=0}^{n-1} \xi(\chi_j, \zeta_j) = \int_V c_E(V) \xi^V \quad (28)$$

where $c_E(V)$ can be computed from $a_E(S)$ and $a_\emptyset(S)$ for $S \subseteq V$ by using (12):

$$c_E(V) = a_E(V) - \sum_{S \subsetneq V} c_E(S) a_\emptyset(V \setminus S) \quad (29)$$

2.3 Generalizations

The above computation is generalizable to k -body interactions without difficulty.

It is possible to compute the self-energy directly using recursion formulas, as sketched in the discussion of Article 1. However, one can derive a more direct recursive formula for the self-energy which is more effective [125]. This can be done with a computational cost $O(3^n)$ as for the Green's function.

One can generalize these techniques to include more general diagrammatic schemes. For example, if one wants to eliminate ladder diagrams (which are required in order to obtain the continuum limit of the unitary Fermi gas) or particle-hole bubbles (which are required to obtain the thermodynamic limit for the electron gas), one has to pay $O((1 + \sqrt{2})^{2n}) = O(5.83^n)$. The fully-dressed (bold) scheme for the Green's function would cost $O(B_n) \sim O((n/\log n)^n)$, where B_n are the Bell numbers.

2.4 Computation of physical correlation functions

We have imposed in Equation (21) that for $\xi = U$ we get back the physical action: $S[U] = S_{\text{physical}}$. Accordingly, we introduce the physical correlation function as

$$G_E = c_E[U] = \sum_{n=0}^{\infty} \int_{V, |V|=n} c_E(V) U^V = \sum_{n=0}^{\infty} C_{E,n} \quad (30)$$

where $C_{E,n}$ is defined by

$$C_{E,n} := \frac{1}{n!} \int_{\chi^{(0)}, \zeta^{(0)}, \dots, \chi^{(n-1)}, \zeta^{(n-1)}} \left(\prod_{j=0}^{n-1} U(\chi^{(j)}, \zeta^{(j)}) \right) c_E(V) \quad (31)$$

where $V = \{(\chi^{(j)}, \zeta^{(j)})\}_{j \in \{0, \dots, n-1\}}$. We can compute this integral by using a Markov-chain Monte Carlo algorithm, with probability measure

$$p_{E,n}(V) := \frac{\left| \left(\prod_{j=0}^{n-1} U(\chi^{(j)}, \zeta^{(j)}) \right) c_E(V) \right|}{n! z_{E,n}} \quad (32)$$

where

$$z_{E,n} := \frac{1}{n!} \int_{\chi^{(0)}, \zeta^{(0)}, \dots, \chi^{(n-1)}, \zeta^{(n-1)}} \left| \left(\prod_{j=0}^{n-1} U(\chi^{(j)}, \zeta^{(j)}) \right) c_E(V) \right| \quad (33)$$

$z_{E,n}$ is easy to compute by Monte Carlo as it is the integral of a positive quantity (see Appendix C for details). Assuming that we know $z_{E,n}$, the order- n contribution $C_{E,n}$ can then be computed from

$$C_{E,n} = z_{E,n} \left\langle \text{sign} \left[\left(\prod_{j=0}^{n-1} U(\chi^{(j)}, \zeta^{(j)}) \right) c_E(V) \right] \right\rangle_{p_{E,n}} \quad (34)$$

where $\langle \cdot \rangle_{p_{E,n}}$ denotes the mean computed with the $p_{E,n}$ distribution. We start from an arbitrary configuration V and we let the system evolve until we reach the equilibrium distribution p_E , from which we start to take data. The estimator for $C_{E,n}$ after visiting the configurations $V_a = \{(\chi_a^{(j)}, \zeta_a^{(j)})\}_{j \in \{0, \dots, n-1\}}$, with $a \in \{0, \dots, N_{MC} - 1\}$ is

$$C_{E,n}(\{V_a\}) := \frac{z_{E,n}}{N_{MC}} \sum_{a=0}^{N_{MC}-1} s_{E,n}(V_a) \quad (35)$$

where $s_{E,n}(V) := \text{sign} \left[\left(\prod_{j=0}^{n-1} U(\chi^{(j)}, \zeta^{(j)}) \right) c_E(V) \right]$. We call the statistical error on $C_{E,n}$ $\epsilon_{E,n,N_{MC}}$. For $N_{MC} \rightarrow \infty$ one has

$$\epsilon_{E,n,N_{MC}} \simeq z_{E,n} \sqrt{1 - \langle s_{E,n} \rangle_{p_{E,n}}^2} \sqrt{\frac{2\tau_{E,n}^{(\text{auto})} + 1}{N_{MC}}} \quad (36)$$

where $\tau_{E,n}^{(\text{auto})}$ is defined by this equation and depends on the details of the Monte Carlo algorithm. In all interesting cases one has $\lim_{n \rightarrow \infty} \langle s_{E,n} \rangle_{p_{E,n}} = 0$, so that for $n \rightarrow \infty$ and $N_{MC} \rightarrow \infty$ one has

$$\epsilon_{E,n,N_{MC}} \simeq z_{E,n} \sqrt{\frac{2\tau_{E,n}^{(\text{auto})} + 1}{N_{MC}}} \quad (37)$$

We will suppose that

$$\tau_{E,n}^{(\text{auto})} \leq C_E^{(\text{auto})} n^{\alpha_E} \quad (38)$$

where $\alpha_E \geq 0$. We have checked numerically that this condition is verified with $\alpha_E = 1$. We present now a conjecture on the large-order behavior of $z_{E,n}$, which is supposed to be valid at least for the Hubbard model

For every E , it exists $C_{z,E} < \infty$ and $R_{z,E} > 0$ such that

$$z_{E,n} \leq C_{z,E} R_{z,E}^{-n} \quad (39)$$

This conjecture should be proved for the Hubbard model with existing techniques⁴¹ In general, it should be correct at finite temperature for lattice models. This conjecture implies in particular

For every E , it exists $C_E < \infty$ and $R_E > 0$ such that

$$|C_{E,n}| \leq C_E R_E^{-n} \quad (40)$$

3 Polynomial-time scaling

We would like to compute a correlation function G_E with a total accuracy of ϵ . For stochastic methods like Quantum Monte Carlo, it is meaningless to talk of

⁴¹J. Magnen, private communication

rigorous bound. Every time the code runs, we obtain a different results, and in principle for any bound ϵ it typically exists a simulation such that the value of the physical result is bigger than ϵ . One has to think in terms of the livelihood that the physical result is within ϵ . We say that a correlation function G_E is computed with a totally accuracy of ϵ if the physical result is within ϵ from the estimate at least $2/3$ of the times the algorithm ran (in the physics literature it is more common use sigma error). More precisely, our estimation G_E^{est} is different from G_E by an amount $\delta := |G_E - G_E^{\text{est}}|$ which is bigger than ϵ no more than $1/3$ of the times.

$$G_E = c_E[U] = \sum_{n=0}^{\infty} C_{E,n} \quad (41)$$

if the series is convergent. Assuming (40) is verified with $R_E > 1$, we have

$$\left| G_E - \sum_{n=0}^{N-1} C_{E,n} \right| \leq \frac{C_E}{1 - R_E} R_E^{-N} \quad (42)$$

We choose N large enough such that the truncation error is smaller than $\epsilon/2$. It is sufficient to impose:

$$N = \max \left(1, \left\lceil \frac{\log \left(\frac{2C_E}{1-R_E} \epsilon^{-1} \right)}{\log R_E} \right\rceil \right) \quad (43)$$

We need to bound the error coming from Monte Carlo. For each $n \in \{1, \dots, N-1\}$, we choose a number of Monte Carlo steps $N_{MC}(n)$ steps needed to achieve a precision of $\epsilon/(2\sqrt{N})$ on each term of the sum:

$$|\epsilon_{E,n,N_{MC}(n)}| \leq \frac{\epsilon}{2\sqrt{N}} \quad (44)$$

In this way, our Monte Carlo estimation $G_E^{(\text{est})}$ is within ϵ from G_E more than two thirds of the times. We have seen that for large n $\epsilon_{E,n,N_{MC}} \sim z_{E,n}/\sqrt{N_{MC}}$. We have seen that the computational cost of CDet per unit Monte Carlo step is of order 3^n for large n , from which we get that the time to do N_{MC} steps at order n is $t_n \sim 3^n N_{MC}$. Therefore for large n , we can write

$$\frac{1}{\sqrt{t_n}} \left(\frac{\sqrt{3}}{R_{z,E}} \right)^n \sim \frac{\epsilon}{2\sqrt{N}} \quad (45)$$

Suppose that $R_{z,E}$ is greater than $\sqrt{3}$. Then, $t_n \rightarrow 0$ for large n , it is easier to compute higher orders, and most of the time is spent to compute the low orders

with high precision. We see that in this case the total computational time to obtain a precision ϵ scales like $1/\epsilon^2$:

$$t(\epsilon) \sim \epsilon^{-2} \quad (46)$$

If $R_{z,E} < \sqrt{3}$, then most of the time is spent on higher orders, nevertheless the computational time is still polynomial

$$t(\epsilon) \sim \epsilon^{-\alpha} \quad (47)$$

with $\alpha = 2 + 2 \frac{\log(R_{z,E}/\sqrt{3})}{\log R_E}$.

Conclusions and outlook

In this part of the text we have presented a new diagrammatic algorithm which allows us to compute the sum of all connected Feynman diagrams at fixed space-time positions of the interaction vertices. The total computational effort increases exponentially with the order of expansion, which is to be compared to the factorial effort needed to compute the order n by sampling Feynman diagram topologies, as in the original formulation of Diagrammatic Monte Carlo.

In order to compare the performances of all possible unbiased numerical methods, we introduced the notion of computational complexity problem (CCP): we say that we have a CCP if the computational time needed to achieve a precision of ϵ (including all sort of error sources in ϵ) on a thermodynamic-limit quantity (e.g. a Green's function) scales more than polynomially with ϵ^{-1} . We find that the algorithm introduced in this part of the text has a polynomial-time scaling when the diagrammatic series is convergent.

We have seen in Article 1 that this method gives results that are already state of the art for the weak-coupling Hubbard model. It would be interesting to extend the results of [32] to lower temperature. In order to achieve this goal, the direct computation of the self-energy [125] is needed. Nevertheless, a fundamental problem is encountered when decreasing the temperature: the radius of convergence of the series approaches zero (at least) logarithmically with the inverse temperature, because of the s -wave phase transition happening for negative values of the interaction, as we have seen in Article 1. As we are interested in positive interaction strength, it is possible to resum the series outside the radius of convergence by using conformal mapping after a careful study of singularities is done. It remains an open question to understand if and with which modifications one can still apply the analysis of the Part I of this text.

Given the generality of the formalism, it is clear that this new algorithm can be applied to any lattice models with arbitrary interactions. In order to consider continuous-space models, one must remove some class of diagrams, and the algorithm can be extended to treat this case. In particular, it would be nice to compare the performances of this algorithm with the Diagrammatic Monte Carlo code for the unitary Fermi gas used to produce the numerical results of Part I.

It would also be interesting to compare the new algorithm with a recently introduced non-equilibrium diagrammatic Monte Carlo algorithm [37], which uses a determinant representation in the Keldysh formalism. The use of the recursive formula is not needed here as the sum over Keldish formalism automatically eliminates disconnected diagrams. It is possible in principle to simulate equilibrium models by taking the long-time evolution starting from a non-interacting state.

Many technical developments of the algorithm are possible, from the point of view of reducing the Monte Carlo variance or the use of non-Monte Carlo techniques, and the extent of which they will speed-up the computation deserves a detailed study.

Appendices of Part II

A Computational cost of the recursive formula

Let V be a set, $|V| = n$. We want to stress that we consider here the case where all the elements of V are different. This is the most difficult case, as the number of subset of a set of a given length is maximal when all elements are different ⁴². Let A_{comp} and M_{comp} be the computational costs of an addition and a multiplication. We assume that we have stored in the memory the values of $c(S)$ and $z(S)$ for all $S \subseteq V$. We first state some preliminary results:

(L1) Let B be a set of k elements. The number of proper subsets of B is $2^k - 1$.

(L2) The number of W such that $W \subseteq V$ and $|W| = k$ is $\binom{n}{k}$.

(L3) Let $W \subseteq V$, $|W| = k$. We assume that we have stored $c(S)$ and $z(S)$ for all $S \subsetneq W$. The cost of computing $c(W)$ from (12) is $(A_{\text{comp}} + M_{\text{comp}})(2^k - 1)$

Indeed, by using **(L1)**, we see that we have to do $2^k - 1$ multiplications and $2^k - 2$ additions to compute the sum in (12), and we have one addition more between the first term and the sum.

We are now in the position to prove

There exists an algorithm to compute $c(V)$ knowing $a(S)$ and $z(S)$ for all $S \subseteq V$ with a cost of $(3^n - 2^n)(A_{\text{comp}} + M_{\text{comp}})$.

Proof: We assume that we have stored $c(S)$ for all $S \subsetneq V$ with $|S| < k$. We then compute $c(W)$ for all $W \subseteq V$, $|W| = k$. By assumption, we have stored $c(S)$ for all $S \subsetneq W$, so that we can apply **(L3)**, that gives a computational cost

⁴²Moreover is the case which is useful for many applications of the recursive formula

of $(A_{\text{comp}} + M_{\text{comp}})(2^k - 1)$ for a given W . From **(L2)**, the number of such W is $\binom{n}{k}$. The total computational cost to compute $c(V)$ is therefore

$$\sum_{k=0}^n [(A_{\text{comp}} + M_{\text{comp}})(2^k - 1)] \binom{n}{k} = (3^n - 2^n)(A_{\text{comp}} + M_{\text{comp}}) \quad (\text{A.1})$$

□

B Computational cost of the determinants

We want to estimate the computation of $a_E(S)$ and $a_\emptyset(S)$ for all $S \subseteq V$, $|V| = n$, with $|E| = m$, for large values of n . It is well known that the computational cost of a determinant of a matrix $N \times N$ is $O(N^3)$. By using the Proposition **(L2)** of Appendix A, we have that the computational cost is of the order of

$$\sum_{k=0}^n \binom{n}{k} [(m + 2k)^3 + (2k)^3] \sim n^3 2^n \quad (\text{B.1})$$

C Hybrid sampling

We will express $z_{E,n}$ in terms of $z_{E,n-1}$. We will use an “hybrid” probability distribution proportional to

$$\begin{aligned} H_E(V) := & (1 - \lambda) \left| \left(\prod_{j=0}^{n-1} U(\chi^{(j)}, \zeta^{(j)}) \right) c_E(V) \right| + \\ & + \lambda \sum_{j=0}^{n-1} \left| f(\chi^{(j)}, \zeta^{(j)}) \left(\prod_{l=0, l \neq j}^{n-1} U(\chi^{(l)}, \zeta^{(l)}) \right) c_E(V \setminus \{(\chi^{(j)}, \zeta^{(j)})\}) \right| \end{aligned} \quad (\text{C.1})$$

for $0 < \lambda < 1$ and $f(\chi, \zeta)$ is an arbitrary function with a finite normalization, $\|f\|_1 := \int_{\chi, \zeta} |f(\chi, \zeta)| < \infty$. One has

$$\int_{\chi^{(0)}, \zeta^{(0)}, \dots, \chi^{(n-1)}, \zeta^{(n-1)}} H_E(V) = n! [(1 - \lambda) z_{E,n} + \lambda \|f\|_1 z_{E,n-1}] \quad (\text{C.2})$$

that means that $h_E(V) := H_E(V) / (n! [(1 - \lambda) z_{E,n} + \lambda \|f\|_1 z_{E,n-1}])$ is a probability distribution. We compute with a Markov chain Monte Carlo algorithm the

mean

$$\left\langle \frac{(1-\lambda) \left| \left(\prod_{j=0}^{n-1} U(\chi^{(j)}, \zeta^{(j)}) \right) c_E(V) \right|}{H_E(V)} \right\rangle_{h_E} = \frac{(1-\lambda) z_{E,n}}{(1-\lambda) z_{E,n} + \lambda \|f\|_1 z_{E,n-1}} \quad (\text{C.3})$$

from which we deduce the ratio between $z_{E,n}$ and $z_{E,n-1}$. The parameter λ is chosen such that the previous mean is not too far from $1/2$.

D Binary representation

Suppose we want to compute the order n contribution for a particular value of the external parameters E . At a particular MC step, we will have a vertex configuration $V = \{(\chi^{(j)}, \beta^{(j)})\}_{j \in \{0, \dots, n-1\}}$. In order to apply the recursive formula, we need to have $a_E(S)$ and $a_\emptyset(S)$ for every $S \subseteq V$, and it would be necessary to store along the way $c_E(S)$ for $S \subseteq V$. The set of subsets of a set (the so-called powerset, denoted by $\mathcal{P}(V)$) is best represented with binary numbers, a 1 represents the presence of a particular element and 0 the absence. We first need to distinguish elements of V , so we introduce an arbitrary ordering

$$V_j := (\chi^{(j)}, \zeta^{(j)}), \quad j \in \{0, \dots, n-1\} \quad (\text{D.1})$$

It is then possible to build a one-to-one mapping between $\{0, \dots, 2^n - 1\}$ (binary numbers with $n-1$ bits) and the set of subsets of V , that we call M_{bin} .

We define $M_{\text{bin}} : \{0, \dots, 2^n - 1\} \mapsto \mathcal{P}(V)$ in this way: for every $x = x_{n-1}x_{n-2} \dots x_0$, with $x_j \in \{0, 1\}$ (this is the binary representation), we build $M_{\text{bin}}(x) \subseteq V$ such that for every $j \in \{0, \dots, n-1\}$, V_j is an element of $M_{\text{bin}}(x)$ if and only if x_j is equal to one.

Let $y \in \{0, \dots, 2^n - 1\}$ such that $M_{\text{bin}}(y) \subseteq M_{\text{bin}}(x)$. Then, if $y = y_{n-1} \dots y_0$ and $x = x_{n-1} \dots x_0$, we have

$$y_j \leq x_j \quad (\text{D.2})$$

for $j \in \{0, \dots, n-1\}$.

For $x \in \{0, \dots, 2^n - 1\}$, we define $\|x\|_b \in \{0, \dots, n - 1\}$ as the number of 1 bits in the binary representation of x

$$\|x\|_b = \sum_{j=0}^{n-1} x_j \quad (\text{D.3})$$

(Indexing functions): For every $x \in \{0, \dots, 2^n - 1\}$ we introduce an indexing function $i_x : \{0, \dots, 2^{\|x\|_b} - 1\} \mapsto \{0, \dots, 2^n - 1\}$ that span all the y such that $M_{\text{bin}}(y) \subseteq M_{\text{bin}}(x)$. More precisely, let $\{u_j\}_{j \in \{0, \dots, \|x\|_b - 1\}}$ be the set of the positions of the 1 bits of x :

$$x = \sum_{j=0}^{n-1} x_j 2^j = \sum_{j=0}^{\|x\|_b - 1} 2^{u_j} \quad (\text{D.4})$$

with $u_j \in \{0, \dots, n - 1\}$, $u_j \neq u_k$ for $j \neq k$. We then define explicitly the indexing function $i_x(s)$ for $s \in \{0, \dots, 2^{\|x\|_b} - 1\}$ written in binary representation $s = s_{\|x\|_b - 1} \dots s_0$

$$i_x(s) := \sum_{j=0}^{\|x\|_b - 1} s_j 2^{u_j} \quad (\text{D.5})$$

We also introduce for convenience the complement of this function $\bar{i}_x : \{0, \dots, 2^{\|x\|_b} - 1\} \mapsto \{0, \dots, 2^n - 1\}$:

$$\bar{i}_x(s) := x - i_x(s) = \sum_{j=0}^{\|x\|_b - 1} (1 - s_j) 2^{u_j} \quad (\text{D.6})$$

Let $x = x_{n-1} \dots x_0$. For every $y = y_{n-1} \dots y_0$ such that $y_j \leq x_j$, with the notations of the previous definition we can associate $s = s_{\|x\|_b - 1} \dots s_0$ such that

$$y = i_x(s) \quad (\text{D.7})$$

by writing

$$s_j = y_{u_j} \quad (\text{D.8})$$

It is clear that the mapping between s and y is one-to-one. The indexing functions can be easily stored in the memory as (two or one dimensional) integer arrays.

For a fixed V , we introduce $x \in \{0, \dots, 2^n - 1\}$

$$\mathbf{a}_E(x) := a_E(M_{\text{bin}}(x)), \quad \mathbf{a}_\emptyset(x) := a_\emptyset(M_{\text{bin}}(x)), \quad \mathbf{c}_E(x) := c_E(M_{\text{bin}}(x)) \quad (\text{D.9})$$

It is clear that \mathbf{a}_E , \mathbf{a}_\emptyset and \mathbf{c}_E can be stored as arrays.

Let $x, y \in \{0, \dots, 2^n - 1\}$ such that $M_{\text{bin}}(y) \subseteq M_{\text{bin}}(x)$. Then

$$M_{\text{bin}}(x) \setminus M_{\text{bin}}(y) = M_{\text{bin}}(x - y) \quad (\text{D.10})$$

Proof. First of all, we see that if $x_{n-1} \dots x_0$ and $y_{n-1} \dots y_0$ are the binary representations x and y , then

$$y_j \leq x_j, \quad j \in \{0, \dots, n-1\} \quad (\text{D.11})$$

so that the subtraction $z = x - y$ produces the binary number $z_{n-1} \dots z_0$, with $z_j = x_j - y_j$. We concentrate now at index j . By enumerating all the possibilities for x_j and y_j , one can easily prove that $V_j \in M_{\text{bin}}(x) \setminus M_{\text{bin}}(y)$ if and only if $V_j \in M_{\text{bin}}(x - y)$. \square

(Binary version of the recursion formula):

One has for $x \in \{0, \dots, 2^n - 1\}$

$$\mathbf{c}_E(x) = \mathbf{a}_E(x) - \sum_{s=0}^{2^{\|x\|_b} - 2} \mathbf{c}_E(i_x(s)) \mathbf{a}_\emptyset(\bar{i}_x(s)) \quad (\text{D.12})$$

Proof. Let $W \subseteq V$. We can write the recursive formula for $c_E(W)$:

$$c_E(W) = a_E(W) - \sum_{S \subseteq W} c_E(S) a_\emptyset(W \setminus S) \quad (\text{D.13})$$

We introduce $x = M_{\text{bin}}^{-1}(W)$. We write

$$\begin{aligned}
\mathbf{c}_E(x) &= c_E(W) = \mathbf{a}_E(x) + \\
&- \sum_{\{y \in \{0, \dots, 2^n - 1\} \mid M_{\text{bin}}(y) \subsetneq M_{\text{bin}}(x)\}} \mathbf{c}_E(y) \mathbf{a}_\emptyset(M_{\text{bin}}(x) \setminus M_{\text{bin}}(y)) = \\
&= \mathbf{a}_E(x) - \sum_{\{y = y_{n-1} \dots y_0 \mid y_j \leq x_j, x \neq y\}} \mathbf{c}_E(y) \mathbf{a}_\emptyset(x - y) = \tag{D.14} \\
&= \mathbf{a}_E(x) - \sum_{s=0}^{2^{\|x\|_b} - 2} \mathbf{c}_E(i_x(s)) \mathbf{a}_\emptyset(x - i_x(s))
\end{aligned}$$

□

Suppose y is such that $M_{\text{bin}}(y) \subsetneq M_{\text{bin}}(x)$. Then $y < x$ (in the sense of integers). This implies that if we know $\mathbf{c}_E(y)$ for all $y < x$, we have all the information to compute $\mathbf{c}_E(x)$ from the binary recursive formula. This means that, in practice, we only need to implement a loop over the value of x from 0 to $2^n - 1$. We put here the pseudo-code that summarizes the algorithm to compute \mathbf{c} .

Algorithm 1 Recursive Linked Cluster

```

1: procedure RECLINCLU( $\mathbf{a}_E, \mathbf{a}_\emptyset, n$ )
2:   for ( $x \leftarrow 0$ ;  $x < 2^n$ ;  $x \leftarrow x + 1$ ) do
3:      $\mathbf{c}_E(x) \leftarrow \mathbf{a}_E(x)$ 
4:      $x_b \leftarrow \|x\|_b$ 
5:     for ( $s \leftarrow 0$ ;  $s < 2^{x_b} - 1$ ;  $s \leftarrow s + 1$ ) do
6:        $\mathbf{c}_E(x) \leftarrow \mathbf{c}_E(x) - \mathbf{c}_E(i_x(s)) \mathbf{a}_\emptyset(i_x(s))$ 
return  $\mathbf{c}_E$ 

```

Part III

Multivaluedness of the Luttinger-Ward functional and applicability of dressed diagrammatic schemes

In this part of the text we study mathematically diagrammatic dressing, that is, diagrammatic series built with dressed propagators or dressed vertices. In particular, we will focus on determining under which conditions this operation is allowed. This study was motivated by numerical evidence by Kozik, Ferrero, and Georges [48] that showed that the fully-dressed diagrammatic expansion is unable to give the correct physical result for strong-enough interactions in some lattice models, as the physical result belong to another non-perturbative branch (that we will call KFG branch). This is related to the fact that the map from the bare Green's function to the full Green's function $G_0 \mapsto G$ is not one-to-one. These findings casted doubts on the numerical results obtained using the fully-dressed formalism, that seemed an uncontrolled method that could even converge to an unphysical result.

We start to study this problem by presenting a simple toy model that displays the following phenomenology:

- The Luttinger-Ward of the toy-model presents a (perturbative) bold branch and a KFG branch: the physical result shifts from the bold branch to the KFG branch when increasing interaction.
- The fully-dressed (bold) scheme converges towards an unphysical result when the KFG branch is the physical one.

We then go beyond phenomenology by studying diagrammatic dressing in a more constructive and systematic way. In practice, we are mainly interested in understanding when we can use dressed diagrammatic schemes. The natural framework to study diagrammatic dressing is by using a shifted action, that is, an action $S^{(z)}$ dependent on a complex parameter z such that the Taylor series in z reproduces term by term the diagrammatic expansion. Essentially, KFG branching is due to singularities of the shifted action which are created by the process of dressing. The applicability condition for dressed diagrammatic schemes is just a condition guaranteeing the analyticity of the shifted action. The main results of this chapter can be summarized as:

- The proposal of a partially-dressed diagrammatic scheme (called semi-bold) that does not suffer from the problem of misleading convergence towards an unphysical result.
- An applicability condition for fully-dressed diagrammatic schemes for lattice models. If this condition is verified, then the bold scheme cannot converge towards an unphysical result.

In this chapter, we will use the word “bold” and “fully-dressed” interchangeably:

$$\text{“bold”} \quad \equiv \quad \text{“fully-dressed”} \quad (1)$$

1 Introduction and overview

Diagrammatic dressing is a powerful tool that allows to use partially (or fully) dressed objects as basic building blocks for perturbative expansions. It allows one to obtain non-perturbative results by selecting the class of diagrams which corresponds to the most important physical effect. Moreover, in some situations, diagrammatic dressing is not only useful, but mandatory, in order to have a well-defined model. For example, in order to define the Unitary Fermi gas, one must first sum up ladder diagrams to infinite order. Another example of mandatory diagrammatic dressing is the screening of long-range interactions: In order to take the thermodynamic limit one has to sum up particle-hole bubble diagrams to infinite order.

It is often useful to express the diagrammatic expansion in terms of the fully-dressed propagators. This is the natural thing to do in certain regimes. For example, Landau's Fermi liquid theory predicts the low-energy low-temperature properties from the interaction between a dilute liquid of quasi-particles, which are defined in terms of the fully-dressed one-particle Green's function. It is expected in this regime that using fully-dressed propagators enhances the convergence properties of the diagrammatic series. Indeed, the interaction between quasi-particles is expected to be weak as the density of quasi-particles is small, even if the bare interaction of the model is not small (this "emergent smallness" is explicitly used within Bold Diagrammatic Monte Carlo in [31]).

We start this chapter by giving a definition of bold series in Section 2.1. We would like to underline the power of some of the techniques introduced in this Section: Instead of using Feynman diagrams, we prefer to use functional techniques and formal power series. The naturalness of this formalism allows us to give rigorous proofs without effort.

One may ask if diagrammatic dressing is an allowed operation from a mathematical point of view. Certainly, the justification of the operation is not obvious a priori. We are moving an infinite set of diagrams from a non-absolutely convergent series, so that the Riemann rearrangement theorem implies that one can get an arbitrary result by reshuffling diagrams. It was found in [48] that the bold series, built on fully-dressed propagators, does not always converges to the physical result. As it is used to give a constructive definition of the Luttinger-Ward functional, this implies that this functional has (at least) two branches. This finding is summarized in section 2.2.

These results casted serious doubts on numerical diagrammatic schemes that used dressed series, and in particular on Bold Diagrammatic Monte Carlo, which uses explicitly the bold series. In particular, there are numerical evidences [126] that the following (catastrophic) scenario is possible: The bold scheme converges misleadingly towards an incorrect result. This is discussed in Section 2.3.

In order to gain insight into the problem, we decided to study the simplest toy-model for fermionic Feynman diagrams, in which all diagrams contribute with the same absolute value. This is the subject of Section 3. The KFG branching phenomenology of Section 2.2 is found in a completely explicit way, see Section 3.3. We also explicitly prove in Section 3.4 that in this toy-model the misleading convergence scenario described in Section 2.3 is present for high-enough interaction strength.

We then decided to undertake the task of the justification of diagrammatic dressing. Bare diagrammatic series are simple Taylor series in the bare coupling constant, and their properties are directly connected to the analytical properties of thermodynamical quantities as a function of the coupling constant. We would like to do the same for dressed diagrammatic series. We introduced an artificial coupling constant such that the dressed series is a simple Taylor expansion built with a modified action, a “shifted” action. This is presented in section 4.1.

The KFG branching is due to the additional non-physical singularities that are created by the process of diagrammatic dressing. In our formalism, it is natural to identify them as singularities of the shifted action. Therefore, if the action is analytical, dressed diagrammatic series are subject to the same applicability condition of the bare diagrammatic series: if they converge, they converge to the right result.

We first propose a particularly convenient partially-dressed diagrammatic scheme for which the shifted action is a polynomial (and therefore an entire function). Hence, it does not suffer from the misleading convergence problem: if it converges, it must converge towards the physical result. In this scheme one uses the propagators obtained by stopping the self-consistent bold procedure at order \mathcal{M} , and using them as basic building blocks. For this reason, we call it semi-bold. We introduce it in Section 4.2

Finally, in Section 5, we derive a sufficient applicability condition that, if satisfied, guarantees that the catastrophic misleading convergence of the bold scheme is not possible. This condition is sharp for the toy-model of Section 3. This result justifies the application of the Bold Diagrammatic Monte Carlo scheme, which is based on a stochastic sampling of the bold series, in some regimes of the phase diagram of lattice models.

2 The dangers of dressing

Diagrammatic dressing, as we have seen, is a powerful tool. A particularly elegant dressing is obtained by using fully-dressed propagators. This gives rise to bold diagrammatic series, that we will denote as “bold” (the bold coming from the historical graphical representation of Feynman diagrams). We introduce the bold

series in subsection 2.1. One is led to believe that the convergence properties are always better when we increase the number of resummed diagrams used in the dressing procedure. Unfortunately, it is found that fully-bold dressing can drastically change the analytical structure. The analytic continuation of the bold series defines only one of the branches, there are additional branches of the self-energy (the KFG branches, from Kozik, Ferrero and Georges, see subsection 2.2), and, most importantly, the physical result can be on the non-perturbative KFG branch for strong enough interaction. Moreover, the bold scheme can still converge to something (unphysical) when the physical result is on the KFG branch (subsection 2.3). This is the real danger of diagrammatic dressing: misleading convergence towards an unphysical result.

The phenomenology described in Section 2.2 was found by Kozik, Ferrero and Georges [48], and reproduced with a simple toy model in Article 3 [127], while the phenomenology of Section 2.3 was first seen numerically for the Hubbard model [126]. We can explicitly prove that the misleading convergence is also present for the toy model of Article 3 (see Section 3).

2.1 The formal definition of the bold series

We use the functional integral representation in terms of Grassmann integrals. For definiteness, we consider the Hubbard model, the generalization is without difficulty. We consider the action

$$S^{(U)}[\bar{\varphi}, \varphi] := - \sum_{\sigma, \mathbf{r}} \int_0^\beta d\tau \bar{\varphi}_\sigma(\mathbf{r}, \tau) (G_0^{-1} \varphi_\sigma)(\mathbf{r}, \tau) + U \sum_{\mathbf{r}} \int_0^\beta (\bar{\varphi}_\uparrow \varphi_\uparrow \bar{\varphi}_\downarrow \varphi_\downarrow)(\mathbf{r}, \tau) \quad (2)$$

where $(\mathbf{r}, \tau) \in \mathbb{Z}^d \times [0, \beta]$ denotes a space-(imaginary)time coordinate. G_0^{-1} stands for the inverse, in the sense of operators, of the free propagator. We introduce the Green's function

$$G(\mathbf{r}, \tau) := - \langle \varphi_\sigma(\mathbf{r}, \tau) \bar{\varphi}_\sigma(0) \rangle := - \frac{\int \mathcal{D}[\varphi, \bar{\varphi}] e^{-S^{(U)}} \varphi_\sigma(\mathbf{r}, \tau) \bar{\varphi}_\sigma(0)}{\int \mathcal{D}[\varphi, \bar{\varphi}] e^{-S^{(U)}}} \quad (3)$$

In order to manipulate diagrammatic series, it is very convenient to use a functional approach. Then, the diagrammatic expansion is a simple Taylor series of some complex parameter z . Diagrammatic dressing in this formalism is simply obtained by using z -dependent functionals. This allows to prove diagrammatic identities in a completely formal (and rigorous) way, without discussing Feynman diagrams.

G can be expanded in a formal U series, the terms of which are computable

in terms of connected Feynman diagrams involving G_0

$$G(U) \hat{=} G_0 + \sum_{n=1}^{\infty} U^n G^{(n)}[G_0] =: G[G_0, U] \quad (4)$$

from which we can define the formal functional $G = G[G_0, U]$. The relation between G_0 and G can be inverted in the ring of formal power series and we can write

$$G_0 = G_0[G, U] := G + \sum_{n=1}^{\infty} U^n G_0^{(n)}[G] \quad (5)$$

The self-energy is defined by the operator equation

$$\Sigma := G_0^{-1} - G^{-1} \quad (6)$$

We introduce the formal functional Σ_{bare} as

$$\Sigma_{\text{bare}}[G_0, U] := G_0^{-1} - (G[G_0, U])^{-1} = \sum_{n=1}^{\infty} U^n \Sigma_{\text{bare}}^{(n)}[G_0] \quad (7)$$

From a diagrammatic point of view, $\Sigma_{\text{bare}}[G_0, U]$ has only diagrams that after cutting one G_0 line, remain connected. We express the self-energy in terms of the bold propagator G , this can be done at least in the ring of formal power series

$$\Sigma_{\text{bold}}[G, U] := \Sigma_{\text{bare}}[G_0[G, U], U] =: \sum_{n=1}^{\infty} U^n \Sigma_{\text{bold}}^{(n)}[G] \quad (8)$$

or, more explicitly:

(Bold formal power series functional):

$$\Sigma_{\text{bold}}[G, U] = \Sigma_{\text{bare}}[(G^{-1} + \Sigma_{\text{bold}}[G, U])^{-1}, U] \quad (9)$$

We give explicit expressions for the first two terms:

$$\Sigma_{\text{bold}}^{(1)}[G] = \Sigma_{\text{bare}}^{(1)}[G] \quad (10)$$

$$\Sigma_{\text{bold}}^{(2)}[G] = \Sigma_{\text{bare}}^{(2)}[G] - \frac{\delta \Sigma_{\text{bare}}^{(1)}[G]}{\delta G} \cdot \Sigma_{\text{bare}}^{(1)}[G] \quad (11)$$

The bold self-energy functional $\Sigma_{\text{bold}}[G, U]$ has a simple description in terms of Feynman diagrams: only diagrams that remain connected after cutting two G

lines have to be considered. The self-energy is not the only quantity that one can “boldify”. The boldification of the grand-canonical partition function leads to the Luttinger-Ward functional. The formal U series for the Luttinger-Ward functional $\Phi[G, U]$, that we call $\Phi_{\text{bold}}[G, U]$, can be related to that of Σ_{bold} by the relation

$$\frac{1}{T} \frac{\delta \Phi_{\text{bold}}[G, U]}{\delta G} \hat{=} \Sigma_{\text{bold}}[G, U] \quad (12)$$

2.2 The Kozik-Ferrero-Georges branch of the Luttinger-Ward functional

Formally, the perturbative (bold) definition of the Luttinger-Ward functional is universal, in the sense that it does not depend explicitly on the bare propagator G_0 . The numerical value associated to the formal power series definition of $\Sigma_{\text{bold}}[G, U]$ (or Φ_{bold}) defines a function in a (hopefully) non-zero neighborhood of the U origin, at least for lattice models. This function should not be expected to be analytic everywhere in the U complex plane, one might expect singularities due to phase transitions in the real U axis or other instabilities for complex U . It was found by Kozik, Ferrero and Georges [48] that in the Hubbard model near half filling (and many other models given the universality of the Luttinger-Ward functional) the process of “boldification” adds other singularities, which are found on the real U axis but are not associated to physical phase transitions.⁴³ Remarkably, they found that the bold self-energy converges to an unphysical answer when evaluated with the true Green’s function G (calculated by other means) when the interaction strength U is strong enough. This implies the existence of another branch of the self-energy functional different from Σ_{bold} , the “Kozik-Ferrero-Georges” branch, denoted by Σ_{KFG} . Schematically, one has:⁴⁴

(KFG branch of the self-energy functional):

$$\Sigma = \Sigma[G(U), U] = \begin{cases} \Sigma_{\text{bold}}[G(U), U] & 0 \leq U \leq U_{\text{KFG}} \\ \Sigma_{\text{KFG}}[G(U), U] & U > U_{\text{KFG}} \end{cases} \quad (13)$$

where $G(U)$ is the physical Green’s function.

⁴³In the shifted-action formalization of diagrammatic dressing, these singularities correspond to singularities of the shifted action itself.

⁴⁴We admit here, for simplicity, the existence of only one KFG branch. This does not seem the general case, in fact in [128] an infinite number of KFG branches were found in many models. This is related to divergences of a vertex function, which is the functional derivative of Σ with respect to G , which just means that the function $G_0 \mapsto G$ is not injective, see[129, 130].

One has also that the point $U = U_{\text{KFG}}$ must be a non-analytic point for $\Sigma = \Sigma[G, U]$, the self-energy expressed as functional of G and U . $U = U_{\text{KFG}}$ is not a singular point for $\Sigma_{\text{bare}}[G_0, U]$ (the self-energy expressed in terms of G_0 and U), or for other correlation functions to our knowledge.

All the discussion translates directly to the Luttinger-Ward functional point of view as we have by definition

$$\frac{1}{T} \frac{\delta \Phi_{\text{LW}}[G, U]}{\delta G} = \Sigma \quad (14)$$

Therefore, one has⁴⁵:

(KFG branch of the Luttinger-Ward functional):

$$\Phi_{\text{LW}}[G(U), U] = \begin{cases} \Phi_{\text{bold}}[G(U), U] & 0 \leq U \leq U_{\text{KFG}} \\ \Phi_{\text{KFG}}[G(U), U] & U > U_{\text{KFG}} \end{cases} \quad (15)$$

where $G(U)$ is the physical Green's function.

This finding is of fundamental importance for self-consistent quantum many-body methods, and in particular for Bold Diagrammatic Monte Carlo, which uses explicitly the bold self-energy functional.

2.3 Misleading convergence of the bold scheme

It turns out that the situation is potentially even more problematic for Bold Diagrammatic Monte Carlo. The natural question one could ask is: What happens to the bold iterative scheme when the bold branch becomes unphysical? One is led to hope that the bold diagrammatic scheme simply does not converge, so that it would be easy to know the applicability region of the bold procedure. However, it was found that in the Hubbard model [126] the bold scheme can converge towards an unphysical result. We have explicitly proved that this also happen in a simple toy model (see Section 3.4).

In Bold Diagrammatic Monte Carlo calculations in essence one aims at computing the Green's function G by a sequence of approximate Green's functions $\tilde{G}_{\mathcal{N}}$, $\mathcal{N} \in \{0, 1, 2, \dots\}$. We define the self-energy sequence (we do not consider here resummation):

$$\Sigma_{\text{bold}}^{(\leq \mathcal{N})}[\tilde{G}_{\mathcal{N}}, U] := \sum_{n=1}^{\mathcal{N}} U^n \Sigma_{\text{bold}}^{(n)}[\tilde{G}_{\mathcal{N}}] \quad (16)$$

⁴⁵See footnote 44.

The Green's function sequence $\tilde{G}_{\mathcal{N}}$ is obtained by imposing the Dyson equation:

$$G_0^{-1} = \tilde{G}_{\mathcal{N}}^{-1} - \Sigma_{\text{bold}}^{(\leq \mathcal{N})}[\tilde{G}_{\mathcal{N}}, U] \quad (17)$$

\tilde{G} is defined by the infinite \mathcal{N} extrapolation of $\tilde{G}_{\mathcal{N}}$:

$$\tilde{G}_{\mathcal{N}} \xrightarrow{\mathcal{N} \rightarrow \infty} \tilde{G} \quad (18)$$

if the limit exists. At this point, we would like to identify \tilde{G} with G , but this is not always true:

(Misleading convergence): Suppose that $\tilde{G}_{\mathcal{N}} \xrightarrow{\mathcal{N} \rightarrow \infty} \tilde{G}$. One has

$$\tilde{G} \stackrel{\text{not always}}{=} G \quad (19)$$

This is the phenomenon of misleading convergence: one has a converging bold procedure $\tilde{G}_{\mathcal{N}} \rightarrow \tilde{G}$, but $\tilde{G} \neq G$.

3 An insightful model

We have seen in Section 2 that Kozik, Ferrero and Georges numerically discovered mathematical difficulties with the bold formalism. They studied not only the Hubbard model in two space dimensions, but also simpler models -the Hubbard atom and the Anderson impurity model- for which there is no spatial coordinate. Here we consider an even simpler toy model for which there is no imaginary-time coordinate either (Article 3). It can be interpreted as the simplest Feynman diagrammatic toy model for fermions. As the Luttinger-Ward functional is universal, one could hope that this model captures the qualitative phenomenology. It is found that the mathematical phenomena of KFG branching appear from elementary algebra. A similar idea was also followed in [131] starting from spin-less fermions, where an extra parameter was introduced to obtain a non-Gaussian theory ⁴⁶.

This section is based on Article 3 and unpublished extensions. The outline is the following. We start by introducing the Feynman diagram definition of the toy model (3.1) and its functional integral representation (3.2). We show then that

⁴⁶With ψ and $\bar{\psi}$ as Grassmann variables one only can form quadratic actions.

- The self-energy functional has two branches (bold and KFG). The “bold” branch gives the physical result for interaction strength smaller than $|U_{\text{KFG}}|$ (3.3), while we get an unphysical result when we evaluate the bold series with the true Green’s function for $|U| > |U_{\text{KFG}}|$. This is the phenomenology of Section 2.2.
- We prove that a Bold Diagrammatic Monte Carlo scheme applied to this model would converge to an unphysical result for $|U| > |U_{\text{KFG}}|$ (3.4). This is the phenomenology of Section 2.3.

3.1 Feynman diagrams definition

We wish to study what one obtains when considering Feynman diagrams with a weight $-1/\mu$ for each propagator line, and a weight U for each two-body interaction vertex between different spin particles. There is no space-time dependence in this model, the space-time fields are numbers. We keep only the fermionic formula for the sign of the diagram, which states that the sign of the diagram is determined by the parity of the number of loops for a given spin component $\sigma \in \{\uparrow, \downarrow\}$. For example, for the Green’s function G

$$G = \frac{1}{\mu} + \sum_{n=1}^{\infty} \sum_{\mathcal{D} \in \mathcal{F}_G^{(c)}(n)} (-1)^{L(\mathcal{D})} \left(-\frac{1}{\mu}\right)^{2n+1} (-U)^n \quad (20)$$

where $\mathcal{D} \in \mathcal{F}_G^{(c)}(n)$ means that \mathcal{D} is a n -th order diagram for the (connected) Green’s function, and $L(\mathcal{D})$ is the number of spin up and spin down loops.

3.2 Grassmann integral representation

We introduce an action S depending on four Grassmann variables $\varphi_\sigma, \bar{\varphi}_\sigma, \sigma \in \{\uparrow, \downarrow\}$

$$S[\bar{\varphi}_\sigma, \varphi_\sigma] := -\mu \sum_{\sigma} \bar{\varphi}_\sigma \varphi_\sigma + U \bar{\varphi}_\uparrow \varphi_\uparrow \bar{\varphi}_\downarrow \varphi_\downarrow \quad (21)$$

μ and U are dimensionless parameters that play the roles of chemical potential and interaction strength. We can compute a “partition function” Z with this action

$$Z = \int \left(\prod_{\sigma} d\varphi_{\sigma} d\bar{\varphi}_{\sigma} \right) e^{-S} \quad (22)$$

and a corresponding propagator

$$G := \langle \bar{\varphi}_\sigma \varphi_\sigma \rangle := \frac{1}{Z} \int \left(\prod_{\sigma} d\varphi_{\sigma} d\bar{\varphi}_{\sigma} \right) e^{-S} \bar{\varphi}_\sigma \varphi_\sigma \quad (23)$$

A simple application of the Feynman rules shows that

The action S reproduces the diagrammatic series described in 3.1.

In what follows we will use the Grassmann representation as it is easier in this framework to perform computations.

3.3 The KFG branch of the toy model

Restricting to $U < 0$, we find that:

- The mapping $G_0 \mapsto G(G_0, U)$ is two-to-one and hence the function $G \mapsto \Sigma(G, U)$ has two branches.
- The bold series $\Sigma_{\text{bold}}(G, U)$, evaluated at the exact $G(\mu, U)$, converges to the correct branch for $|U| < |U_{\text{KFG}}|$, where $U_{\text{KFG}} := -\mu^2$, and to the wrong branch for $|U| > |U_{\text{KFG}}|$.

This can be derived very directly from the above definitions. Expanding the exponentials in Eqs. (22,23) yields

$$Z(\mu, U) = \mu^2 - U \quad (24)$$

$$G(\mu, U) = \frac{\mu}{\mu^2 - U}. \quad (25)$$

The propagator for $U = 0$ is

$$G_0(\mu) = \frac{1}{\mu}. \quad (26)$$

The self-energy Σ , defined as usual by the Dyson equation $G^{-1} = G_0^{-1} - \Sigma$, reads

$$\Sigma(\mu, U) = \frac{U}{\mu}. \quad (27)$$

We note that for $U > 0$, an obvious pathology appears in this model around $U = \mu^2$; namely, Z changes sign, and G diverges. Therefore we restrict to $U < 0$.

Eliminating μ between Eqs. (25,26) gives

$$G(G_0, U) = \frac{G_0}{1 - UG_0^2}. \quad (28)$$

The map $G_0 \mapsto G(G_0, U)$ is two-to-one, because the G_0 's that correspond to a given G are the solutions of the second order equation

$$UGG_0^2 + G_0 - G = 0, \quad (29)$$

which has the two solutions

$$G_0^{(\pm)}(G, U) = \frac{-1 \pm \sqrt{1 + 4UG^2}}{2UG}. \quad (30)$$

These solutions are real provided (G, U) belongs to the physical manifold $\{(G(\mu, U), U)\}$; indeed,

$$4|U|G(\mu, U)^2 \leq 1. \quad (31)$$

The corresponding self-energies (given by the Dyson equation) are

$$\Sigma^{(\pm)}(G, U) = \frac{-1 \pm \sqrt{1 + 4UG^2}}{2G}. \quad (32)$$

The correct self-energy $\Sigma(\mu, U)$ is recovered from $\Sigma^{(s)}(G(\mu, U), U)$ provided one takes the determination

$$s = \text{sign}(\mu^2 - |U|). \quad (33)$$

We turn to a discussion of the bold diagrammatic series $\Sigma_{\text{bold}}(G, U)$ for the self-energy Σ in terms of fully dressed propagator G and bare vertex U . We find that $\Sigma_{\text{bold}}(G, U)$ is the $U \rightarrow 0$ Taylor series of $\Sigma^{(+)}(G, U)$. Before deriving this, we note that, obviously, $\Sigma_{\text{bold}}(G, U)$ can never be the Taylor series of $\Sigma^{(-)}(G, U)$, since the former vanishes at $U = 0$ while the latter does not. For the derivation, it is convenient to introduce $g := \sqrt{|U|}G$ and $g_0 := \sqrt{|U|}G_0$, so that Eqs.(28,30) simplify to $g(g_0) = g_0/(1+g_0^2)$ and $g_0^{(\pm)}(g) = (1 \mp \sqrt{1-4g^2})/(2g)$. The key point is that $g_0^{(+)}(g(g_0)) \hat{=} g_0$, where the symbol $\hat{=}$ means equality in the sense of formal power series. This is because the inverse mapping of $g(g_0)$ is $g_0^{(+)}(g)$ for small g_0 and g . Let us then denote by $\Sigma_{\text{bare}}(G_0, U)$ the diagrammatic series for the self-energy in terms of bare propagators and vertices. Setting $\Sigma_{\text{bold}}(G, U) =: \sqrt{|U|}\sigma_{\text{bold}}(g)$ and $\Sigma_{\text{bare}}(G_0, U) =: \sqrt{|U|}\sigma_{\text{bare}}(g_0)$, a defining property of σ_{bold} is that $\sigma_{\text{bold}}(g(g_0)) \hat{=} \sigma_{\text{bare}}(g_0)$. In the present toy model, we simply have $\Sigma_{\text{bare}}(G_0, U) = UG_0$, i.e., $\sigma_{\text{bare}}(g_0) = -g_0$. Hence, $\sigma_{\text{bold}}(g) \hat{=} -g_0^{(+)}(g)$, i.e., $\Sigma_{\text{bold}}(G, U) \hat{=} UG_0^{(+)}(G, U) = \Sigma^{(+)}(G, U)$.

It is natural to evaluate the bold series at the exact $G(\mu, U)$. The obtained series always converges, as follows from the inequality (31). The convergence is always to $\Sigma^{(+)}(G(\mu, U), U)$, which as we have seen is the correct result for $|U| < \mu^2$, and the wrong one for $|U| > \mu^2$. The convergence speed is slow for $|U|$ close to μ^2 , and gets faster not only in the small $|U|$ limit, but also in the large $|U|$ limit. This is qualitatively identical to the numerical observations of Kozik *et al.* in non-zero space-time dimensions. We note that the series converges even at the critical value $|U| = \mu^2$, albeit very slowly (the summand behaving as $1/n^{3/2}$ for large n); at this point, the boundary of the series' convergence disc is

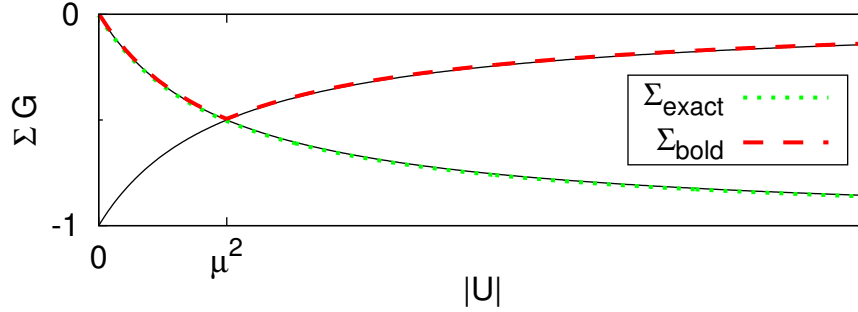


Figure 6: The two branches of the self-energy Σ , multiplied for convenience by G , as a function of the interaction strength $|U|$, for fixed μ . Dotted line: exact self-energy $\Sigma_{\text{exact}} = \Sigma(\mu, U)$, dashed line: bold series $\Sigma_{\text{bold}}(G, U)$. The upper branch corresponds to $\Sigma^{(+)}(G, U)$, the lower branch to $\Sigma^{(-)}(G, U)$. Here, G stands for the exact $G(\mu, U)$.

reached. Explicitly, expanding the square root in Eq. (32) yields

$$\Sigma_{\text{bold}}(G, U) = \sum_{n=1}^{\infty} \frac{(-1)^{n-1} (2n-2)!}{n! (n-1)!} G^{2n-1} U^n. \quad (34)$$

We can therefore write:

(KFG branch of the toy model): For $U \leq 0$ one has

$$\Sigma(G, U) = \begin{cases} \Sigma_{\text{bold}}(G, U) & |U| \leq |U_{\text{KFG}}| \\ \Sigma_{\text{KFG}}(G, U) & |U| > |U_{\text{KFG}}| \end{cases} \quad (35)$$

with $U_{\text{KFG}} = -\mu^2$, Σ_{bold} is the Taylor series in U of the function $\Sigma^{(+)}(G, U)$, and we defined $\Sigma_{\text{KFG}} := \Sigma^{(-)}$, where

$$\Sigma^{(\pm)}(G, U) = \frac{-1 \pm \sqrt{1 + 4UG^2}}{2G}. \quad (36)$$

In Figure 3.3 we plot the quantity ΣG , which, for the exact Σ , is equal to U times the double occupancy $\langle \bar{\varphi}_{\uparrow} \varphi_{\uparrow} \bar{\varphi}_{\downarrow} \varphi_{\downarrow} \rangle$, versus $|U|$ for fixed μ . The picture is qualitatively identical to Fig. 2(a) of Kozik *et al.*

Geometrically, the mapping $U \mapsto \Sigma(G, U)$ can be viewed as single-valued on a two-sheeted Riemann-surface with a branch point at $-1/(4G^2)$. Let us vary U from 0 to $-\infty$ for fixed μ . For small $|U|$, the point U is far away from the branch point and the bold series converges quickly. The result corresponds to the

correct Riemann-sheet. Upon increasing $|U|$, the point U and the branch point $-1/(4G^2(\mu, U))$ both move leftwards. The point U catches up the branch point when $|U| = |U_{\text{KFG}}| = \mu^2$. For larger $|U|$, U is again to the right of the branch point, and the bold series converges again, but the result corresponds to the wrong sheet. In principle, the correct result can be recovered from $\Sigma_{\text{bold}}(G, U)$ by analytic continuation along a path where U rotates once around the branch point. We point out that in the present zero space-time dimensional model, both branches $G_0^{(\pm)}(G, U)$ are physical in the sense that they are the non-interacting propagator for certain parameters of the model. This is not the case for the Hubbard atom and the Hubbard model [48].

3.4 Misleading convergence of the bold scheme within the toy model

In this section, we show that the possibility described in Section 2.3, that is, the convergence of the bold scheme towards an incorrect result, it is realized in the toy model.⁴⁷ This possibility was first found numerically within a Bold Diagrammatic Monte Carlo simulation of the Hubbard model [126].

The truncated Dyson equation is

$$\Sigma_{\text{bold}}^{(\leq \mathcal{N})}(\tilde{G}_{\mathcal{N}}, U) = \frac{1}{G_0} - \frac{1}{\tilde{G}_{\mathcal{N}}} \quad (37)$$

Using the re-scaled variables g , g_0 and σ defined in the previous section, this can be rewritten:

$$\sigma_{\text{bold}}^{(\leq \mathcal{N})}(\tilde{g}_{\mathcal{N}}) = \frac{1}{g_0} - \frac{1}{\tilde{g}_{\mathcal{N}}} \quad (38)$$

One has for $0 \leq x \leq 1/2$:

$$\sigma_{\text{bold}}(x) = \text{Taylor} \left(\frac{-1 + \sqrt{1 - 4x^2}}{2x} \right) = - \sum_{n=1}^{\infty} \frac{(2n-2)!}{n!(n-1)!} x^{2n-1} \quad (39)$$

and

$$\sigma_{\text{bold}}^{(\leq \mathcal{N})}(x) = - \sum_{n=1}^{\mathcal{N}} \frac{(2n-2)!}{n!(n-1)!} x^{2n-1} \quad (40)$$

We introduce

$$h_{\mathcal{N}}(x) := \sigma_{\text{bold}}^{(\leq \mathcal{N})}(x) + \frac{1}{x}, \quad h(x) := \sigma_{\text{bold}}(x) + \frac{1}{x} \quad (41)$$

⁴⁷This interesting fact was discovered numerically and then proved by F. Werner [132]. In this section we present an alternative derivation.

so that the Dyson equation (38) can be written

$$h_{\mathcal{N}}(\tilde{g}_{\mathcal{N}}) = \frac{1}{g_0} \quad (42)$$

We consider $g_0 > 0$ and $\tilde{g}_{\mathcal{N}}$ from now on.

$h_{\mathcal{N}}(x)$ is a continuous function that for $x \in (0, \infty)$ that takes values in $(-\infty, \infty)$, therefore the equation $h_{\mathcal{N}}(\tilde{g}_{\mathcal{N}}) = 1/g_0 > 0$ has always a solution. Moreover, $h_{\mathcal{N}}(x)$ is a monotonically decreasing function of x , therefore the solution is unique. We have therefore shown that

For every g_0 and \mathcal{N} , there exists a unique $\tilde{g}_{\mathcal{N}}(g_0)$ solution of (42).

One has that $h_{\mathcal{N}}(x)$ is a monotonically decreasing function of \mathcal{N} . This implies that the positive sequence $\tilde{g}_{\mathcal{N}}$ is monotonically decreasing with \mathcal{N} , therefore it converges to a non-negative number. Hence, one has

One has $\tilde{g}_{\mathcal{N}} \downarrow \tilde{g} \geq 0$ as $\mathcal{N} \rightarrow \infty$, for every $g_0 > 0$.

We have seen that the bold scheme $\tilde{g}_{\mathcal{N}}$ always converges monotonically to some value \tilde{g} . Suppose $\tilde{g} > 1/2$. Using the monotonicity of $h_{\mathcal{N}}$, we have

$$h_{\mathcal{N}}(\tilde{g}_{\mathcal{N}}) \leq h_{\mathcal{N}}(\tilde{g}) \quad (43)$$

but the right hand side tends to $-\infty$ as \mathcal{N} goes to infinity.

Suppose $\tilde{g} < 1/2$. There exists \mathcal{N}^* such that for all $\mathcal{N} \geq \mathcal{N}^*$, one has $\tilde{g}_{\mathcal{N}} < (1/2 + \tilde{g})/2$. We have therefore for $\mathcal{N} \geq \mathcal{N}^*$

$$\frac{1}{g_0} = \frac{1}{\tilde{g}_{\mathcal{N}}} + \sum_{n=1}^{\infty} \tilde{g}_{\mathcal{N}}^{2n-1} \sigma_{\text{bold}, 2n-1} - \sum_{n=\mathcal{N}+1}^{\infty} \tilde{g}_{\mathcal{N}}^{2n-1} \sigma_{\text{bold}, 2n-1} \quad (44)$$

In the second term of the equation we can apply the Lebesgue dominated convergence theorem for the $\mathcal{N} \rightarrow \infty$, while the third term can be bounded by

$$\left| \sum_{n=\mathcal{N}+1}^{\infty} \tilde{g}_{\mathcal{N}}^{2n-1} \sigma_{\text{bold}, 2n-1} \right| \leq \sum_{n=\mathcal{N}+1}^{\infty} 2^{-2n+1} |\sigma_{\text{bold}, 2n-1}| \underset{\mathcal{N} \rightarrow \infty}{=} 0 \quad (45)$$

so by taking the $\mathcal{N} \rightarrow \infty$ we have for $\tilde{g} < 1/2$

$$\frac{1}{g_0} = \sigma_{\text{bold}}(\tilde{g}) + \frac{1}{\tilde{g}} \quad (46)$$

which gives the correct result for $0 \leq g_0 < 1$. For $g_0 \geq 1$, the only possibility is therefore $\tilde{g} = 1/2$:

(Misleading convergence of the bold scheme): The bold scheme always converges monotonically $\tilde{g}_N \underset{N \rightarrow \infty}{=} \tilde{g} \in \mathbb{R}^+$. One has

$$\tilde{g} = \begin{cases} g & \text{for } g_0 \leq 1 \\ \frac{1}{2} \neq g & \text{for } g_0 > 1 \end{cases} \quad (47)$$

The bold scheme always converges to $\tilde{g} = 1/2$ for $g_0 \geq 1$, which is the wrong result for $g_0 > 1$.

4 Semi-bold scheme: partial dressing with no misleading convergence

Diagrammatic dressing is the process of expressing the diagrammatic series in terms of dressed objects, which are built by re-summing some class of diagrams. The use of renormalized objects can be very useful in some physical situations, and even mandatory when the bare expansion is ill-defined. Here we present a discussion of dressing by the use of a shifted-action expansion (Article 4 [87]), that allows to formalize diagrammatic dressing in a convenient framework, and to justify diagrammatic dressing.

The idea behind shifted-action expansions is very simple: we want to introduce an action such that the Taylor expansion in some parameter reproduces order by order the dressed expansion. After having given a formal definition of the shifted action (Section 4.1), we present the semi-bold scheme in Section 4.2.

4.1 Shifted-action expansion

We consider a generic fermionic many-body problem described by an action

$$S[\psi, \bar{\psi}] = -\langle \psi | G_0^{-1} | \psi \rangle + S_{\text{int}}[\psi, \bar{\psi}] \quad (48)$$

where $\psi, \bar{\psi}$ are Grassmann fields [133], and we use bra-ket notations to suppress space, imaginary time, possible internal quantum numbers, and integrals/sums over them, *i.e.*, $\langle \psi | G_0^{-1} | \psi \rangle$ denotes the integral/sum over \mathbf{r}, τ and σ of $\bar{\psi}_\sigma(\mathbf{r}, \tau) (G_{0,\sigma}^{-1} \psi_\sigma)(\mathbf{r}, \tau)$. G_0^{-1} stands for the inverse, in the sense of operators, of the free propagator. The full propagator G and the self-energy Σ are related through the Dyson equation $G^{-1} = G_0^{-1} - \Sigma$. The bare Feynman diagrammatic expansion corresponds to perturbation theory in S_{int} . In order to generate a diagrammatic expansion built on a partially dressed single-particle propagator \tilde{G}_N ,

we introduce an auxiliary (shifted) action of the form

$$S_{\mathcal{N}}^{(\xi)}[\psi, \bar{\psi}] = -\langle \psi | G_{0,\mathcal{N}}^{-1}(\xi) | \psi \rangle + \xi S_{\text{int}}[\psi, \bar{\psi}], \quad (49)$$

where

$$G_{0,\mathcal{N}}^{-1}(\xi) = \tilde{G}_{\mathcal{N}}^{-1} + \xi \Lambda_1 + \dots + \xi^{\mathcal{N}} \Lambda_{\mathcal{N}}, \quad (50)$$

ξ is an auxiliary complex parameter, and $\Lambda_1, \dots, \Lambda_{\mathcal{N}}$ are appropriate operators. $\tilde{G}_{\mathcal{N}}$ is the single particle propagator for $S_{\mathcal{N}}^{(\xi=0)}$. At $\xi \neq 0$, one can still view $\tilde{G}_{\mathcal{N}}$ as the free propagator, provided one includes in the interaction terms not only ξS_{int} , but also the quadratic terms $\langle \psi | \xi^n \Lambda_n | \psi \rangle$. Accordingly, ξ is interpreted as a coupling constant, and the $\xi^n \Lambda_n$ acquire the meaning of counter-terms. These counter-terms can be tuned to cancel out reducible diagrams, thereby enforcing the dressed character of the diagrammatic expansion. A natural requirement is that $S_{\mathcal{N}}^{(\xi=1)}$ coincides with the physical action S , *i.e.*, that

$$\tilde{G}_{\mathcal{N}}^{-1} + \sum_{n=1}^{\mathcal{N}} \Lambda_n = G_0^{-1}. \quad (51)$$

For given G_0 , this should be viewed as an equation to be solved for $\tilde{G}_{\mathcal{N}}$ (it is non-linear if the Λ_n 's depend on $\tilde{G}_{\mathcal{N}}$). The unperturbed action for the dressed expansion, $\langle \psi | \tilde{G}_{\mathcal{N}}^{-1} | \psi \rangle$, is shifted by the Λ_n 's with respect to the unperturbed action for the bare expansion, $\langle \psi | G_0^{-1} | \psi \rangle$.

We can then use any action of the generic class (49) for producing physical answers in the form of Taylor expansion in powers of ξ , provided the propagator $\tilde{G}_{\mathcal{N}}$ and the shifts Λ_n satisfy Eq. (51). More precisely, consider the full single-particle propagator $G_{\mathcal{N}}(\xi)$ of the action $S_{\mathcal{N}}^{(\xi)}$, and the corresponding self-energy

$$\Sigma_{\mathcal{N}}(\xi) := G_{0,\mathcal{N}}^{-1}(\xi) - G_{\mathcal{N}}^{-1}(\xi). \quad (52)$$

Note that since $S_{\mathcal{N}}^{(\xi=1)} = S$, we have $G_{\mathcal{N}}(\xi=1) = G$ and hence also $\Sigma_{\mathcal{N}}(\xi=1) = \Sigma$. We assume for simplicity that $\Sigma_{\mathcal{N}}(\xi)$ is analytic at $\xi = 0$, and that its Taylor series $\sum_{n=1}^{\infty} \Sigma_{\mathcal{N}}^{(n)}[\tilde{G}_{\mathcal{N}}] \xi^n$, converges at $\xi = 1$. We expect these assumptions to hold for fermionic lattice models at finite temperature in a broad parameter regime, given that the action $S_{\mathcal{N}}^{(\xi)}$ is analytic in ξ [46, 134, 28, 29, 33, 135, 31]. Then, since $S_{\mathcal{N}}^{(\xi)}$ is an entire function of ξ , we can conclude that

$$\Sigma = \sum_{n=1}^{\infty} \Sigma_{\mathcal{N}}^{(n)}[\tilde{G}_{\mathcal{N}}], \quad (53)$$

i.e., the physical self-energy is equal to the dressed diagrammatic series.

This last step of the reasoning can be justified using the following presumption: *Let \mathcal{D} be a connected open region of the complex plane containing 0. Assume that $S^{(\xi)}$ is analytic in \mathcal{D} , that the corresponding self-energy $\Sigma(\xi)$ is analytic at $\xi = 0$, and that $\Sigma(\xi)$ admits an analytic continuation $\tilde{\Sigma}(\xi)$ in \mathcal{D} . Then, Σ and $\tilde{\Sigma}$ coincide on \mathcal{D} .* This presumption is based on the following argument: Since $S^{(\xi)}$ is analytical, if no phase transition occurs when varying ξ in \mathcal{D} , then $\Sigma(\xi)$ is analytical on \mathcal{D} , and by the identity theorem for analytic functions, Σ and $\tilde{\Sigma}$ coincide on \mathcal{D} . If a phase transition would be crossed as a function of ξ in \mathcal{D} , analytic continuation through the phase transition would not be possible [136], contradicting the above assumption on the existence of $\tilde{\Sigma}$. Applying this presumption to $\tilde{\Sigma}(\xi) := \sum_{n=1}^{\infty} \Sigma_{\mathcal{N}}^{(n)}[\tilde{G}_{\mathcal{N}}] \xi^n$, which has a radius of convergence $R \geq 1$ (from the Cauchy-Hadamard theorem), and taking for \mathcal{D} the open disc of radius R , we directly obtain Eq. (53) provided $R > 1$. If $R=1$, we can still derive Eq. (53), using Abel's theorem and assuming that $\Sigma_{\mathcal{N}} * (\xi)$ is continuous at $\xi=1$, which, given that the action is entire in ξ , is generically expected (except for physical parameters fined-tuned precisely to a first-order phase transition, where Σ is not uniquely defined).

4.2 Semi-bold scheme

We first focus on the choice

$$\Lambda_n = \Sigma_{\text{bold}}^{(n)}[\tilde{G}_{\mathcal{N}}] \quad (54)$$

where $\Sigma_{\text{bold}}^{(n)}[\mathcal{G}]$ is the sum of all bold diagrams of order n , built with the propagator \mathcal{G} and the bare interaction vertex corresponding to S_{int} , that remain connected when cutting two \mathcal{G} lines. This means that $\tilde{G}_{\mathcal{N}}$ is the solution of the bold scheme for maximal order \mathcal{N} , cf. Eq. (51). For a given \mathcal{N} , higher-order dressed graphs can then be built on $\tilde{G}_{\mathcal{N}}$. The numerical protocol corresponding to this 'semi-bold' scheme consists of two independent parts: Part 1 is the Bold Diagrammatic Monte Carlo simulation of the truncated order- \mathcal{N} bold sum employed to solve iteratively for $\tilde{G}_{\mathcal{N}}$ satisfying Eqs. (51,54); Part 2 is the diagrammatic Monte Carlo simulation of higher-order terms, $\Sigma_{\mathcal{N}}^{(n)}[\tilde{G}_{\mathcal{N}}]$, $n > \mathcal{N}$, that uses $\tilde{G}_{\mathcal{N}}$ as the bare propagator. Note that here \mathcal{N} is fixed (contrarily to the conventional bold scheme discussed below), and the infinite-order extrapolation is done only in Part 2.

The Feynman rules for the semi-bold scheme are as follows:

$$\Sigma_{\mathcal{N}}^{(n)}[\tilde{G}_{\mathcal{N}}] = \Sigma_{\text{bold}}^{(n)}[\tilde{G}_{\mathcal{N}}] \quad \text{for } n \leq \mathcal{N}; \quad (55)$$

while for $n \geq \mathcal{N} + 1$, $\Sigma_{\mathcal{N}}^{(n)}[\tilde{G}_{\mathcal{N}}]$ is the sum of all bare diagrams, built with $\tilde{G}_{\mathcal{N}}$ as free propagator and the bare interaction vertex corresponding to S_{int} , which

do not contain any insertion of a sub-diagram contributing to $\Sigma_{\text{bold}}^{(n)}[\tilde{G}_{\mathcal{N}}]$ with $n \leq \mathcal{N}$. Indeed, each such insertion is exactly compensated by the corresponding counterterm. To derive Eq. (55), we will use the relation

$$\Sigma_{\mathcal{N}}(\xi) \hat{=} \sum_{n=1}^{\infty} \Sigma_{\text{bold}}^{(n)}[G_{\mathcal{N}}(\xi)] \xi^n \quad (56)$$

where $\hat{=}$ stands for equality in the sense of formal power series in ξ , and we will show the proposition

$$\Sigma_{\mathcal{N}}(\xi) \hat{=} \sum_{n=1}^k \Sigma_{\text{bold}}^{(n)}[\tilde{G}_{\mathcal{N}}] \xi^n + O(\xi^{k+1}) \quad (\text{Pr}_k)$$

for any $k \in \{0, \dots, \mathcal{N} + 1\}$, by recursion over k . $(\text{Pr}_{k=0})$ clearly holds. If (Pr_k) holds for some $k \leq \mathcal{N}$, then we have $G_{\mathcal{N}}(\xi) \hat{=} \tilde{G}_{\mathcal{N}} + O(\xi^{k+1})$, as follows from Eqs. (52), (50) and (54). Substitution into Eq. (56) then yields (Pr_{k+1}) .

5 Applicability of the bold scheme

We turn to the conventional scheme in which diagrams are built on the *fully* dressed single-particle propagator. The corresponding numerical protocol is identical to Part 1 of the above one, with the additional step of extrapolating \mathcal{N} to infinity, as done in [42, 12, 33, 135, 31]. Accordingly, we assume that the 'bold sequence' $\tilde{G}_{\mathcal{N}}$ converges to a limit \tilde{G} when $\mathcal{N} \rightarrow \infty$. The crucial question is under what conditions one can be confident that \tilde{G} is the genuine propagator G of the original model. The answer comes from the properties of the sequence of functions $L_{\mathcal{N}}(\xi)$:

(Applicability of the bold scheme): Let us define

$$L_{\mathcal{N}}^{(\xi)} := \sum_{n=1}^{\mathcal{N}} \Sigma_{\text{bold}}^{(n)}[\tilde{G}_{\mathcal{N}}] \xi^n. \quad (57)$$

Let us show that $\tilde{G} = G$ holds under the following sufficient condition:

- (i) for any ξ in a disc $\mathcal{D} = \{|\xi| < R\}$ of radius $R > 1$, and for all (\mathbf{p}, τ) , $L_{\mathcal{N}}^{(\xi)}(\mathbf{p}, \tau)$ converges for $\mathcal{N} \rightarrow \infty$; moreover this sequence is uniformly bounded, *i.e.*, there exists a function $C_1(\mathbf{p}, \tau)$ such that $\forall \xi \in \mathcal{D}, \forall (\mathcal{N}, \mathbf{p}, \tau), |L_{\mathcal{N}}^{(\xi)}(\mathbf{p}, \tau)| \leq C_1(\mathbf{p}, \tau)$; and
- (ii) $\tilde{G}_{\mathcal{N}}(\mathbf{p}, \tau)$ is uniformly bounded, *i.e.*, there exists a constant C_2 such that for all $(\mathcal{N}, \mathbf{p}, \tau), |\tilde{G}_{\mathcal{N}}(\mathbf{p}, \tau)| \leq C_2$.

Our derivation is based on the action

$$S_\infty^{(\xi)} := \lim_{\mathcal{N} \rightarrow \infty} S_{\mathcal{N}}^{(\xi)}. \quad (58)$$

Clearly,

$$S_\infty^{(\xi)} = \langle \psi | \tilde{G}^{-1} + L^{(\xi)} | \psi \rangle + \xi S_{\text{int}} \quad (59)$$

with

$$L^{(\xi)}(\mathbf{p}, \tau) := \lim_{\mathcal{N} \rightarrow \infty} L_{\mathcal{N}}^{(\xi)}(\mathbf{p}, \tau). \quad (60)$$

Since $S_{\mathcal{N}}^{(\xi=1)} = S$, we have $S_\infty^{(\xi=1)} = S$, and thus $G_\infty(\xi=1) = G$ where $G_\infty(\xi)$ is the full propagator of the action $S_\infty^{(\xi)}$.

We first observe that $L^{(\xi)}(\mathbf{p}, \tau)$ is an analytic function of $\xi \in \mathcal{D}$ for all (\mathbf{p}, τ) , and that

$$\frac{1}{n!} \frac{\partial^n}{\partial \xi^n} L^{(\xi)}(\mathbf{p}, \tau) \Big|_{\xi=0} = \Sigma_{\text{bold}}^{(n)}[\tilde{G}](\mathbf{p}, \tau). \quad (61)$$

This follows from conditions (i,ii), given that momenta are bounded for lattice models. Indeed, for any triangle \mathcal{T} included in \mathcal{D} , $\oint_{\mathcal{T}} d\xi L_{\mathcal{N}}^{(\xi)}(\mathbf{p}, \tau) = 0$. Thanks to condition (i), the dominated convergence theorem is applicable, yielding $\oint_{\mathcal{T}} d\xi L^{(\xi)}(\mathbf{p}, \tau) = 0$. The analyticity of $\xi \mapsto L^{(\xi)}(\mathbf{p}, \tau)$ follows by Morera's theorem. To derive Eq. (61) we start from

$$\frac{1}{n!} \frac{\partial^n}{\partial \xi^n} L_{\mathcal{N}}^{(\xi)}(\mathbf{p}, \tau) \Big|_{\xi=0} = \Sigma_{\text{bold}}^{(n)}[\tilde{G}_{\mathcal{N}}](\mathbf{p}, \tau). \quad (62)$$

By Cauchy's integral formula, the l.h.s. of Eq. (62) equals

$1/(2i\pi) \oint_{\mathcal{C}} d\xi L_{\mathcal{N}}^{(\xi)}(\mathbf{p}, \tau)/\xi^{n+1}$ where \mathcal{C} is the unit circle. Using again condition (i) and the dominated convergence theorem, when $\mathcal{N} \rightarrow \infty$, this tends to $1/(2i\pi) \oint_{\mathcal{C}} d\xi L^{(\xi)}(\mathbf{p}, \tau)/\xi^{n+1}$, which equals the l.h.s. of Eq. (61). To show that $\Sigma_{\text{bold}}^{(n)}[\tilde{G}_{\mathcal{N}}](\mathbf{p}, \tau)$ tends to $\Sigma_{\text{bold}}^{(n)}[\tilde{G}](\mathbf{p}, \tau)$, we consider each Feynman diagram separately; the dominated convergence theorem is applicable thanks to condition (ii), the boundedness of the integration domain for internal momenta and imaginary times, and assuming that interactions decay sufficiently quickly at large distances for the bare interaction vertex to be bounded in momentum representation.

Hence

$$L^{(\xi)} = \sum_{n=1}^{\infty} \Sigma_{\text{bold}}^{(n)}[\tilde{G}] \xi^n. \quad (63)$$

As a consequence, the action $S_\infty^{(\xi)}$ generates the fully dressed bold series built on \tilde{G} , i.e., its self-energy $\Sigma_\infty(\xi)$ has the Taylor expansion $\sum_{n=1}^{\infty} \Sigma_{\text{bold}}^{(n)}[\tilde{G}] \xi^n$, and

the Taylor series of $G_\infty(\xi)$ reduces to the ξ -independent term \tilde{G} . This can be derived in the same way as Eq. (55), by showing by recursion over k that for any $k \geq 0$, $\Sigma_\infty(\xi) = \sum_{n=1}^k \Sigma_{\text{bold}}^{(n)}[\tilde{G}] \xi^n + O(\xi^{k+1})$. Furthermore, having shown above the analyticity of $L^{(\xi)}$, i.e., of $S_\infty^{(\xi)}$, we again expect that $G_\infty(\xi)$ is analytic at $\xi = 0$ (for fermions on a lattice at finite temperature), and we can use again the above presumption to conclude that $G_\infty(\xi = 1) = G = \tilde{G}$.

6 Conclusions and outlook

In this part of the dissertation we have studied the problem of diagrammatic dressing. Kozik *et al.* have found that the Luttinger-Ward functional has multiple branches, and the perturbative “bold” branch cannot always give the physical result. Inspired by this, we have studied a toy model for fermionic Feynman diagrams which has this phenomenology. Moreover, we have proven that the misleading convergence of the bold scheme towards an unphysical result (for which there was numerical evidence [126]), does happen for the toy model.

After having gained insight with the toy model, we went beyond phenomenology. We have first shown that for a large class of partially dressed schemes (containing the semi-bold scheme), misleading convergence cannot happen. For the bold scheme, we have provided an applicability theorem that guarantees that the misleading convergence is impossible if a condition is satisfied.

The semi-bold scheme seems a very good candidate for the substitution of the bold scheme when the latter cannot be applied. For example, the 1-semi-bold scheme was successfully applied for the Hubbard model in Article 1, and it converges much faster than the bare scheme.

The applicability theorem only works when we are inside the radius of convergence, therefore it would be interesting to generalize the arguments leading to the result when we are outside the radius of convergence. In particular, it would be useful to generalize the applicability theorem to continuous-space models (e.g. the unitary Fermi gas), where the radius of convergence is zero. This would add to the mathematical justification of the Bold Diagrammatic Monte Carlo approach for the unitary Fermi gas presented in Part I.

Article 3: Skeleton series and multivaluedness of the self-energy functional

Skeleton series and multivaluedness of the self-energy functional in zero space-time dimensions

Riccardo Rossi¹ and Félix Werner²

¹Laboratoire de Physique Statistique, Ecole Normale Supérieure, UPMC, Université Paris Diderot, CNRS, 24 rue Lhomond, 75005 Paris, France

²Laboratoire Kastler Brossel, Ecole Normale Supérieure, UPMC, Collège de France, CNRS, 24 rue Lhomond, 75005 Paris, France

E-mail: rossi@lps.ens.fr

Received 30 April 2015, revised 3 September 2015

Accepted for publication 7 October 2015

Published 29 October 2015



Abstract

Recently, Kozik, Ferrero and Georges discovered numerically that for a family of fundamental models of interacting fermions, the self-energy $\Sigma[G]$ is a multi-valued functional of the fully dressed single-particle propagator G , and that the skeleton diagrammatic series $\Sigma_{\text{bold}}[G]$ converges to the wrong branch above a critical interaction strength. We consider the zero space-time dimensional case, where the same mathematical phenomena appear from elementary algebra. We also find a similar phenomenology for the fully bold formalism built on the fully dressed single-particle propagator and pair propagator.

Keywords: Luttinger-Ward functional, Feynman diagrams, self-consistent quantum field theory

(Some figures may appear in colour only in the online journal)

In quantum many-body physics, an important role is played by the self-consistent field-theoretical formalism, where the self-energy Σ is expressed in terms of the exact propagator G (see, e.g., [1] and Refs. therein). In a recent article, Kozik, Ferrero and Georges numerically discovered mathematical difficulties with this formalism [2]. They studied not only the Hubbard model in two space dimensions, but also simpler models—the Hubbard atom and the Anderson impurity model—for which there is no spatial coordinate. Here we consider an even simpler toy-model for which there is no imaginary-time coordinate either. This idea was also followed in the very recent article [3]. For fermionic many-body problems, the partition function can be written as a functional integral over Grassmann fields in $(d + 1)$ space-time

dimensions (d spatial coordinates and one imaginary-time coordinate) [4]. Accordingly, we consider the zero space-time dimensional model defined by a ‘partition function’ given by a simple Grassmann integral,

$$Z = \int \left(\prod_{\sigma} d\varphi_{\sigma} d\bar{\varphi}_{\sigma} \right) e^{-S[\bar{\varphi}_{\sigma}, \varphi_{\sigma}]} \quad (1)$$

with the action

$$S[\bar{\varphi}_{\sigma}, \varphi_{\sigma}] = -\mu \sum_{\sigma} \bar{\varphi}_{\sigma} \varphi_{\sigma} + U \bar{\varphi}_{\uparrow} \varphi_{\uparrow} \bar{\varphi}_{\downarrow} \varphi_{\downarrow}, \quad (2)$$

and a corresponding propagator

$$G = \langle \bar{\varphi}_{\sigma} \varphi_{\sigma} \rangle = \frac{1}{Z} \int \left(\prod_{\sigma} d\varphi_{\sigma} d\bar{\varphi}_{\sigma} \right) e^{-S[\bar{\varphi}_{\sigma}, \varphi_{\sigma}]} \bar{\varphi}_{\sigma} \varphi_{\sigma}. \quad (3)$$

Here $\sigma \in \{ \uparrow, \downarrow \}$ is the spin index, while μ and U are dimensionless parameters that play the roles of chemical potential and interaction strength. Diagrammatically, the Feynman rules for the present toy-model are analogous to the ones of the physical ($d + 1$) dimensional models, with the simplification that space-time variables are absent and that the propagators are constants

In this exactly solvable toy-model, we observe a similar phenomenology than the one found by Kozik *et al* in non-zero space-time dimensions. More precisely, restricting to $U < 0$, we find that:

- The mapping $G_0 \mapsto G(G_0, U)$ is two-to-one and hence the function $G \mapsto \Sigma(G, U)$ has two branches.
- The skeleton series $\Sigma_{\text{bold}}(G, U)$, evaluated at the exact $G(\mu, U)$, converges to the correct branch for $|U| < \mu^2$, and to the wrong branch for $|U| > \mu^2$.

This can be derived very directly from the above definitions. Expanding the exponentials in equations (1) and (3) yields

$$Z(\mu, U) = \mu^2 - U \quad (4)$$

$$G(\mu, U) = \frac{\mu}{\mu^2 - U}. \quad (5)$$

The propagator for $U = 0$ is

$$G_0(\mu) = \frac{1}{\mu}. \quad (6)$$

The self-energy Σ , defined as usual by the Dyson equation $G^{-1} = G_0^{-1} - \Sigma$, reads

$$\Sigma(\mu, U) = \frac{U}{\mu}. \quad (7)$$

We note that for $U > 0$, an obvious pathology appears in this model around $U = \mu^2$; namely, Z changes sign, and G diverges. Therefore we restrict to $U < 0$.

Eliminating μ between equations (5, 6) gives

$$G(G_0, U) = \frac{G_0}{1 - U G_0^2}. \quad (8)$$

The map $G_0 \mapsto G(G_0, U)$ is two-to-one, because the G_0 's that correspond to a given G are the solutions of the second order equation

$$UG G_0^2 + G_0 - G = 0, \quad (9)$$

which has the two solutions

$$G_0^{(\pm)}(G, U) = \frac{-1 \pm \sqrt{1 + 4UG^2}}{2UG}. \quad (10)$$

These solutions are real provided (G, U) belongs to the physical manifold $\{(G(\mu, U), U)\}$; indeed,

$$4|U|G(\mu, U)^2 \leq 1. \quad (11)$$

The corresponding self-energies (given by the Dyson equation) are

$$\Sigma^{(\pm)}(G, U) = \frac{-1 \pm \sqrt{1 + 4UG^2}}{2G}. \quad (12)$$

The correct self-energy $\Sigma(\mu, U)$ is recovered from $\Sigma^{(s)}(G(\mu, U), U)$ provided one takes the determination

$$s = \text{sign}(\mu^2 - |U|). \quad (13)$$

We turn to a discussion of the skeleton diagrammatic series $\Sigma_{\text{bold}}(G, U)$ for the self-energy Σ in terms of fully dressed propagator G and bare vertex U . We find that $\Sigma_{\text{bold}}(G, U)$ is the $U \rightarrow 0$ Taylor series of $\Sigma^{(+)}(G, U)$. Before deriving this, we note that obviously, $\Sigma_{\text{bold}}(G, U)$ can never be the Taylor series of $\Sigma^{(-)}(G, U)$, since the former vanishes at $U = 0$ while the latter does not. For the derivation, it is convenient to introduce $g := \sqrt{|U|} G$ and $g_0 := \sqrt{|U|} G_0$, so that equations (8, 10) simplify to $g(g_0) = g_0/(1 + g_0^2)$ and $g_0^{(\pm)}(g) = (1 \mp \sqrt{1 - 4g^2})/(2g)$. The key point is that $g_0^{(+)}(g(g_0)) \doteq g_0$, where the symbol \doteq means equality in the sense of formal power series. This is because the inverse mapping of $g(g_0)$ is $g_0^{(+)}(g)$ for small g_0 and g . Let us then denote by $\Sigma_{\text{bare}}(G_0, U)$ the diagrammatic series for the self-energy in terms of bare propagators and vertices. Setting $\Sigma_{\text{bold}}(G, U) =: \sqrt{|U|} \sigma_{\text{bold}}(g)$ and $\Sigma_{\text{bare}}(G_0, U) =: \sqrt{|U|} \sigma_{\text{bare}}(g_0)$, a defining property of σ_{bold} is that $\sigma_{\text{bold}}(g(g_0)) \doteq \sigma_{\text{bare}}(g_0)$. In the present toy-model, we simply have $\Sigma_{\text{bare}}(G_0, U) = U G_0$, i.e., $\sigma_{\text{bare}}(g_0) = -g_0$. Hence, $\sigma_{\text{bold}}(g) \doteq -g_0^{(+)}(g)$, i.e., $\Sigma_{\text{bold}}(G, U) \doteq U G_0^{(+)}(G, U) = \Sigma^{(+)}(G, U)$.

Explicitly, expanding the square root in equation (12) yields

$$\Sigma_{\text{bold}}(G, U) = \sum_{n=1}^{\infty} \frac{(-1)^{n-1} (2n-2)!}{n! (n-1)!} G^{2n-1} U^n. \quad (14)$$

It is natural to evaluate the bold series at the exact $G(\mu, U)$. The obtained series always converges, as follows from the inequality (11). The convergence is always to $\Sigma^{(+)}(G(\mu, U), U)$, which, as we have seen, is the correct result for $|U| < \mu^2$, and the wrong one for $|U| > \mu^2$. The convergence speed is slow for $|U|$ close to μ^2 , and gets faster not only in the small $|U|$ limit, but also in the large $|U|$ limit. This is qualitatively identical to the numerical observations of Kozik *et al* in non-zero space-time dimensions. We note that the series converges even at the critical value $|U| = \mu^2$, albeit very slowly (the summand behaving as $1/n^{3/2}$ for large n); at this point, the boundary of the series' convergence disc is reached.

In the figure 1 we plot the quantity ΣG , which, for the exact Σ , is equal to U times the double occupancy $\langle \bar{\varphi}_\uparrow \varphi_\uparrow \bar{\varphi}_\downarrow \varphi_\downarrow \rangle$, versus $|U|$ for fixed μ . The picture is qualitatively identical to figure 2(a) of Kozik *et al*.

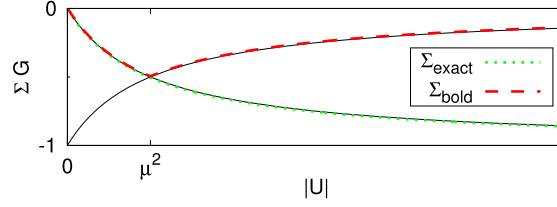


Figure 1. The two branches of the self-energy Σ , multiplied for convenience by G , as a function of the interaction strength $|U|$, for fixed μ . Dotted line: exact self-energy $\Sigma_{\text{exact}} = \Sigma(\mu, U)$, dashed line: skeleton series $\Sigma_{\text{bold}}(G, U)$. The upper branch corresponds to $\Sigma^{(+)}(G, U)$, the lower branch to $\Sigma^{(-)}(G, U)$. Here, G stands for the exact $G(\mu, U)$.

Geometrically, the mapping $U \mapsto \Sigma(G, U)$ can be viewed as single-valued on a two-sheeted Riemann-surface with a branch point at $-1/(4G^2)$. Let us vary U from 0 to $-\infty$ for fixed μ . For small $|U|$, the point U is far away from the branch point and the bold series converges quickly. The result corresponds to the correct Riemann-sheet. Upon increasing $|U|$, the point U and the branch point $-1/(4G^2(\mu, U))$ both move leftwards. The point U catches up the branch point when $|U| = \mu^2$. For larger $|U|$, U is again to the right of the branch point, and the bold series converges again, but the result corresponds to the wrong sheet. In principle, the correct result can be recovered from $\Sigma_{\text{bold}}(G, U)$ by analytic continuation along a path where U rotates once around the branch point.

As emphasized by Kozik *et al*, since the self-energy is the functional derivative of the Luttinger-Ward functional $\Phi[G, U]$ with respect to G , and since $\Sigma[G, U]$ is multivalued, Φ must also be multivalued. This can also be seen explicitly in the present model. The Luttinger-Ward functional (which is actually a function in the present model) can be constructed following the usual procedure (see, e.g., [1]). Starting from the free energy $F(\mu, U) = -\ln Z(\mu, U)$, and noting that

$$\frac{\partial F}{\partial \mu}(\mu, U) = -2 G, \tag{15}$$

the Baym-Kadanoff functional is defined by Legendre transformation:

$$\Omega(G, U) = F(\mu, U) + 2 \mu G \tag{16}$$

with $\mu(G, U)$ such that equation (15) holds. The Luttinger-Ward functional is then defined by

$$\Phi(G, U) = \Omega(G, U) - \Omega(G, 0). \tag{17}$$

This leads to the expression

$$\Phi_{\pm}(G, U) = -\ln \left| \Sigma^{(\mp)}(G, U) \right| - \ln |G| - 2 G \Sigma^{(\mp)}(G, U) - 2. \tag{18}$$

There are two branches because equation (15) has two solutions. Accordingly, the mapping $\mu \mapsto F(\mu, U)$ is neither convex nor concave. Finally one can check that³

$$\frac{\partial \Phi_{\pm}}{\partial G}(G, U) = 2 \Sigma^{(\pm)}(G, U). \tag{19}$$

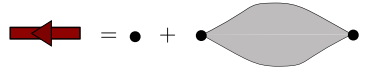
³ The unconventional factors 2 in equations (15), (16), and (19) could be removed by working with spin-dependent μ and G .

We point out that in the present zero space-time dimensional model, both branches $G_0^{(\pm)}(G, U)$ are physical in the sense that they are the non-interacting propagator for certain parameters of the model. This is not the case for the Hubbard atom and the Hubbard model [2]. More generally, the absence of imaginary-time coordinate constitutes a drastic simplification, and while we have observed similar phenomena than in [2], it remains an open question to which extent the underlying mechanisms are similar.

Finally we briefly treat the fully bold formalism built not only on the fully dressed G but also on the fully dressed pair propagator Γ . This formalism was used, e.g., in [5, 6]. One defines

$$\Gamma = U - U^2 \langle \varphi_{\uparrow} \varphi_{\uparrow} \bar{\varphi}_{\uparrow} \bar{\varphi}_{\uparrow} \rangle \quad (20)$$

or diagrammatically



$$\leftarrow = \bullet + \text{pair propagator} \quad (21)$$

The pair self-energy Π is defined by the Dyson equation $\Gamma^{-1} = U^{-1} - \Pi$.

The dressed G and Γ are given in terms of the bare G_0 and U by equation (8) and

$$\Gamma = U \frac{1 - 2U G_0^2}{1 - U G_0^2}. \quad (22)$$

Eliminating U yields a cubic equation for G_0 , which reads

$$\gamma g_0^3 + 2g_0^2 - 3g_0 + 1 = 0 \quad (23)$$

in terms of the rescaled quantities

$$g_0 := G_0/G \quad (24)$$

$$\gamma := \Gamma G^2. \quad (25)$$

In the relevant range $0 < |\gamma| \leq 2\sqrt{3}/9$ the three solutions are

$$g_0^{(l)} = \frac{2}{3\gamma} \left[\sqrt{9\gamma + 4} \cos\left(\frac{\theta(\gamma) + 2\pi l}{3}\right) - 1 \right], \quad l \in \{-1, 0, 1\} \quad (26)$$

where $\theta(\gamma) = \arg(-27\gamma^2 - 54\gamma - 16 - 3i\sqrt{3}|\gamma|\sqrt{4 - 27\gamma^2}) \in (-\pi, \pi)$. The fully bold diagrammatic series $\Sigma_{\text{bold}}(G, \Gamma)$ and $\Pi_{\text{bold}}(G, \Gamma)$, evaluated at the exact $G(\mu, U)$ and $\Gamma(\mu, U)$, always converge to the $l = 1$ branch⁴, which coincides with the exact result for $|U|/\mu^2 < (1 + \sqrt{3})/2$. Above this critical interaction strength, the exact result is the $l = -1$ branch, so that the bold series converges to a wrong result. At this critical interaction, the boundary of the series' convergence disc is reached. In summary, a similar phenomenology occurs again.

The consequences for the Bold Diagrammatic Monte Carlo approach [5–9] of the findings of [2] and of the present work is left for future study.

Acknowledgments

We thank E Kozik, N Prokof'ev and K Van Houcke for discussions. We acknowledge support from CNRS, ERC and IFRAF-NanoK (grants PICS 06220, 'Thermodynamix', and

⁴ Explicitly, we have $\Sigma_{\text{bold}}(G, \Gamma) \doteq [1/g_0^{(+1)}(\gamma) - 1]/G$ and $\Pi_{\text{bold}}(G, \Gamma) \doteq \Sigma_{\text{bold}}(G, \Gamma)/[G g_0^{(+1)}(\gamma)]$.

‘Atomix’). Our host institutions are members of ‘Paris Sciences et Lettres’, ‘Sorbonne Universités’, and ‘Sorbonne Paris Cité’.

References

- [1] Haussmann R 1999 *Self-Consistent Quantum-Field Theory and Bosonization for Strongly Correlated Electron Systems* (Berlin: Springer)
- [2] Kozik E, Ferrero M and Georges A 2015 *Phys. Rev. Lett.* **114** 156402
- [3] Stan A, Romaniello P, Rigamonti S, Reining L and Berger J *New J. Phys.* **17** 093045
- [4] Negele J W and Orland H 1988 *Quantum Many-particle Systems* (Reading, MA: Addison-Wesley)
- [5] Van Houcke K, Werner F, Kozik E, Prokof'ev N, Svistunov B, Ku M J H, Sommer A T, Cheuk L W, Schirotzek A and Zwierlein M W 2012 *Nature Phys.* **8** 366
Van Houcke K, Werner F, Prokof'ev N and Svistunov B arXiv:1305.3901
- [6] Deng Y, Kozik E, Prokof'ev N V and Svistunov B V 2015 *EPL* **110** 57001
- [7] Prokof'ev N and Svistunov B 2007 *Phys. Rev. Lett.* **99** 250201
Prokof'ev N and Svistunov B 2008 *Phys. Rev. B* **77** 125101
- [8] Kulagin S, Prokof'ev N, Starykh O, Svistunov B and Varney C 2013 *Phys. Rev. Lett.* **110** 070601
Kulagin S, Prokof'ev N, Starykh O, Svistunov B and Varney C 2013 *Phys. Rev. B* **87** 024407
- [9] Mishchenko A S, Nagaosa N and Prokof'ev N 2014 *Phys. Rev. Lett.* **113** 166402

Article 4: Shifted-action expansion and applicability of dressed diagrammatic schemes

Shifted-action expansion and applicability of dressed diagrammatic schemes

Riccardo Rossi,¹ Félix Werner,² Nikolay Prokof'ev,^{3,4} and Boris Svistunov^{3,4,5}

¹Laboratoire de Physique Statistique, Ecole Normale Supérieure, UPMC, Université Paris Diderot, CNRS, Paris Sciences et Lettres, Sorbonne Universités, Sorbonne Paris Cité, 24 rue Lhomond, 75005 Paris, France

²Laboratoire Kastler Brossel, Ecole Normale Supérieure, UPMC, Collège de France, CNRS, Paris Sciences et Lettres, Sorbonne Universités, 24 rue Lhomond, 75005 Paris, France

³Department of Physics, University of Massachusetts, Amherst, Massachusetts 01003, USA

⁴Russian Research Center "Kurchatov Institute," 123182 Moscow, Russia

⁵Wilczek Quantum Center, Zhejiang University of Technology, Hangzhou 310014, China

(Received 14 August 2015; revised manuscript received 29 February 2016; published 5 April 2016)

While bare diagrammatic series are merely Taylor expansions in powers of interaction strength, dressed diagrammatic series, built on fully or partially dressed lines and vertices, are usually constructed by reordering the bare diagrams, which is an *a priori* unjustified manipulation, and can even lead to convergence to an unphysical result [E. Kozik, M. Ferrero, and A. Georges, *Phys. Rev. Lett.* **114**, 156402 (2015)]. Here we show that for a broad class of partially dressed diagrammatic schemes, there exists an action $S^{(\xi)}$ depending analytically on an auxiliary complex parameter ξ , such that the Taylor expansion in ξ of correlation functions reproduces the original diagrammatic series. The resulting applicability conditions are similar to the bare case. For fully dressed skeleton diagrammatics, analyticity of $S^{(\xi)}$ is not granted, and we formulate a sufficient condition for converging to the correct result.

DOI: 10.1103/PhysRevB.93.161102

Much of theoretical physics is formulated in the language of Feynman diagrams, in various fields such as condensed matter, nuclear physics, and quantum chromodynamics (QCD). A powerful feature of the diagrammatic technique, used in each of the above fields, is the possibility to build diagrams on partially or fully dressed propagators or vertices (see, e.g., Refs. [1–5]). In quantum many-body physics, notable examples include dilute gases, whose description is radically improved if ladder diagrams are summed up so that the expansion is done in terms of the scattering amplitude instead of the bare interaction potential, and Coulomb interactions, which one has to screen to have a meaningful diagrammatic technique.

With the development of diagrammatic Monte Carlo, it becomes possible to compute Feynman diagrammatic expansions to high order for fermionic strongly correlated quantum many-body problems [6–11]. The number of diagrams grows factorially with the order, even for a fully irreducible skeleton scheme [12]. Nevertheless, for fermionic systems on a lattice at finite temperature, diagrammatic series (of the form $\sum_n a_n$ with a_n the sum of all order- n diagrams) are typically convergent in a broad range of parameters, due to a nearly perfect cancellation of contributions of different sign within each order, as proven mathematically [13] and seen numerically [6,7,9–11].

One might think that partial or full renormalization of diagrammatic elements (propagators, interactions, vertices, etc.) always leads to more compact and better behaving diagrammatic expansions. However, such a dressed diagrammatic series cannot be used blindly: Even when it converges, the result is not guaranteed to be correct, since it is *a priori* not allowed to reorder the terms of a series that is not absolutely convergent (the sum of the absolute values of *individual diagrams* is typically infinite, due to factorial scaling of the number of diagrams with the order). And indeed, for a skeleton series, i.e., a series built on the fully dressed propagator, convergence to a wrong result does occur in the case of the Hubbard model in the strongly correlated regime

near half filling [14], and preliminary results suggest that the corresponding self-consistent skeleton scheme converges to a wrong result as a function of the maximal self-energy diagram order \mathcal{N} [15]. Both of these phenomena are clearly seen in the exactly solvable zero space-time dimensional case [16,17].

In this Rapid Communication, we establish a condition that is necessarily violated in the event of convergence to a wrong result of the self-consistent skeleton scheme. Furthermore, we show that this convergence issue is absent for a broad class of partially dressed schemes. In particular, we propose a simple scheme based on the truncated skeleton series. The underlying idea is to construct an action $S^{(\xi)}$ that depends on an auxiliary complex parameter ξ such that the Taylor series in ξ of correlation functions reproduces the dressed diagrammatic series built on a given partially or fully dressed propagator. This makes the dressed scheme as mathematically justified as a bare scheme, provided $S^{(\xi)}$ is analytic with respect to ξ and $S^{(\xi=1)}$ coincides with the physical action; these conditions hold automatically in the partially dressed case, while in the fully dressed case they hold under a simple sufficient condition which we provide. Our construction applies to a general class of diagrammatic schemes built on dressed lines and vertices, including two-particle ladders and screened long-ranged potentials.

Partially dressed single-particle propagator. We consider a generic fermionic many-body problem described by an action

$$S[\psi, \bar{\psi}] = \langle \psi | G_0^{-1} | \psi \rangle + S_{\text{int}}[\psi, \bar{\psi}], \quad (1)$$

where $\psi, \bar{\psi}$ are Grassmann fields [18], and we use bracket notations to suppress space, imaginary time, possible internal quantum numbers, and integrals/sums over them, i.e., $\langle \psi | G_0^{-1} | \psi \rangle$ denotes the integral/sum over \mathbf{r}, τ and σ of $\bar{\psi}_\sigma(\mathbf{r}, \tau)(G_{0,\sigma}^{-1}\psi_\sigma)(\mathbf{r}, \tau)$. G_0^{-1} stands for the inverse, in the sense of operators, of the free propagator. The full propagator G and the self-energy Σ are related through the Dyson equation

$G^{-1} = G_0^{-1} - \Sigma$. The bare Feynman diagrammatic expansion corresponds to perturbation theory in S_{int} . In order to generate a diagrammatic expansion built on a partially dressed single-particle propagator $\tilde{G}_{\mathcal{N}}$, we introduce an auxiliary action of the form

$$S_{\mathcal{N}}^{(\xi)}[\psi, \bar{\psi}] = \langle \psi | G_{0,\mathcal{N}}^{-1}(\xi) | \psi \rangle + \xi S_{\text{int}}[\psi, \bar{\psi}], \quad (2)$$

where

$$G_{0,\mathcal{N}}^{-1}(\xi) = \tilde{G}_{\mathcal{N}}^{-1} + \xi \Lambda_1 + \dots + \xi^{\mathcal{N}} \Lambda_{\mathcal{N}}, \quad (3)$$

ξ is an auxiliary complex parameter, and $\Lambda_1, \dots, \Lambda_{\mathcal{N}}$ are appropriate operators. $\tilde{G}_{\mathcal{N}}$ is the single-particle propagator for $S_{\mathcal{N}}^{(\xi=0)}$. At $\xi \neq 0$, one can still view $\tilde{G}_{\mathcal{N}}$ as the free propagator, provided one includes in the interaction terms not only ξS_{int} , but also the quadratic terms $\langle \psi | \xi^n \Lambda_n | \psi \rangle$. Accordingly, ξ is interpreted as a coupling constant, and the $\xi^n \Lambda_n$ acquire the meaning of counterterms. These counterterms can be tuned to cancel out reducible diagrams, thereby enforcing the dressed character of the diagrammatic expansion. A natural requirement is that $S_{\mathcal{N}}^{(\xi=1)}$ coincides with the physical action S , i.e., that

$$\tilde{G}_{\mathcal{N}}^{-1} + \sum_{n=1}^{\mathcal{N}} \Lambda_n = G_0^{-1}. \quad (4)$$

For given G_0 , this should be viewed as an equation to be solved for $\tilde{G}_{\mathcal{N}}$ (it is nonlinear if the Λ_n 's depend on $\tilde{G}_{\mathcal{N}}$). The unperturbed action for the dressed expansion $\langle \psi | \tilde{G}_{\mathcal{N}}^{-1} | \psi \rangle$ is shifted by the Λ_n 's with respect to the unperturbed action for the bare expansion $\langle \psi | G_0^{-1} | \psi \rangle$.

We can then use any action of the generic class (2) for producing physical answers in the form of a Taylor expansion in powers of ξ , provided the propagator $\tilde{G}_{\mathcal{N}}$ and the shifts Λ_n satisfy Eq. (4). More precisely, consider the full single-particle propagator $G_{\mathcal{N}}(\xi)$ of the action $S_{\mathcal{N}}^{(\xi)}$, and the corresponding self-energy

$$\Sigma_{\mathcal{N}}(\xi) := G_{0,\mathcal{N}}^{-1}(\xi) - G_{\mathcal{N}}^{-1}(\xi). \quad (5)$$

Note that since $S_{\mathcal{N}}^{(\xi=1)} = S$, we have $G_{\mathcal{N}}(\xi=1) = G$ and hence also $\Sigma_{\mathcal{N}}(\xi=1) = \Sigma$. We assume for simplicity that $\Sigma_{\mathcal{N}}(\xi)$ is analytic at $\xi=0$, and that its Taylor series, $\sum_{n=1}^{\infty} \Sigma_{\mathcal{N}}^{(n)}[\tilde{G}_{\mathcal{N}}] \xi^n$, converges at $\xi=1$. We expect these assumptions to hold for fermionic lattice models at finite temperature in a broad parameter regime, given that the action $S_{\mathcal{N}}^{(\xi)}$ is analytic in ξ [6,7,9-11,13,19]. Then, since $S_{\mathcal{N}}^{(\xi)}$ is an entire function of ξ , we can conclude that

$$\Sigma = \sum_{n=1}^{\infty} \Sigma_{\mathcal{N}}^{(n)}[\tilde{G}_{\mathcal{N}}], \quad (6)$$

i.e., the physical self-energy is equal to the dressed diagrammatic series.

This last step of the reasoning can be justified using the following presumption: *Let \mathcal{D} be a connected open region of the complex plane containing 0. Assume that $S^{(\xi)}$ is analytic in \mathcal{D} , that the corresponding self-energy $\Sigma(\xi)$ is analytic at $\xi=0$, and that $\Sigma(\xi)$ admits an analytic continuation $\tilde{\Sigma}(\xi)$ in \mathcal{D} . Then, Σ and $\tilde{\Sigma}$ coincide on \mathcal{D} .* This presumption is based on the following argument: Since $S^{(\xi)}$ is analytical, if no phase

transition occurs when varying ξ in \mathcal{D} , then $\Sigma(\xi)$ is analytical on \mathcal{D} , and by the identity theorem for analytic functions, Σ and $\tilde{\Sigma}$ coincide on \mathcal{D} . If a phase transition would be crossed as a function of ξ in \mathcal{D} , analytic continuation through the phase transition would not be possible [20], contradicting the above assumption on the existence of $\tilde{\Sigma}$. Applying this presumption to $\tilde{\Sigma}(\xi) := \sum_{n=1}^{\infty} \Sigma_{\mathcal{N}}^{(n)}[\tilde{G}_{\mathcal{N}}] \xi^n$, which has a radius of convergence $R \geq 1$ (from the Cauchy-Hadamard theorem), and taking for \mathcal{D} the open disk of radius R , we directly obtain Eq. (6) provided $R > 1$. If $R = 1$, we can still derive Eq. (6), using Abel's theorem and assuming that $\Sigma_{\mathcal{N}}(\xi)$ is continuous at $\xi=1$, which, given that the action is entire in ξ , is generically expected (except for physical parameters finely-tuned precisely to a first-order phase transition, where Σ is not uniquely defined).

Semibold scheme. We first focus on the choice

$$\Lambda_n = \Sigma_{\text{bold}}^{(n)}[\tilde{G}_{\mathcal{N}}] \quad (1 \leq n \leq \mathcal{N}), \quad (7)$$

where $\Sigma_{\text{bold}}^{(n)}[\mathcal{G}]$ is the sum of all skeleton diagrams of order n , built with the propagator \mathcal{G} and the bare interaction vertex corresponding to S_{int} , that remain connected when cutting two \mathcal{G} lines. This means that $\tilde{G}_{\mathcal{N}}$ is the solution of the bold scheme for maximal order \mathcal{N} [cf. Eq. (4)]. For a given \mathcal{N} , higher-order dressed graphs can then be built on $\tilde{G}_{\mathcal{N}}$. The numerical protocol corresponding to this ‘‘semibold’’ scheme consists of two independent parts: Part I is the bold diagrammatic Monte Carlo simulation of the truncated order- \mathcal{N} skeleton sum employed to solve iteratively for $\tilde{G}_{\mathcal{N}}$ satisfying Eqs. (4) and (7); part II is the diagrammatic Monte Carlo simulation of higher-order terms, $\Sigma_{\mathcal{N}}^{(n)}[\tilde{G}_{\mathcal{N}}]$, $n > \mathcal{N}$, that uses $\tilde{G}_{\mathcal{N}}$ as the bare propagator. Note that here \mathcal{N} is fixed (contrarily to the conventional skeleton scheme discussed below), and the infinite-order extrapolation is done only in part II.

The Feynman rules for this scheme are as follows:

$$\Sigma_{\mathcal{N}}^{(n)}[\tilde{G}_{\mathcal{N}}] = \Sigma_{\text{bold}}^{(n)}[\tilde{G}_{\mathcal{N}}] \quad \text{for } n \leq \mathcal{N}, \quad (8)$$

while for $n \geq \mathcal{N} + 1$, $\Sigma_{\mathcal{N}}^{(n)}[\tilde{G}_{\mathcal{N}}]$ is the sum of all bare diagrams, built with $\tilde{G}_{\mathcal{N}}$ as free propagator and the bare interaction vertex corresponding to S_{int} , which do not contain any insertion of a subdiagram contributing to $\Sigma_{\text{bold}}^{(n)}[\tilde{G}_{\mathcal{N}}]$ with $n \leq \mathcal{N}$. Indeed, each such insertion is exactly compensated by the corresponding counterterm. To derive Eq. (8), we will use the relation

$$\Sigma_{\mathcal{N}}(\xi) \hat{=} \sum_{n=1}^{\infty} \Sigma_{\text{bold}}^{(n)}[G_{\mathcal{N}}(\xi)] \xi^n, \quad (9)$$

where $\hat{=}$ stands for equality in the sense of formal power series in ξ , and we will show the proposition

$$\Sigma_{\mathcal{N}}(\xi) \hat{=} \sum_{n=1}^k \Sigma_{\text{bold}}^{(n)}[\tilde{G}_{\mathcal{N}}] \xi^n + O(\xi^{k+1}) \quad (\mathcal{P}_k)$$

for any $k \in \{0, \dots, \mathcal{N} + 1\}$, by recursion over k . ($\mathcal{P}_{k=0}$) clearly holds. If (\mathcal{P}_k) holds for some $k \leq \mathcal{N}$, then we have $G_{\mathcal{N}}(\xi) \hat{=} \tilde{G}_{\mathcal{N}} + O(\xi^{k+1})$, as follows from Eqs. (5), (3), and (7). Substitution into Eq. (9) then yields (\mathcal{P}_{k+1}).

Alternatively to the semibold scheme Eq. (7), other choices are possible for the shifts $\Lambda_1, \dots, \Lambda_{\mathcal{N}}$ and the dressed

propagator $\tilde{G}_{\mathcal{N}}$. For example, the shifts can be based on diagrams containing the original bare propagator G_0 instead of $\tilde{G}_{\mathcal{N}}$. In the absence of exact cancellation, all diagrams should be simulated in part II of the numerical protocol, and Λ_n will enter the theory explicitly. This flexibility of choosing the form of Λ_n 's, along with the obvious option of exploring different \mathcal{N} 's, provides a tool for controlling systematic errors coming from truncation of the ξ series.¹

Skeleton scheme. We turn to the conventional scheme in which diagrams are built on the *fully* dressed single-particle propagator. The corresponding numerical protocol is identical to part I of the above one, with the additional step of extrapolating \mathcal{N} to infinity, as done in Refs. [8–11,21]. Accordingly, we assume that the “skeleton sequence” $\tilde{G}_{\mathcal{N}}$ converges to a limit \tilde{G} when $\mathcal{N} \rightarrow \infty$. The crucial question is under what conditions one can be confident that \tilde{G} is the genuine propagator G of the original model. The answer comes from the properties of the sequence of functions

$$L_{\mathcal{N}}^{(\xi)} := \sum_{n=1}^{\mathcal{N}} \Sigma_{\text{bold}}^{(n)}[\tilde{G}_{\mathcal{N}}] \xi^n. \quad (10)$$

Let us show that $\tilde{G} = G$ holds under the following sufficient conditions: (i) For any ξ in a disk $\mathcal{D} = \{|\xi| < R\}$ of radius $R > 1$, and for all (\mathbf{p}, τ) , $L_{\mathcal{N}}^{(\xi)}(\mathbf{p}, \tau)$ converges for $\mathcal{N} \rightarrow \infty$; moreover, this sequence is uniformly bounded, i.e., there exists a function $C_1(\mathbf{p}, \tau)$ such that $\forall \xi \in \mathcal{D}, \forall (\mathcal{N}, \mathbf{p}, \tau), |L_{\mathcal{N}}^{(\xi)}(\mathbf{p}, \tau)| \leq C_1(\mathbf{p}, \tau)$; and (ii) $\tilde{G}_{\mathcal{N}}(\mathbf{p}, \tau)$ is uniformly bounded, i.e., there exists a constant C_2 such that for all $(\mathcal{N}, \mathbf{p}, \tau), |\tilde{G}_{\mathcal{N}}(\mathbf{p}, \tau)| \leq C_2$.

Our derivation is based on the action

$$S_{\infty}^{(\xi)} := \lim_{\mathcal{N} \rightarrow \infty} S_{\mathcal{N}}^{(\xi)}. \quad (11)$$

Clearly,

$$S_{\infty}^{(\xi)} = \langle \psi | \tilde{G}^{-1} + L^{(\xi)} | \psi \rangle + \xi S_{\text{int}} \quad (12)$$

with

$$L^{(\xi)}(\mathbf{p}, \tau) := \lim_{\mathcal{N} \rightarrow \infty} L_{\mathcal{N}}^{(\xi)}(\mathbf{p}, \tau). \quad (13)$$

Since $S_{\mathcal{N}}^{(\xi=1)} = S$, we have $S_{\infty}^{(\xi=1)} = S$, and thus $G_{\infty}(\xi = 1) = G$, where $G_{\infty}(\xi)$ is the full propagator of the action $S_{\infty}^{(\xi)}$.

We first observe that $L^{(\xi)}(\mathbf{p}, \tau)$ is an analytic function of $\xi \in \mathcal{D}$ for all (\mathbf{p}, τ) , and that

$$\frac{1}{n!} \frac{\partial^n}{\partial \xi^n} L^{(\xi)}(\mathbf{p}, \tau) \Big|_{\xi=0} = \Sigma_{\text{bold}}^{(n)}[\tilde{G}](\mathbf{p}, \tau). \quad (14)$$

This follows from conditions (i) and (ii), given that momenta are bounded for lattice models. Indeed, for any triangle \mathcal{T} included in \mathcal{D} , $\oint_{\mathcal{T}} d\xi L_{\mathcal{N}}^{(\xi)}(\mathbf{p}, \tau) = 0$. Owing to condition (i), the dominated convergence theorem is applicable, yielding $\oint_{\mathcal{T}} d\xi L^{(\xi)}(\mathbf{p}, \tau) = 0$. The analyticity of $\xi \mapsto L^{(\xi)}(\mathbf{p}, \tau)$ follows

¹The case where $\mathcal{N} = 1$ and Λ_1 is a number is known as Screened Perturbation Theory in thermal ϕ^4 theory; its extension to gauge theories is known as Hard-Thermal-Loop Perturbation Theory [4]. We thank E. Braaten for pointing this out.

by Morera's theorem. To derive Eq. (14) we start from

$$\frac{1}{n!} \frac{\partial^n}{\partial \xi^n} L_{\mathcal{N}}^{(\xi)}(\mathbf{p}, \tau) \Big|_{\xi=0} = \Sigma_{\text{bold}}^{(n)}[\tilde{G}_{\mathcal{N}}](\mathbf{p}, \tau). \quad (15)$$

By Cauchy's integral formula, the left-hand side of Eq. (15) equals $1/(2i\pi) \oint_{\mathcal{C}} d\xi L_{\mathcal{N}}^{(\xi)}(\mathbf{p}, \tau)/\xi^{n+1}$, where \mathcal{C} is the unit circle. Using again condition (i) and the dominated convergence theorem, when $\mathcal{N} \rightarrow \infty$, this tends to $1/(2i\pi) \oint_{\mathcal{C}} d\xi L^{(\xi)}(\mathbf{p}, \tau)/\xi^{n+1}$, which equals the left-hand side of Eq. (14). To show that $\Sigma_{\text{bold}}^{(n)}[\tilde{G}_{\mathcal{N}}](\mathbf{p}, \tau)$ tends to $\Sigma_{\text{bold}}^{(n)}[\tilde{G}](\mathbf{p}, \tau)$, we consider each Feynman diagram separately; the dominated convergence theorem is applicable owing to condition (ii), the boundedness of the integration domain for internal momenta and imaginary times, and assuming that interactions decay sufficiently quickly at large distances for the bare interaction vertex to be bounded in momentum representation.

Hence

$$L^{(\xi)} = \sum_{n=1}^{\infty} \Sigma_{\text{bold}}^{(n)}[\tilde{G}] \xi^n. \quad (16)$$

As a consequence, the action $S_{\infty}^{(\xi)}$ generates the fully dressed skeleton series built on \tilde{G} , i.e., its self-energy $\Sigma_{\infty}(\xi)$ has the Taylor expansion $\sum_{n=1}^{\infty} \Sigma_{\text{bold}}^{(n)}[\tilde{G}] \xi^n$, and the Taylor series of $G_{\infty}(\xi)$ reduces to the ξ -independent term \tilde{G} . This can be derived in the same way as Eq. (8), by showing by recursion over k that for any $k \geq 0$, $\Sigma_{\infty}(\xi) = \sum_{n=1}^k \Sigma_{\text{bold}}^{(n)}[\tilde{G}] \xi^n + O(\xi^{k+1})$. Furthermore, having shown above the analyticity of $L^{(\xi)}$, i.e., of $S_{\infty}^{(\xi)}$, we again expect that $G_{\infty}(\xi)$ is analytic at $\xi = 0$ (for fermions on a lattice at finite temperature), and we can use again the above presumption to conclude that $G_{\infty}(\xi = 1) = G = \tilde{G}$.

Dressed pair propagator. So far we have discussed dressing of the single-particle propagator while keeping the bare interaction vertices. We turn to diagrammatic schemes built on dressed pair propagators. We restrict to spin-1/2 fermions with on-site interaction,

$$S_{\text{int}}[\psi, \bar{\psi}] = U \sum_{\mathbf{r}} \int_0^{\beta} d\tau (\bar{\psi}_{\uparrow} \bar{\psi}_{\downarrow} \psi_{\downarrow} \psi_{\uparrow})(\mathbf{r}, \tau), \quad (17)$$

where U is the bare interaction strength. For simplicity we discuss dressing of the pair propagator while keeping the bare G_0 . It is necessary to perform a Hubbard-Stratonovich transformation in order to construct the appropriate auxiliary action. Introducing a complex scalar Hubbard-Stratonovich field η leads to the action

$$\mathcal{S}[\psi, \bar{\psi}, \eta, \bar{\eta}] = \langle \psi | G_0^{-1} | \psi \rangle - \langle \eta | \Gamma_0^{-1} | \eta \rangle - \langle \eta | \Pi_0 | \eta \rangle + \langle \eta | \psi_{\downarrow} \psi_{\uparrow} \rangle + \langle \psi_{\downarrow} \psi_{\uparrow} | \eta \rangle, \quad (18)$$

where $\Pi_0(\mathbf{r}, \tau) = -(G_{0,\uparrow} G_{0,\downarrow})(\mathbf{r}, \tau)$ and Γ_0 is the sum of the ladder diagrams, $\Gamma_0^{-1}(\mathbf{p}, \Omega_n) = U^{-1} - \Pi_0(\mathbf{p}, \Omega_n)$, with Ω_n the bosonic Matsubara frequencies.

We first consider the diagrammatic scheme built on G_0 and Γ_0 . We denote by $\Sigma_{\text{lad}}^{(n)}[G_0, \Gamma_0]$ the sum of all self-energy diagrams of order n , i.e., containing n Γ_0 lines. This diagrammatic series is generated by the shifted action

$$\mathcal{S}_{\text{lad}}^{(\xi)}[\psi, \bar{\psi}, \eta, \bar{\eta}] = \langle \psi | G_0^{-1} | \psi \rangle - \langle \eta | \Gamma_0^{-1} | \eta \rangle - \xi^2 \langle \eta | \Pi_0 | \eta \rangle + \xi (\langle \eta | \psi_{\downarrow} \psi_{\uparrow} \rangle + \langle \psi_{\downarrow} \psi_{\uparrow} | \eta \rangle), \quad (19)$$

in the sense that self-energy $\Sigma_{\text{lad}}(\xi)$ corresponding to this action has the Taylor series $\sum_{n=1}^{\infty} \Sigma_{\text{lad}}^{(n)}[G_0, \Gamma_0] \xi^{2n}$. Indeed, the counterterm $\xi^2 \Pi_0$ cancels out the reducible diagrams containing $G_0 G_0$ bubbles. Therefore, if this diagrammatic series converges, then it yields the physical self-energy. This follows from the same reasoning as below Eq. (5). The same applies to the series for the pair self-energy Π in terms of $[G_0, \Gamma_0]$. Here Π is defined by $\Gamma^{-1} = \Gamma_0^{-1} - \Pi$, where Γ denotes the fully dressed pair propagator, used in Refs. [8, 11].

More complex schemes, built on dressed pair propagators other than Γ_0 , can be generated by the shifted action

$$\mathcal{S}_{\mathcal{N}}^{(\xi)}[\psi, \bar{\psi}, \eta, \bar{\eta}] = \langle \psi | G_0^{-1} | \psi \rangle - \langle \eta | \Gamma_{0, \mathcal{N}}^{-1}(\xi) | \eta \rangle - \xi^2 \langle \eta | \Pi_0 | \eta \rangle + \xi \langle (\eta | \psi_{\downarrow} \psi_{\uparrow}) + (\psi_{\downarrow} \psi_{\uparrow} | \eta) \rangle, \quad (20)$$

where

$$\Gamma_{0, \mathcal{N}}^{-1}(\xi) = \Gamma_0^{-1} + \xi^2 \Omega_1 + \dots + \xi^{2\mathcal{N}} \Omega_{\mathcal{N}} \quad (21)$$

and one imposes $\Gamma_{0, \mathcal{N}}(\xi = 1) = \Gamma_0$. In particular, the semibold scheme is defined by

$$\Omega_n = \Pi_{\text{bold}}^{(n)}[\tilde{\Gamma}_{\mathcal{N}}], \quad (22)$$

where $\Pi_{\text{bold}}^{(n)}[\gamma]$ is the sum of all skeleton diagrams of order n built with the pair-propagator γ that remain connected when cutting two γ lines. As usual, $\Pi_{\text{bold}}^{(1)} = -GG + G_0 G_0$. This scheme was introduced previously for $\mathcal{N} = 1$ [22].

Finally, we consider the skeleton scheme built on G_0 and Γ . Assuming that the skeleton sequence $\tilde{\Gamma}_{\mathcal{N}}$ converges to some $\tilde{\Gamma}$, one can show analogously to the above reasoning that $\tilde{\Gamma}$ is equal to the exact Γ under the following sufficient conditions: (i) For any ξ in a disk $\mathcal{D} = \{|\xi| < R\}$ of radius $R > 1$, and for all (\mathbf{p}, Ω_n) , $M_{\mathcal{N}}^{(\xi)}(\mathbf{p}, \Omega_n) := \sum_{n=1}^{\mathcal{N}} \Pi_{\text{bold}}^{(n)}[\tilde{\Gamma}_{\mathcal{N}}](\mathbf{p}, \Omega_n) \xi^n$ converges for $\mathcal{N} \rightarrow \infty$; moreover, this sequence is uniformly bounded, i.e., there exists $C(\mathbf{p}, \Omega_n)$ such that $\forall \xi \in \mathcal{D}, \forall (\mathcal{N}, \mathbf{p}, \Omega_n), |M_{\mathcal{N}}^{(\xi)}(\mathbf{p}, \Omega_n)| \leq C(\mathbf{p}, \Omega_n)$; and (ii) $\tilde{\Gamma}_{\mathcal{N}}(\mathbf{p}, \Omega_n)$ is uniformly bounded.

Screened interaction potential. Finally, we briefly address the procedure of dressing the interaction line, which is particularly important for long-range interaction potentials. Restricting for simplicity to a spin-independent interaction potential $V(\mathbf{r})$, the interaction part of the action writes

$$\frac{1}{2} \sum_{\sigma, \sigma'} \sum_{\mathbf{r}, \mathbf{r}'} \int_0^{\beta} d\tau (\bar{\psi}_{\sigma} \psi_{\sigma})(\mathbf{r}, \tau) V(\mathbf{r} - \mathbf{r}') (\bar{\psi}_{\sigma'} \psi_{\sigma'})(\mathbf{r}', \tau). \quad (23)$$

We again keep the bare G_0 for simplicity and consider dressing of V only. Introducing a real scalar Hubbard-Stratonovich field

χ leads to the action

$$\mathcal{S}[\psi, \bar{\psi}, \chi] = \langle \psi | G_0^{-1} | \psi \rangle + \frac{1}{2} \langle \chi | V^{-1} | \chi \rangle + i \sum_{\sigma} \langle \chi | \bar{\psi}_{\sigma} \psi_{\sigma} \rangle. \quad (24)$$

Here we assume that the Fourier transform $V(\mathbf{q})$ of the interaction potential is positive, so that the quadratic form $\langle \chi | V^{-1} | \chi \rangle = (2\pi)^{-d} \int_0^{\beta} d\tau \int d^d q |\chi(\mathbf{q}, \tau)|^2 / V(\mathbf{q})$ is positive definite. The auxiliary action takes the form

$$\mathcal{S}_{\mathcal{N}}^{(\xi)}[\psi, \bar{\psi}, \chi] = \langle \psi | G_0^{-1} | \psi \rangle + \frac{1}{2} \langle \chi | \tilde{V}_{\mathcal{N}}^{-1} + \xi^2 \Omega_1 + \dots + \xi^{2\mathcal{N}} \Omega_{\mathcal{N}} | \chi \rangle + i \xi \sum_{\sigma} \langle \chi | \bar{\psi}_{\sigma} \psi_{\sigma} \rangle. \quad (25)$$

The semibold scheme corresponds to $\Omega_n = \Pi_{\text{bold}}^{(n)}[\tilde{V}_{\mathcal{N}}]$, where Π now stands for the polarization. In particular, \tilde{V}_1 is the random phase approximation (RPA) screened interaction.

Summarizing, we have revealed an analytic structure behind dressed-line diagrammatics. More precisely, we have exhibited the function which analytically continues a dressed diagrammatic series. This function originates from an action that depends on an auxiliary parameter ξ . When the action is a polynomial in ξ , the situation reduces to the one of a bare expansion. Within this category, a particular case well suited for numerical implementation is the semibold scheme for which the bare propagator is taken from the truncated bold self-consistent equation. For the fully bold scheme, we construct an appropriate auxiliary action, but only under a certain condition. If this condition is verified numerically, it is safe to use the fully bold scheme. If not, the semibold scheme remains applicable.

Furthermore, we have demonstrated the generality of the shifted-action construction by treating the case of a dressed pair propagator and of a screened long-range interaction. Further extensions left for future work are dressing of three-point vertices, as well as justifying resummation of divergent diagrammatic series by considering non-disk-shaped analyticity domains \mathcal{D} .

We are grateful to Youjin Deng, Evgeny Kozik, and Kris Van Houcke for valuable exchanges. This work was supported by the National Science Foundation under Grant No. PHY-1314735, The Simons Collaboration on the Many Electron Problem, the MURI Program ‘‘New Quantum Phases of Matter’’ from AFOSR, CNRS, ERC, and IFRAF-NanoK (Grants PICS 06220, *Thermodynamix*, and *Atomix*).

- [1] L. D. Landau, E. M. Lifshitz, and L. P. Pitaevskii, *Statistical Physics Part 2* (Butterworth-Heinemann, Oxford, U.K., 2000).
- [2] A. Abrikosov, L. Gor'kov, and I. Y. Dzyaloshinskii, *Methods of Quantum Field Theory in Statistical Physics* (Dover, New York, 1975).
- [3] W. H. Dickhoff and C. Barbieri, *Prog. Part. Nucl. Phys.* **52**, 377 (2004).

- [4] J. O. Andersen and M. Strickland, *Ann. Phys.* **317**, 281 (2005).
- [5] M. G. Alford, A. Schmitt, K. Rajagopal, and T. Schäfer, *Rev. Mod. Phys.* **80**, 1455 (2008).
- [6] K. Van Houcke, E. Kozik, N. Prokof'ev, and B. Svistunov, *Phys. Procedia* **6**, 95 (2010).
- [7] E. Kozik, K. Van Houcke, E. Gull, L. Pollet, N. Prokof'ev, B. Svistunov, and M. Troyer, *Europhys. Lett.* **90**, 10004 (2010).

- [8] K. Van Houcke, F. Werner, E. Kozik, N. Prokof'ev, B. Svistunov, M. J. H. Ku, A. T. Sommer, L. W. Cheuk, A. Schirotzek, and M. W. Zwierlein, *Nat. Phys.* **8**, 366 (2012).
- [9] S. A. Kulagin, N. Prokof'ev, O. A. Starykh, B. Svistunov, and C. N. Varney, *Phys. Rev. Lett.* **110**, 070601 (2013).
- [10] A. S. Mishchenko, N. Nagaosa, and N. Prokof'ev, *Phys. Rev. Lett.* **113**, 166402 (2014).
- [11] Y. Deng, E. Kozik, N. V. Prokof'ev, and B. V. Svistunov, *Europhys. Lett.* **110**, 57001 (2015).
- [12] L. Molinari and N. Manini, *Eur. Phys. J. B* **51**, 331 (2006).
- [13] G. Benfatto, A. Giuliani, and V. Mastropietro, *Ann. Henri Poincaré* **7**, 809 (2006).
- [14] E. Kozik, M. Ferrero, and A. Georges, *Phys. Rev. Lett.* **114**, 156402 (2015).
- [15] Y. Deng and E. Kozik (private communication).
- [16] R. Rossi and F. Werner, *J. Phys. A* **48**, 485202 (2015).
- [17] R. Rossi and F. Werner (unpublished).
- [18] J. W. Negele and H. Orland, *Quantum Many-Particle Systems* (Addison-Wesley, Reading, MA, 1988).
- [19] A. Abdesselam and V. Rivasseau, *Lett. Math. Phys.* **44**, 77 (1998).
- [20] S. N. Isakov, *Commun. Math. Phys.* **95**, 427 (1984).
- [21] N. V. Prokof'ev and B. V. Svistunov, *Phys. Rev. B* **77**, 125101 (2008).
- [22] K. Van Houcke (unpublished).

Bibliography

- [1] D. M. Ceperley. Path integrals in the theory of condensed helium. Rev. Mod. Phys., 67:279–355, Apr 1995.
- [2] M. Boninsegni, N. V. Prokof'ev, and B. V. Svistunov. Worm algorithm and diagrammatic Monte Carlo: A new approach to continuous-space path integral Monte Carlo simulations. Phys. Rev. E, 74:036701, Sep 2006.
- [3] Lode Pollet. Recent developments in quantum Monte Carlo simulations with applications for cold gases. Reports on Progress in Physics, 75(9):094501, 2012.
- [4] S. Trotzky, L. Pollet, F. Gerbier, U. Schnorrberger, I. Bloch, N. V. Prokof'ev, B. Svistunov, and M. Troyer. Suppression of the critical temperature for superfluidity near the Mott transition. Nature Physics, 6:998–1004, 2010.
- [5] E. Y. Loh, J. E. Gubernatis, R. T. Scalettar, S. R. White, D. J. Scalapino, and R. L. Sugar. Sign problem in the numerical simulation of many-electron systems. Phys. Rev. B, 41:9301–9307, May 1990.
- [6] Ceperley D. M. Path integral Monte Carlo methods for fermions. Monte Carlo and Molecular Dynamics of Condensed Matter Systems, 49, 1996.
- [7] D. M. Ceperley. Quantum Monte Carlo Methods for Fermions. Proceedings of the Les Houches Summer School, Strongly Interacting Fermions ed B. Doucot and J. Zinn-Justin, 56, 1995.
- [8] F.F. Assaad and H.G. Evertz. World-line and Determinantal Quantum Monte Carlo Methods for Spins, Phonons and Electrons. Springer Berlin Heidelberg, pages 277–356, 2008.
- [9] Zwerger, W. (ed.). The BCS-BEC Crossover and the Unitary Fermi Gas. Lecture Notes in Physics, Volume 836. Springer, Berlin, 2012.

- [10] A. Altmeyer, S. Riedl, C. Kohstall, M. J. Wright, R. Geursen, M. Bartenstein, C. Chin, J. Hecker Denschlag, and R. Grimm. Precision Measurements of Collective Oscillations in the BEC-BCS Crossover. Phys. Rev. Lett., 98:040401, 2007.
- [11] S. Nascimbène, N. Navon, K. J. Jiang, F. Chevy, and C. Salomon. Nature, 463:1057, 2010.
- [12] Kris Van Houcke, Félix Werner, Evgeny Kozik, Nikolay Prokof'ev, Boris Svistunov, MJH Ku, AT Sommer, LW Cheuk, Andre Schirotzek, and MW Zwierlein. Feynman diagrams versus Fermi-gas Feynman emulator. Nature Physics, 8(5):366–370, 2012.
- [13] M. Ku, A. Sommer, L. W. Cheuk, and M. W. Zwierlein. Science, 335:563, 2012.
- [14] Sascha Hoinka, Marcus Lingham, Kristian Fenech, Hui Hu, Chris J. Vale, Joaquín E. Drut, and Stefano Gandolfi. Precise Determination of the Structure Factor and Contact in a Unitary Fermi Gas. Phys. Rev. Lett., 110:055305, Jan 2013.
- [15] Russell A Hart, Pedro M Duarte, Tsung-Lin Yang, Xinxing Liu, Thereza Paiva, Ehsan Khatami, Richard T Scalettar, Nandini Trivedi, David A Huse, and Randall G Hulet. Observation of antiferromagnetic correlations in the Hubbard model with ultracold atoms. Nature, 519(7542):211–214, 2015.
- [16] Daniel Greif, Gregor Jotzu, Michael Messer, Rémi Desbuquois, and Tilman Esslinger. Formation and Dynamics of Antiferromagnetic Correlations in Tunable Optical Lattices. Phys. Rev. Lett., 115:260401, Dec 2015.
- [17] Maxwell F. Parsons, Anton Mazurenko, Christie S. Chiu, Geoffrey Ji, Daniel Greif, and Markus Greiner. Site-resolved measurement of the spin-correlation function in the Fermi-Hubbard model. Science, 353(6305):1253–1256, 2016.
- [18] Lawrence W. Cheuk, Matthew A. Nichols, Katherine R. Lawrence, Melih Okan, Hao Zhang, Ehsan Khatami, Nandini Trivedi, Thereza Paiva, Marcos Rigol, and Martin W. Zwierlein. Observation of spatial charge and spin correlations in the 2D Fermi-Hubbard model. Science, 353(6305):1260–1264, 2016.
- [19] J. H. Drewes, L. A. Miller, E. Cocchi, C. F. Chan, N. Wurz, M. Gall, D. Pertot, F. Brennecke, and M. Köhl. Antiferromagnetic Correlations in

Two-Dimensional Fermionic Mott-Insulating and Metallic Phases. Phys. Rev. Lett., 118:170401, Apr 2017.

- [20] A. Mazurenko, C. S. Chiu, G. Ji, M. F. Parsons, M. Kanász-Nagy, R. Schmidt, F. Grusdt, E. Demler, D. Greif, and M. Greiner. A cold-atom Fermi-Hubbard antiferromagnet. Nature, 545:462–466, May 2017.
- [21] Nikolai V. Prokof'ev and Boris V. Svistunov. Polaron Problem by Diagrammatic Quantum Monte Carlo. Phys. Rev. Lett., 81:2514–2517, Sep 1998.
- [22] Nikolay Prokof'ev and Boris Svistunov. Fermi-polaron problem: Diagrammatic Monte Carlo method for divergent sign-alternating series. Phys. Rev. B, 77:020408, Jan 2008.
- [23] N. V. Prokof'ev and B. V. Svistunov. Bold diagrammatic Monte Carlo: A generic sign-problem tolerant technique for polaron models and possibly interacting many-body problems. Phys. Rev. B, 77:125101, Mar 2008.
- [24] Jonas Vlietinck, Jan Ryckebusch, and Kris Van Houcke. Quasiparticle properties of an impurity in a Fermi gas. Phys. Rev. B, 87:115133, Mar 2013.
- [25] Jonas Vlietinck, Jan Ryckebusch, and Kris Van Houcke. Quasiparticle properties of an impurity in a Fermi gas. Phys. Rev. B, 87:115133, Mar 2013.
- [26] Peter Kroiss and Lode Pollet. Diagrammatic Monte Carlo study of quasi-two-dimensional Fermi polarons. Phys. Rev. B, 90:104510, Sep 2014.
- [27] Olga Goulko, Andrey S. Mishchenko, Nikolay Prokof'ev, and Boris Svistunov. Dark continuum in the spectral function of the resonant Fermi polaron. Phys. Rev. A, 94:051605, Nov 2016.
- [28] Kris Van Houcke, Evgeny Kozik, N. Prokof'ev, and B. Svistunov. Diagrammatic Monte Carlo. Physics Procedia, 6:95 – 105, 2010.
- [29] E. Kozik, K. Van Houcke, E. Gull, L. Pollet, N. Prokof'ev, B. Svistunov, and M. Troyer. Diagrammatic Monte Carlo for correlated fermions. EPL (Europhysics Letters), 90(1):10004, 2010.
- [30] Jan Gukelberger, Evgeny Kozik, Lode Pollet, Nikolay Prokof'ev, Manfred Sgrist, Boris Svistunov, and Matthias Troyer. *p*-Wave Superfluidity by Spin-Nematic Fermi Surface Deformation. Phys. Rev. Lett., 113:195301, Nov 2014.

- [31] Youjin Deng, Evgeny Kozik, Nikolay V. Prokof'ev, and Boris V. Svistunov. Emergent BCS regime of the two-dimensional fermionic Hubbard model: Ground-state phase diagram. EPL (Europhysics Letters), 110(5):57001, 2015.
- [32] Wei Wu, Michel Ferrero, Antoine Georges, and Evgeny Kozik. Controlling Feynman diagrammatic expansions: Physical nature of the pseudogap in the two-dimensional Hubbard model. Phys. Rev. B, 96:041105, Jul 2017.
- [33] S. A. Kulagin, N. Prokof'ev, O. A. Starykh, B. Svistunov, and C. N. Varney. Bold Diagrammatic Monte Carlo Method Applied to Fermionized Frustrated Spins. Phys. Rev. Lett., 110:070601, Feb 2013.
- [34] S. A. Kulagin, N. Prokof'ev, O. A. Starykh, B. Svistunov, and C. N. Varney. Bold diagrammatic Monte Carlo technique for frustrated spin systems. Phys. Rev. B, 87:024407, Jan 2013.
- [35] Yuan Huang, Kun Chen, Youjin Deng, Nikolay Prokof'ev, and Boris Svistunov. Spin-Ice State of the Quantum Heisenberg Antiferromagnet on the Pyrochlore Lattice. Phys. Rev. Lett., 116:177203, Apr 2016.
- [36] Buividovich, P. V. A method for resummation of perturbative series based on the stochastic solution of Schwinger-Dyson equations. Nuclear Physics B, 3:688–709, 2011.
- [37] Rosario E. V. Profumo, Christoph Groth, Laura Messio, Olivier Parcollet, and Xavier Waintal. Quantum Monte Carlo for correlated out-of-equilibrium nanoelectronic devices. Phys. Rev. B, 91:245154, Jun 2015.
- [38] Riccardo Rossi. Determinant diagrammatic Monte Carlo algorithm in the thermodynamic limit. ArXiv, 1612.05184, 2016.
- [39] Tobias Pfeffer and Lode Pollet. A stochastic root finding approach: the homotopy analysis method applied to Dyson-Schwinger equations. New Journal of Physics, 19(4):043005, 2017.
- [40] Buividovich, P. V. Feasibility of Diagrammatic Monte-Carlo based on weak-coupling expansion in asymptotically free theories: case study of $O(N)$ sigma-model in the large- N limit. PoS(LATTICE 2015), 293, 2015.
- [41] Buividovich, P. V. and Davody, A. . Diagrammatic Monte-Carlo study of the convergent weak-coupling expansion for the large- N $U(N)\times U(N)$ principal chiral model. arXiv, 1705.03368, 2017.

- [42] Nikolay Prokof'ev and Boris Svistunov. Bold Diagrammatic Monte Carlo Technique: When the Sign Problem Is Welcome. Phys. Rev. Lett., 99:250201, Dec 2007.
- [43] LN Lipatov. Divergence of the perturbation-theory series and the quasi-classical theory. JETP, 45(2):216, 1977.
- [44] E. Brézin, J. C. Le Guillou, and J. Zinn-Justin. Perturbation theory at large order. I. The φ^{2N} interaction. Phys. Rev. D, 15:1544–1557, Mar 1977.
- [45] J. Zinn-Justin. Quantum field theory and critical phenomena. Quantum Field Theory and Critical Phenomena, Clarendon Press; 4th edition, 2002.
- [46] G. Benfatto, A. Giuliani, and V. Mastropietro. Fermi liquid behavior in the 2D Hubbard model at low temperatures. Annales H. Poincare, 7:809–898, 2006.
- [47] Alessandro Giuliani and Vieri Mastropietro. Rigorous construction of ground state correlations in graphene: Renormalization of the velocities and ward identities. Phys. Rev. B, 79:201403, May 2009.
- [48] Evgeny Kozik, Michel Ferrero, and Antoine Georges. Nonexistence of the Luttinger-Ward Functional and Misleading Convergence of Skeleton Diagrammatic Series for Hubbard-Like Models. Phys. Rev. Lett., 114:156402, Apr 2015.
- [49] R. Rossi, N. Prokof'ev, B. Svistunov, K. Van Houcke, and F. Werner. Polynomial complexity despite the fermionic sign. EPL (Europhysics Letters), 118(1):10004, 2017.
- [50] X. Leyronas and R. Combescot. Superfluid Equation of State of Dilute Composite Bosons. Phys. Rev. Lett., 99:170402, 2007.
- [51] D. S. Petrov, C. Salomon, and G. V. Shlyapnikov. Weakly Bound Dimers of Fermionic Atoms. Phys. Rev. Lett., 93:090404, 2004.
- [52] A. J. Leggett and S. Zhang. Lecture Notes in Physics, 836:33, 2012. in [9].
- [53] M. Randeria, W. Zwerger, and M. Zwierlein. The BCS–BEC Crossover and the Unitary Fermi Gas, pages 1–32. Springer Berlin Heidelberg, Berlin, Heidelberg, 2012.
- [54] M.W. Zwierlein, J.R. Abo-Shaeer, A. Schirotzek, C.H. Schunck, and W. Ketterle. Nature, 435:1047, 2005.

- [55] Ultra-Cold Fermi gases. Proceedings of the International School of Physics "Enrico Fermi", M. Inguscio, W. Ketterle and C. Salomon eds. SIF, Bologna, 2007.
- [56] Giacomo Valtolina, Alessia Burchianti, Andrea Amico, Elettra Neri, Klejda Xhani, Jorge Amin Seman, Andrea Trombettoni, Augusto Smerzi, Matteo Zaccanti, Massimo Inguscio, and Giacomo Roati. Josephson effect in fermionic superfluids across the BEC-BCS crossover. Science, 350(6267):1505–1508, 2015.
- [57] Dominik Husmann, Shun Uchino, Sebastian Krinner, Martin Lebrat, Thierry Giamarchi, Tilman Esslinger, and Jean-Philippe Brantut. Connecting strongly correlated superfluids by a quantum point contact. Science, 350(6267):1498–1501, 2015.
- [58] I. Ferrier-Barbut, M. Delehaye, S. Laurent, A. T. Grier, M. Pierce, B. S. Rem, F. Chevy, and C. Salomon. A mixture of Bose and Fermi superfluids. Science, 345(6200):1035–1038, 2014.
- [59] Yvan Castin, Igor Ferrier-Barbut, and C. Salomon. The Landau critical velocity for a particle in a Fermi superfluid. Comptes Rendus Physique, 16:241, 2015.
- [60] Marion Delehaye, Sébastien Laurent, Igor Ferrier-Barbut, Shuwei Jin, Frédéric Chevy, and Christophe Salomon. Critical Velocity and Dissipation of an Ultracold Bose-Fermi Counterflow. Phys. Rev. Lett., 115:265303, Dec 2015.
- [61] Yong-il Shin. Determination of the equation of state of a polarized Fermi gas at unitarity. Phys. Rev. A, 77:041603(R), 2008.
- [62] N. Navon, S. Nascimbène, F. Chevy, and C. Salomon. Science, 328:729, 2010.
- [63] M. Horikoshi, S. Nakajima, M. Ueda, and T. Mukaiyama. Science, 327:442, 2010.
- [64] M.J.H. Ku, A.T. Sommer, L.W. Cheuk, and M.W. Zwierlein. Revealing the Superfluid Lambda Transition in the Universal Thermodynamics of a Unitary Fermi Gas. Science, 335:563, 2012.
- [65] Munekazu Horikoshi, Masato Koashi, Hiroyuki Tajima, Yoji Ohashi, and Makoto Kuwata-Gonokami. Ground-state thermodynamic quantities of homogeneous spin-1/2 fermions from the BCS region to the unitarity limit.

- [66] G. B. Partridge, K. E. Strecker, R. I. Kamar, M. W. Jack, and R. G. Hulet. Molecular Probe of Pairing in the BEC-BCS Crossover. Phys. Rev. Lett., 95:020404, 2005.
- [67] F. Werner, L. Tarruell, and Y. Castin. Number of closed-channel molecules in the BEC-BCS crossover. Eur. Phys. J. B, 68:401, 2009.
- [68] J. T. Stewart, J. P. Gaebler, T. E. Drake, and D. S. Jin. Verification of Universal Relations in a Strongly Interacting Fermi Gas. Phys. Rev. Lett., 104(23):235301, 2010.
- [69] E. D. Kuhnle, S. Hoinka, P. Dyke, H. Hu, P. Hannaford, and C. J. Vale. Temperature Dependence of the Universal Contact Parameter in a Unitary Fermi Gas. Phys. Rev. Lett., 106:170402, 2011.
- [70] Yoav Sagi, Tara E. Drake, Rabin Paudel, and Deborah S. Jin. Measurement of the Homogeneous Contact of a Unitary Fermi gas. Phys. Rev. Lett., 109:220402, 2012.
- [71] Sébastien Laurent, Matthieu Pierce, Marion Delehay, Tarik Yefsah, Frédéric Chevy, and Christophe Salomon. Connecting Few-Body Inelastic Decay to Quantum Correlations in a Many-Body System: A Weakly Coupled Impurity in a Resonant Fermi Gas. Phys. Rev. Lett., 118:103403, 2017.
- [72] J. T. Stewart, J. P. Gaebler, and D. S. Jin. Using photoemission spectroscopy to probe a strongly interacting Fermi gas. Nature, 454:744, 2008.
- [73] J. P. Gaebler, J. T. Stewart, T. E. Drake, D. S. Jin, A. Perali, P. Pieri, and G. C. Strinati. Nature Physics, 6:569, 2010.
- [74] Tung-Lam Dao, Antoine Georges, Jean Dalibard, Christophe Salomon, and Iacopo Carusotto. Measuring the one-particle excitations of ultra-cold fermionic atoms by stimulated Raman spectroscopy. Phys. Rev. Lett., 98:240402, 2007.
- [75] Biswaroop Mukherjee, Zhenjie Yan, Parth B. Patel, Zoran Hadzibabic, Tarik Yefsah, Julian Struck, and Martin W. Zwierlein. Homogeneous Atomic Fermi Gases. Phys. Rev. Lett., 118:123401, Mar 2017.
- [76] C. Cao, E. Elliott, J. Joseph, H. Wu, J. Petricka, T. Schaefer, and J. E. Thomas. Universal Quantum Viscosity in a Unitary Fermi Gas. Science, 331:58, 2011.

- [77] J. A. Joseph, E. Elliott, and J. E. Thomas. Shear Viscosity of a Unitary Fermi Gas Near the Superfluid Phase Transition. Phys. Rev. Lett., 115:020401, Jul 2015.
- [78] Tilman Enss, Rudolf Haussmann, and Wilhelm Zwerger. Ann. Phys., 326:770, 2011.
- [79] Piotr Magierski, Gabriel Wlazłowski, Aurel Bulgac, and Joaquín E. Drut. Finite-Temperature Pairing Gap of a Unitary Fermi Gas by Quantum Monte Carlo Calculations. Phys. Rev. Lett., 103:210403, Nov 2009.
- [80] J. E. Drut, T. A. Lähde, and T. Ten. Momentum Distribution and Contact of the Unitary Fermi gas. Phys. Rev. Lett., 106:205302, 2011.
- [81] O. Goulko and M. Wingate. Thermodynamics of balanced and slightly spin-imbalanced Fermi gases at unitarity. Phys. Rev. A, 82:053621, 2010.
- [82] Olga Goulko and Matthew Wingate. Numerical study of the unitary Fermi gas across the superfluid transition. Phys. Rev. A, 93:053604, May 2016.
- [83] Félix Werner and Yvan Castin. General relations for quantum gases in two and three dimensions: Two-component fermions. Phys. Rev. A, 86:013626, Jul 2012.
- [84] K. Van Houcke, F. Werner, N. Prokof'ev, and B. Svistunov. Bold diagrammatic Monte Carlo for the resonant Fermi gas. ArXiv e-prints, May 2013.
- [85] R. Combescot, X. Leyronas, and M. Yu. Kagan. Phys. Rev. A, page 023618, 2006.
- [86] G. C. Strinati. Lecture Notes in Physics, 836:99, 2012.
- [87] Rossi, Riccardo and Werner, Félix and Prokof'ev, Nikolay and Svistunov, Boris. Shifted-action expansion and applicability of dressed diagrammatic schemes. Phys. Rev. B, 93:161102, Apr 2016.
- [88] R. Haussmann. Phys. Rev. B, 49:12975, 1994.
- [89] R. Haussmann, W. Rantner, S. Cerrito, and W. Zwerger. Thermodynamics of the BCS-BEC crossover. Phys. Rev. A, 75:023610, 2007.
- [90] G. Parisi. Asymptotic estimates in perturbation theory with fermions. Physics Letters B, 66:382–384, February 1977.

- [91] C. Itzykson, G. Parisi, and J-B. Zuber. Asymptotic estimates in quantum electrodynamics. Phys. Rev. D, 16:996–1013, Aug 1977.
- [92] R. Balian, C. Itzykson, J. B. Zuber, and G. Parisi. Asymptotic estimates in quantum electrodynamics. II. Phys. Rev. D, 17:1041–1052, Feb 1978.
- [93] E. B. Bogolmony and V.A. Fateyev. The Dyson instability and asymptotics of the perturbation series in QED. Phys. Lett. B, 76:210–212, May 1978.
- [94] Marcos Marino. Instantons and large N: an introduction to non-perturbative methods in quantum field theory. Cambridge University Press, 2015.
- [95] Hardy, Godfrey Harold. Divergent series. Chelsea Publishing Company, 1991.
- [96] J. P. Ramis. Les series κ — sommables et leurs applications, pages 178–199. Springer Berlin Heidelberg, Berlin, Heidelberg, 1980.
- [97] Balser, W. From Divergent Power Series to Analytic Functions. Lecture notes in Mathematics, Springer-Verlag, 1991.
- [98] E. B. Bogomolny. Calculation of the Green functions by the coupling constant dispersion relations. Physics Letters B, 67:193–194, March 1977.
- [99] K. Van Houcke, F. Werner, E. Kozik, N. Prokof'ev, and B. Svistunov. Contact and momentum distribution of the unitary fermi gas by bold diagrammatic monte carlo. arXiv:1303.6245.
- [100] Shimpei Endo and Yvan Castin. The interaction-sensitive states of a trapped two-component ideal Fermi gas and application to the virial expansion of the unitary Fermi gas. Journal of Physics A: Mathematical and Theoretical, 49(26):265301, 2016.
- [101] Yangqian Yan and D. Blume. Path-Integral Monte Carlo Determination of the Fourth-Order Virial Coefficient for a Unitary Two-Component Fermi Gas with Zero-Range Interactions. Phys. Rev. Lett., 116:230401, Jun 2016.
- [102] Olga Goulko, Andrey S. Mishchenko, Lode Pollet, Nikolay Prokof'ev, and Boris Svistunov. Numerical analytic continuation: Answers to well-posed questions. Phys. Rev. B, 95:014102, Jan 2017.
- [103] M. Punk and W. Zwerger. Theory of rf-Spectroscopy of Strongly Interacting Fermions. Phys. Rev. Lett., 99:170404, 2007.

- [104] R. Haussmann, M. Punk, and W. Zwerger. Phys. Rev. A, 80:063612, 2009.
- [105] Frederic Chevy and Christophe Mora. Ultra-cold polarized Fermi gases. Reports on Progress in Physics, 73(11):112401, 2010.
- [106] M. Punk, P.T. Dumitrescu, and W. Zwerger. Polaron-to-molecule transition in a strongly imbalanced Fermi gas. Phys. Rev. A, 80:053605, 2009.
- [107] S. Nascimbène, N. Navon, K. J. Jiang, L. Tarruell, M. Teichmann, J. McKeever, F. Chevy, and C. Salomon. Phys. Rev. Lett., 103:170402, 2010.
- [108] A. Schirotzek, C.-H. Wu, A. Sommer, and M. W. Zwierlein. Phys. Rev. Lett., 102:230402, 2009.
- [109] M.P. Fry. Vacuum energy density in large orders of perturbation theory for the scalar yukawa² field theory. Physics Letters B, 80(1):65 – 67, 1978.
- [110] Pierre Renouard. Analyticité et sommabilité “de Borel” des fonctions de Schwinger du modèle de Yukawa en dimension $d=2$. I. Approximation “à volume fini”. Annales de l’I.H.P. Physique théorique, 27:237–277, 1977.
- [111] Pierre Renouard. Analyticité et sommabilité “de Borel” des fonctions de Schwinger du modèle de Yukawa en dimension $d=2$. II. La limite adiabatique. Annales de l’I.H.P. Physique théorique, 31:235–318, 1979.
- [112] Jesper Levinsen and Meera M. Parish. Strongly interacting two-dimensional Fermi gases, chapter 1, pages 1–75. WORLD SCIENTIFIC, 2015.
- [113] Marianne Bauer, Meera M. Parish, and Tilman Enss. Universal Equation of State and Pseudogap in the Two-Dimensional Fermi Gas. Phys. Rev. Lett., 112:135302, Apr 2014.
- [114] B. Fröhlich, M. Feld, E. Vogt, M. Koschorreck, M. Köhl, C. Berthod, and T. Giamarchi. Two-Dimensional Fermi Liquid with Attractive Interactions. Phys. Rev. Lett., 109:130403, Sep 2012.
- [115] Marco Koschorreck, Daniel Pertot, Enrico Vogt, and Michael Köhl. Universal spin dynamics in two-dimensional Fermi gases. Nature Phys., 9:405, 2013.
- [116] Vasiliy Makhalov, Kirill Martiyanov, and Andrey Turlapov. Ground-State Pressure of Quasi-2D Fermi and Bose Gases. Phys. Rev. Lett., 112:045301, Jan 2014.

- [117] I. Boettcher, L. Bayha, D. Kedar, P. A. Murthy, M. Neidig, M. G. Ries, A. N. Wenz, G. Zürn, S. Jochim, and T. Ess. Equation of State of Ultracold Fermions in the 2D BEC-BCS Crossover Region. Phys. Rev. Lett., 116:045303, Jan 2016.
- [118] Klaus Hueck, Niclas Luick, Lennart Sobirey, Jonas Siegl, Thomas Lompe, and Henning Moritz. Two-Dimensional Homogeneous Fermi Gases. arXiv:1704.06315.
- [119] F. J. Dyson. Divergence of Perturbation Theory in Quantum Electrodynamics. Phys. Rev., 85:631–632, Feb 1952.
- [120] C. A. R. Sá de Melo, Mohit Randeria, and Jan R. Engelbrecht. Crossover from BCS to Bose superconductivity: Transition temperature and time-dependent Ginzburg-Landau theory. Phys. Rev. Lett., 71:3202–3205, Nov 1993.
- [121] Barry Simon. Notes on infinite determinants of Hilbert space operators. Advances in Mathematics, 24(3):244 – 273, 1977.
- [122] E. Lieb and M. Loss. Analysis. Graduate Studies in Mathematics, 14, 2001.
- [123] Barry Simon. Large orders and summability of eigenvalue perturbation theory: A mathematical overview. International Journal of Quantum Chemistry, 21(1):3–25, 1982.
- [124] H. J. Haubold, A. M. Mathai, and R. K. Saxena. Mittag-Leffler Functions and Their Applications. Journal of Applied Mathematics, 298628:51, 2011.
- [125] Ferrero, M., and Moutenet, A. "Talk at Diagrammatic Monte Carlo workshop, Flatiron Institute, New York", June 2017.
- [126] Y. Deng and E. Kozik. (private communication).
- [127] Riccardo Rossi and Félix Werner. Skeleton series and multivaluedness of the self-energy functional in zero space-time dimensions. Journal of Physics A: Mathematical and Theoretical, 48(48):485202, 2015.
- [128] T. Schäfer, S. Ciuchi, M. Wallerberger, P. Thunström, O. Gunnarsson, G. Sangiovanni, G. Rohringer, and A. Toschi. Nonperturbative landscape of the Mott-Hubbard transition: Multiple divergence lines around the critical endpoint. Phys. Rev. B, 94:235108, Dec 2016.

- [129] O. Gunnarsson, G. Rohringer, T. Schafer, G. Sangiovanni, and A. Toschi. Breakdown of traditional many-body theories for correlated electrons. arXiv, page 1703.06478, 2017.
- [130] W. Tarantino, P. Romaniello, A. Berger, and L. Reining. arXiv, page 1703.05587, 2017.
- [131] Adrian Stan, Pina Romaniello, Santiago Rigamonti, Lucia Reining, and J A Berger. Unphysical and physical solutions in many-body theories: from weak to strong correlation. New Journal of Physics, 17(9):093045, 2015.
- [132] Felix Werner. (unpublished).
- [133] J.W. Negele and H. Orland. Quantum Many-particle Systems. Advanced Books Classics. Westview Press, 2008.
- [134] A. Abdesselam and V. Rivasseau. Explicit fermionic tree expansions. Letters in Mathematical Physics, 44(1):77–88, Apr 1998.
- [135] Andrey S. Mishchenko, Naoto Nagaosa, and Nikolay Prokof'ev. Diagrammatic Monte Carlo Method for Many-Polaron Problems. Phys. Rev. Lett., 113:166402, Oct 2014.
- [136] S. N. Isakov. Nonanalytic Features of the First Order Phase Transition in the Ising Model. Commun. Math. Phys., 95:427, 1984.